ULTIMATE CAPACITY OF OFFSHORE PLATFORM CONDUCTOR STRINGS

by

David McGowan

Thesis submitted to the faculty of the
Virginia Polytechnic Institute and State University
in partial fulfillment of the requirements for the degree of

MASTER OF SCIENCE

in

Civil Engineering

APPROVED:

W. Samuel Easterling, Chairman

Thomas M. Murray

Siegfried M. Holzer

April 1991

Blacksburg, Virginia 24061

LD
5655
V855
1991
M4494
c.2

ULTIMATE CAPACITY OF OFFSHORE PLATFORM CONDUCTOR STRINGS

by

David McGowan

Committee Chairman: W. Samuel Easterling

Civil Engineering

(ABSTRACT)

The ultimate capacity of offshore platform conductor strings is studied. The unique way in which conductors are loaded is described and the various design methods that exist are presented. Previous research in the field of tubular member behavior is also reviewed.

The results of seven experimental tests are evaluated and compared with the existing conductor design criteria. The test matrix calls for various amounts of lateral loading to be imposed on the conductor system. Axial load, applied to simulate the weight of inner casings, is then applied until failure.

Results indicate that internally applied axial loads do not induce stability related failure in the outer conductor. Additionally, the design internal moment, which is based on an inner casing being as eccentric as possible, accurately represents the upper limit for the bending moment observed in the experimental tests. The flexural stiffness of the inner casing serves to strengthen the conductor system. Therefore, a design method that considers the strength of the outer conductor and the inner casings is recommended.

ACKNOWLEDGEMENTS

I am very grateful to Dr. W. Samuel Easterling for his continuous support and guidance in this project. I would also like to thank my committee members, Dr. Thomas M. Murray and Dr. Siegfried M. Holzer, for their help during my graduate studies. I thank UNOCAL Corp., particularly Dr. William B. Lamport, for their sponsorship of this research project.

I wish to thank all of my fellow graduate (and undergraduate) students who have assisted me in this project. You have made working at the Structures Lab enjoyable and entertaining. I thank lab technicians Brett Farmer and Dennis Huffman for their support and friendship. A special thanks is due to Ann Crate for helping in the preparation of this report.

I thank my parents, William and Lucy McGowan, along with the rest of my family for the support they have given me over the years. Lastly, I wish to thank my future wife, Tracy Steiner, for her love and understanding during my graduate studies.

TABLE OF CONTENTS

	Page
List of Figures	vi
List of Tables	ix
CHAPTER 1 Introduction	1
1.1 Offshore Platform Conductor Strings	1
1.2 Literature Survey	3
1.2.1 Tubular Member Behavior	3
1.2.2 Conductor String Behavior	9
1.3 Scope of Research	13
1.4 Overview of Research	14
CHAPTER 2 Experimental Details	16
2.1 Stub Column Details	16
2.2 Tensile Coupon Details	17
2.3 Residual Stress Determination	18
2.4 Model Test Details	19
2.5 Full Size Test Details	21
2.5.1 Full Scale Specimen Details	21
2.5.2 Full Scale Test Set Up	24
2.5.3 Full Scale Test Procedures	29
CHAPTER 3 Experimental Results	31
3.1 General	31
3.2 Stub Column Results	33
3.3 Tensile Coupon Results	34
3.4 Residual Stress Determination	34
3.5 Model Test Results	37
3.5.1 Model Test 1	37
3.5.2 Model Test 2	42
3.6 Full Scale Test Results	42
3.6.1 Test FS-1	45
3.6.2 Test FS-2	46
3.6.3 Test FS-3	47
3.6.4 Test FS-4	49
3.6.5 Test FS-5	51
3.6.6 Test FS-6	53
3.6.7 Test FS-7	54

TABLE OF CONTENTS (continued)

	Page
CHAPTER 4 Interpretation of Results	55
4.1 Overview of Conductor String Design Methods	55
4.2 Evaluation of Model Tests	56
4.3 Outer Conductor Stability	58
4.4 Evaluation of Current Design Procedures	69
4.5 Inner Casing Test Data	72
4.6 Conductor String Behavior	77
CHAPTER 5 Summary, Conclusions and Recommendations	84
5.1 Summary	84
5.2 Conclusions	85
5.3 Recommendations	86
References	88
Appendix A	90
Appendix B	103
Appendix C	117
Appendix D	129
Appendix E	146
Appendix F	162
Appendix G	179
Appendix H	191
Vita	196

LIST OF FIGURES

Figure		Page
1.1	Detail of Typical Conductor String	2
1.2	Column Strength Curves	6
1.3	Strength Interaction Curves	8
2.1	Model Test Details	20
2.2	Full Scale Test Configuration (Vertical)	25
2.3	Full Scale Test Configuration (Horizontal)	26
2.4	Support Frame Detail	27
3.1	Conversion of Strains to Bending Moment	32
3.2	Stress-Strain Diagram: 6-5/8 in. Pipe	35
3.3	Stress-Strain Diagram: 3-1/2 in. Pipe	36
3.4	Results of Residual Stress Determination	38
3.5	Model Test 1 Axial Load vs. Tip Deflection	40
3.6	Model Test 1 Load vs. Bending Moment	41
3.7	Model Test 2 Axial Load vs. Tip Deflection	43
3.8	Model Test 2 Load vs. Bending Moment	44
3.9	FS-5 Local Buckle	52
4.1	Results vs. Existing Column Strength Criteria	61
4.2	Results vs. AISC(ASD) Stability Interaction Criteria	65
4.3	Results vs. Toma & Chen Stability Interaction Criteria	66
4.4	Results vs. AISC(LRFD) Stability Interaction Criteria	67
4.5	Results vs. AISI 76 Stability Interaction Criteria	68
4.6	Results vs. Stahl & Baur Interaction Curve Using the Manley Design Method	76
4.7	Conductor System with Eccentric Inner Casing	79
4.8	Conductor System with Eccentric Inner Casing	80
4.9	FS-1 Bending Moment over length of Outer Conductor	82
A.1	FS-1 Strain Gage Locations	92
A.2	FS-1 Outer Conductor Material Properties	93
A.3	FS-1 Inner Casing Material Properties	94
A.4	FS-1 Bending Moment at load point 26	95
A.5	FS-1 Axial Load vs. Outer Conductor Lateral Deflection	96
A.6	FS-1 Outer Conductor Midspan Chord Deflection	97
A.7	FS-1 Axial Load vs. Outer Conductor Bending Moment	98
A.8	FS-1 Axial Load vs. Outer Conductor Bending Moment	99
A.9	FS-1 Axial Load vs. Outer Conductor Bending Moment	100
A.10	FS-1 Axial Load vs. Outer Conductor Bending Moment	101
A.11	FS-1 Axial Load vs. Outer Conductor Bending Moment	102
B.1	FS-2 Strain Gage Locations	105
B.2	FS-2 Outer Conductor Material Properties	106
B.3	FS-2 Inner Casing Material Properties	107
B.4	FS-2 Bending Moment at load point 14	108
B.5	FS-2 Axial Load vs. Outer Conductor Lateral Deflection	109
B.6	FS-2 Outer Conductor Midspan Chord Deflection	110
B.7	FS-2 Axial Load vs. Outer Conductor Bending Moment	111

LIST OF FIGURES (continued)

Figure		Page
B.8	FS-2 Axial Load vs. Outer Conductor Bending Moment	112
B.9	FS-2 Axial Load vs. Outer Conductor Bending Moment	113
B.10	FS-2 Axial Load vs. Outer Conductor Bending Moment	114
B.11	FS-2 Axial Load vs. Outer Conductor Bending Moment	115
B.12	FS-2 Measured Axial Load in Inner Casing	116
C.1	FS-3 Strain Gage Locations	119
C.2	FS-3 Outer Conductor Material Properties	120
C.3	FS-3 Inner Casing Material Properties	121
C.4	FS-3 Bending Moment at load point 15	122
C.5	FS-3 Axial Load vs. Outer Conductor Lateral Deflection	123
C.6	FS-3 Outer Conductor Midspan Chord Deflection	124
C.7	FS-3 Axial Load vs. Outer Conductor Bending Moment	125
C.8	FS-3 Axial Load vs. Outer Conductor Bending Moment	126
C.9	FS-3 Axial Load vs. Outer Conductor Bending Moment	127
C.10	FS-3 Axial Load vs. Outer Conductor Bending Moment	128
D.1	FS-4 Strain Gage Locations	131
D.2	FS-4 Outer Conductor Material Properties	132
D.3	FS-4 Inner Casing Material Properties	133
D.4	FS-4 Bending Moment at load point 15	134
D.5	FS-4 Lateral Load vs. Outer Conductor Lat. Defl.	135
D.6	FS-4 Axial Load vs. Outer Conductor Lat. Defl.	136
D.7	FS-4 Outer Conductor Midspan Chord Defl.	137
D.8	FS-4 Outer Conductor Bending Moment at L = 1'-0"	138
D.9	FS-4 Outer Conductor Bending Moment at L = 3'-0"	139
D.10	FS-4 Outer Conductor Bending Moment at L = 4'-0"	140
D.11	FS-4 Outer Conductor Bending Moment at L = 5'-0"	141
D.12	FS-4 Outer Conductor Bending Moment at L = 7'-0"	142
D.13	FS-4 Outer Conductor Bending Moment at L = 9'-0"	143
D.14	FS-4 Outer Conductor Bending Moment at L = 11'-0"	144
D.15	FS-4 Measured Axial Load in Inner Casing	145
E.1	FS-5 Strain Gage Locations	148
E.2	FS-5 Outer Conductor Material Properties	149
E.3	FS-5 Inner Casing Material Properties	150
E.4	FS-5 Bending Moment at load point 12	151
E.5	FS-5 Lateral Load vs. Outer Conductor Lat. Defl.	152
E.6	FS-5 Axial Load vs. Outer Conductor Lat. Defl.	153
E.7	FS-5 Outer Conductor Midspan Chord Deflection	154
E.8	FS-5 Outer Conductor Bending Moment at L = 1'-0"	155
E.9	FS-5 Outer Conductor Bending Moment at L = 3'-0"	156
E.10	FS-5 Outer Conductor Bending Moment at L = 4'-0"	157
E.11	FS-5 Outer Conductor Bending Moment at L = 5'-0"	158
E.12	FS-5 Outer Conductor Bending Moment at L = 7'-0"	159
E.13	FS-5 Outer Conductor Bending Moment at L = 9'-0"	160
E.14	FS-5 Outer Conductor Bending Moment at L = 11'-0"	161

LIST OF FIGURES (continued)

Figure		Page
F.1	FS-6 Strain Gage Locations	164
F.2	FS-6 Outer Conductor Material Properties	165
F.3	FS-6 Inner Casing Material Properties	166
F.4	FS-6 Bending Moment at load point 13	167
F.5	FS-6 Lateral Load vs. Outer Conductor Lat. Defl.	168
F.6	FS-6 Axial Load vs. Outer Conductor Lat. Defl.	169
F.7	FS-6 Outer Conductor Midspan Chord Deflection	170
F.8	FS-6 Outer Conductor Bending Moment at L = 2'-0"	171
F.9	FS-6 Outer Conductor Bending Moment at L = 3'-0"	172
F.10	FS-6 Outer Conductor Bending Moment at L = 4'-0"	173
F.11	FS-6 Outer Conductor Bending Moment at L = 5'-0"	174
F.12	FS-6 Outer Conductor Bending Moment at L = 7'-0"	175
F.13	FS-6 Outer Conductor Bending Moment at L = 9'-0"	176
F.14	FS-6 Outer Conductor Bending Moment at L = 11'-0"	177
F.15	FS-6 Measured Axial Load in Inner Casing	178
G.1	FS-7 Strain Gage Locations	181
G.2	FS-7 Outer Conductor Material Properties	182
G.3	FS-7 Inner Casing Material Properties	183
G.4	FS-7 Bending Moment at load point 30	184
G.5	FS-7 Axial Load vs. Outer Conductor Bending Moment	185
G.6	FS-7 Axial Load vs. Outer Conductor Bending Moment	186
G.7	FS-7 Axial Load vs. Outer Conductor Bending Moment	187
G.8	FS-7 Axial Load vs. Outer Conductor Bending Moment	188
G.9	FS-7 Axial Load vs. Outer Conductor Bending Moment	189
G.10	FS-7 Measured Axial Load in Inner Casing	190

LIST OF TABLES

TABLE		PAGE
2.1	Outer Conductor Specimen Details	23
2.2	Test Matrix for Full Scale Tests	30
4.1	Model Test Predicted Failure Loads	57
4.2	Observed 1st Peak Load / Predicted Values	63
4.3	Observed Max. Load (From Load Cells) / Predicted Values	71
4.4	Observed Max. Load (From Strain Gages) / Predicted Values	75

LIST OF SYMBOLS

P = Axial Load

P_y = Yield axial load = $F_y(A)$

M = Bending moment

M_p = plastic moment = $Z(F_y)$

P_E = Euler buckling load = $[\pi^2 E/(KL/r)^2](A)$

P_{cr} = Buckling load

P_i = Internal axial load

P_e = External axial load

M_i = Internal bending moment

M_e = external bending moment

C_m = Coefficient defined in AISC specification

L = Length or distance from base

D = sweep (out-of-straightness)

e = annulus separating outer conductor and inner casing

KL = effective length

F_y = yield stress

CHAPTER I

INTRODUCTION

1.1 Offshore Platform Conductor Strings

Conductor strings in offshore oil platforms are the link between the platform and the oil reservoir. Initially, all of the drilling operations are performed through the conductor string and ultimately, the conductor string is the pathway through which oil is transported to the platform.

Typically, a conductor string will consist of as many as 5 or 6 concentric tubular steel members. The outermost tubular member, referred to as the outer conductor, extends from the platform deck into the borehole in the sea floor. The outer conductor usually will consist of a 20 or 26 in. diameter steel tube and is the first part of the conductor string to be set in place. Between the platform deck and the borehole in the sea floor, the outer conductor is laterally supported at various points along its length by conductor guide frames (Graff 1981).

Once the outer conductor is set in place, it serves as a foundation for the drilling operation. During drilling, other strings of steel tubes are placed inside of the outer conductor. These steel tubes extend deeper into the well and serve the purpose of protecting the well line. As the well deepens, its diameter gets smaller and the diameter of the protective casing is reduced. A deep well may require many strings of protective casing, each placed within the previous, with the last casing string extending the entire length of the well. A diagram of a conductor string is shown in Fig. 1.1.

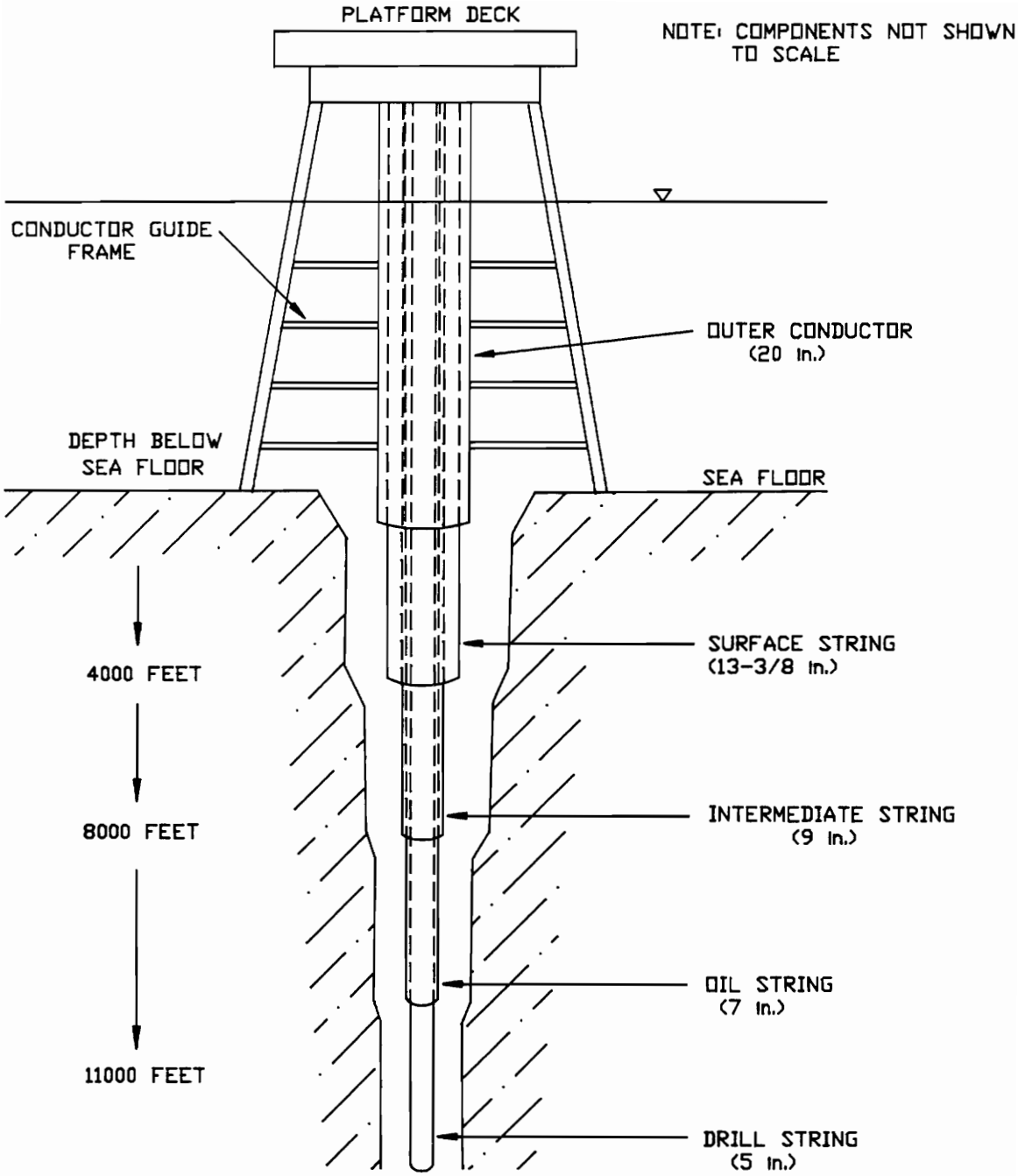

FIG. 1.1 DETAILS OF TYPICAL CONDUCTOR STRING

When a casing string is placed inside the outer conductor, it is supported at its top by simply hanging that string from the top of the outer conductor. This practice results in the inner casing string being in tension due to its own weight, while the outer conductor is put into compression by the weight of the inner casing. Each subsequent inner casing string is supported in a similar manner, simply hanging that casing string from the top of the tubes outside of it. The result is that the outer conductor can be subjected to tremendous axial compression from the self-weight of the inner casings as well as its own self-weight. Depending on the depth of the well, as much as 400 tons of casing can be used in a single well.

The conductor string must resist additional axial compression in the form of the blowout preventer stack (BOP). The BOP is placed on top of the outer conductor and controlls the pressure in the well while drilling operations are taking place. A typical BOP weighs in excess of 20 tons. Between the platform and the sea floor, lateral loading comes in the form of wave and current action on the conductor string.

1.2 Literature Survey

1.2.1 Tubular Member Behavior

Most current design criteria for structural members have been developed from the behavior of hot-rolled, wide-flanged shapes. With the increasing use of tubular members in offshore structures as well as multistory buildings, the engineer is faced with the problem of choosing a reliable design guide.

Unlike wide-flanged shapes, most tubular members are not hot-rolled, but are fabricated from a flat piece of plate material. This flat piece of plate is cold-rolled until opposite edges of the plate come together and a cylinder is formed. These two edges are then welded together longitudinally to complete the cylinder. Fabrication limitations restrict the length of plate that can be cold- rolled. But, long sections of pipe can be fabricated by connecting sections of pipe with circumferential welds.

This fabrication process induces both longitudinal and circumferential residual stresses in the tube. The cold-rolling of the flat plate and the circumferential welds that connect sections of pipe induce circumferential residual stresses that vary through the thickness of the pipe. Longitudinal welding of the pipe induces longitudinal residual stresses that vary around the circumference of the pipe. These residual stresses, combined with possible geometric imperfections from the fabrication process, affect the behavior of tubular members (Chen and Ross 1977).

Considerable research has been conducted on both the strength and stability of fabricated tubular columns. Chen and Ross (1976) conducted tests to determine the axial strength and behavior of cylindrical columns. Included in their test was a determination of the distribution of both longitudinal and circumferential residual stresses in the pipe. The longitudinal residual stresses were determined by the "slicing gage" technique. In this technique, the cross-section of the tubular member is divided into longitudinal strips. A Whittemore gage is then used to measure the strain in the strips as they are cut from the cross-section of the pipe. From the measured data, a distribution of longitudinal residual stresses around the cross-section of the pipe is developed. Chen and Ross also conducted tests

on ten fabricated tubular steel columns that varied from 18 ft. to 36 ft. in length. Results from these tests were compared to analytical column curves developed by the Column Research Council (CRC) and the American Institute of Steel Construction (AISC). The curves are referred to as the CRC-AISC curves. The comparison indicated that the CRC-AISC ultimate column strength equation gave reasonably accurate but slightly conservative predictions of the column strength.

Wagner et al (1976) conducted studies in which ultimate load capacities of tubular steel beam-columns were determined. In their research, a computer model was used to generate beam-column response. Of particular interest in their computer program was the inclusion of a longitudinal residual stress distribution. Moment curvature diagrams were developed for varying amounts of axial load; however, no interaction equations were derived.

Toma and Chen (1979) analyzed the behavior of fabricated tubular columns. A computer model that accounted for the effects of out-of-roundness, out-of-straightness, and residual stresses in the tube was developed. Verification of this computer model was made through comparisons with the experimental data collected in the ten full-scale tests reported by Chen and Ross (1976). Using this computer model, a column strength curve for tubular members was developed and compared with the CRC-AISC column design formulas. The computed column strength curve was found to be slightly below the CRC-AISC curve. This indicates that the CRC-AISC curve may tend to give slightly unconservative results for tubular columns. Also, the computer model showed that imperfections, such as out- of-straightness, can greatly influence the strength of the column. Modified column strength equations were developed from the results of the computer analysis.

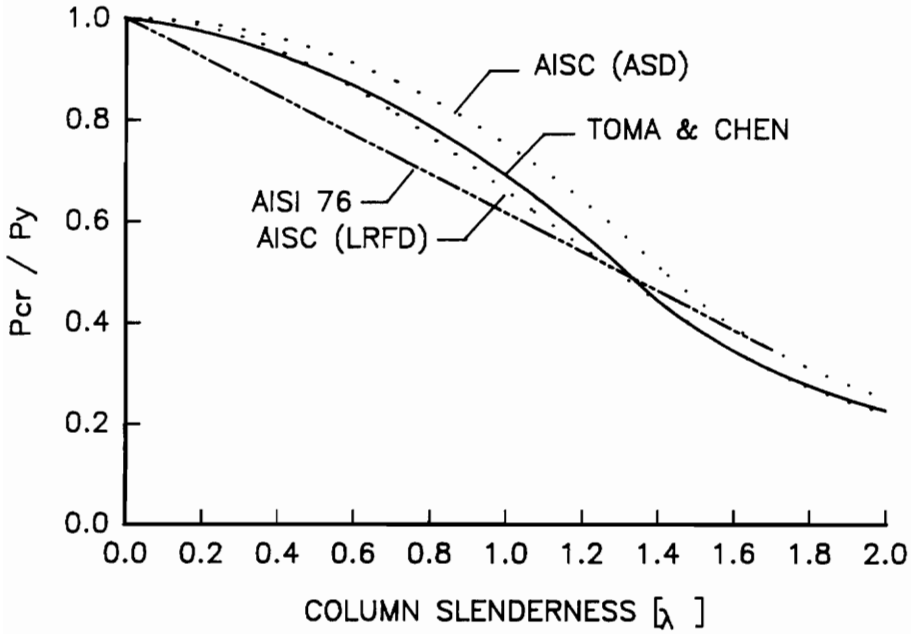

$$\lambda = \frac{KL}{r\pi}\sqrt{\frac{F_y}{E}}$$

FIG. 1.2 COLUMN STRENGTH CURVES

The study (Toma and Chen 1979) included an evaluation of the interaction between axial force, P/Py, and bending moment, M/Mp. This interaction curve was computed for a tubular cross-section. Residual stress effects, both circumferential and longitudinal, as well as cross-section out-of-roundness effects were incorporated in the analytical model. It was found that the out-of-roundness had very little effect on the strength of the cross-section. Further, the residual stresses had no effect whatsoever on the ultimate strength of the tubular cross-section. The strength interaction curve developed was verified through comparison with previous data. Comparison with strength interaction curves developed for wide-flanged shapes indicates that the computed curve tends to be slightly above that given by the AISC formula.

In 1988, the Structural Stability Research Council (SSRC), formerly the Column Research Council, addressed the topic of column strength curves in the Guide to Stability Design Criteria for Metal Structures (Galambos 1988). Recognizing the wide range of structural shapes that can be used as columns, the SSRC has developed a multiple column curve approach to design that takes into account the variables that effect column strength. Accordingly, the SSRC has developed a column strength curve for tubular columns. This curve is similar to the column curve used by AISC in the Load and Resistance Factor Design (LRFD) specification (1986).

One additional column strength curve to be considered for application to tubular columns is a curve denoted as AISI 76 (Stability 1982). This curve was developed specifically for tubular members and recognizes that the high residual stresses in tubular members greatly influence column strength. Although developed for square and rectangular cold-formed hollow sections, the curve

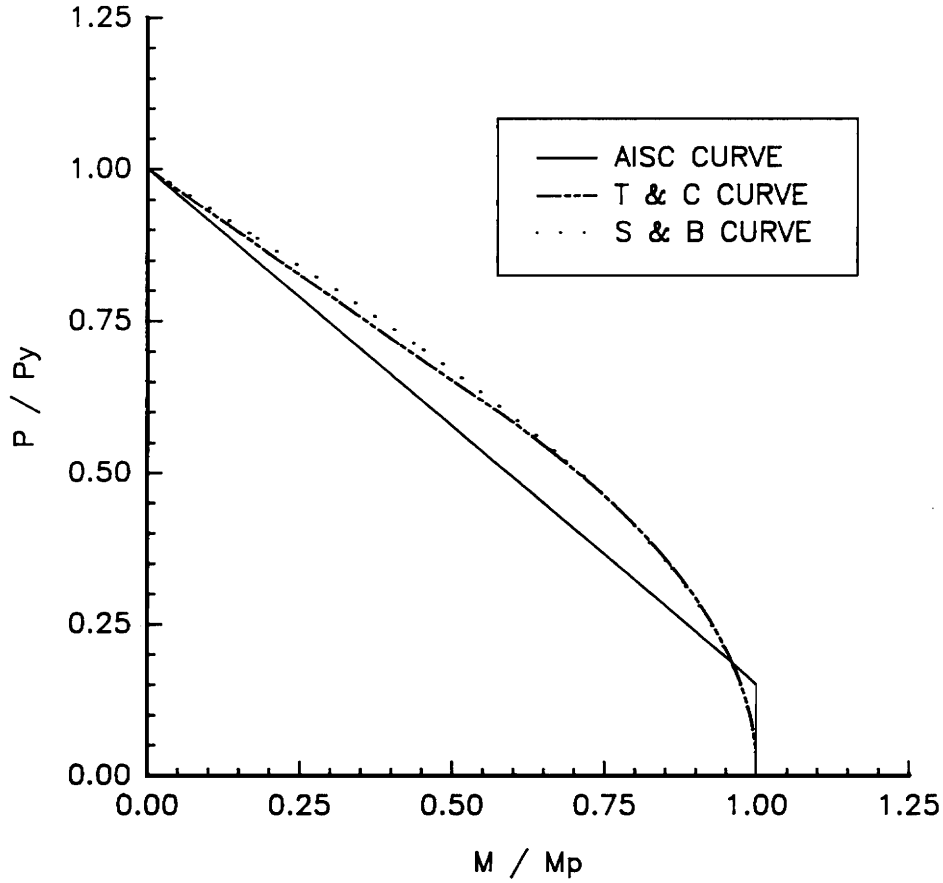

FIG. 1.3 STRENGTH INTERACTION CURVES

could be equally applicable to cold-formed cylindrical tubes. The AISI 76 curve lies considerably below the AISC-LRFD curve.

Column strength curves are shown in Fig. 1.2. Strength interaction curves are shown in Fig. 1.3.

1.2.2 Conductor String Behavior

Currently, the American Petroleum Institute (API) addresses the design of structural steel in the publication "API Recommended Practice for Planning, Designing, and Constructing Fixed Offshore Platforms" (API 1979). In this manual, API essentially adopts those equations given by AISC for structural steel design. Given this information, the design of the outer conductor requires that it meet the AISC requirements for cylindrical members subjected to axial compression and bending. The outer conductor is subjected to axial compression from the weight of the inner casings and the BOP stack, and bending from the lateral current and wave loading as well as eccentricity of the axial load. According to AISC plastic design, the outer conductor would need to satisfy the interaction equations for both strength and stability given by equations N4-2 and N4-3 in the AISC allowable stress design specification (Specification 1989). These equations are:

$$\frac{P}{P_{cr}} + \frac{C_m M}{(1-\frac{P}{P_E})M_M} \leq 1.0 \qquad \text{(Stability)} \qquad (1\text{-}1)$$

$$\frac{P}{P_y} + \frac{M}{1.18\ M_p} \leq 1.0 \quad M \leq M_P \qquad \text{(Strength)} \qquad (1\text{-}2)$$

Stahl and Baur (1980) addressed the design of offshore platform conductors. Design equations were developed for conductors. These equations were modified versions of the AISC equations. The modifications proposed by Stahl and Baur were based upon the fundamental principle that axial loads and bending moments on the conductor due to the weight of the inner casings produce no buckling tendencies in the outer conductor. Based upon this fundamental principle, Stahl and Baur modified Eq. (1-1) to the form shown below.

$$\frac{P_i}{P_y} + \frac{P_e}{P_{crm}} + \frac{C_M(M_i+M_e)}{(1-\frac{Pe}{P_E})M_p} \leq 1.0 \qquad (1\text{-}3)$$

The major difference between Eq. (1-3) and Eq. (1-1) is that the axial load term and the moment term are separated into internally applied terms (due to weight of inner casings) and externally applied terms (due to BOP stack and environmental loadings). In Eq. (1-3), the internally applied loads are represented by axial load, Pi, and bending moment, Mi (due to eccentricity of inner casings). Based on the premise that internally applied axial loads do not induce buckling, the internal axial load term is divided by a yield load, Py, rather than a buckling load, Pcr. Additionally, the critical buckling load for the external axial load has been modified to account for the fact that the pipe is at a higher level of stress due to the internal axial loads.

In their example design problem, Stahl and Baur analyzed the outer conductor and those inner casings that were in compression as a composite conductor system. For their example design, only the next inner casing was in compression. This next inner casing was grouted along its entire length to the outer conductor; however, only section properties for the steel alone were

computed. In the example, the authors showed how the modified design equations can result in significant financial savings (millions of dollars) for a typical platform. A computer model was used to verify the author's design method and an alternative interaction equation was presented for use with tubular members (Stahl and Baur 1983). This interaction equation is shown in Fig. 1.3.

In presenting their fundamental principle that internal casing string loads produce no buckling tendencies in the outer conductor, Stahl and Baur used energy considerations to show how these loads do not lead to buckling. This principle was also applied to the design of prestressed concrete compression members. Lin and Burns (1981) showed how prestressed elements in concrete can induce buckling in the concrete. It was shown that for the case where the prestressing element is in direct contact with the concrete all along its length, there will be no buckling tendencies due to the prestressing.

It was pointed out that if an annulus were present between the prestressing element and the concrete, the concrete would behave as a column. However, the column behavior is limited. The concrete in compression, due to the prestressing, will tend to deflect laterally. At first, this deflection will not affect the prestressing element. But should the concrete deflect enough to come into contact with the prestressing element, the two would begin to deflect together. Stahl and Baur account for this effect in their modified design equations by assuming the axial load is eccentric by an amount proportional to the annulus separating the outer conductor and the inner casing.

Manley (1985) developed a design procedure slightly different than the Stahl and Baur approach for the design of tieback conductor systems. Tieback conductor systems differ from standard conductor systems in that the conductors

are "tied into" existing wellheads on the sea floor. In these systems, additional moments (called tieback overshot moments) are imposed upon the system due to misalignment of the conductor and the wellhead. Manley found that it was inconsistent to consider a composite section only involving those strings that were in compression. Large discontinuities in the interaction ratio could result depending upon whether an internal casing string was either slightly in compression or slightly in tension.

Manley's revised design methodology calls for a strength check to be performed for each internal casing. While performing this strength check, a reserve moment capacity is computed for the internal casing string. This reserve moment capacity is then added to the moment capacity of the outer conductor when performing a stability check for the outer conductor. Stability of the inner casings is not an issue, according to Manley, because lateral support is provided by the outer conductor.

Manley restates the basic premise of Stahl and Baur that internal casing string loads do not induce buckling tendencies. However, his design differs from Stahl and Baur in that he considers the effect of all the inner casings on the strength and stability of the system (Manley 1985).

Imm and Stahl (1988) also addressed the design of platform conductors, specifically, the design of deepwater conductor systems. In their design procedure, the inner casings are considered when determining the effect of the external load applied at the top of the conductor. In deepwater conductor systems, the outer conductor may be long enough in relation to the inner casings to justify examining how the external load is distributed to both the outer conductor and the inner casings. In such cases, the application of the external

weight at the top of the conductor system can have the effect of reducing the internal axial load on the outer conductor.

Although not directly modeled after conductor strings, the lateral stability of piles in ungrouted jacket legs may offer some insight into conductor behavior. Flick and Green (1983) evaluate the strength of piles that are driven inside of lightly stressed jacket legs. If there is no annulus between the pile and the jacket leg, the capacity of the column would simply be the sum of the capacities of the pile and jacket leg. However, the presence of an annulus between the pile and the jacket leg weakens the system. Still, the jacket leg does provide some lateral resistance to the pile and serves some strengthening functions. Though not directly applicable to the behavior of conductor strings, some parallels may be drawn between the analysis processes for this system and the conductor string system.

Designers of offshore platform conductor strings are confronted with differing design procedures. Presently, no experimental research has been done to evaluate the varying design methods. It is the purpose of this study to evaluate the procedures experimentally and to assess their accuracy in predicting the ultimate capacity of offshore platform conductor strings.

1.3 Scope of Research

The purpose of this research is to study the behavior of conductor string systems. In the experimental phase of the research, an outer conductor is simulated with a 6-5/8 in. diameter pipe while an inner casing is modeled with a 3-1/2 in. diameter pipe. Axial compression is placed upon the outer conductor by tensioning the inner casing with hydraulic rams. Dead weight is used to load the

conductor system laterally to model the environmental loading on a conductor due to current and wave action. By varying the amount of lateral loading, the behavior of a conductor system under combined internal axial loads and external lateral loading is evaluated. Results are then used to evaluate the various design methods that exist for offshore platform conductor strings.

Also included in the research program are two small scale model conductor tests. In these tests, an outer conductor is modeled with a 1-1/4 in. diameter schedule 40 steel tube while an inner casing is modeled with a 1-1/8 in. diameter steel rod. A universal testing machine is used to tension the inner casing.

Additionally, an attempt is made to investigate the distribution of longitudinal residual stresses in the 6-5/8 in. diameter pipe used in the full scale tests. These results are then compared with other available research on the distribution of residual stresses. Finally, stress-strain relationships are found for both the 6-5/8 in. and the 3-1/2 in. diameter pipes used in the tests.

1.4 Overview of Research

In Chapter II of this report, the set ups and procedures used in the experimental research program are described. In addition to the full-scale tests, details are given for the stub column tests, tensile coupon tests, residual stress test and model conductor tests.

In Chapter III, the results of the experimental tests performed are given. Included in the test results are highlights of the tests as well as any observations that may be significant to the analysis of the results.

Chapter IV is an interpretation of the results of the experimental research. Here, the data collected from the experimental tests is evaluated and analyzed. Current design methods are compared with the observed test results. Conductor string behavior is analyzed and explained.

Finally, in Chapter V, the research project is summarized and conclusions and recommendations on the design of offshore platform conductor strings are presented. Possible future work in the area is also recommended.

In this study, those tests where the outer conductor is a 1-1/4 in. diameter schedule 40 steel tube are referred to as model tests. Tests where the outer conductor is a 6-5/8 in. diameter steel tube are referred to as full scale tests. In actuality, both of these are model conductor systems.

CHAPTER II

EXPERIMENTAL DETAILS

2.1 Stub Column Details

Stub column tests were performed on specimens cut from the 6-5/8 in. diameter pipes used to model the outer conductor in the full size tests. The purpose of these tests was to develop the compression stress-strain relationship for the pipe section. The behavior of welded steel tubing in compression is largely affected by the residual stresses in the pipe that result from the forming process. These residual stresses cause the stress-strain curve to exhibit a gradual yielding of the cross-section instead of a sharp yield plateau.

The specimens used in the stub column tests were cold-sawed from a stock piece. The length of the stub column was not less than 20 in. (3 x diameter), and not greater than 45.5 in. (20 x radius of gyration), as prescribed by SSRC (Galambos 1988). The actual lengths of the specimens tested varied, but all were between 20 and 22 in. in length. The ends of the columns were milled to be perpendicular to the longitudinal axis of the column.

Electrical resistance strain gages measured strains during testing. Four strain gages were used on each stub column and were placed at mid-height, at quarter points around the circumference of the pipe as recommended by the SSRC (Galambos 1988).

The stub column was tested in a 300 kip capacity universal testing machine. Bearing plates provided flat surfaces at each end of the stub column. The testing procedure called for the axial load on the stub column to be increased

in steps. Once the load on the column reached a preset value, the specimen was allowed time for both the strains and the load to stabilize. Readings were then taken and the load was increased until the next step was reached. The tests were carried out until the specimen failed by local buckling. The stress-strain curve was then developed by converting the axial load to a stress, and averaging the four strains recorded for each load point.

2.2 Tensile Coupon Details

Tensile coupon tests were performed on specimens cut from both the 6-5/8 in. diameter pipe and the 3-1/2 in. diameter pipe. The purpose of these tests was to develop the tensile stress-strain relationship for the material as well as to determine the modulus of elasticity, yield stress, and ultimate strength.

The coupons for the outer conductor were cold-sawed from a stock piece of tubing. Specifically, the specimens were cut from a location on the cross-section approximately 180 degrees from the longitudinally welded seam. This was done because the residual stresses in the tubing tend to decrease in magnitude as the distance from the seam is increased.

After the coupons were milled, any paint or rust that was on the metal was removed. The dimensions of the coupon were measured to the nearest 0.001 in. with dial calipers. It should be noted that these coupons were cut from the curved cross-section of the steel pipe. No attempt was made to flatten the coupons, but rather they were merely left as curved coupons. Given the geometry of the coupons, the cross-sectional area of the coupon was computed for conversion of loads to stresses. The effect of the curved surfaces of the coupons had minimal effect on the cross-sectional area of the coupon.

Strains were measured from a single electrical resistance strain gage which was mounted on the specimen at the center of the milled down region. The standard testing procedure was to have the specimen loaded at a constant load rate up to approximately 80% of its expected yield stress. The specimen was then loaded at a constant displacement rate that would enable data to be collected throughout the yield plateau. The test continued until ultimate strength was reached and the specimen fractured. A 0.2% offset was used to determine the yield stress of the material.

2.3 Residual Stress Determination

Tests were performed to determine the distribution of longitudinal residual stresses in the cross-section of the 6-5/8 in. diameter outer conductor pipe. The longitudinal welding of the seam in cold-formed steel tubing results in significant residual stresses.

The method of sectioning was used to measure these residual stresses. In this method, the cross-section of the pipe is divided into longitudinal sections. The strains in each section are then measured as that piece is cut from the cross-section.

A section of pipe to be tested was cold-sawed from stock and the ends were milled square. The cross-section of the pipe was then divided into 3/4 in. wide sections. Symmetry was exploited by laying out sections, beginning from the welded seam, for only half of the circumference of the pipe. Since the longitudinal residual stresses result from the welding of the tube, the residual stress distributions on either side of the weld should be nearly identical.

Strains were measured with electrical resistance strain gages that were mounted on both the inside surface and outside surface of each section. The use of electrical resistance strain gages enabled a much shorter section of pipe to be used than would have been necessary had the strains been determined by measuring a change in gage length. By mounting the strain gages on both surfaces of the section, the curvature of the section that resulted as it was cut from the cross-section was eliminated and the middle surface strain was determined. Assuming linear stress-strain behavior, the middle surface strain was then converted into a residual stress for that section of pipe. By plotting the results around the cross-section, the distribution of longitudinal residual stresses was determined.

2.4 Model Test Details

The main purpose of the model tests was to investigate what might be expected in the full-size tests. In addition, the model tests could be used to analyze conductor string behavior. A section of 1-1/4 in. schedule 40 steel pipe was used to model the outer conductor. This piece was cut from stock at a length of 3.5 ft. and the ends were milled square. The inner casing was modeled with a section of 1-1/8 in. A36 steel rod.

A schematic of the test set up can be seen in Fig. 2.1. The specimen was tested in a universal testing machine. Due to the configuration of the testing machine, the specimen was tested in an inverted position. The testing procedure was designed to simulate the axial compression of an outer conductor due to the weight of inner casing strings. As can be seen in Fig. 2.1, the 1-1/4 in. outer conductor is supported at its base by a base plate that rests on a fixed crosshead

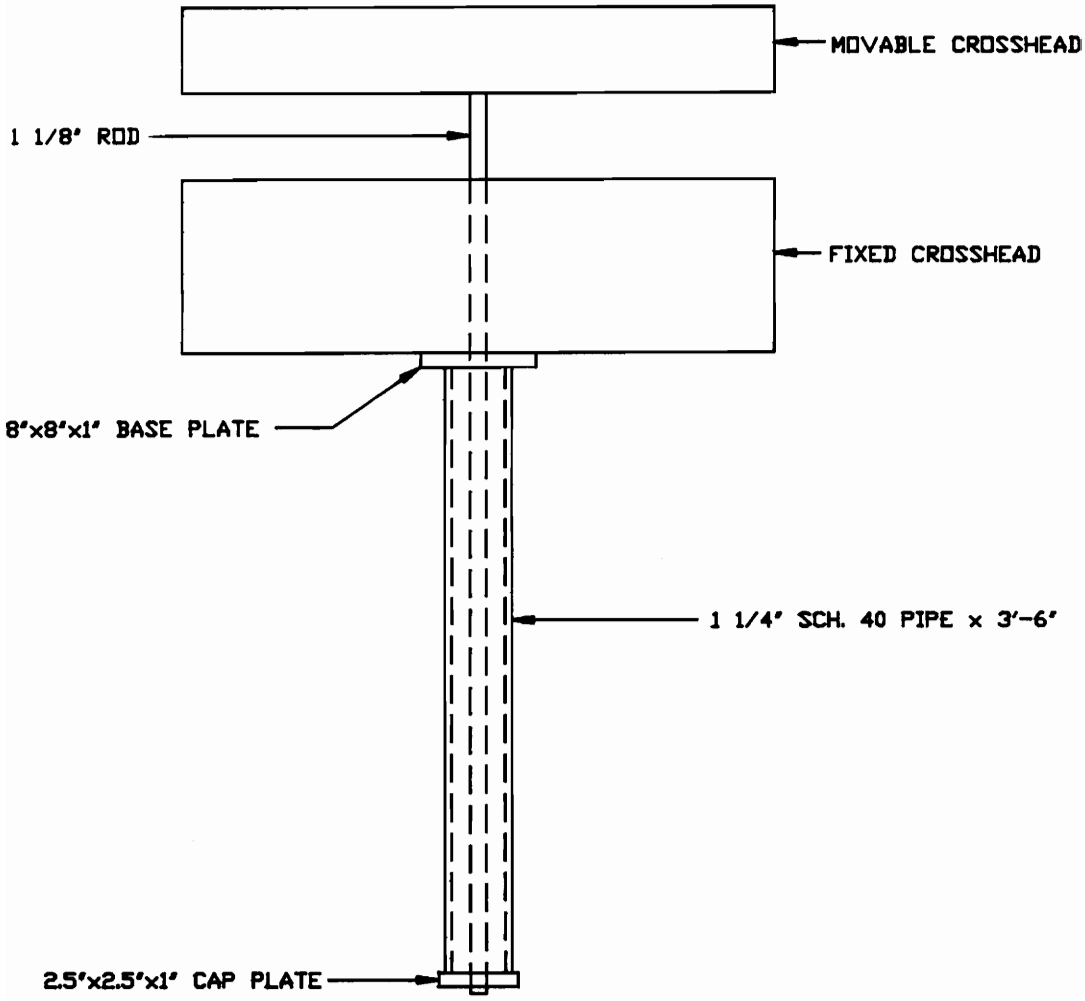

FIG. 2.1 MODEL TEST DETAILS

of the testing machine. The 1-1/8 in. inner casing is attached to a cap plate at the top of the outer conductor with a simple nut/washer connection. The inner casing then passes through the base plate and fixed crosshead and is gripped at the movable crosshead. By moving this crosshead upward, the inner casing is tensioned while the outer conductor is compressed with an equal load.

Electrical resistance strain gages were used to measure strains during the experiment. Specifically, 12 strain gages were placed on the outer conductor, four at each quarter point of the pipe at 90 degree intervals around the cross-section. The vertical and horizontal deflections of the tip of the outer conductor were measured with displacement transducers.

The testing procedure in model test 1 called for load values of 7 and then 13 kips to be placed on the system. The load then increased in one kip increments up to a maximum value of 31 kips. In model test 2, load was applied in one kip increments up to approximately 24 kips. At this point, smaller increments of load were applied until the maximum value of 32.05 kips was reached. In both tests, the system was allowed time to stabilize at each load point. Data readings were taken after the strains and displacements had stabilized.

2.5 Full Size Test Details

2.5.1 Full Size Specimen Details

The specimens used to model the outer conductor in the full scale tests were 6-5/8 in. A53 Grade B-E steel pipe with a wall thickness of 0.188 in. The specified minimum yield stress of this pipe is 35 ksi. Specimens were cut from stock pieces of approximately 42 ft. in length. The lengths of the specimens

varied, but in general, two specimens could be cut from a single stock section. After the specimen was cut, the ends were milled square. Data measured for each outer conductor specimen included both initial out-of-straightness and out-of-roundness of the tubular, length of the section, and the material's stress-strain relationship in both tension and compression.

The specimens used to model the inner casing in the full scale tests were 3-1/2 in. grade X80 steel pipe with a wall thickness of 0.250 in. The specified minimum yield stress for this pipe was 80 ksi. It should be noted that this pipe was not fabricated steel tubing, but was hot-rolled pipe. The stock pieces for this particular pipe varied in length between approximately 25 ft. and 33 ft. Accordingly, only one test specimen was used from each stock piece. The specimens came with tapered threads and couplings at each end of the pipe. For reasons that will be discussed later, one end of the test specimen was always a threaded end. The inner casing specimens to be tested were cold-sawed from the stock piece. Tensile coupons were also cut from stock for determination of the stress-strain relationship.

After the outer conductor specimens were cut from stock and the out-of-straightness and out-of-roundness measurements were taken, strain gages were mounted on the specimen. The number of strain gages applied and their locations on the specimen varied between tests (see appendices). However, some general comments about the strain gages can be made. Four strain gages were applied at each chosen cross-section of the specimen. These four strain gages were placed at quarter points around the circumference of the pipe. By applying four gages at each cross-section, the forces and moments acting at a given location along the length of the specimen could be determined.

Table 2.1 Outer Conductor Specimen Details

Test	Length (ft.)	F_y (ksi)	D/L*
FS-1	15.17	46.3	1/1625
FS-2	15.00	48.1	1/643
FS-3	13.92	46.3	1/2650
FS-4	13.00	48.1	1/1130
FS-5	13.00	47.9	1/1182
FS-6	13.00	47.9	1/1575
FS-7	16.00	46.0	1/1401

*Initial out-of-straightness

The process of mounting strain gages on the inner casing differed from that of the outer conductor. To protect the strain gage's lead wires on the inner casing, small holes were drilled in the inner casing and the wires were run inside the pipe. This process was used for all tests except FS-1, where the wires were simply placed along the outside of the inner casing.

General information about the outer conductor test specimens is given in Table 2.1. Refer to the appendices for more specific data regarding the locations of strain gages.

2.5.2 Full Scale Test Set Up

The testing configuration for the full scale tests was designed to place axial compression on the outer conductor pipe by tensioning the inner casing. For tests FS-1 through FS-3, the outer conductor was tested in a vertical position (see Fig. 2.2). For tests FS-4 through FS-7, the outer conductor was tested in a horizontal position (see Fig. 2.3).

In all tests, the same support frame was used to support the outer conductor (see Fig. 2.4). This support frame allowed the 3-1/2 in. inner casing to pass through the bottom of the frame. The outer conductor was anchored in the support frame by two plates. The first was a 9"x9"x1/2" base plate that was welded to the base of the outer conductor and bolted to the bottom plate of the test frame. The second plate used to anchor the outer conductor in the support frame was a 20"x18"x1/2" support plate that was welded to the side of the outer conductor and bolted to the top plate of the support frame.

The inner casing pipe passed through holes in the support frame and out the bottom. The inner casing was connected to a short fabricated loading beam

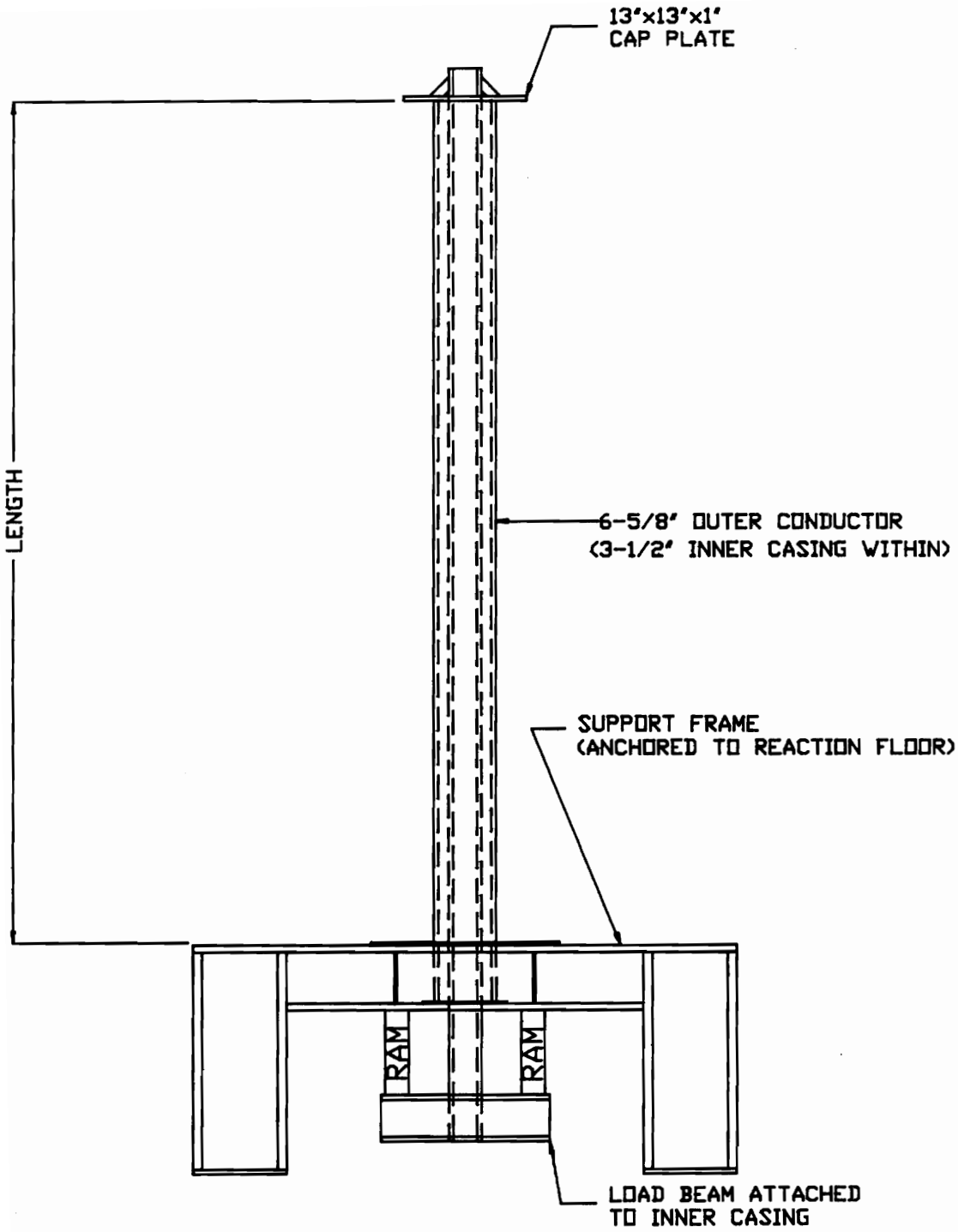

FIG. 2.2 FULL SCALE TEST CONFIGURATION (VERTICAL POSITION)

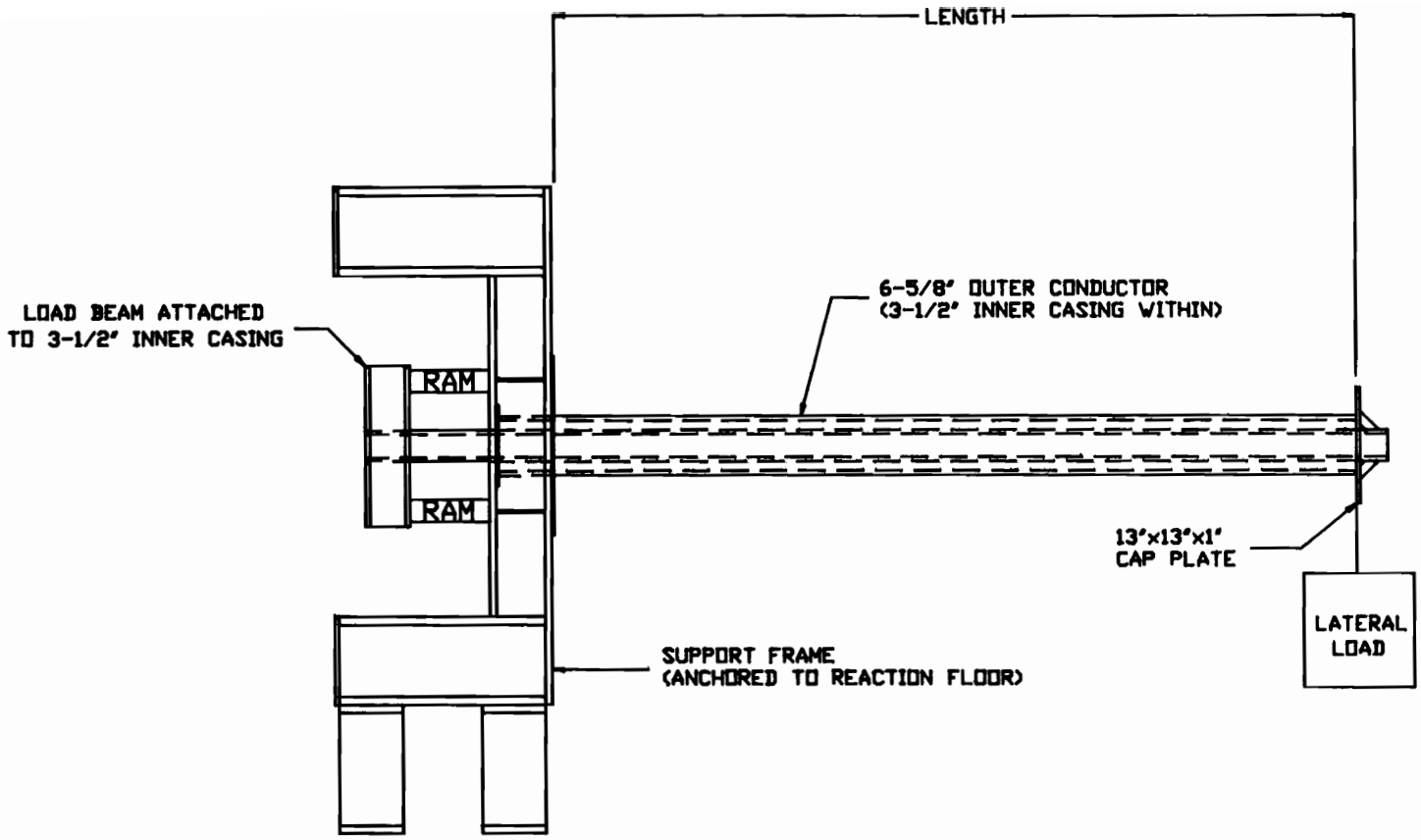

FIG. 2.3 FULL SCALE TEST CONFIGURATION (HORIZONTAL POSITION)

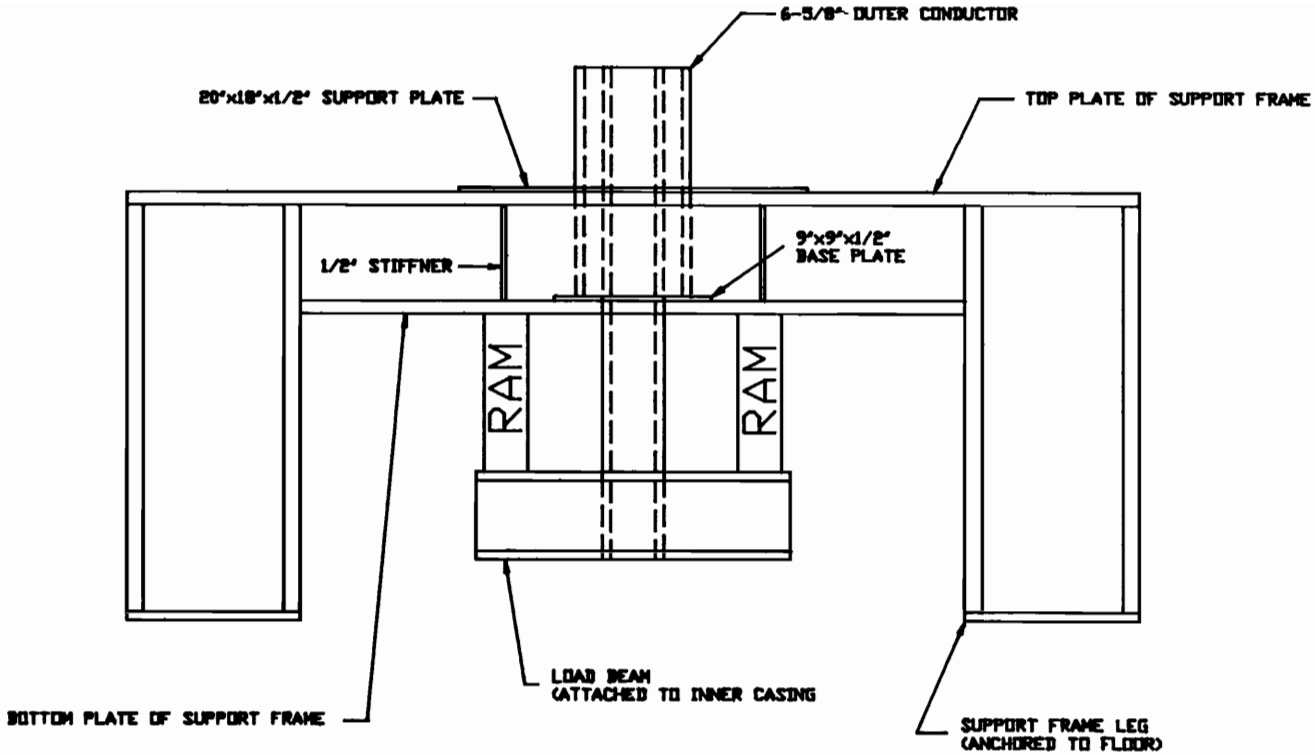

FIG. 2.4 SUPPORT FRAME DETAIL

by means of the threads on the inner casing and a coupling. This set up enabled the load beam to be reused from test to test. At the opposite end, the inner casing was welded to a cap plate which was, in turn, welded to the top of the outer conductor. Except for FS-3, the inner casing was centered in the outer conductor at the cap plate. In all tests, the inner casing was centered in the outer conductor at the base of the outer conductor by virtue of the location of the holes in the support frame.

The inner casing was tensioned by two 120 kip capacity hydraulic rams that were connected to a single hand operated pump. These rams, each connected in series with a 500 kip load cell, were placed between the load beam at the base of the inner casing and the bottom plate of the load frame. By pushing down on the load beam, the inner casing was tensioned and, hence, the outer conductor was put into compression.

Those tests in which lateral loading was applied to the outer conductor were all conducted in the horizontal position (see Fig. 2.3). In these tests, the outer conductor (and inner casing) were simply cantilevered out from the support frame. The lateral loading was placed on the system by hanging a dead weight from the cap plate of the outer conductor. Test FS-7 was conducted in the horizontal position but no lateral loading was applied to the system. In addition, test FS-7 differed from the other horizontal tests because the outer conductor was a propped cantilever.

In all full scale tests, most of the data was collected using a micro-computer based data acquisition system. All strain gages, displacement transducers and load cells were monitored through the data acquisition system. Typically, the lateral deflection of the outer conductor was measured at mid length

and at the tip by linear voltage displacement transducers. Dial gages were also used to measure the movement of the outer conductor near the support frame.

2.5.3 Full Scale Test Procedures

The testing procedure for the full scale tests began by configuring the data acquisition system. Critical values were monitored continuously. In those tests where only axial loads were applied (FS-1, FS-2, FS-3, FS-7), a small amount of load (less than 5 kips) was placed on the pipe, and then released, to seat the specimen and check instrumentation.

In those tests in which lateral load was placed on the structure (FS-4, FS-5, FS-6), the lateral loads were imposed on the conductor as testing began, prior to any axial loading. The lateral weights were applied incrementally and time was allowed for the strain and displacements to stabilize. The amount of lateral loading applied varied between tests. By doing this, various interaction curves for combined axial compression and bending could be evaluated or developed. After the designated amount of lateral weight had been applied, the axial loading of the outer conductor began and was continued until failure.

In general, axial loads were increased in 10 kip increments initially. These increments were made smaller as the predicted failure load of the conductor was approached. Displacement increments were used as warranted. Quick analytical checks on the specimen's behavior were done during testing to check instrumentation and loading procedures. In all tests, time was allowed for the loads, strains and displacements to stabilize before the data was recorded. Failure was determined by either local buckling or excessive deflections.

The parameters for each full scale test are shown in Table 2.2.

Table 2.2 Test Matrix for Full-Scale Tests

Test	Length (ft.)	Position	Applied Lateral Loading	Lateral (lb.)	$M_{applied}/M_p$ (outer cond.)
FS-1	15.17	Vertical	No	--	--
FS-2	15.00	Vertical	No	--	--
FS-3	13.92	Vertical	No	--	--
FS-4	13.00	Horizontal*	Yes	920	0.44
FS-5	13.00	Horizontal*	Yes	1720	0.78
FS-6	13.00	Horizontal*	Yes	481	0.26
FS-7	16.00	Horizontal**	No	--	--

*Simple Cantilever
**Propped Cantilever

CHAPTER III

EXPERIMENTAL RESULTS

3.1 General

The results of the stub column and tensile coupon tests are found in graphical form in the appendices. For these tests, a stress-strain relationship was derived for the material. In addition, a 0.2% offset was used to determine the yield stress for the material from the tensile coupon tests.

Strains measured at a given cross-section in the model tests are used to determine the bending moment acting on the cross-section at a given load point. The process of converting the raw strains into a bending moment is described in Fig. 3.1. The same procedure is used to determine the bending moments on the outer conductor in the full scale tests as well. While this conversion can only be expected to give an approximation of the actual bending moment, the results appear to be quite good. In fact, when lateral load was applied to the cantilever test configuration in FS-4, FS-5, and FS-6, the method produced bending moments that correlated very closely with expected results. However, it should be noted that the assumptions made in converting the strains to a bending moment are based on linear theory. They can, therefore, be expected to give less reliable results as significant amounts of yielding take place in the conductor.

The data gathered in the full scale tests is presented in detail in the appendices. Data collected includes applied loads, lateral deflections of the outer conductor at certain key points and strains at several cross-sections. Computed bending moments are also presented at various cross-sections of the pipe.

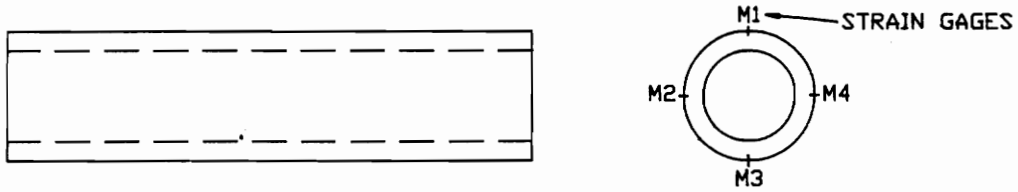

1) For a given load point, convert measured strains (M1 - M4) into stresses (S1 - S4) using material's stress-strain relationship

2) Average the 4 stresses to obtain the stress due to axial load

$$(S1+S2+S3+S4)/4 = S\ axial$$

3) Compute the stress at each point due to bending by taking the difference between each measured stress and the average stress

$$B1 = S1 - S(axial)$$
$$B2 = S2 - S(axial)$$
$$B3 = S3 - S(axial)$$
$$B4 = S4 - S(axial)$$

4) Determine the maximum stress due to bending at the cross section by

$$\sqrt{\left[\frac{(B1-B3)}{2}\right]^2 + \left[\frac{(B2-B4)}{2}\right]^2} = S(max)$$

5) Convert S(max) to bending moment by

$$S(max) = Mc/I$$

Figure 3.1 Conversion of Measured Strains to Bending Moment

Some of the terminology used in the explanation of the test results should be defined. The term unstable is often used in reference to the outer conductor. In this report, unstable simply means that the compression member being considered cannot sustain any additional axial compression and would collapse under a service load. Stability, as defined by the SSRC (Galambos 1988), is "the capacity of a compression member or element to remain in position and support load, even if forced slightly out of line or position by an added lateral force." The buckling load is the load at which a compression member would collapse if in service. For the compression members tested in this research, the member is said to have buckled laterally if it passes from a stable state to an unstable state.

By imposing axial compression with hydraulic rams, the unstable path of a column can be evaluated. Had the system been loaded with dead weight, instability of the system would result in collapse.

The term excessive deflections, or large deflections, is often stated as a reason for the termination of a test. These terms simply mean that the deflections of the specimen have either reached a limit set by the test fixtures, or they have reached a level where the test did not need to be continued to assess the strength of the system. These terms in no way refer to a system's state of stability.

3.2 Stub Column Results

The results of the stub column tests performed on the 6-5/8 in. outer conductor pipe show that the pipe exhibited a gradual yielding of the cross-section. This is directly attributed to the residual stresses in the pipe that are induced by the welding of the longitudinal seam. Results of a typical stub column

test are given in Fig. 3.2(A). The ultimate mode of failure for the stub column was local buckling. The local buckling occurred at axial loads that ranged between 201 kips and 210 kips.

3.3 Tensile Coupon Results

The results of tensile coupon tests of the 6-5/8 in. outer conductor were used to obtain the yield strength of the outer conductor. A typical stress-strain relationship for the outer conductor in tension is given in Fig. 3.2(B). Again, the material did not exhibit a well defined yield point, but rather yielded gradually. A 0.2% offset was used to define the yield strength of the outer conductor. Observed values of the modulus of elasticity ranged from 29540 ksi to 32820 ksi.

Tensile coupon tests on the 3-1/2 in. inner casing showed that it had a much sharper yield point than the 6-5/8 in. outer conductor. A typical stress-strain diagram for an inner casing tensile coupon is given in Fig. 3.3. The sharp yield point observed with the 3-1/2 in. pipe was expected since the pipe was hot-rolled, seamless pipe, and thus had very low residual stresses.

3.4 Residual Stress Determination

To determine residual stress patterns, strain gages were mounted on both the inside and outside surfaces of a section of 6-5/8 in. pipe. The gages were placed at these locations to determine the middle surface strain of a section as it was cut free from the pipe. However, those strain gages on the inside surface did not give consistent, reliable data. Therefore, only those strain gages on the outside surface were considered in the residual stress determination.

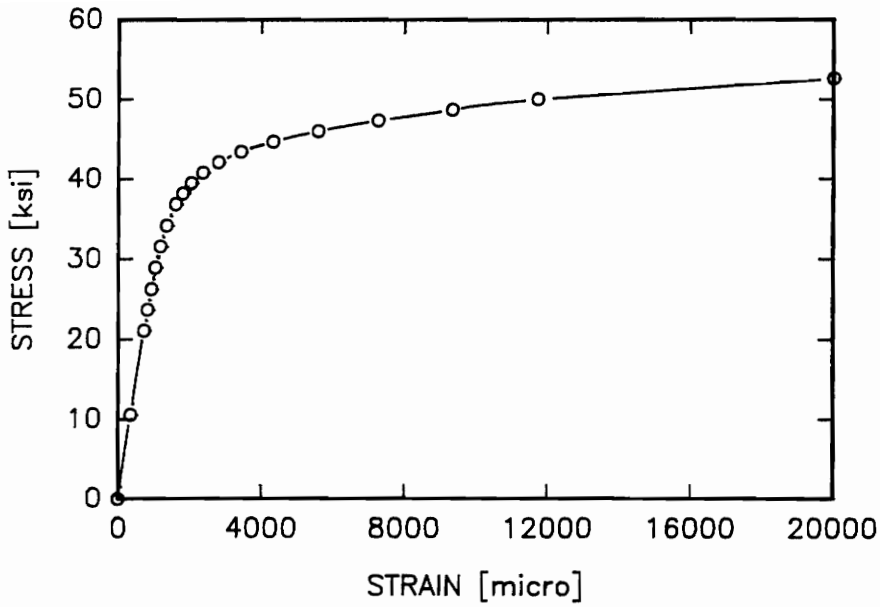

A) STUB COLUMN RESULTS

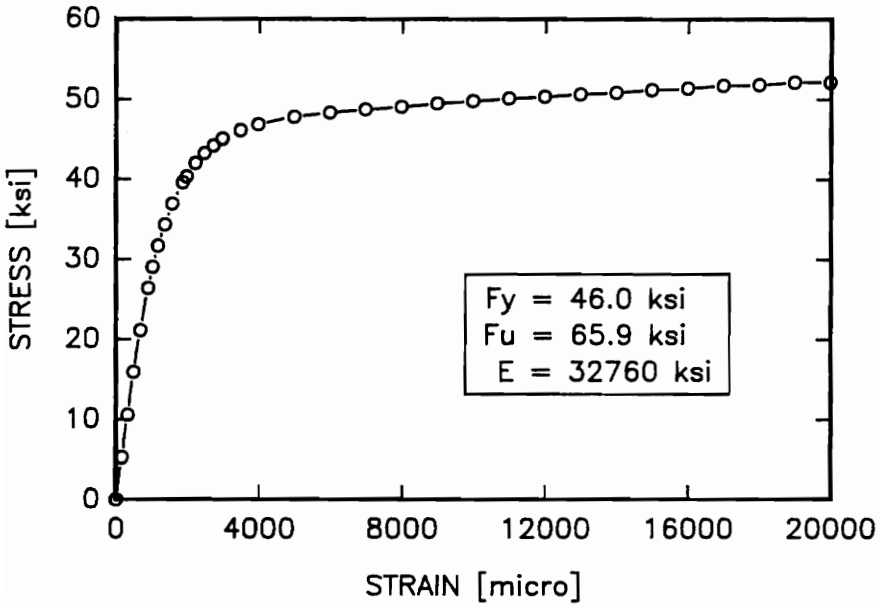

B) TENSILE COUPON RESULTS

FIG. 3.2 TYPICAL STRESS–STRAIN DIAGRAM: 6–5/8" PIPE

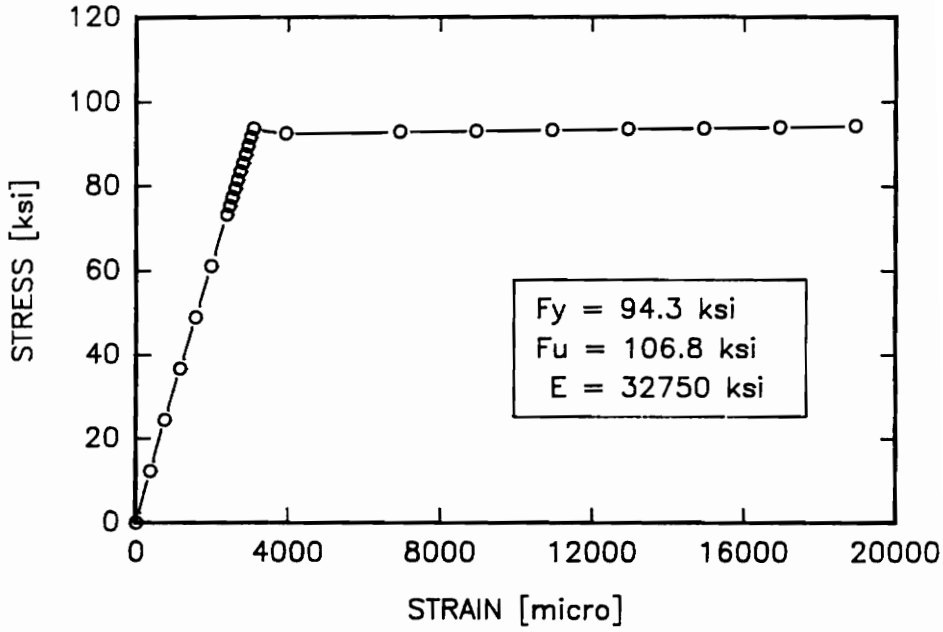

FIG. 3.3 TYPICAL STRESS–STRAIN DIAGRAM: 3–1/2" PIPE

Assuming that the curvature of each section is identical as it is cut from the pipe, the middle surface strain for each section is determined based on the fact that the net longitudinal residual stress on the pipe as a whole must equal zero. Therefore, the middle surface strain is determined by 1) finding the average strain on the outside surface of the sections cut from the pipe and then 2) finding the difference between each individual section and the average strain of all the sections. Strains are then converted to stresses based on the modulus of elasticity for that section of pipe. The results of the residual stress determination test are plotted against data from previous research in Fig. 3.4.

3.5 Model Test Results

Results of model test 1 are shown in Fig. 3.5 and Fig. 3.6. Model test 2 results can be seen in Fig. 3.7 and Fig. 3.8.

3.5.1 Model Test 1

The testing procedure for model test 1 called for axial load to be put on the model conductor system in increments to a maximum load of 31 kips. The model conductor deflected very little to an axial load of approximately 22 kips. At this point, the tip of the outer conductor began to deflect laterally in increasing amounts as shown in Fig. 3.5. However, at no point did the system appear to be unstable. The system continued to hold increasing axial load to a maximum value of 31 kips. The maximum observed lateral deflection of the tip of the outer conductor was 2.28 in. The maximum observed vertical deflection of the tip of the outer conductor was 0.68 in.

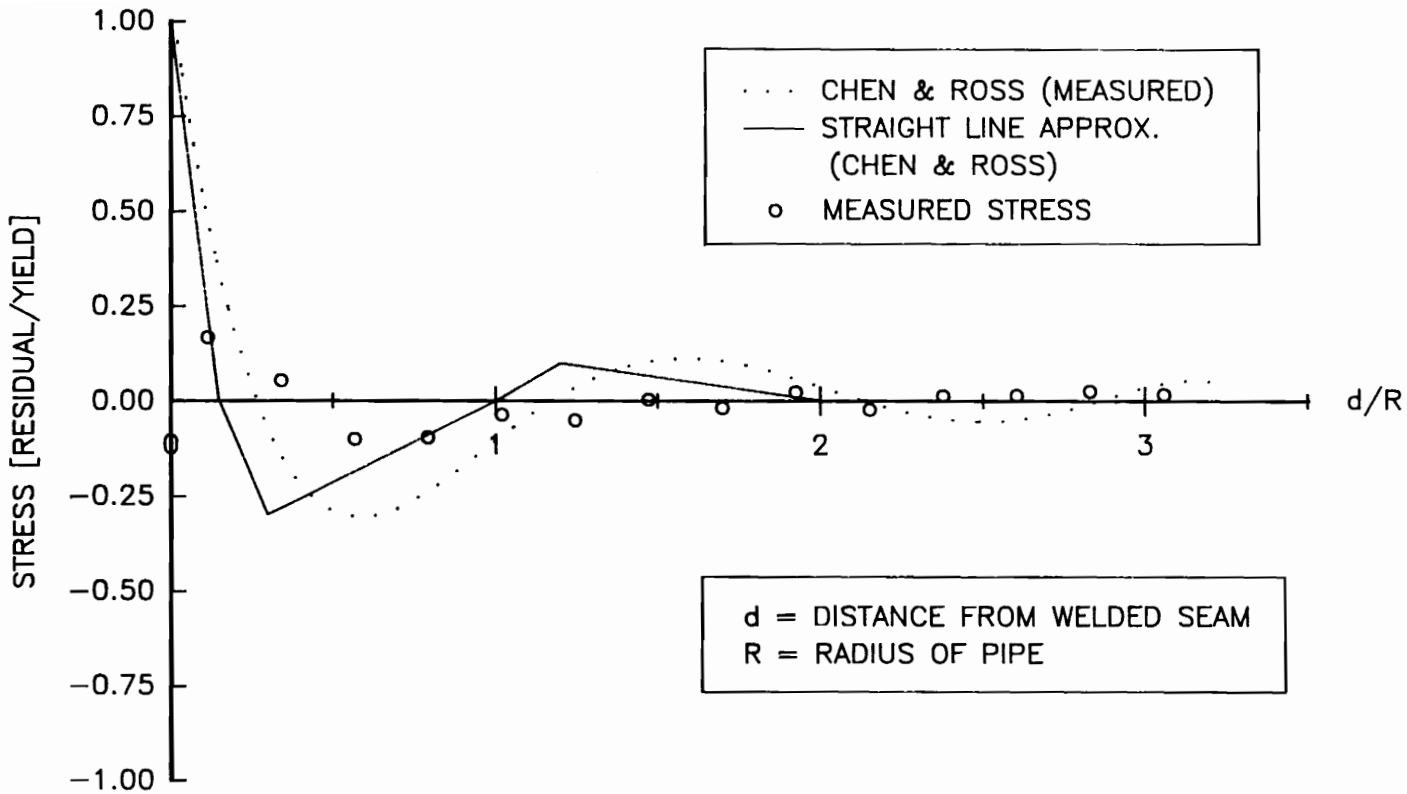

FIG. 3.4 RESULTS OF RESIDUAL STRESS DETERMINATION TEST

As seen in Fig. 3.6, some bending due to eccentricity of the axial load was present from the beginning of the test. Initially, the bending moment on the outer conductor increased linearly with the applied axial load. This suggests that the axial load was eccentric by some distance. The dotted line in Fig. 3.6 represents the bending moment resulting from the axial load being 0.128 in. eccentric. This distance (0.128 in.) is the annulus that exists between the 1-1/4 in. schedule 40 outer conductor pipe and the 1-1/8 in. inner casing rod. Because the bending moment, computed from measured strains, exceeds the value 0.128P at some points, the axial load must be eccentric by a distance greater than 0.128 in. Various factors could explain such behavior. Most likely, the eccentricity of the axial load was caused by the nut and washer of the inner rod not sitting flush on the cap plate of the outer conductor.

As seen in Fig. 3.6, the measured bending moments on the outer conductor began to decrease at an axial load of 22 kips, the same time at which the tip of the outer conductor began to deflect laterally in increasing amounts. This is exactly the opposite of what would be expected in a traditional externally loaded column. With a traditional column, increased deflections result in increased bending moments. However in the model test system, the inner rod provides lateral support to the outer conductor. This lateral support helps to stabilize the outer conductor.

After the outer conductor pipe had deflected a sufficient distance laterally, the outer conductor came into contact with the inner casing rod. The rod then provided some resistance to further lateral displacement of the outer conductor. Any further lateral displacement necessitated the deflection of both the inner casing and the outer conductor.

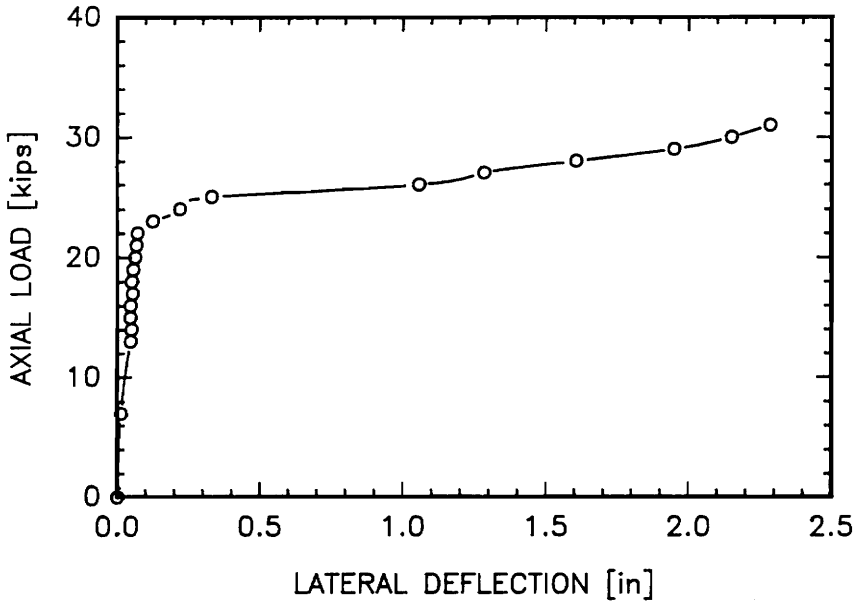

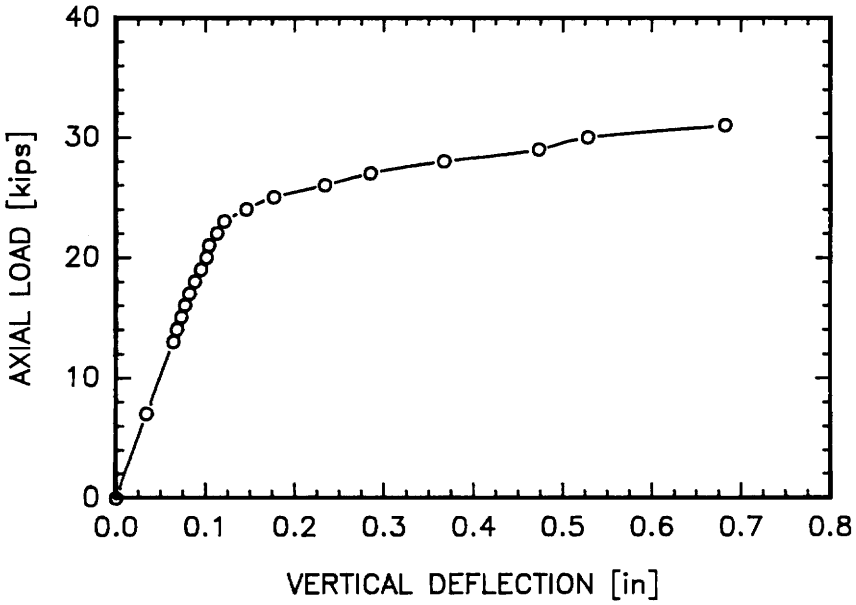

FIG. 3.5 MODEL TEST 1 AXIAL LOAD VS. TIP DEFLECTION

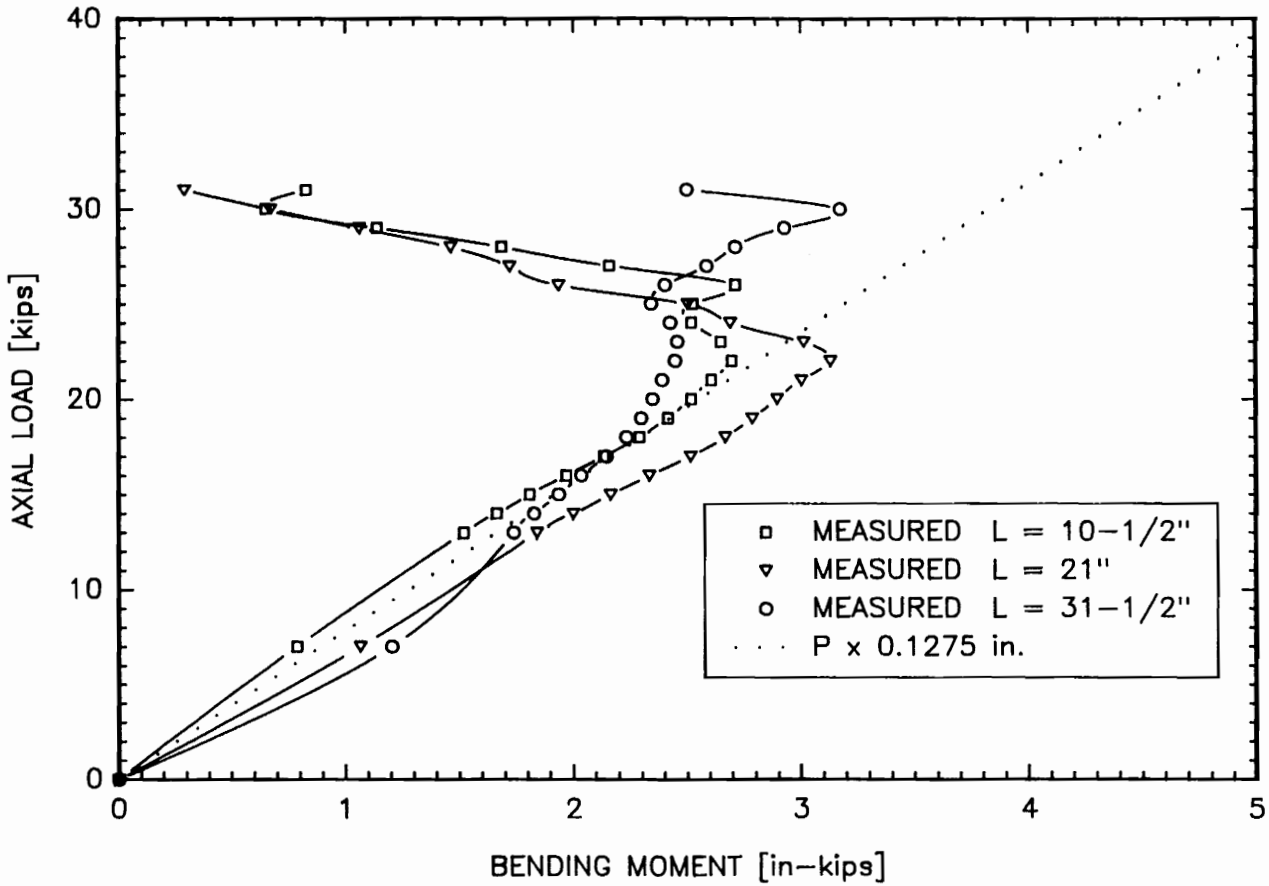

FIG. 3.6 MODEL TEST 1 LOAD VS. BENDING MOMENT

3.5.2 Model Test 2

In model test 2, load was placed on the model conductor system in one kip increments to approximately 24 kips. Within this range, the response of the conductor was essentially linear. That is, both the vertical and lateral deflection of the conductor increased linearly with the axial load (see Fig. 3.7). Within this range of the test, the computed bending moment in the outer conductor also increased roughly linearly with the axial load (see Fig. 3.8).

However, after reaching an axial load of 24.52 kips at load point 26, the system began to deflect laterally and the axial load on the system began to drop. This indicates that the outer conductor buckled laterally. As the axial load on the conductor dropped after load point 26, the computed bending moments in the outer conductor increased sharply. This is further evidence that the outer conductor buckled laterally.

After the axial load dropped to 23.78 kips, the conductor system began to hold increasing amounts of axial load. However, the conductor continued to deflect laterally. The computed bending moments in the outer conductor decreased in this part of the test. The system continued to hold axial load until the test was stopped at a load of 32.05 kips.

3.6 Full Scale Test Results

Detailed results for the full scale tests are found in the appendices. Included in these appendices is information such as:

- material stress-strain information
- load vs. deflection plots
- load vs. computed bending moment plots

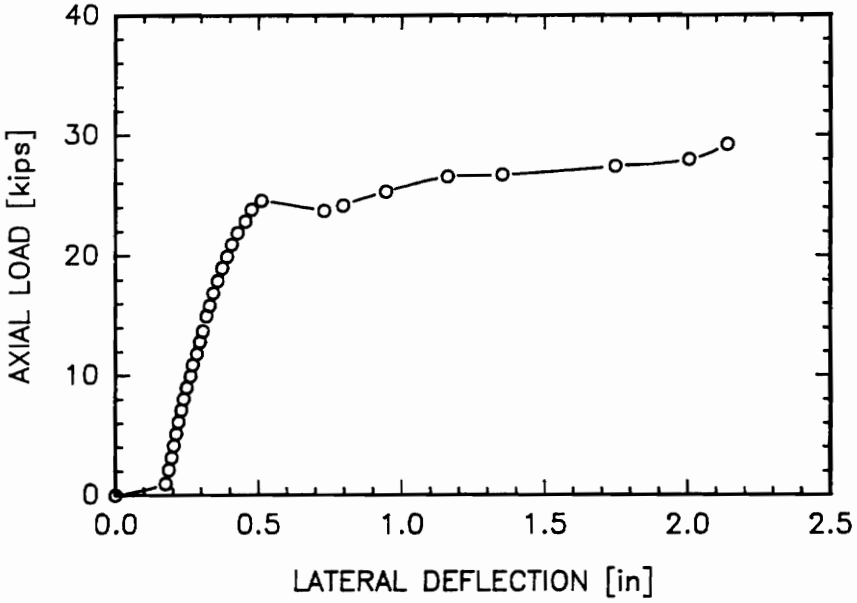

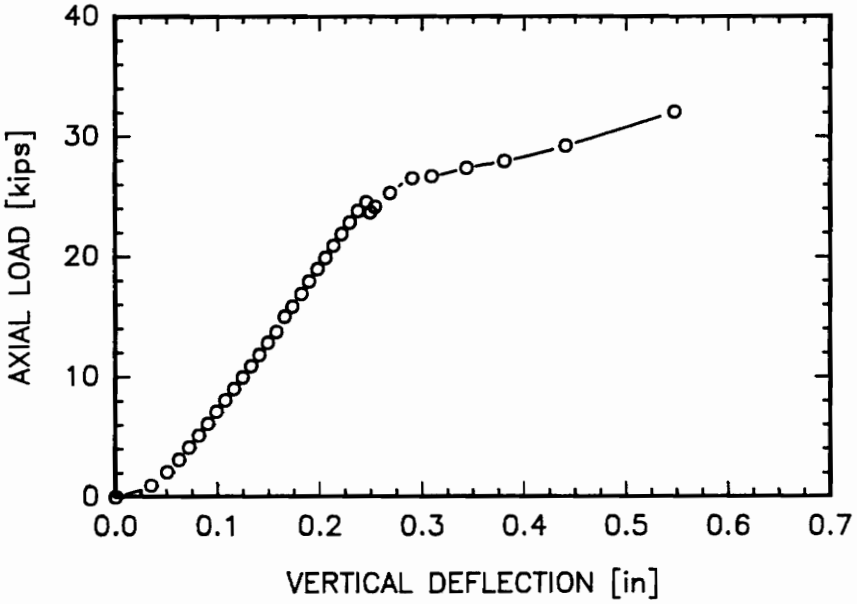

FIG. 3.7 MODEL TEST 2 AXIAL LOAD VS. TIP DEFLECTION

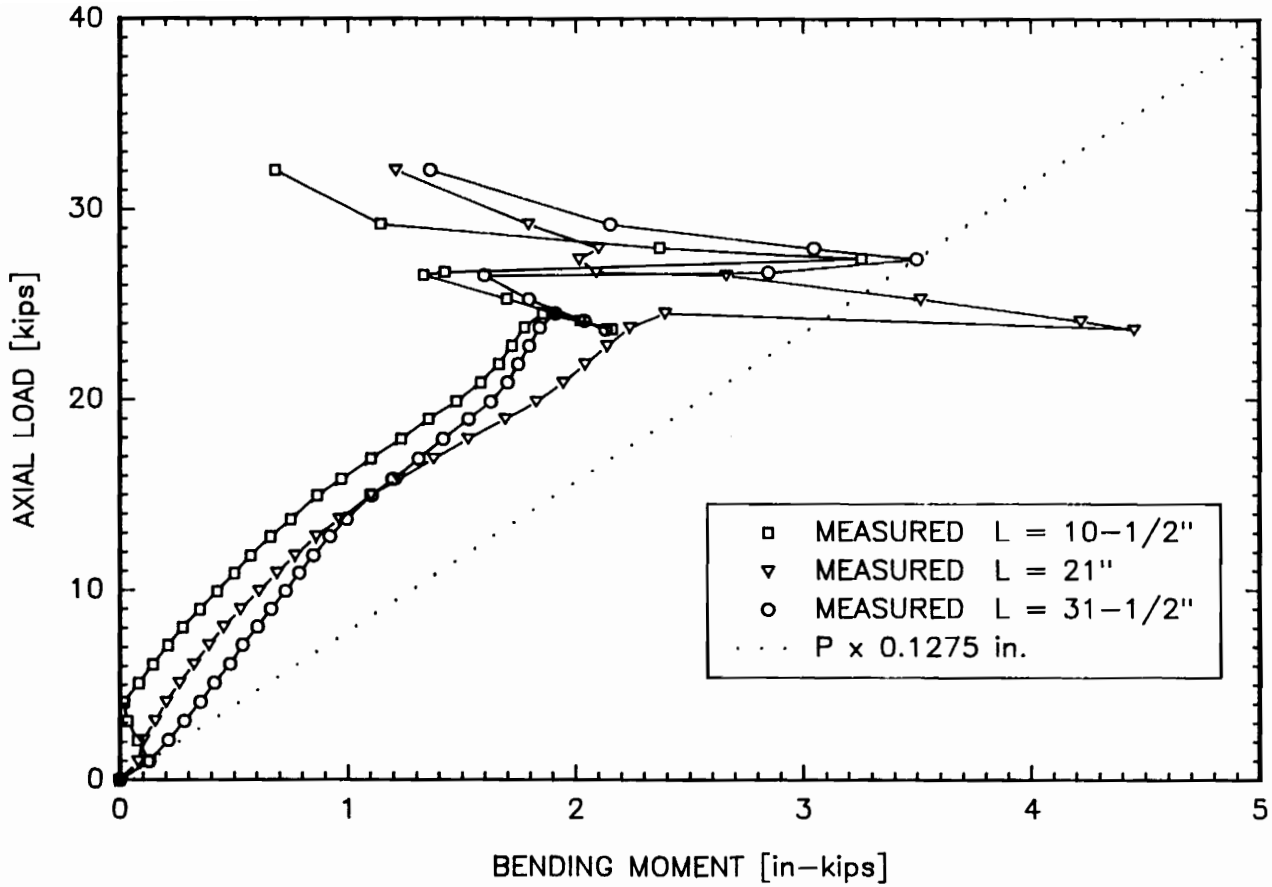

FIG. 3.8 MODEL TEST 2 LOAD VS. BENDING MOMENT

3.6.1 Test FS-1

Detailed results from test FS-1 are found in Appendix A. The outer conductor specimen used in FS-1 was 15.17 ft. in length and was tested in the vertical position. Only axial load was applied to the system. No external lateral load was applied.

Initially, axial load was applied in increments of 10 kips until the total load reached approximately 90 kips. At this point, the load was increased in smaller increments. The system reached a relative maximum load of 107.6 kips at load point 26. At this point, the system began to lose its load carrying capacity. The axial load on the conductor began to drop and the lateral deflection of the outer conductor increased.

This first peak, or relative maximum, that the conductor system reached represents a buckling load for the outer conductor. By plotting the computed bending moment over the length of the outer conductor for load point 26, inflection points are identified, and an effective length for the buckling mode observed in FS-1 is determined (see Fig. A.4). Additionally, as seen in plots of bending moment at various points along the length of the outer conductor (see App. A), the bending moment increased as the load dropped after load point 26. Again this illustrates a buckling, or instability, of the outer conductor.

The axial load on the conductor system continued to decrease until a minimum load of 100.5 kips was reached at load point 31. At this point, the outer conductor had deflected laterally enough to come into contact with the inner casing. Just as in the model test, the inner casing provided lateral support for the outer conductor. With this added support from the inner casing, the conductor system began to hold increasing amounts of axial load.

After load point 31, the axial load increased until the test was stopped at an axial load of 144.6 kips. The test was stopped due to excessive deflections and not due to any instability of the conductor system. That is, the conductor was still holding increasing amounts of axial load when the test was stopped. The maximum measured lateral deflection of the tip of the outer conductor was approximately 33.9 in.

In App. A, the computed bending moment at various cross-sections is plotted vs. the applied axial load. In these graphs, the dotted line represents a moment due to the axial load being eccentric by 1.37 in. The value of 1.37 in. represents the annulus between the 6-5/8 in. outer conductor and the 3-1/2 in. inner casing. In the conductor design procedure proposed by Stahl and Baur (1980), the axial load times 1.37 in. (1.37 P) represents the design internal moment for the outer conductor. In these graphs, the measured bending moment can be compared with the design bending moment for the conductor system. The axial load vs. bending moment graphs are found in Appendix A.

3.6.2 Test FS-2

Detailed results from test FS-2 are given in App. B. In test FS-2, the outer conductor tested was 15.0 ft. in length and was tested in the vertical position. Axial load only was applied to the conductor system. Test FS-2 was designed to be the same as test FS-1 except for conductor length.

The outer conductor behavior in FS-2 was very similar to that in FS-1. A relative maximum load of 108.8 kips was reached at load point 14. This was considered to be a buckling value for the outer conductor since the axial load on the outer conductor dropped after this value was reached. Again, the bending

moment was computed at various cross-sections along the length of the outer conductor for load point 14 to determine the effective length for the buckling mode of FS-2 (see Fig. B.4).

After reaching 108.8 kips of axial load at load point 14, the axial load on the outer conductor dropped off to 106.4 kips. At this point, the outer conductor had deflected laterally a sufficient distance to come into contact with the inner casing. With the lateral support provided by the inner casing, the conductor system was able to hold increasing amounts of axial load.

The axial load on the system reached a maximum value of 168.9 kips, at which time the test was stopped. The reason for stopping the test was excessive deflections and not any instability of the conductor system. The maximum observed lateral deflection of the tip of the outer conductor was 33.2 in. Upon completion of testing, considerable plastic deformations had occurred in both the outer conductor and the inner casing.

In Appendix B, the computed bending moment values are shown for various cross-sections along the length of the outer conductor. Again, the dotted line in these graphs represents the design internal moment proposed by Stahl and Baur and is based on the axial load being eccentric by a distance equal to the annulus between the inner casing and the outer conductor.

3.6.3 Test FS-3

Appendix C contains detailed results from test FS-3. The outer conductor used in test FS-3 was 13.9 ft. in length and was tested in the vertical position. Axial load only was applied in this test. Test FS-3 differed from the previous two tests as well as the tests that followed in that the inner casing was positioned as

eccentric as possible at the top (cap plate) of the outer conductor. This was done to determine what effect an eccentric inner casing would have upon the conductor system. The inner casing was still centered at the base of the outer conductor by virtue of the holes in the support frame through which the inner casing passed.

Unlike tests FS-1 and FS-2, test FS-3 did not reach a relative maximum, or first peak, load. However, as seen in Fig. C.5, the outer conductor appeared to be approaching a relative maximum until the inner casing provided lateral support. The presence of the lateral support provided by the inner casing was first observed at load point 15 (P = 110.4 kips). Additional evidence that shows the outer conductor was beginning to buckle at load point 15 is seen in the computed bending moment plots of the appendix. At certain points along the outer conductor, the computed bending moments were increasing dramatically just prior to load point 15. This indicates that the outer conductor was moving towards instability prior to the lateral support being provided by the inner casing. Some analysis of the stability of the outer conductor at load point 15 may be justified despite the fact that a relative maximum load was never reached.

After load point 15, the conductor system continued to hold increasing amounts of axial load up to 178.7 kips, at which point the test was stopped. Again, the test was stopped due to excessive deflections and not due to any sudden instability of the conductor. The lateral deflection of the tip of the outer conductor exceeded 40 in. when the test was stopped.

The eccentricity of the inner casing appeared to have no effect on the ultimate strength of the conductor. However, the behavior of the outer conductor was influenced by the inner casing being eccentric. This influence was especially

evident in the initial loading of the conductor, up to load point 15. Unlike tests FS-1 and FS-2, the outer conductor of test FS-3 began to deflect laterally when small amounts of axial load were applied. This was expected since the eccentricity of the load would result in additional bending moments. The computed bending moments for the outer conductor of FS-3 illustrate this principle. Considerable moments on the pipe were measured and, at least initially, increased linearly with the axial load (see App. C).

3.6.4 Test FS-4

Detailed results for test FS-4 are found in appendix D. The outer conductor used in FS-4 was 13 ft. in length and was tested in the horizontal position. A lateral load of 0.92 kips was applied at the tip of the 13 ft. cantilevered outer conductor.

The lateral loading was applied to the conductor system in increments. Dead weight of steel plates and angles were used for the lateral loading and were attached to the cap plate of the outer conductor with a single 3/4 in. bolt as shown schematically in Fig. 2.3. The measured deflections for the outer conductor due to the lateral loading were slightly greater than those predicted for a simple cantilever. However, this was expected since the support frame for the conductor was not a perfectly rigid base. Instead, the frame acts as a very stiff rotational spring.

After the 0.92 kips of lateral load were applied, the axial load was applied until failure. As in test FS-3, a relative maximum or first peak in the axial load did not occur. The outer conductor came into contact with the inner casing before any loss of stability in the outer conductor could occur. Still, the outer conductor

was close to reaching instability before the inner casing provided lateral support at load point 15 (P=82.7 kips). Some analysis regarding the stability of the outer conductor at load point 15 may be warranted.

After the inner casing provided lateral support to the outer conductor, the conductor system was able to sustain increasing amounts of axial load up until a maximum load of 145.5 kips was reached. The test was stopped due to excessive deflections and not due to any loss of load carrying capacity. When the maximum load was reached, the tip of the outer conductor had deflected laterally approximately 30 in.

The computed bending moments are plotted for various cross-sections of the outer conductor against both the lateral load and the axial load, in App. D. In the graphs of the bending moment vs. the lateral load, the theoretical (dotted) line is based on simple cantilever beam behavior. Hence, this line varies with the different cross-sections considered, depending upon their moment arm. In the graphs of the bending moment in relation to the axial load, the dotted line represents the design bending moment proposed by Stahl and Baur and includes both internal and external moments. Because the external moment varies over the length of the pipe, this design moment also varies over the length of the pipe. Therefore, the design moment will depend upon which cross-section of the pipe is being analyzed.

As was the case in all of the full scale tests, the inner casing and the outer conductor were inseparable after all loads on the system were released. In some places, the lateral force of the inner casing on the outer conductor caused the cross-section of the outer conductor to distort and become elliptical. This was

limited to that section of pipe where the inner casing was actually bearing on the inside wall of the outer conductor.

3.6.5 Test FS-5

Detailed results for test FS-5 are found in appendix E. As in FS-4, the specimen for test FS-5 was 13 ft. in length and was tested in the horizontal position. A total load of 1.72 kips was hung from the tip of the cantilevered outer conductor to represent lateral loading.

The lateral load was applied incrementally at the tip of the outer conductor. With 1.72 kips of weight applied laterally to the conductor, the outer conductor began to yield (on both the tension and compression side of the pipe) near the support frame. The total applied lateral weight resulted in the 13 ft. cantilever deflecting approximately 5.8 in. at the tip of the cantilever.

After the 1.72 kips of lateral load was applied, axial load was incrementally applied on the system until failure. The outer conductor behaved independently of the inner casing up until load point 12 (P=43.5 kips). At this point, the outer conductor had laterally deflected enough to come into contact with the inner casing. With the added lateral support of the inner casing, the conductor system exhibited increased stiffness and held increasing amounts of axial load.

The conductor reached a maximum axial load of 100.8 kips at load point 24. After this point, a local buckle formed on the compression side of the outer conductor where it entered the support frame, as seen in Fig. 3.9. The load carrying capacity of the conductor system decreased dramatically after the local buckle formed. The lateral deflection of the tip of the outer conductor at load point 24 (P=100.8 kips) was approximately 26.5 in. After the local buckle had

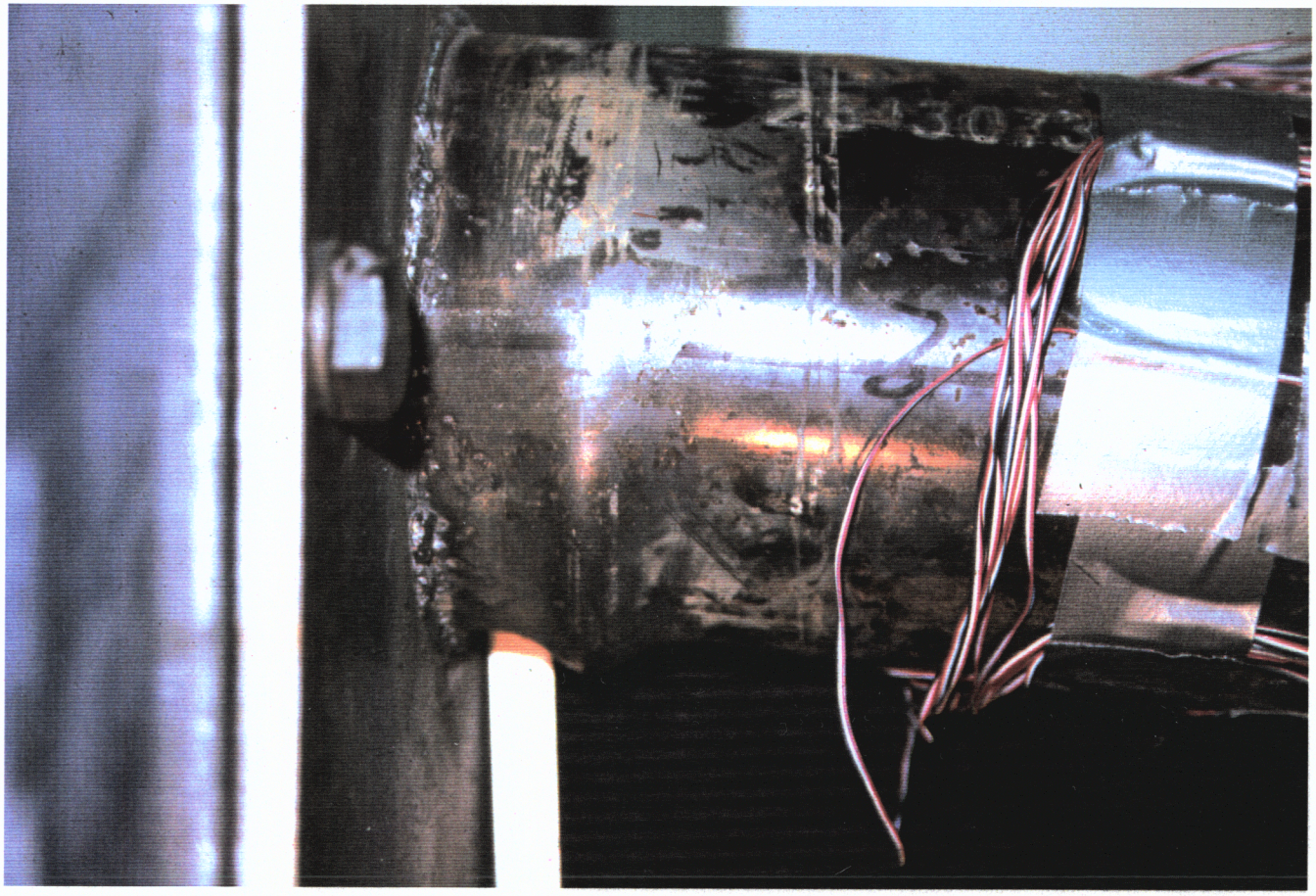

FIG. 3.9 FS-5 Local Buckle

formed, additional displacement was induced to visibly emphasize the failed location.

3.6.6 Test FS-6

Specific results for FS-6 are found in App. F. The outer conductor specimen tested in FS-6 was 13 ft. in length and was tested in the horizontal position. A lateral load of 0.48 kips was applied incrementally at the tip of the cantilevered outer conductor and axial load was then applied until failure.

Initially, the 0.48 kips of weight was applied laterally to the tip of the outer conductor in the absence of axial load. The outer conductor deflected approximately 1.25 in. due to the lateral weight. Axial load was then applied to the conductor system by tensioning the inner casing.

As the axial load was applied to the conductor system, the outer conductor behaved independently of the inner casing up until load point 13. At this point, the outer conductor had deflected laterally enough to come into contact with the inner casing. No relative maximum or first peak load in the outer conductor was reached. The additional stiffness of the inner casing prevented any instability from occurring in the outer conductor. Given the behavior of the outer conductor in FS-6, a stability analysis may be warranted for the outer conductor at load point 13 (P=90.4 kips).

With the added stiffness of the inner casing, the conductor system was able to sustain increasing amounts of axial load up to a maximum of 160.3 kips. The test was stopped at this point due to excessive deflections and not due to any loss of load carrying capacity. The lateral deflection of the tip of the outer conductor at maximum load was 39.25 in.

3.6.7 Test FS-7

Complete results for test FS-7 are found in App. G. The outer conductor specimen tested in FS-7 was 16 ft. in length and was tested in the horizontal position. However, the conductor was not a cantilever (as in FS-4, FS-5, FS-6). Instead, the conductor was supported at its base by the support frame and at its tip with a pin support. This change in the test set up was made to investigate the effect of different boundary conditions. Additionally, other than the self-weight of the components involved, no lateral load was placed on the conductor. Axial load only was applied to the system and was continued until failure.

As the system was loaded, the outer conductor behaved as a conventional column and was not affected by the inner casing. This continued until a relative maximum or first peak load was reached at load point 28 (P = 130.6 kips). Here the system lost its axial load carrying capacity and the outer conductor continued to deflect as the axial load on the conductor decreased. At this point, the outer conductor had laterally buckled and could carry no further axial load.

After deflecting enough to come into contact with the inner casing, the outer conductor began to hold increasing amounts of axial load. This continued until the test was stopped at an axial load of 160.4 kips. Excessive deflections caused the test to be stopped, not any loss of load carrying capacity in the outer conductor.

Unfortunately, no pertinent or reliable lateral deflection data was available for test FS-7. However, after the specimen had been unloaded, lateral deflections of the outer conductor were measured. The maximum lateral deflection of the outer conductor was approximately 7.5 in.

CHAPTER IV

INTERPRETATION OF RESULTS

In this chapter, the results of the experimental tests are evaluated. Data collected is analyzed and the behavior of the conductor system is studied. Current design procedures are compared with the test results.

4.1 Overview of Conductor String Design Methods

Two different design methods are used to analyze and predict the behavior of the experimental models tested in this research program. They are referred to as the Stahl and Baur (SB) approach and the Manley approach. Both of these methods were discussed in Sec. 1.2.2.

The SB approach, when applied to the experimental models, considers the outer conductor alone. The Manley approach, however, considers the effect of both the outer conductor and the inner casing on the system strength. Both methods are based on the fundamental principle that internal axial compressive forces do not induce any buckling tendencies in the outer conductor. Considering that the axial loads placed on the models in this research are all internal axial loads, both of these design methods are strength (not stability) related approaches.

Within both of these design methods, three different strength interaction curves are considered. They are the AISC plastic design curve, a curve proposed by Toma and Chen (1979), and a curve proposed by Stahl and Baur (1980).

These curves are shown in Fig. 1.3. Both the Toma and Chen and the Stahl and Baur strength curves were developed specifically for tubular members. The AISC curve was developed primarily for wide-flanged shapes.

4.2 Evaluation of Model Tests

Results of model test 1 and model test 2 are shown in Fig. 3.5 - 3.8. The predicted failure loads for the model tests are shown in Table 4.1 The failure loads predicted by the Manley method were computed based on an assumed yield strength of 42 ksi for the 1-1/8 in. rod used to model the inner casing.

Both of the model tests conducted reached axial loads approximately equal to the yield load (Py) for the outer conductor. The tests were not stopped because of instability but rather because the axial load had reached the yield load for the pipe.

At one point during model test 2 (load point 27), the axial load on the conductor decreased while the measured bending moments and deflections increased. This indicates that the outer conductor had become unstable. However, the presence of the inner casing limited the lateral deflection of the outer conductor, thus enabling the application of additional load.

The collected data indicates that the point at which both model tests began to deflect in increasing amounts (behave non-linearly) is directly attributed to the outer conductor becoming unstable. However, a detailed stability analysis of the outer conductor at these points is not possible since an effective length for the conductor was not determined.

The lateral support provided by the inner casing prevented any stability failure in the outer conductor. This support is seen graphically in Fig. 3.6. The

Table 4.1 Model Test Predicted Failure Loads (kips)

Stahl & Baur Method			Manley Method		
AISC	T&C	S&B	AISC	T&C	S&B
25.40	26.27	26.61	26.51	27.32	27.62

Model Test 1: Max Load = 31.00 kips

Model Test 2: Max Load = 32.05 kips

measured bending moment at midspan of the outer conductor in model test 1 starts to decrease just as the tip of the outer conductor begin to deflect in increasing amounts (load point 11). This is the opposite of what would be expected in a traditional externally loaded column.

The design internal moment proposed by Stahl and Baur, shown by the dotted lines in Fig. 3.6 and Fig. 3.8, is calculated based on the axial load being eccentric by a distance equal to the annulus between the outer conductor and the inner casing. This moment was exceeded in both the model tests. However, the annulus for the model tests was very small (0.1275 in.) and the measured moments were equally small. With such a small annulus, other factors, such as out-of-straightness of the conductor, could have resulted in higher bending moments.

In summary, the model tests show that the lateral support provided by the inner casing prevents any instability related failure of the conductor system. However, the point at which the outer conductor began to deflect laterally appears to be stability related.

4.3 Full Scale Tests - Outer Conductor Stability

When axial compression was first applied to the outer conductor in the full scale tests, the outer conductor and the inner casing were in contact with each other only through the cap plate at the top of the conductor system. Without any lateral support between end points, the outer conductor was expected to behave as an externally loaded column. This behavior would continue until the outer conductor came into contact with the inner casing along its length.

The midspan chord deflection of the outer conductor is computed by taking one half of the tip deflection and subtracting the measured midspan deflection. The chord deflection represents the deflection of the outer conductor in relation to its endpoints. From the figures in the appendices of axial load vs. midspan chord deflection, one can determine the point where the outer conductor comes into contact with the inner casing. This is evident by a sudden jump in stiffness and load carrying capacity. The annulus separating the outer conductor and inner casing in the full scale tests was 1.37 in. (based on a centralized inner casing). The plots of axial load vs. midspan chord deflection show that the lateral support of the inner casing becomes effective once the outer conductor has deflected approximately this distance.

Prior to the point where the inner casing contacts the outer conductor, the outer conductor behaves as a conventional column. In some tests (FS-1, FS-2, FS-7), the outer conductor reached a relative maximum load, or buckling load, prior to contacting the inner casing. In these tests, the stability of the column was evaluated at these peak loads. In other tests (FS-3, FS-4, FS-6), a relative maximum, or buckling, load was not reached prior to contacting the inner casing. However, the outer conductor in these tests appeared close to reaching instability when it contacted the inner casing. Thus, the stability of the outer conductor in these tests was evaluated. In test FS-5, the outer conductor was not close to reaching instability when the support of the inner casing was felt. Therefore, any stability analysis for test FS-5 should be considered as a lower bound.

In those tests where only axial load was applied to the conductor (FS-1, FS-2, FS-3, FS-7), the outer conductor was expected to behave as a conventional column providing that it did not come into contact with the inner casing along its

length. In tests FS-1, FS-2 and FS-7, the conductor reached a relative maximum load prior to contacting the inner casing. By analyzing the data collected from the outer conductor at the relative maximum load, the various column strength curves discussed in chapter 1 were evaluated. While test FS-3 did not achieve a relative maximum load, it appeared to be close to reaching a peak. It, therefore, was also used to evaluate the various column strength criteria.

In order to evaluate the various column strength curves, an effective length for the outer conductor must be determined. This was accomplished by using data from the strain gages that were mounted at various cross sections of the outer conductor. As was discussed in section 3.6, these strains converted into a bending moment. By plotting the bending moment over the length of the outer conductor at the peak load, an effective length for the outer conductor was determined (see appendices). The effective length was determined by finding the distance between the points of zero moment on the conductor. In some of the tests, the data was extrapolated to determine the effective length for the outer conductor.

Once an effective length was determined, the various column strength curves were evaluated. Fig. 4.1 shows the results of the four tests that only had axial load applied by comparing them with the four column strength curves discussed in chapter 1. The column slenderness values for the four tests ranged from 0.702 to 0.989. Within this range, the AISC(ASD) column curve results in the least conservative predictions. On the average, the observed peak loads were only 81% of the values predicted by the AISC(ASD) curve. Previous research conducted by Flick and Green (1983) indicates that the AISC(ASD) column curve

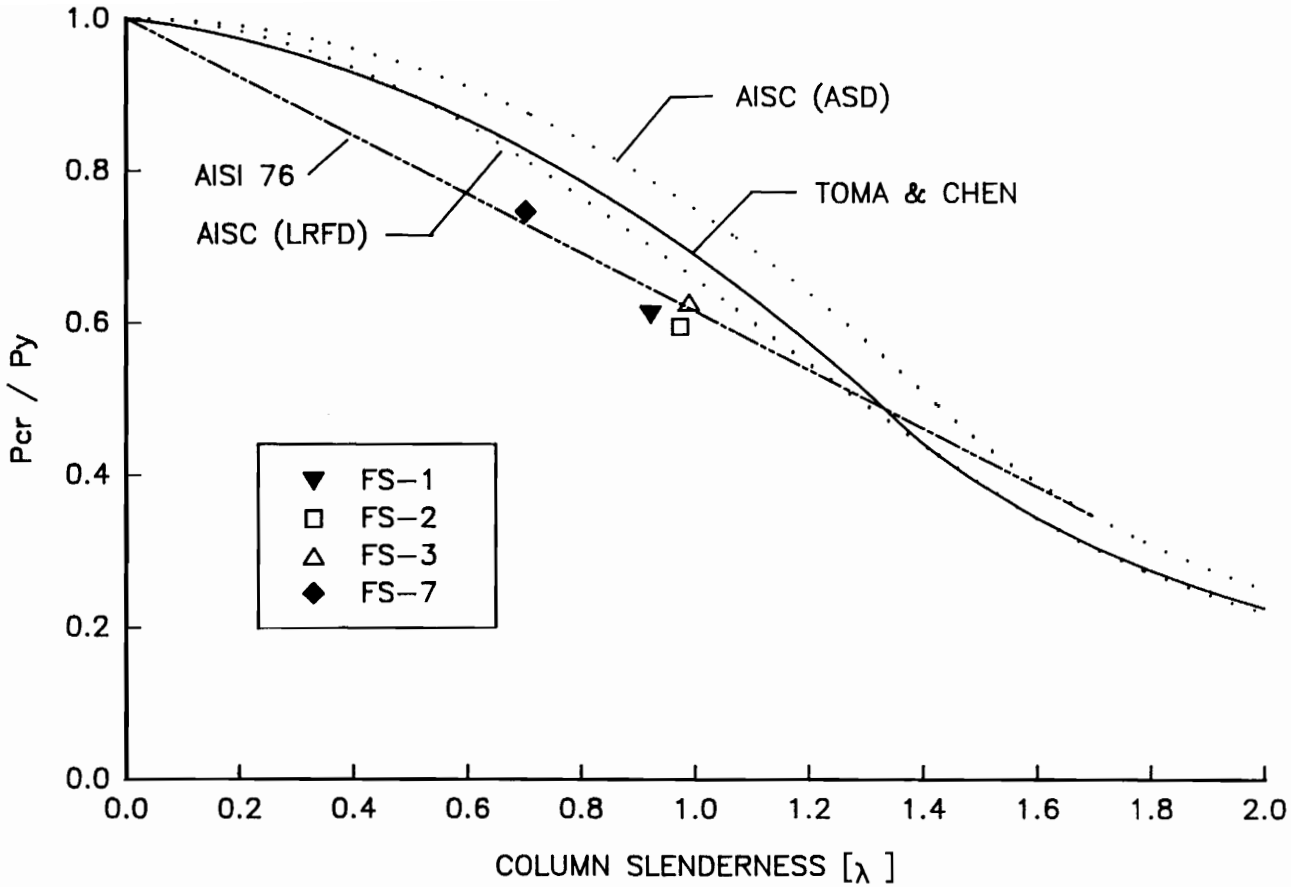

FIG. 4.1 COMPARISON OF TEST RESULTS WITH EXISTING COLUMN STRENGTH CRITERIA

can be expected to give unconservative results for tubular columns similar to those of this study.

The observed peak loads were on the average 87% of the predicted values based on the Toma and Chen column strength criteria, 90% of the values predicted by AISC(LRFD) criteria and 98% of the values predicted by AISI 76 criteria. Results for each individual test are shown seen in Table 4.2.

In those tests where some lateral loading was applied to the structure (FS-4, FS-5, FS-6), the outer conductor was analyzed as a conventional column with some imposed bending moment, up to the point where the inner casing contacts the outer conductor. In none of these three tests did the outer conductor reach a relative maximum load prior to contacting the inner casing. However, in tests FS-4 and FS-6, the outer conductor appeared close enough to reaching a relative maximum to warrant a stability evaluation. Test FS-5 stability analysis results should be considered as a lower bound since the outer conductor in this test did not appear to be close to reaching a relative maximum when it contacted the inner casing.

A structural member subjected to combined axial compression and bending must satisfy (according to AISC) the stability interaction equation shown below:

$$\frac{P}{P_{cr}} + \frac{C_M M}{(1-\frac{P}{P_E})M_M} \leq 1.0 \qquad (4\text{-}1)$$

In evaluating tests FS-4, FS-5 and FS-6, the Pcr term was calculated using one of the four column strength curves discussed previously. In order to determine the effective length for each particular test, the computed bending moment was

Table 4.2 Observed 1st Peak Load/Values Predicted by Stability Criteria

	AISC (ASD)	T & C	AISC (LRFD)	AISI 76
FS-1	0.78	0.84	0.87	0.95
FS-2	0.78	0.85	0.88	0.95
FS-3	0.83	0.90	0.94	1.01
FS-4	0.92	0.97	0.99	1.07
FS-5*	0.77*	0.81*	0.83*	0.89*
FS-6	0.91	0.96	0.99	1.06
FS-7	0.85	0.90	0.93	1.02
Average	0.85	0.90	0.93	1.01
Range	.78-.92	.84-.97	.87-.99	.95-1.07

*Lower Bound

plotted over the length of the outer conductor. However, the effect of the external lateral loading on the computed bending moment was removed from this graph. This was done in order to determine the bending moments induced by the axial loading alone. As before, the effective length was determined by finding the distance between the zero moment (inflection) points on the outer conductor.

For the analysis of tests FS-4, FS-5 and FS-6, a value of 0.60 was assumed for Cm. This was done because the test results indicated that the experimental configuration closely resembled a pinned-pinned column with a concentrated moment at one end. While the tip of the conductor could displace laterally (in which case Cm = 0.85), the axial load applied would remain on an axis that connects the endpoints of the outer conductor. Because the axial load was applied by tensioning the inner casing, the axial load will be in line with the endpoints of the outer conductor. The system, therefore, more closely resembled a pinned-pinned column than a fixed-free column.

The results of the stability analysis for FS-4, FS-5 and FS-6 are found in Fig. 4.2 through Fig. 4.5 for the four different column criteria. Again, the results for test FS-5 should be taken as a lower bound and not as a definitive value.

The observed peak loads are on the average 92% of those predicted by AISC(ASD) interaction criteria, 97% of those predicted by the Toma and Chen interaction curve, 99% of those predicted by the AISC(LRFD) method, and 107% of those predicted using the AISI 76 column curve. Specific results for each individual test are found in Table 4.2. The average values shown in Table 4.2 do not include the results of test FS-5.

As has been discussed, the outer conductor behaves similarly to an externally loaded conventional column provided that there is no contact between

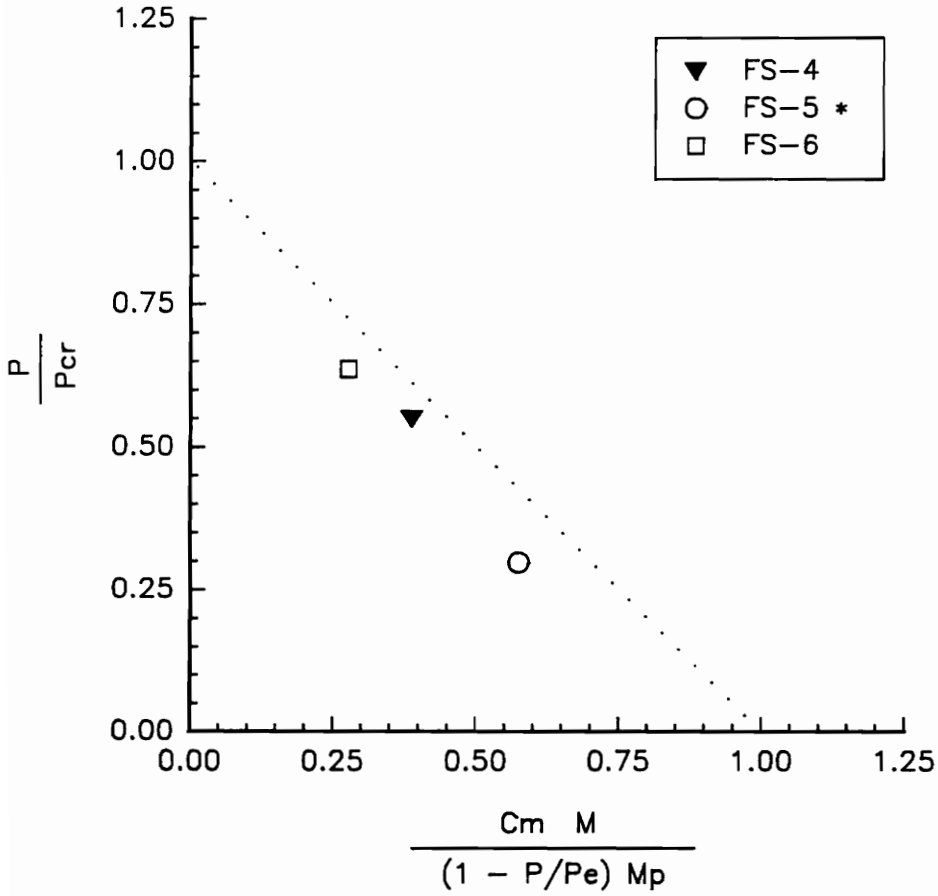

* LOWER BOUND VALUE

FIG. 4.2 COMPARISON OF TEST RESULTS WITH AISC(ASD) STABILITY INTERACTION CRITERIA

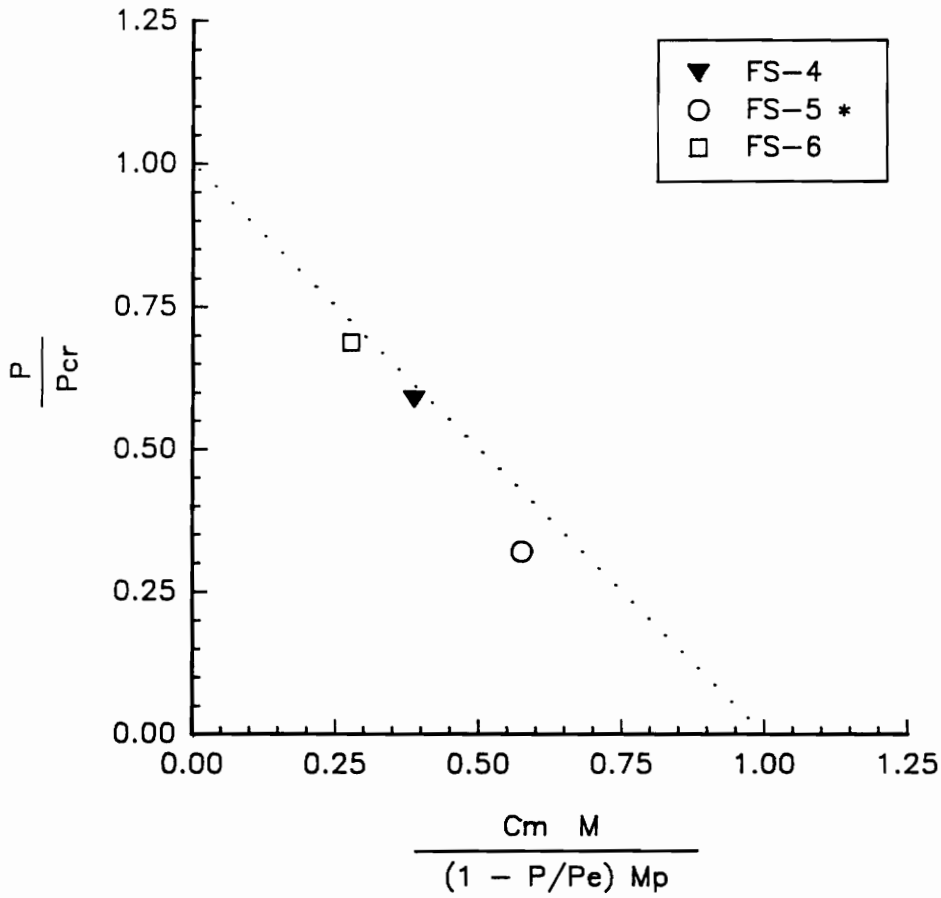

* LOWER BOUND VALUE

FIG. 4.3 COMPARISON OF TEST RESULTS WITH TOMA & CHEN STABILITY INTERACTION CRITERIA

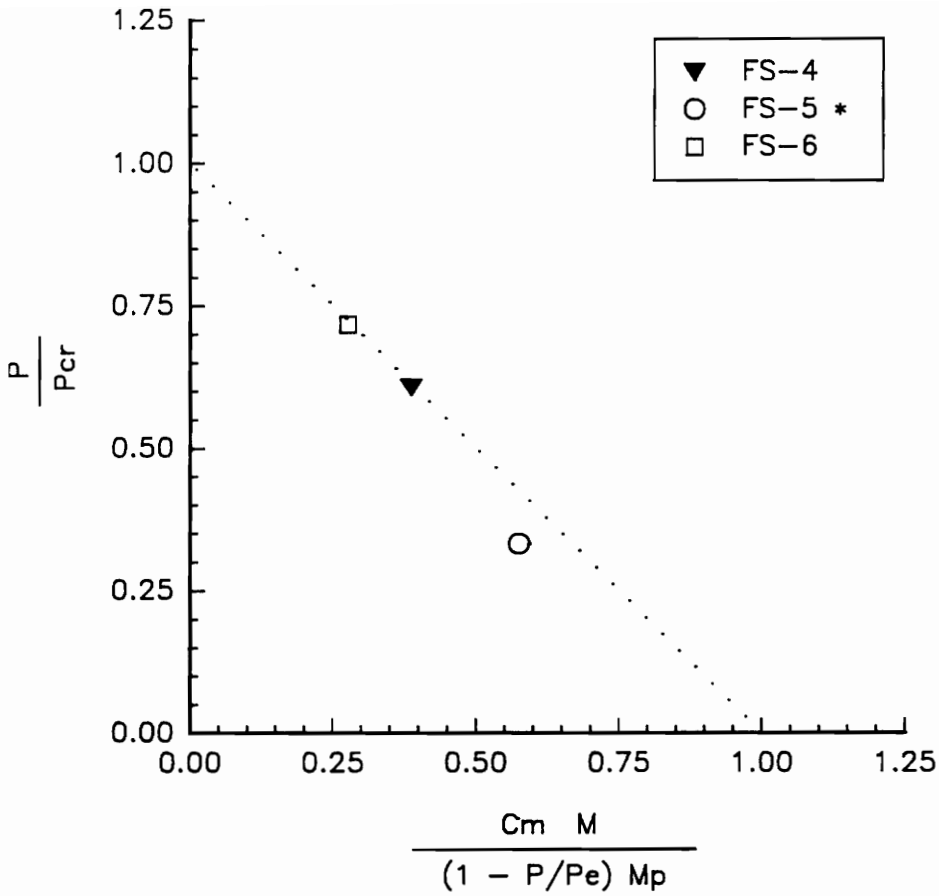

* LOWER BOUND VALUE

FIG. 4.4 COMPARISON OF TEST RESULTS WITH AISC(LRFD) STABILITY INTERACTION CRITERIA

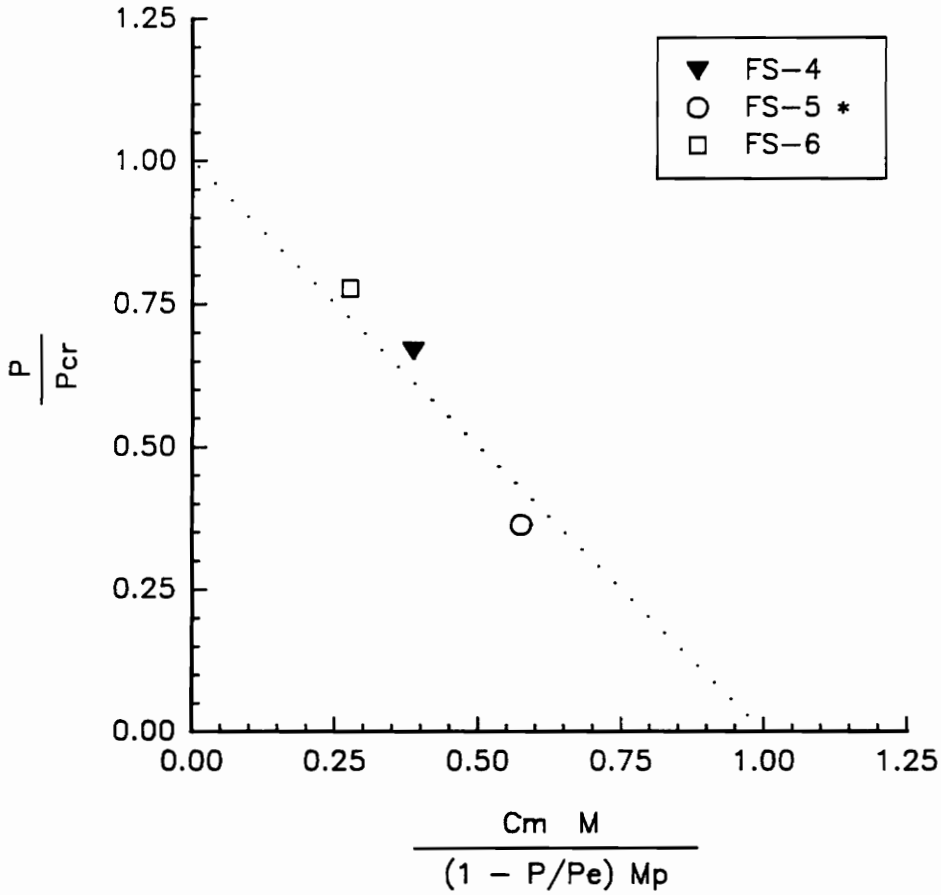

* LOWER BOUND VALUE

FIG. 4.5 COMPARISON OF TEST RESULTS WITH AISI 76 STABILITY INTERACTION CRITERIA

the inner casing and the outer conductor along the length of the system. For tests FS-1, FS-2, FS-3 and FS-7, the column strength curves discussed in chapter 1 yielded rather unconservative results. The AISI 76 column strength curve best predicted the axial load capacity of the outer conductor while the AISC(ASD) curve yielded the most unconservative results. Similar results were observed in those tests where some lateral loading was imposed on the conductor system.

It is concluded that the internal axial compression placed on the outer conductor by the inner casing can induce buckling tendencies in the outer conductor. That is, up until the outer conductor comes into contact with the inner casing along its length, the outer conductor behaves as an externally loaded column.

4.4 Evaluation of Current Design Procedures

The conductor systems tested in this research were evaluated by the two conductor design methods presented earlier (Stahl & Baur and Manley). As was stated previously, when applied to the conductors in this research, the two design procedures reduce to the evaluation of an interaction ratio for strength. In the Stahl and Baur method, the outer conductor alone is evaluated. The outer conductor and the inner casing are evaluated in the Manley method.

Both of the design methods reduce to strength checks since they are based on the principle that internal axial loads do not induce buckling tendencies in the outer conductor. In addition, a design internal moment is assumed in these design methods that is dependent upon the axial load being eccentric by a distance equal to the annulus separating the outer conductor and the inner casing.

Table 4.3 shows the test results compared to the values predicted by the two design methods. Three different strength interaction curves were used to evaluate the system for each design method. For all the tests, the conductor design methods gave conservative predictions of the systems strength.

In general, the Stahl and Baur method was more conservative than the Manley method. This was particularly true in those tests where some lateral loading was imposed on the system. In fact, as the imposed bending moment increased, the Stahl and Baur predictions became overly conservative. On the other hand, the Manley method yielded more consistent results over the range of applied bending moment. This indicates that the strength of the inner casing has a definite effect on the strength of the conductor system. Of the three strength interaction curves, the AISC curve generally yielded the most conservative results while the Stahl and Baur curve was the least conservative.

A special effort was made to analyze the bending moments in the outer conductor. As discussed in section 3.1, the strains measured during testing have been converted to bending moments for the various cross sections which were monitored during testing. These computed bending moments can then be compared with the bending moments assumed in the conductor design methods.

The appendices contain the graphs of the computed bending moments (referred to as measured moments) vs. the applied loads (axial and lateral). On these plots, the dotted line represents the design moment used in the conductor design methods discussed previously. Included in the design moment is an external moment (due to the imposed lateral loading) and an internal moment (due to the eccentricity of the axial load). From the figures in the appendices, it is evident that the design moment accurately represents a limiting value for the

Table 4.3 Full Scale Tests: Observed Maximum Load (From Load Cells)/Predicted Maximum Load

	Stahl & Baur Method			Manley Method		
Test	AISC	T&C	S&B	AISC	T&C	S&B
FS-1	1.29	1.21	1.19	1.16	1.09	1.07
FS-2	1.45	1.36	1.33	1.30	1.23	1.21
FS-3	1.59	1.49	1.47	1.40	1.32	1.30
FS-4	2.00	1.73	1.73	1.50	1.33	1.31
FS-5	2.56	2.37	2.39	1.35	1.14	1.14
FS-6	1.77	1.58	1.57	1.42	1.29	1.27
FS-7	1.44	1.35	1.32	1.29	1.22	1.20
Avg.	1.73	1.58	1.57	1.35	1.23	1.21

bending moment in the outer conductor. This is evident, in the tests, when the outer conductor comes into contact with the inner casing. For instance, from Fig. B.4, it appears that the curvature of the outer conductor is such that it would contact the inner casing approximately 6 ft. from the base of the conductor. Referring to Fig. B.8(B), it is apparent that the measured bending moment approaches the design moment as the outer conductor comes into contact with the inner casing. However, the bending moment does not surpass the design moment. Rather, the inner casing supports the outer conductor and prevents the bending moment from exceeding the design moment. Similar behavior was observed in all of the tests conducted, including those with some external moment imposed on the system. The measured bending moment approached the design moment as the outer conductor came into contact with the inner casing, but did not exceed it.

Given the results of the experimental tests, it appears that the design moment proposed by both Stahl and Baur and Manley is an accurate upper bound for the bending moment observed in the outer conductor. This supports the principle that internal casing string loads do not induce any buckling tendencies in the outer conductor.

4.5 Inner Casing Test Data

Although strain gages were mounted on the inner casing in all seven of the full scale tests, data from only four of the tests was complete enough to analyze. In many of the tests, the strain gages were damaged or destroyed either during the test set up or during testing. However, enough data was collected from tests

FS-2, FS-4, FS-6 and FS-7 to investigate the behavior of the inner casing during the tests.

The strains measured at a given cross section of the inner casing were converted into an axial load and bending moment acting on that cross section by means of the procedure shown in Fig. 3.1. It was felt that given the elastic behavior of the inner casing material, this procedure could accurately analyze the inner casing behavior.

Generally, as the axial load was initially applied to the conductor system, the inner casing was tensioned and very little bending moment was observed in the inner casing. This continued until the outer conductor came into contact with the inner casing along its length. At this point, the lateral force put on the inner casing by the outer conductor resulted in the inner casing contacting the support frame where it passed through the hole in the bottom plate (see Fig. 2.4).

This created a special problem because the friction between the inner casing and the support frame absorbed a portion of the axial load applied by the rams. This discrepancy was not accounted for in the load cells. However, the amount of axial load actually reaching the conductor system was measured with the strain gages that were mounted on the inner casing. In addition, by measuring the axial load at various points along the length of the inner casing, the amount of axial load lost due to friction between the inner casing and outer conductor was determined.

Fig. B.12 shows the amount of axial load measured in the inner casing at various points along its length in test FS-2. It can be seen that the load cells accurately measured the amount of axial load in the inner casing up until approximately load point 15. At this point, the load cells began to measure more

load than was actually getting to the conductor system. Ultimately, when the test was terminated at load point 30, the load cells measured 168.9 kips of axial load on the conductor while strain gages on the inner casing indicated that only 142 kips of axial load were on the inner casing 12 ft. from the base.

Similar results occurred in test FS-4 (see Fig. D.15). At load point 32 in test FS-4, the load cells measured a total of 145.5 kips of axial load on the system. However, the strain gages mounted on the inner casing 9.75 ft. from the base indicated that only 119.5 kips of axial load were in the inner casing. Similarly, at load point 32 in test FS-6, the load cells measured 160.2 kips of load while strain gages indicated that only 137.4 kips of load were on the inner casing (see Fig. F.15). In test FS-7, the load cells measured a maximum of 160.4 kips of load on the inner casing while strain gages indicated that only 155.7 kips were on the inner casing (see Fig. G.10). While it is true that some axial load is dissipated along the length of the conductor due to friction between the inner casing and the outer conductor, Fig. B.12 indicates that this amount is small in comparison to the amount of load lost to friction between the inner casing and the support frame.

Based on the axial load measured by the strain gages on the inner casing, the observed maximum loads for tests FS-2, FS-4, FS-6 and FS-7 have been adjusted and compared with those values predicted by the conductor design methods discussed earlier. The results of this analysis are shown in Table 4.4.

By considering the results presented in Table 4.4, one can conclude that all of the conductor design methods are conservative in predicting failure loads for the tests. The Stahl and Baur method is more conservative than the Manley method. This is particularly true when some lateral loading is applied to the conductor (FS-4, FS-6). In these tests, the Stahl and Baur method is extremely

Table 4.4 Full Scale Tests: Maximum Measured Load (From Strain Gages on Inner Casing)/Predicted Maximum Load

	Stahl & Baur Method			Manley Method		
Test	AISC	T&C	S&B	AISC	T&C	S&B
FS-2	1.22	1.14	1.12	1.10	1.03	1.01
FS-4	1.64	1.42	1.42	1.23	1.09	1.08
FS-6	1.52	1.35	1.34	1.21	1.11	1.09
FS-7	1.40	1.31	1.29	1.26	1.18	1.16
Avg.	1.45	1.31	1.29	1.20	1.10	1.09

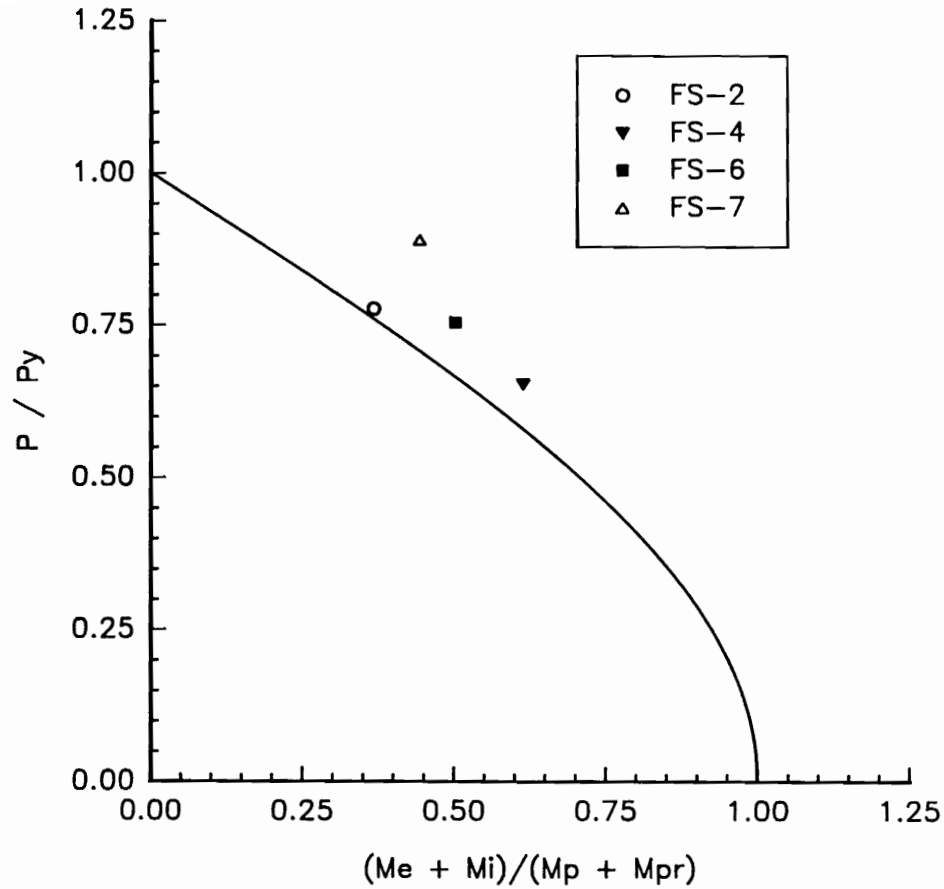

FIG. 4.6 COMPARISON OF TEST RESULTS WITH STAHL & BAUR INTERACTION CURVE USING THE MANLEY DESIGN METHOD (BASED ON AXIAL LOAD MEASURED BY STRAIN GAGES)

conservative. On the other hand, the Manley method is consistently conservative in predicting the failure loads for the conductor system despite the loading conditions. This indicates that the stiffness of the inner casing has a definite effect on the strength of the conductor system. The Manley method considers this strength while the Stahl and Baur method does not. The strength interaction curve proposed by Stahl and Baur best predicts the strength of the conductor system in both of the design methods.

Considering the revised data shown in Table 4.4, as well as the original data shown in Table 4.3, it is concluded that the Manley design method best predicts the strength of the conductor system. Additionally, the Stahl and Baur curve appears to be the interaction curve best suited to predicting the behavior of the tubular members used in the conductor system tested in this research (see Fig. 4.6).

4.6 Conductor String Behavior

In this section, the physical behavior of a conductor system loaded axially by an internal casing string is analyzed. This behavior is then used to assess the various conductor design methods that exist.

In the testing program, the inner casing was centralized in the outer conductor in all of the tests except for test FS-3. When axial compression was first placed on the outer conductor by tensioning the inner casing, the outer conductor received no lateral support along its length by the centralized inner casing. Given this configuration, the outer conductor was expected to behave as an externally loaded conventional column. In such case, the compression caused

by the internal casing string would induce buckling tendencies in the outer conductor.

The tests conducted in this project confirm this theory. The outer conductor behaved as an externally loaded column until the point where contact occurred with the inner casing. In fact, in three of the tests (FS-1, FS-2, FS-7) the outer conductor buckled laterally prior to contacting the inner casing. In the other tests, the outer conductor appeared to be close to buckling laterally when it contacted the inner casing.

However, the column action of the outer conductor is limited. Once the outer conductor has deflected laterally enough to come into contact with the inner casing, the boundary conditions for the outer conductor change. The lateral support of the inner casing helps to strengthen the outer conductor.

To gain an understanding of how this support influences the design of conductor strings, a worst-case scenario is analyzed. Consider the conductor system shown in Fig. 4.7. In this system, an outer conductor is loaded from an eccentric internal casing that can sustain axial loads but has no flexural stiffness. It is seen that at all points along the length of the conductor, the axial load on the conductor is eccentric by the distance e. The tension membrane action of the inner casing limits the lateral deflection of the outer conductor. Given this configuration, the moment in the outer conductor at any point is simply P x e. No secondary moments are induced as the conductor deflects laterally. The internal casing string load would, therefore, not induce any buckling tendencies in the outer conductor.

To design the conductor system shown in Fig. 4.7, only the outer conductor need be considered since the inner casing has no flexural stiffness. In

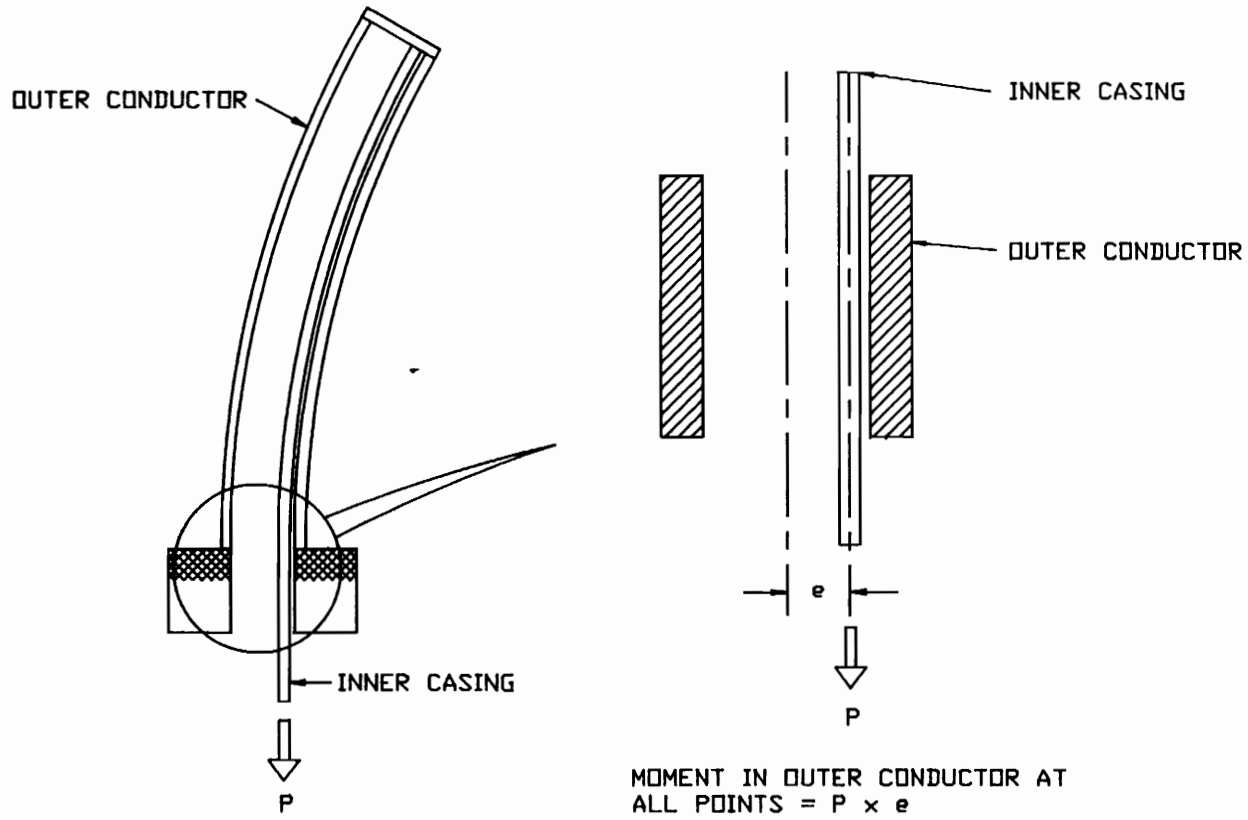

FIG. 4.7 CONDUCTOR SYSTEM WITH ECCENTRIC INNER CASING
(INNER CASING HAS NO FLEXURAL STIFFNESS)

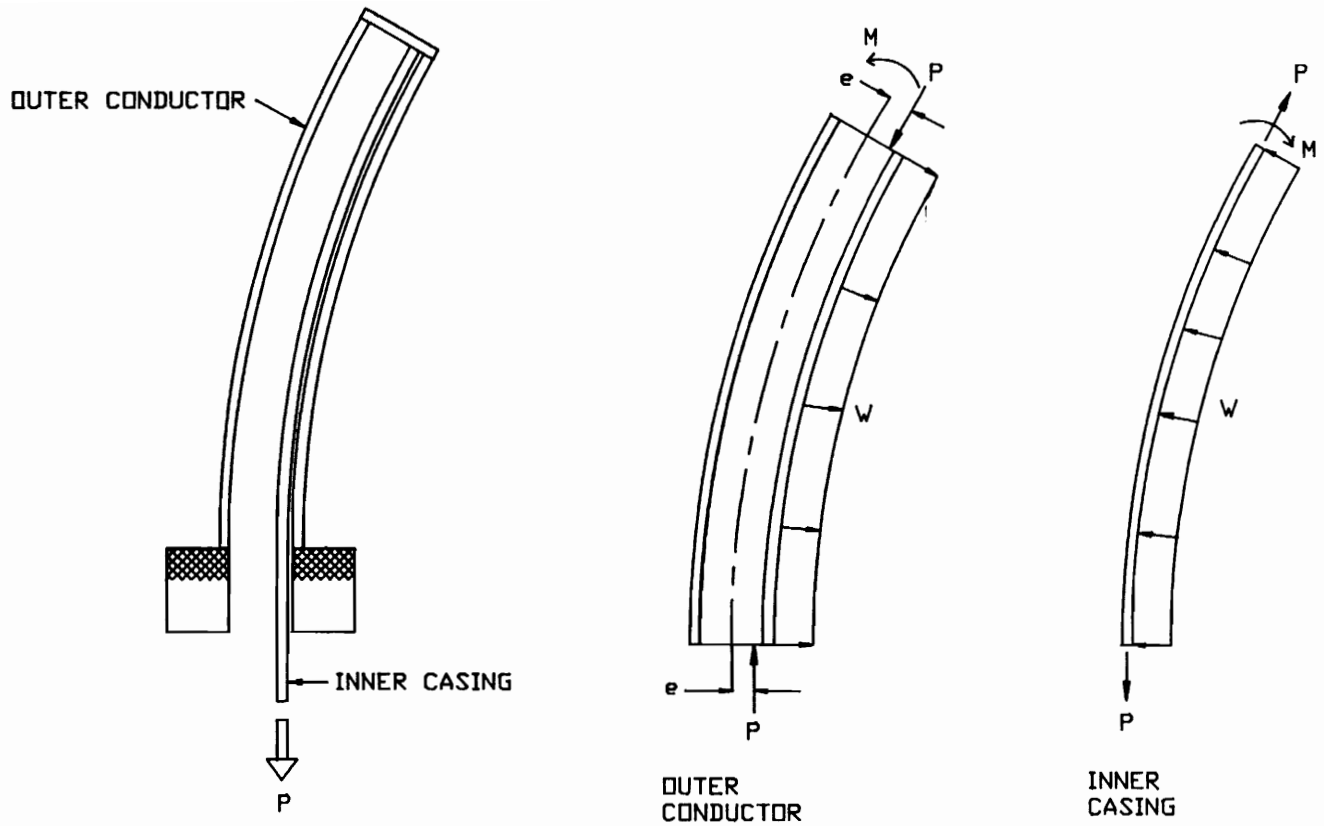

FIG. 4.8 CONDUCTOR SYSTEM WITH ECCENTRIC INNER CASING
(INNER CASING HAS SOME FLEXURAL STIFFNESS)

this case, the Stahl and Baur conductor design method would be used to determine the ultimate capacity of the conductor system.

In actuality, the inner casing will have some flexural capacity in addition to its axial load carrying capacity. Now consider the conductor system shown in Fig. 4.8. The boundary conditions for this conductor system are identical to those of Fig. 4.7 except that the inner casing has some flexural stiffness. In addition to the support provided by the tensile membrane action of the inner casing, the outer conductor is supported by the flexural stiffness of the inner casing. That is, the inner casing will carry some bending moment that results from the outer conductor pushing laterally against the inner casing. This however, does not affect the total bending moment acting on the conductor system. The lateral force of the outer conductor on the inner casing (shown as W in Fig. 4.8) results in an increase in the bending of the inner casing (shown as M in Fig. 4.8). However, this is countered with an equal and opposite effect that reduces the bending moment on the outer conductor. The total bending moment acting at any point of the system is, therefore, independent of the lateral support provided by the inner casing and remains as P x e for any point in the conductor system.

Test data shows that the lateral support of the inner casing reduces the moment acting on the outer conductor. Fig. 4.9 shows that the computed bending moment in the outer conductor of FS-1 reduces after coming into contact with the inner casing. In this figure, at load point 26, the outer conductor had not yet contacted the inner casing. At load point 32, the outer conductor had just contacted the inner casing. At load point 38, the lateral support of the inner casing had reduced the bending moment in the outer conductor at a cross section located 6 ft. from the base of the conductor. Unfortunately, not enough

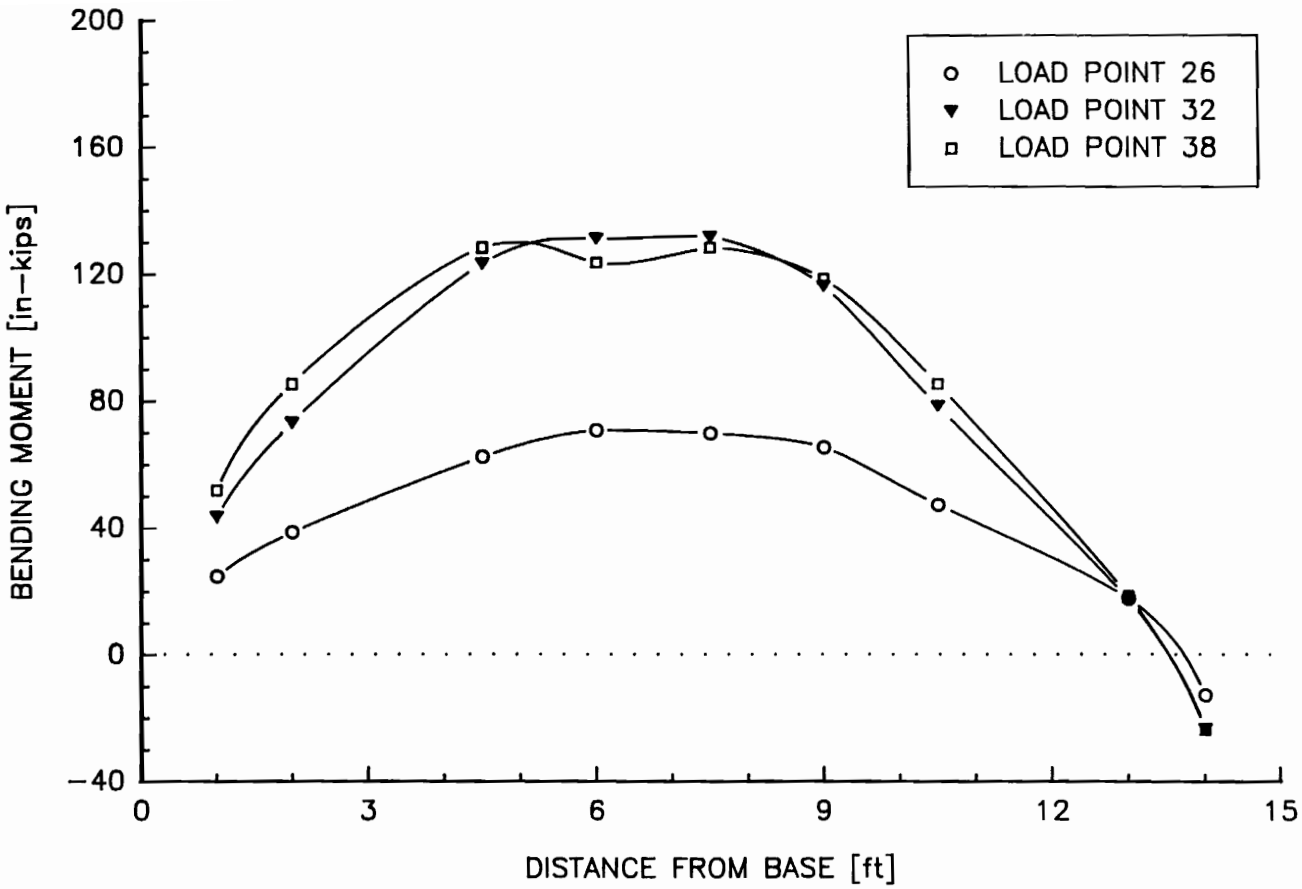

FIG. 4.9 FS-1 MEASURED BENDING MOMENT OVER THE LENGTH OF THE OUTER CONDUCTOR

data was collected from the inner casing to accurately analyze its behavior. However, the strains that were recorded indicate that the inner casing underwent considerable bending after it came into contact with the outer conductor.

The flexural stiffness of the inner casing helps to strengthen the conductor system shown in Fig. 4.8. The Manley design approach takes the inner casing into consideration by computing the reserve moment capacity for the inner casing and adding it to the moment capacity of the outer conductor. The results of the experimental tests indicate that the Manley design method consistently gives reasonably conservative estimates of the ultimate capacity of the conductor system.

CHAPTER V

SUMMARY, CONCLUSIONS AND RECOMMENDATIONS

5.1 Summary

In summary, two small scale model tests and seven full scale tests have been conducted to analyze the behavior of a conductor system subjected to combined internal axial loading and external lateral loading. Data gathered in these tests include the applied loads, critical deflections, and strains at certain locations on both the outer conductor and inner casing. The data gathered from the strain gages was used to determine the bending moment acting on the outer conductor.

In three tests, the outer conductor buckled laterally prior to contacting the inner casing along its length. Given these results, various column strength curves were compared with the observed values.

None of the experimental tests were stopped due to instability of the outer conductor. Test results indicate that the internal axial loads do not result in a stability related failure of the outer conductor. Additionally, the design moment proposed by Stahl and Baur appears to accurately represent an upper bound for the moment in the outer conductor.

The maximum loads imposed on the experimental specimens were compared with those values predicted by the various conductor design methods. Results indicate that all design methods are conservative in predicting the

system's strength. However, the Stahl and Baur design approach becomes overly conservative as the amount of external lateral loading is increased. The Manley design method is consistently conservative in predicting the strength of the system.

5.2 Conclusions

Based on the experimental tests conducted in this research and the evaluation of conductor string behavior, the following conclusions are made.

1) Based on those tests where the outer conductor buckles laterally, the AISI 76 curve best predicts the column strength of the tubular members tested in this research. The AISC(ASD) column strength curve yields unconservative results for column strength.

2) Based on the model tests and full scale tests, it is concluded that internal axial compression forces in the outer conductor can not result in a stability related failure of the outer conductor.

3) The bending moment proposed by Stahl and Baur as the design internal moment (P x e), where P is the internal axial load and e is the annulus separating the outer conductor and the inner casing, accurately represents the upper bound for the bending moment observed in the outer conductor.

4) The Stahl and Baur design method, where only the strength of the outer conductor is considered, conservatively predicts the strength of a conductor system. However, as the external lateral loading on the conductor is increased, this method becomes overly conservative.

5) The Manley design method, where the strengths of both the inner casing and the outer conductor are considered, consistently predicts the strength of the conductor systems tested in this research.

6) Of the three strength interaction curves considered (AISC plastic design, Toma and Chen, Stahl and Baur), the Stahl and Baur curve appears to best predict the strength of the tubular members tested in this research. The AISC curve, developed primarily for hot-rolled, wide-flanged sections, is conservative when used with tubular members.

7) Based on test FS-3, it is concluded that an eccentric inner casing does not affect the ultimate strength of the conductor system.

8) Given the conductor behavior described in section 4.6, the value of P x e accurately represents the internal bending moment in the conductor system. This moment is carried by both the outer conductor and the inner casing.

5.3 Recommendations

Based on this research program, several recommendations can be made for the design of offshore platform conductor strings.

1) When evaluating the interaction ratio for the outer conductor, the axial compression from the weight of the inner casings should be divided by a yield load for the outer conductor (P_y). However, an additional moment term should be included that results from the axial load being eccentric by a distance equal to the annulus separating the outer conductor and inner casing (Pxe). This is seen in Eq. 1-3.

2) The reserve bending moment capacities of the inner casings should be added to the moment capacity of the outer conductor when evaluating the strength of the conductor system.

Based on this research program, several recommendations are made for future experimental work on the strength of conductor systems.

1) The axial load and bending moment in the inner casing is of significant importance to the strength of the system. Therefore, more strain gages should be mounted on the inner casing in future tests so that the behavior of the inner casing can be more completely studied.

2) To more closely model an actual conductor system, a continuous span could be constructed using small diameter pipe to model the outer conductor. Lateral loading between the supports could model wave and current action.

3) In addition to the internal axial load applied in this test, external axial loads could be applied to simulate the weight of the BOP stack. It is felt that the inner casings may significantly increase the system's capacity to withstand external axial load. Also, the effective length factors used in the design of conductor strings can be evaluated or modified.

4) Instrumentation of an actual conductor system as it is installed may also identify additional factors to be considered in the design process.

REFERENCES

"API Recommended Practice for Planning, Designing and Constructing Fixed Offshore Platforms." (1979). American Petroleum Institute.

Bjorhovde, R. (1988). "Columns: From Theory to Practice." Engineering Journal, AISC, 25(1), 21-34.

Chen, W.F. and Ross, D.A. (1976). "The Axial Strength and Behavior of Cylindrical Columns." Proceedings of the 8th Offshore Technology Conference, May 3, 741-753.

Chen, W.F. and Ross, D.A. (1977). "Tests of Fabricated Tubular Columns." Journal of the Structural Divison, ASCE, 103(3), 619-634.

Flick, L.D. and Green, D.J. (1983). "Lateral Stability of Piles in Ungrouted Jacket Legs." Proceedings of the 15th Offshore Technology Conference, May 2, 557-564.

Galambos, T.V., ed. (1988). Guide to Stability Design Criteria for Metal Structures, 4th edit. Wiley-Interscience, New York, N.Y.

Graff, W.J. (1981). Introduction to Offshore Structures. Gulf Publishing Co., Houston, TX.

Imm, G.R. and Stahl, B. (1988). "Design of Concentric Tubular Members." Proceeding of the 20th Offshore Technology Conference, May 2, 263-271.

Lin, T.Y. and Burns, N.H. (1981). Design of Prestressed Concrete Structures. John Wiley & Sons, Inc., New York, N.Y.

"Load and Resistance Factor Design Specification for Structural Steel Buildings." (1986). AISC, Chicago, IL.

Manley, R.B. (1985). "Design Methodology for Offshore Platform Tieback Conductors." Proceedings of the 17th Offshore Technology Conference, May 6, 259-268.

"Specification of Structural Steel Buildings - Allowable Stress and Plastic Design." (1989). AISC, Chicago, IL.

"Stability for Metal Structures - A World View." (Draft Copy). SSRC.

Stahl, B. and Baur, M.P. (1980). "Design Methodology for Offshore Platform Conductors." Proceedings of the 12th Offshore Technology Conference, May 5, 465-478.

Toma, S. and Chen, W.F. (1979). "Analysis of Fabricated Tubular Columns." Journal of the Structural Division, ASCE, 105(11), 2343-2366.

Wagner, A.L. et al. (1976). "Design Interaction Curves for Tubular Steel Beam-Columns." Proceedings of the 8th Offshore Technology Conference, May 3, 755-764.

Whitehead, H. (1976). An A-Z of Offshore Oil and Gas. Kogan Page, London.

APPENDIX A

TEST FS-1 DATA

UNOCAL

TEST DATA SHEET

Test: UNOCAL FS-1

Test Date: June 25, 1990

Dimensions:

	Outer	Inner
Diameter (in.)	6.625	3.500
Wall Thickness (in.)	0.188	0.250
Yield Stress (ksi)	46.3	91.8

Parameters: Specimen Length = 15'-2"

Test Position - vertical

Axial Load Only Applied

Max. Axial Load: 144.6 kips

Failure Mode: Stopped Test - Large Deflections

Predicted Failure Loads (AISC Criteria):

Stahl & Baur Method 112.2 kips

Manley Method 124.5 kips

Discussion:

- Specimen first reached relative maximum load of 107.6 kips, after which load dropped off to 100.5 kips.
- Specimen continued to hold increasing amount of load up to 144.6 kips.
- Maximum lateral deflection at tip of specimen = 33.9 in.

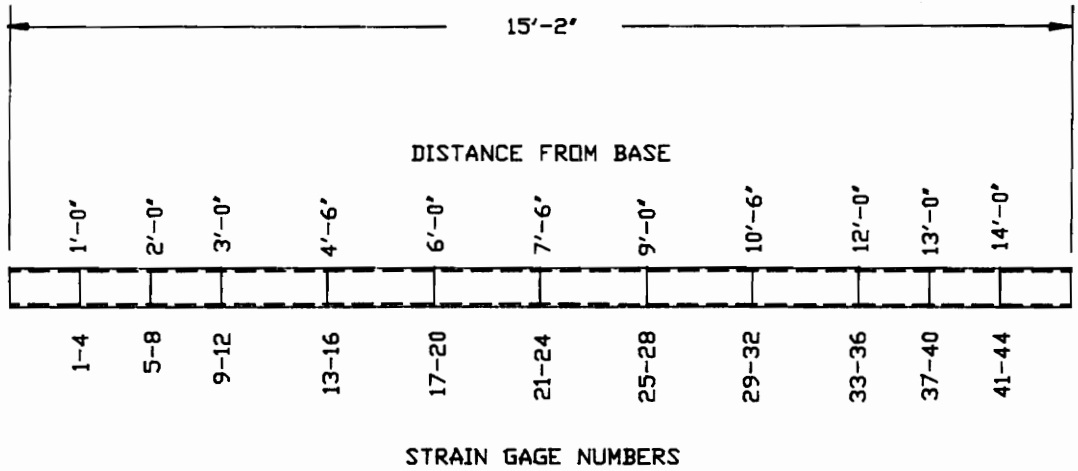

A) 6-5/8" OUTER CONDUCTOR PIPE

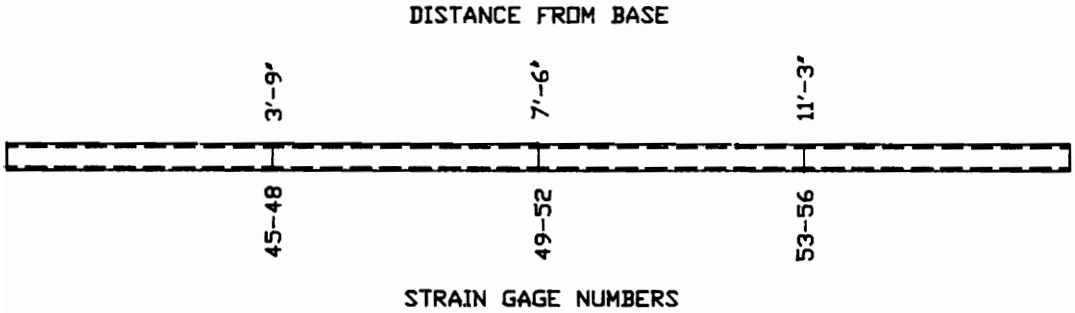

B) 3-1/2" INNER CASING PIPE

FIG. A.1 FS-1 STRAIN GAGE LOCATIONS

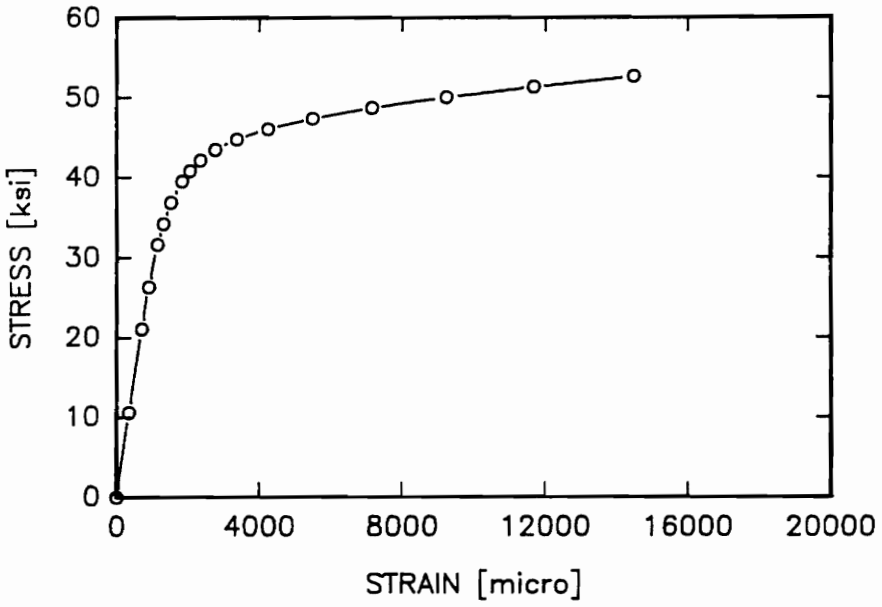

A) STUB COLUMN RESULTS

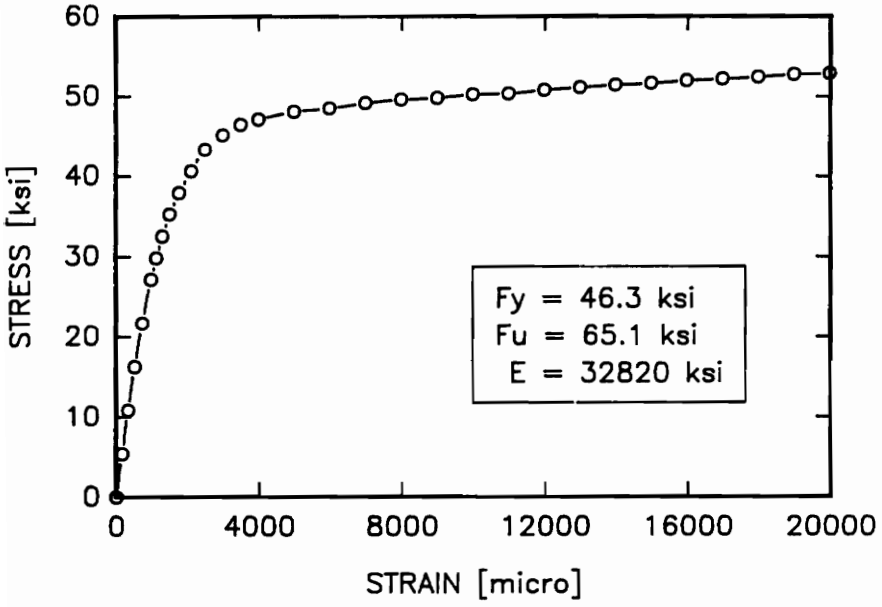

B) TENSILE COUPON RESULTS

FIG. A.2 FS−1 OUTER CONDUCTOR MATERIAL PROPERTIES

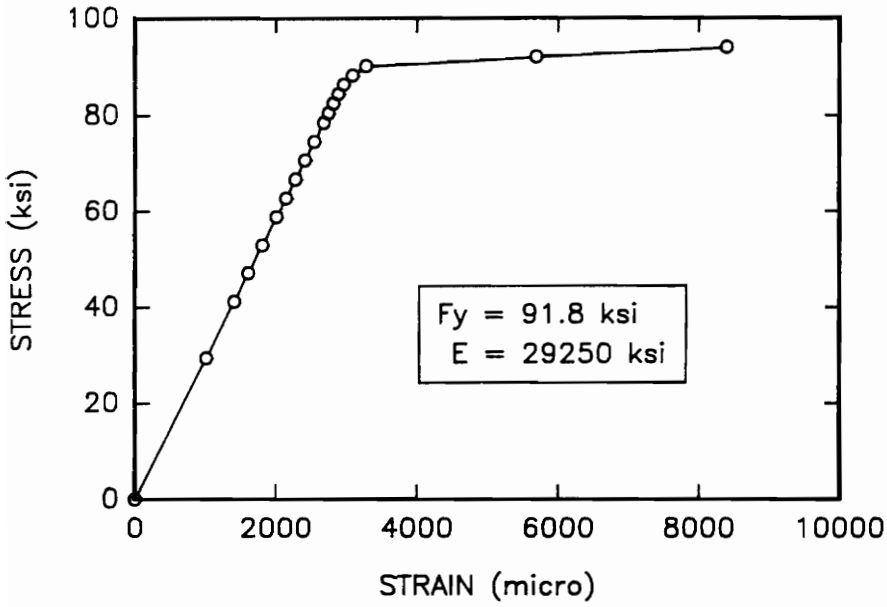

FIG. A.3 FS−1 INNER CASING MATERIAL PROPERTIES

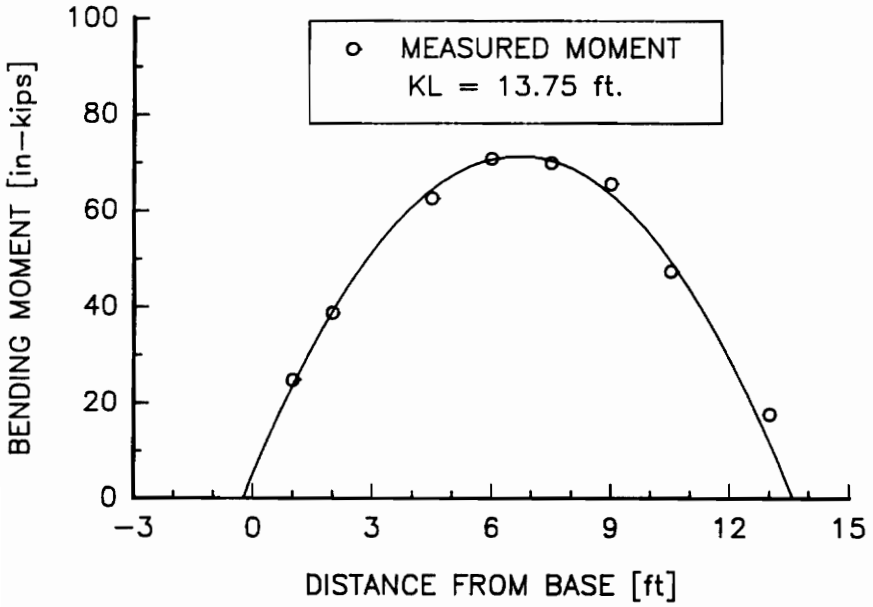

FIG. A.4 FS-1 BENDING MOMENT OVER THE LENGTH OF THE OUTER CONDUCTOR AT LOAD POINT 26

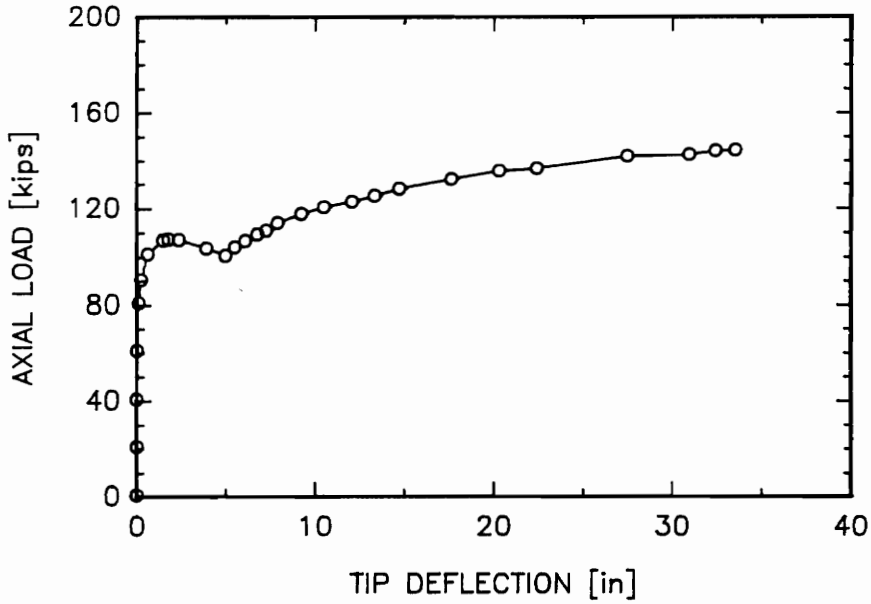

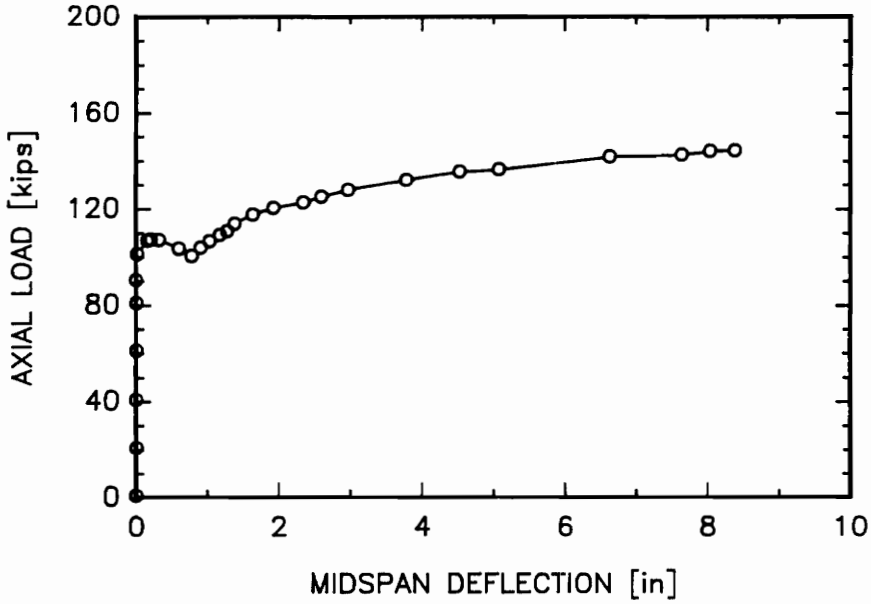

FIG. A.5 FS−1 AXIAL LOAD VS. OUTER CONDUCTOR LATERAL DEFLECTION

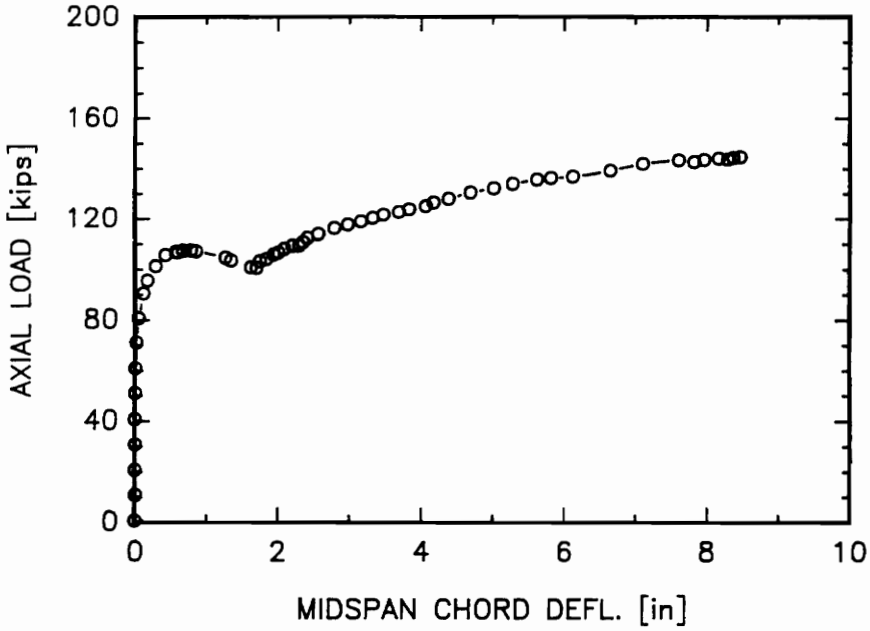

FIG. A.6 FS–1 OUTER CONDUCTOR MIDSPAN CHORD DEFLECTION

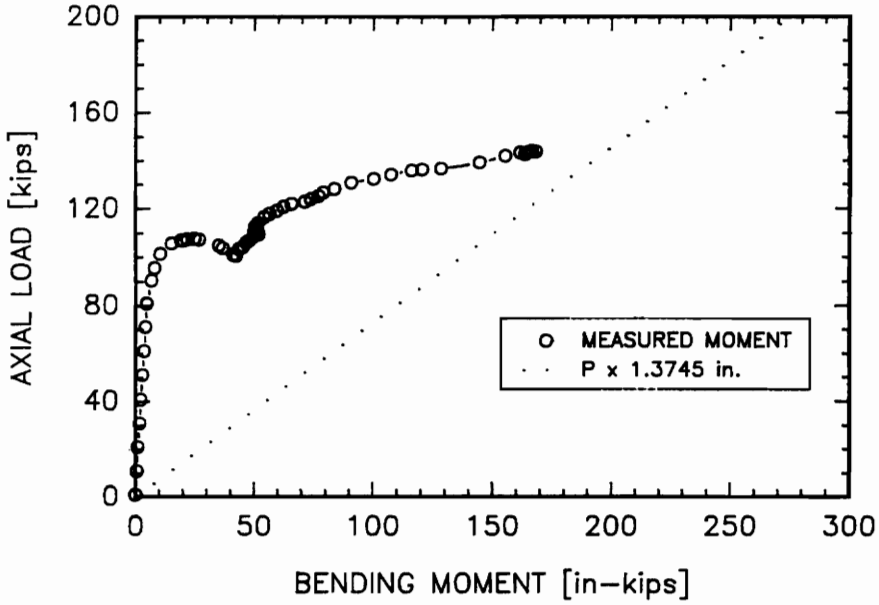

A) L = 1'-0"

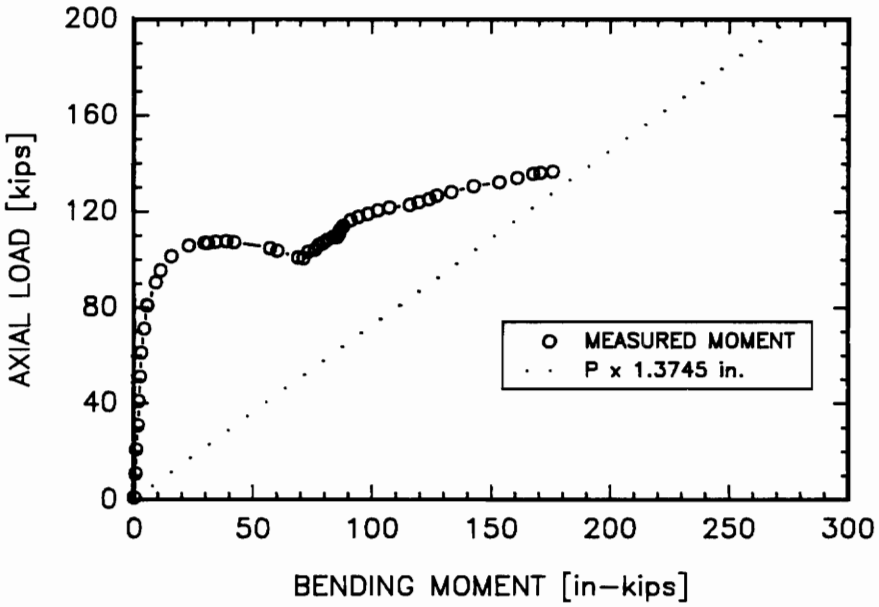

B) L = 2'-0"

FIG. A.7 FS-1 AXIAL LOAD VS. OUTER CONDUCTOR BENDING MOMENT

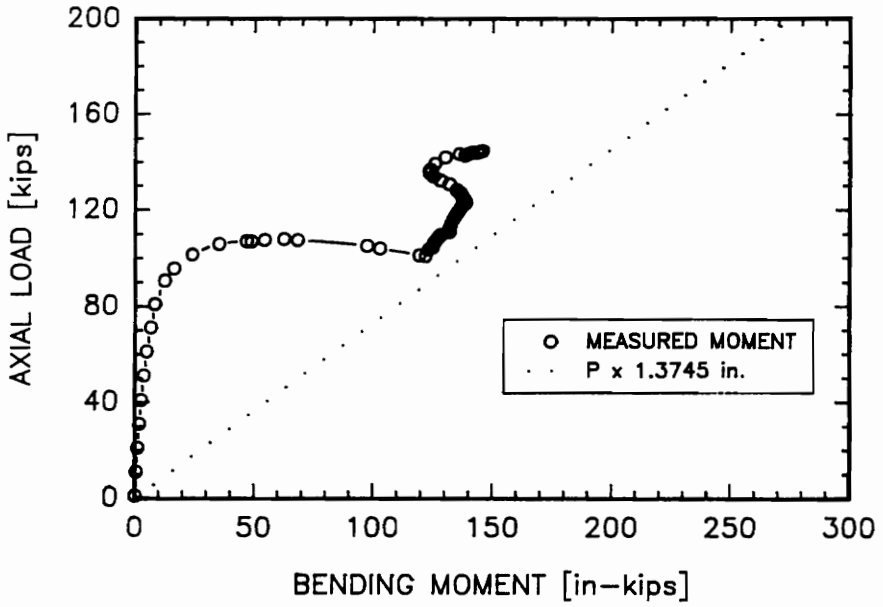

A) L = 4'-6"

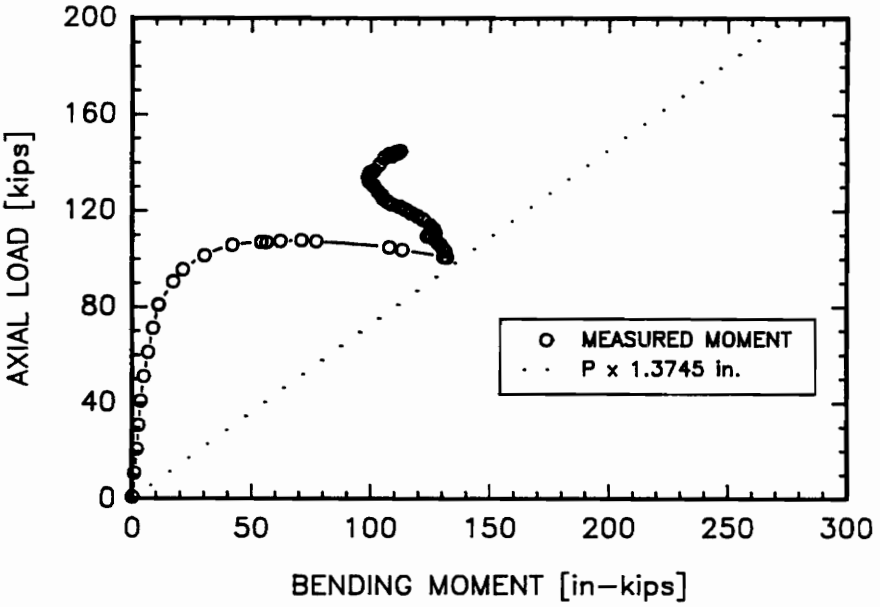

B) L = 6'-0"

FIG. A.8 FS-1 AXIAL LOAD VS. OUTER CONDUCTOR BENDING MOMENT

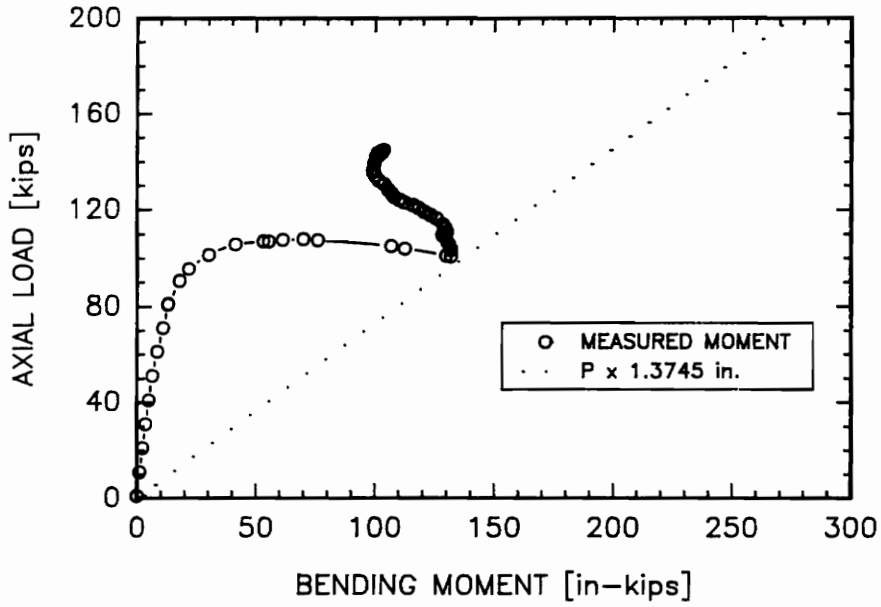

A) L = 7'-6"

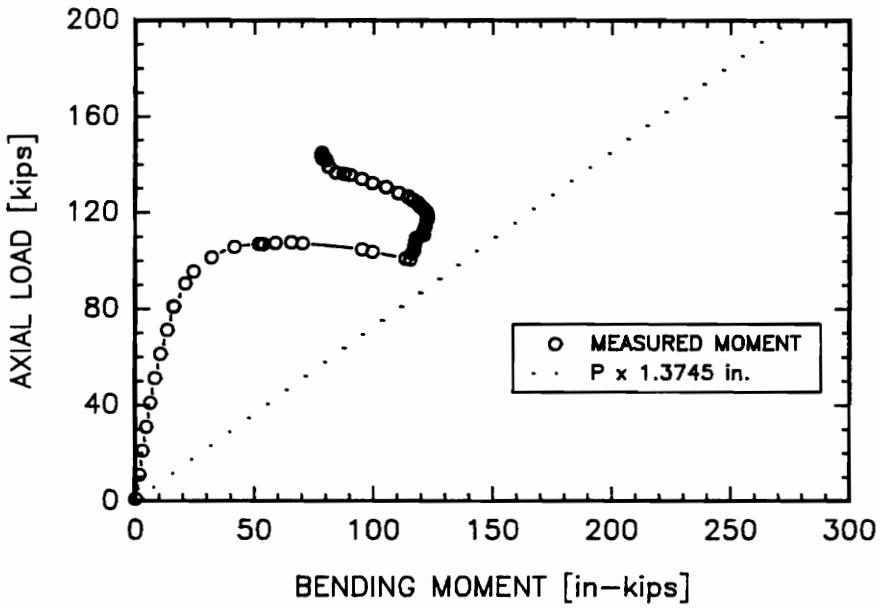

B) L = 9'-0"

FIG. A.9 FS-1 AXIAL LOAD VS. OUTER CONDUCTOR BENDING MOMENT

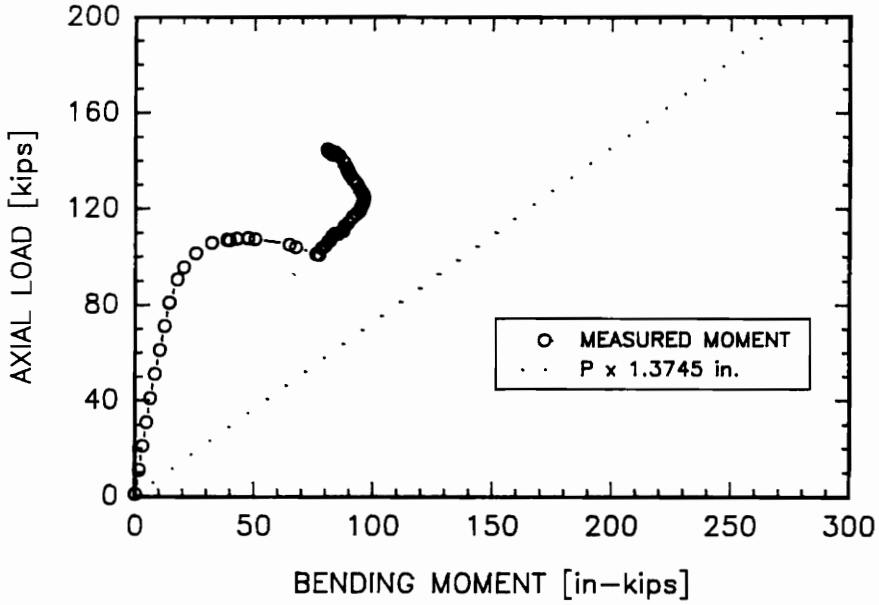

A) L = 10'-6"

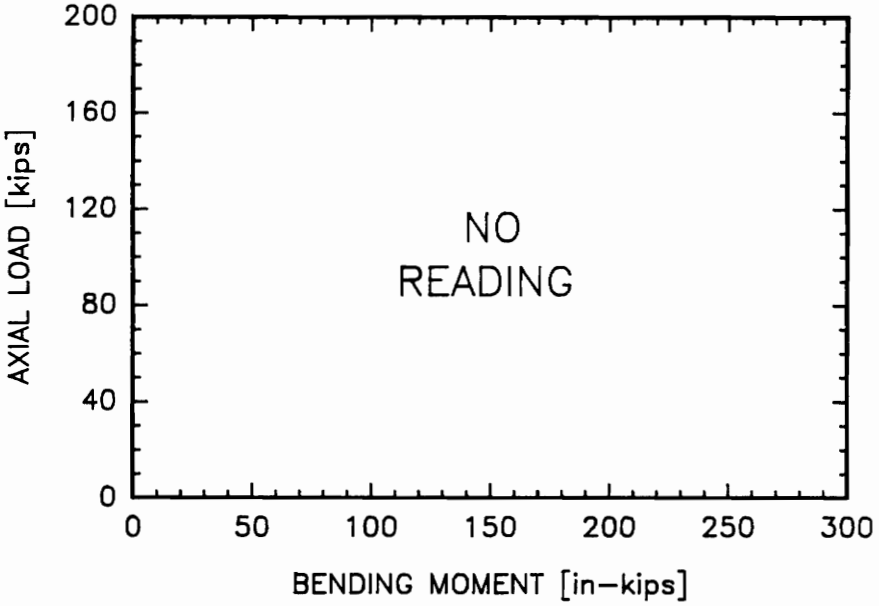

B) L = 12'-0"

FIG. A.10 FS-1 AXIAL LOAD VS. OUTER CONDUCTOR BENDING MOMENT

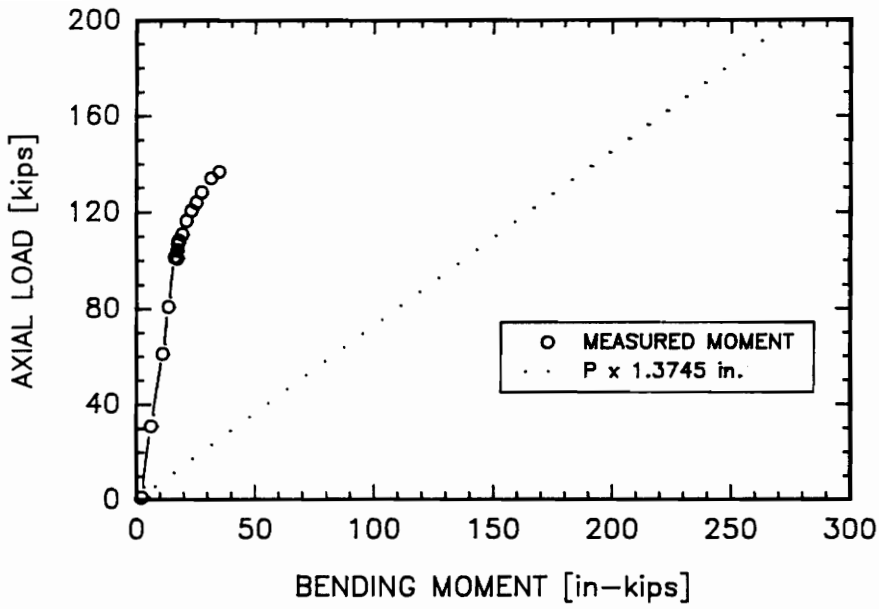

A) L = 13'-0"

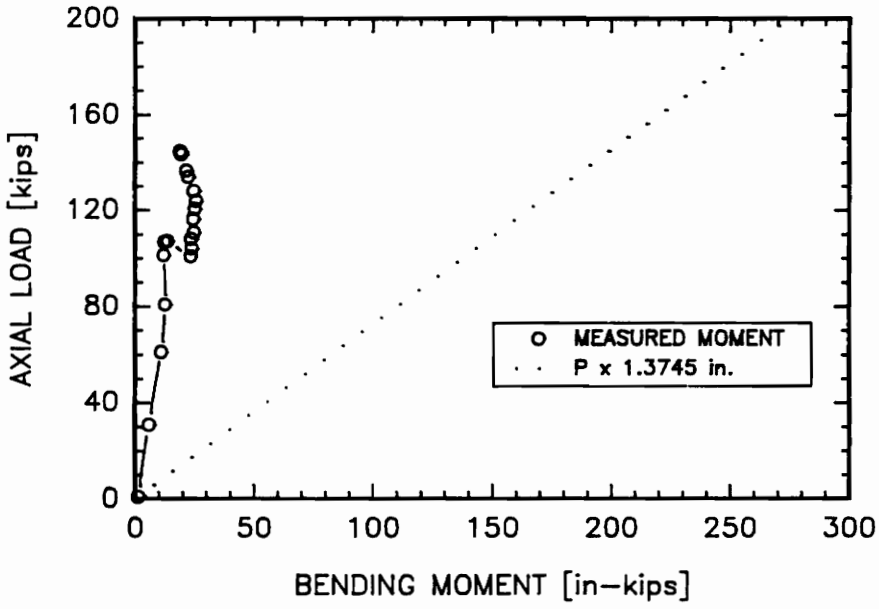

B) L = 14'-0"

FIG. A.11 FS-1 AXIAL LOAD VS. OUTER CONDUCTOR BENDING MOMENT

APPENDIX B

TEST FS-2 DATA

UNOCAL

TEST DATA SHEET

Test: UNOCAL FS-2

Test Date: July 18, 1990

Dimensions:

	Outer	Inner
Diameter (in.)	6.625	3.500
Wall Thickness (in.)	0.188	0.250
Yield Stress (ksi)	48.1	96.5

Parameters: Specimen Length = 15'-0"

Test Position - Vertical

Axial Load Only Applied

Max. Axial Load: 168.9 kips

Failure Mode: Stopped Test - Large Deflections

Predicted Failure Loads (AISC Criteria):

Stahl & Baur Method 116.6 kips

Manley Method 129.6 kips

Discussion:

- Specimen first reached relative maximum load of 108.8 kips, after which load dropped off to 106.4 kips.
- Specimen continued to hold increasing amount of load up to 168.9 kips.
- Maximum lateral deflection at tip of specimen = 33.2 in.

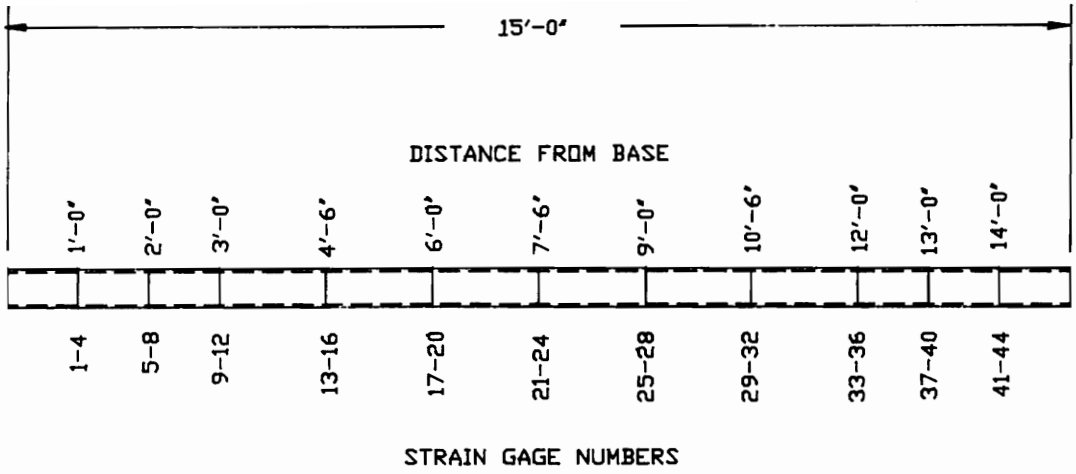

A) 6-5/8" OUTER CONDUCTOR PIPE

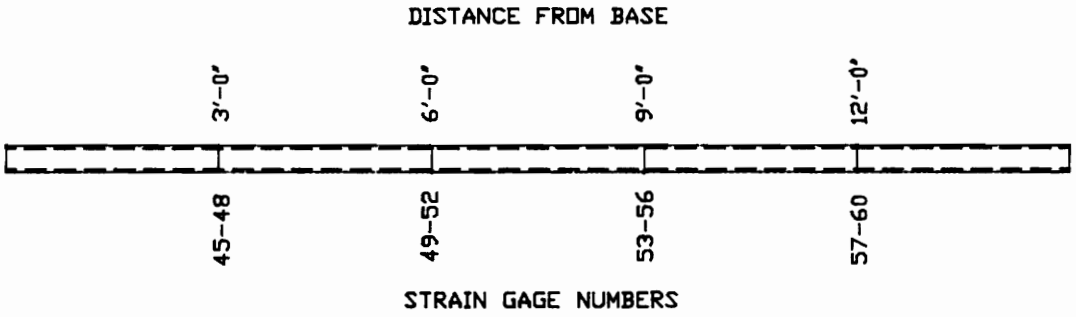

B) 3-1/2" INNER CASING PIPE

FIG. B.1 FS-2 STRAIN GAGE LOCATIONS

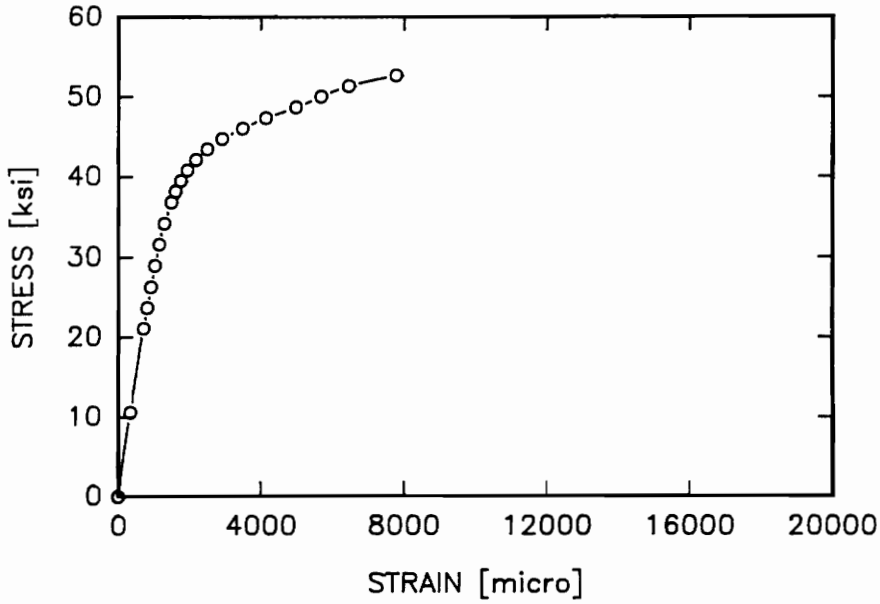

A) STUB COLUMN RESULTS

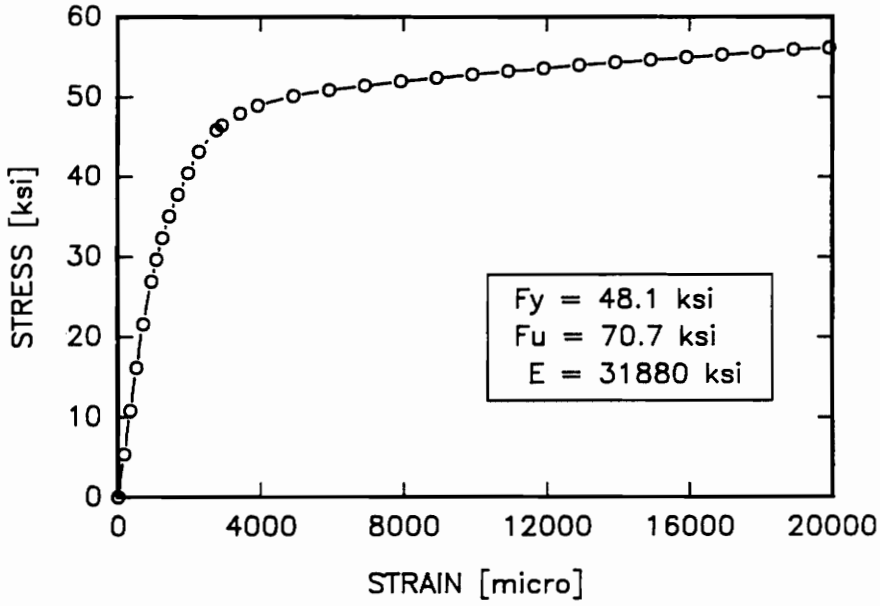

B) TENSILE COUPON RESULTS

FIG. B.2 FS–2 OUTER CONDUCTOR MATERIAL PROPERTIES

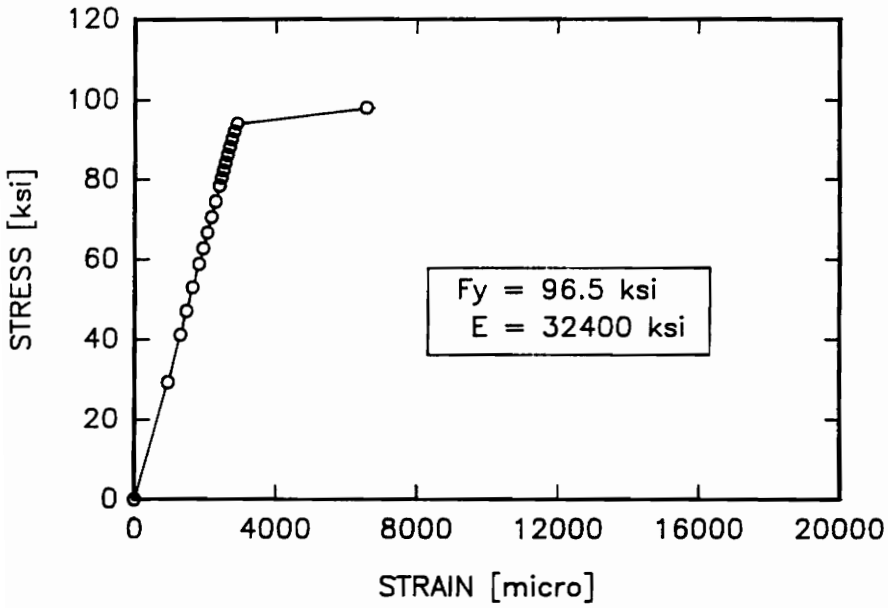

FIG. B.3 FS–2 INNER CASING MATERIAL PROPERTIES

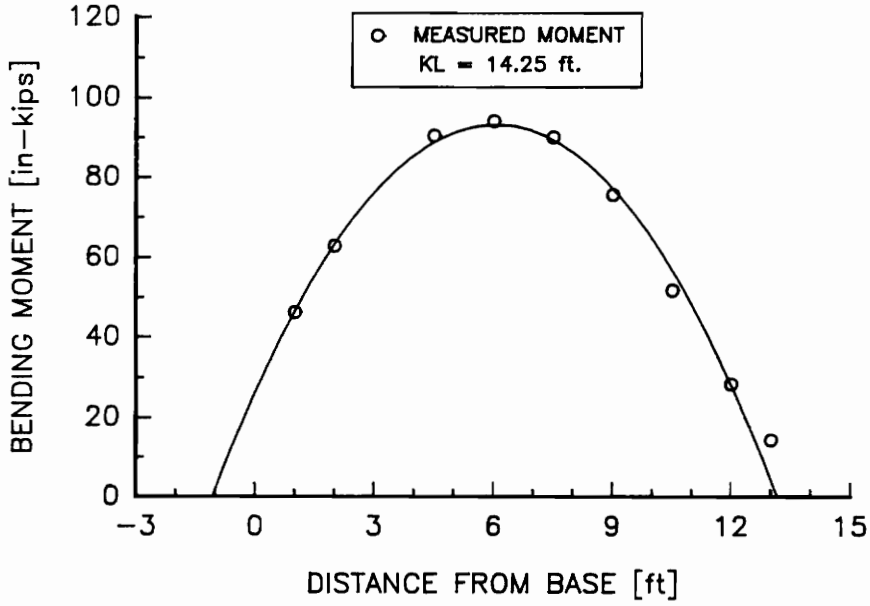

FIG. B.4 FS-2 BENDING MOMENT OVER THE LENGTH OF THE OUTER CONDUCTOR AT LOAD POINT 14.

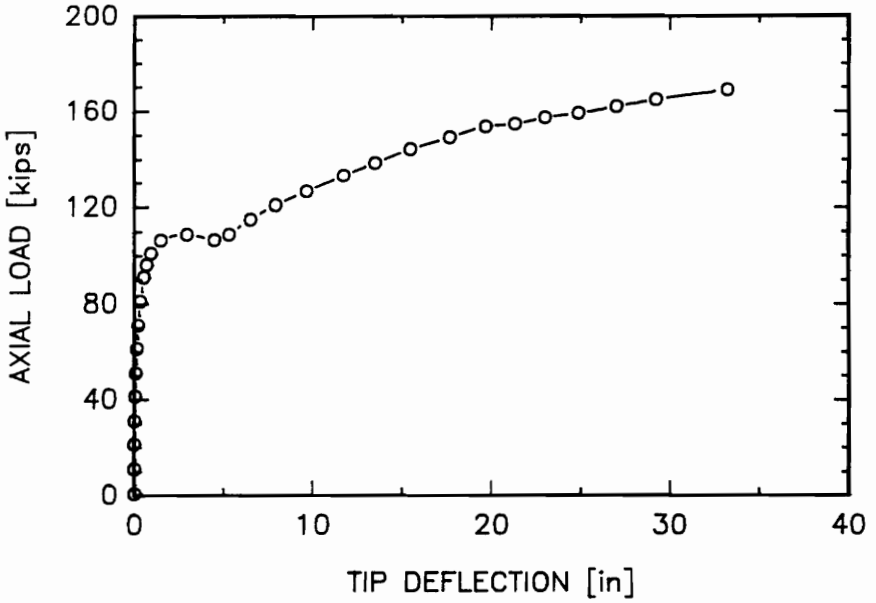

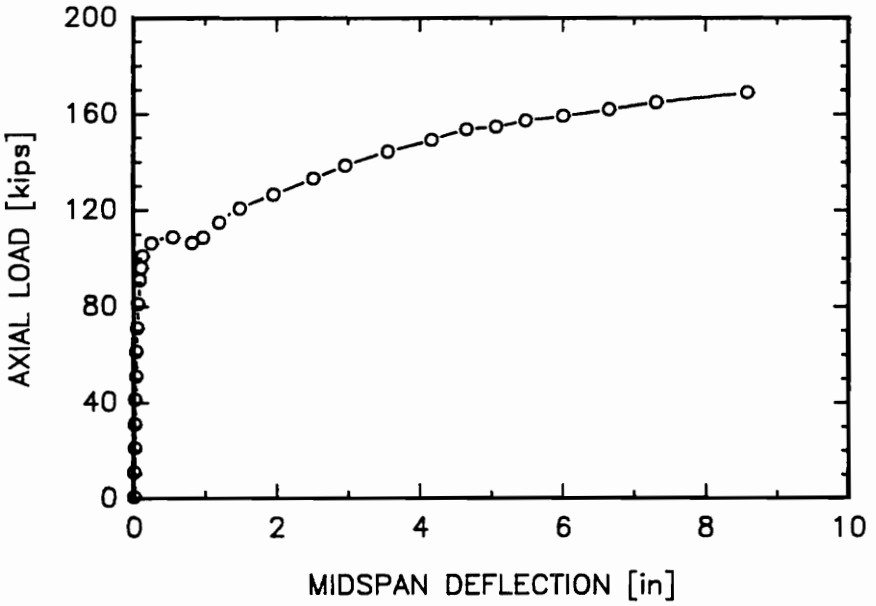

FIG. B.5 FS−2 AXIAL LOAD VS. OUTER CONDUCTOR LATERAL DEFLECTION

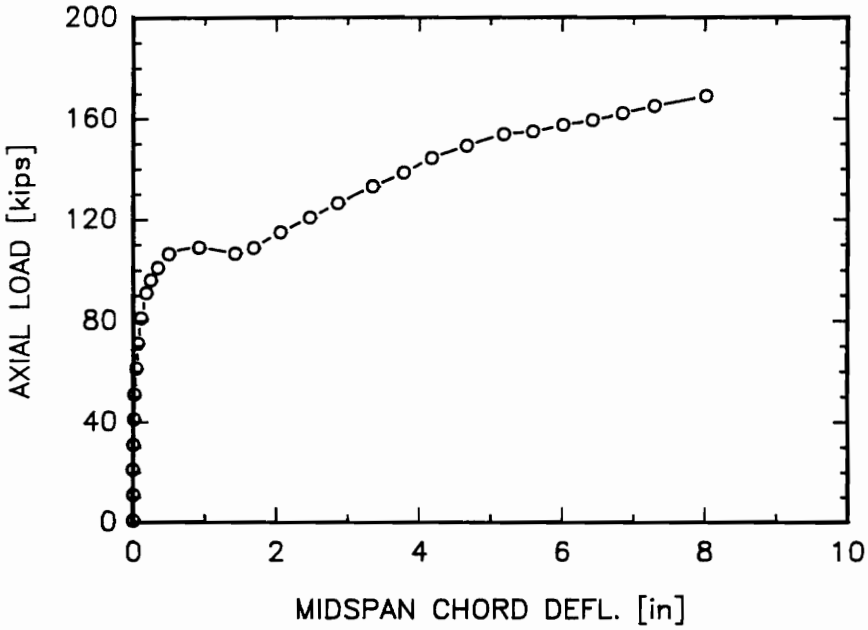

FIG. B.6 FS–2 OUTER CONDUCTOR MIDSPAN CHORD DEFLECTION

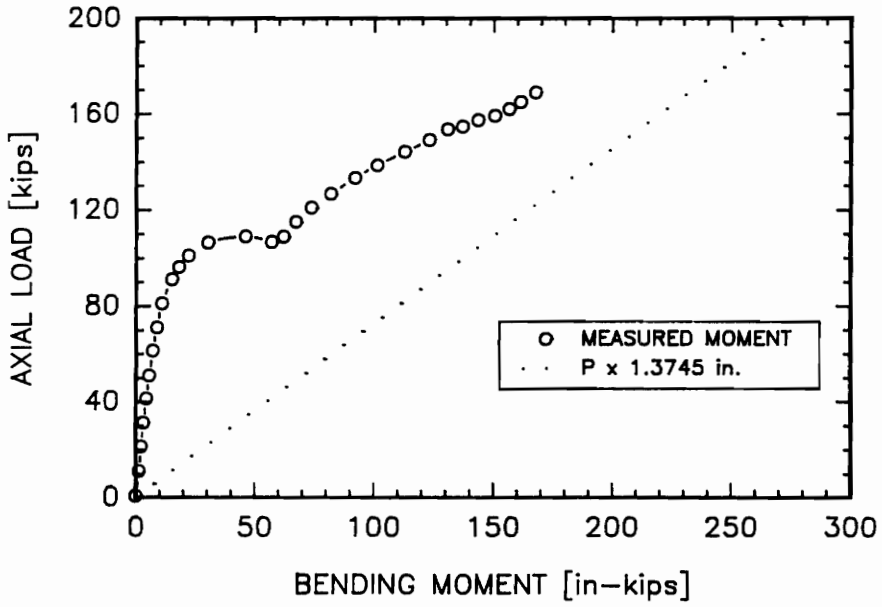

A) L = 1'-0"

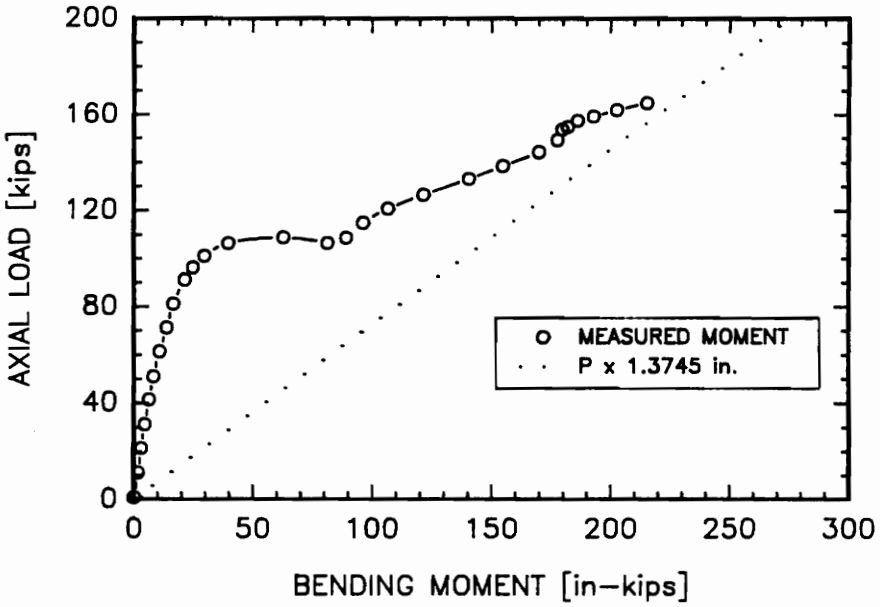

B) L = 2'-0"

FIG. B.7 FS-2 AXIAL LOAD VS. OUTER CONDUCTOR BENDING MOMENT

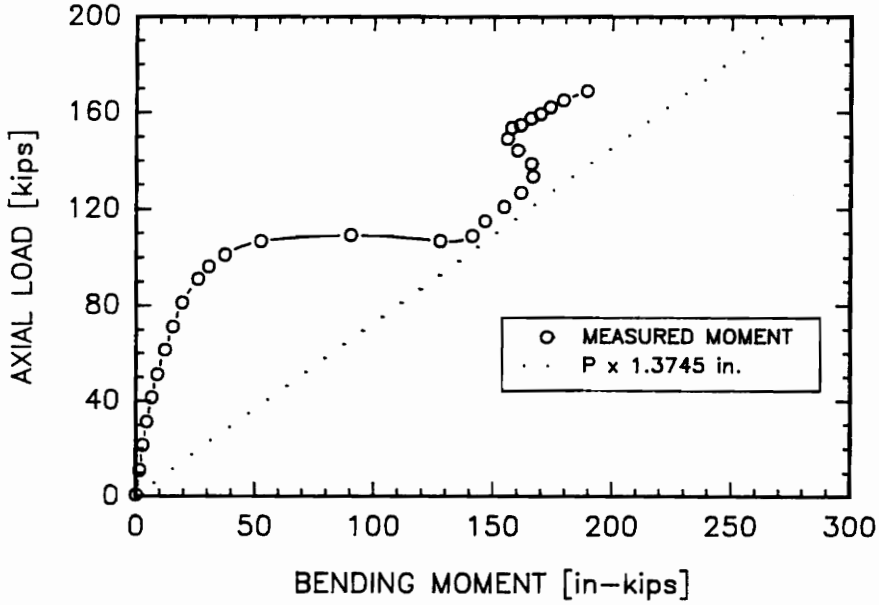

A) L = 4'-6"

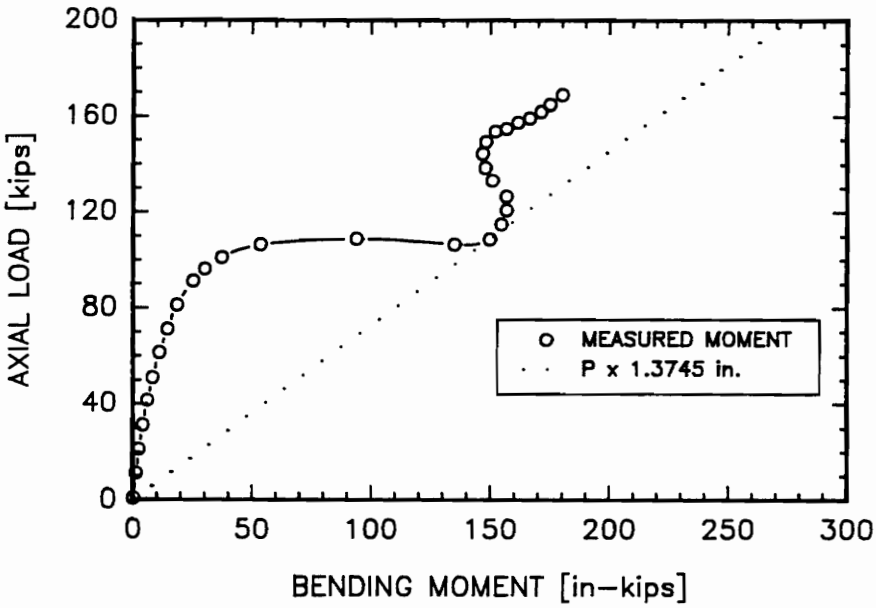

B) L = 6'-0"

FIG. B.8 FS-2 AXIAL LOAD VS. OUTER CONDUCTOR BENDING MOMENT

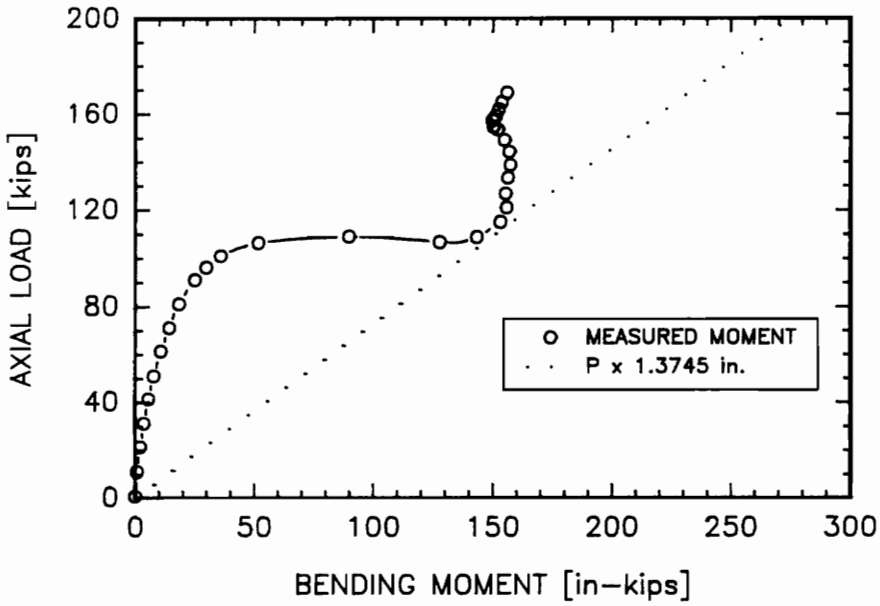

A) L = 7'-6"

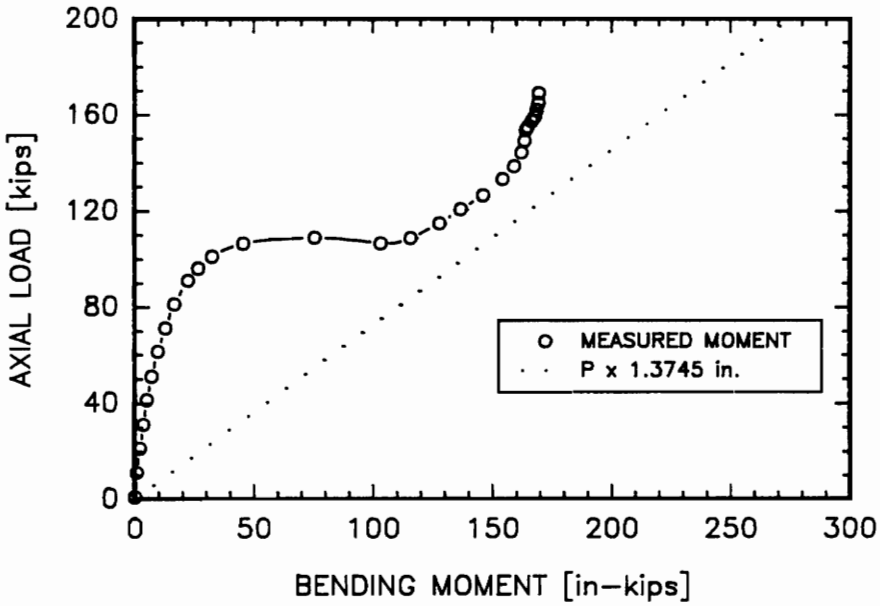

B) L = 9'-0"

FIG. B.9 FS-2 AXIAL LOAD VS. OUTER CONDUCTOR BENDING MOMENT

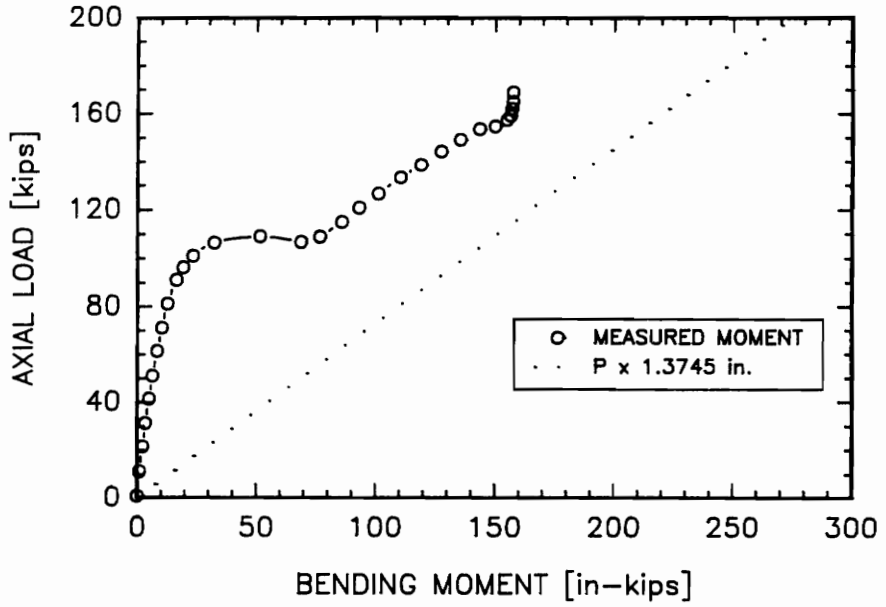

A) L = 10'-6"

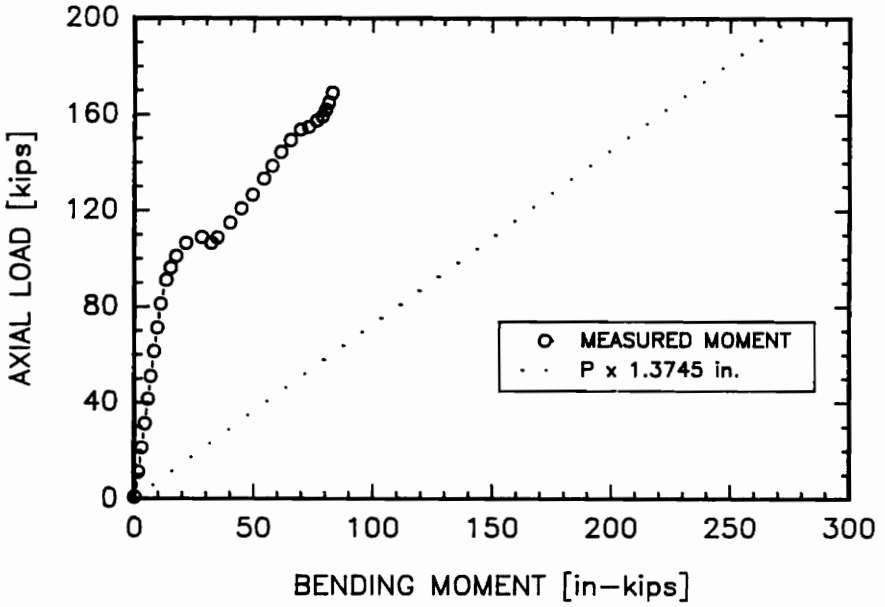

B) L = 12'-0"

FIG. B.10 FS-2 AXIAL LOAD VS. OUTER CONDUCTOR BENDING MOMENT

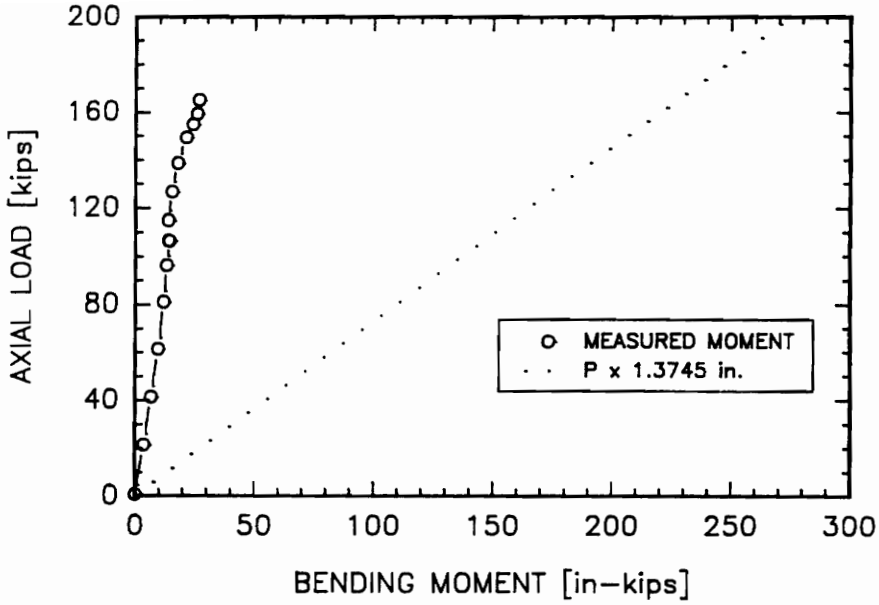

A) L = 13'-0"

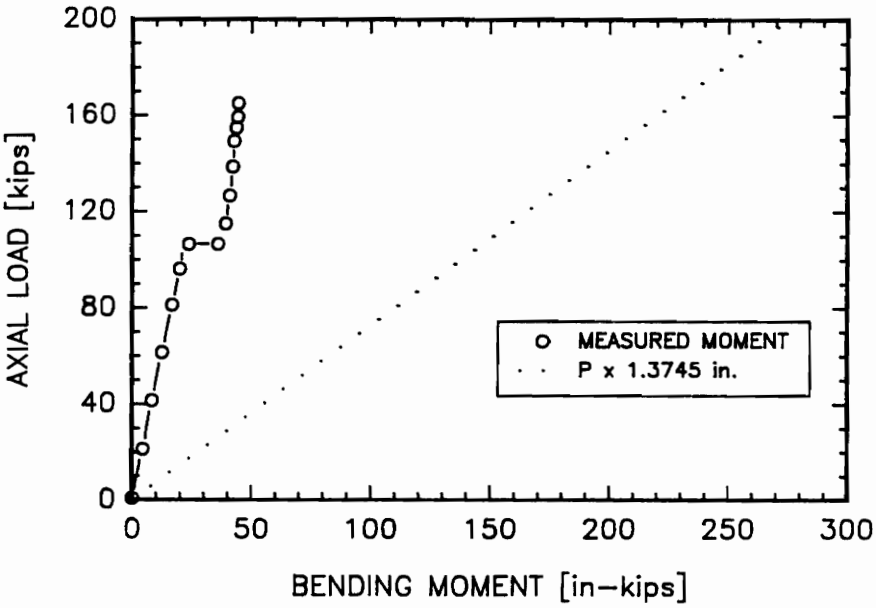

B) L = 14'-0"

FIG. B.11 FS-2 AXIAL LOAD VS. OUTER CONDUCTOR BENDING MOMENT

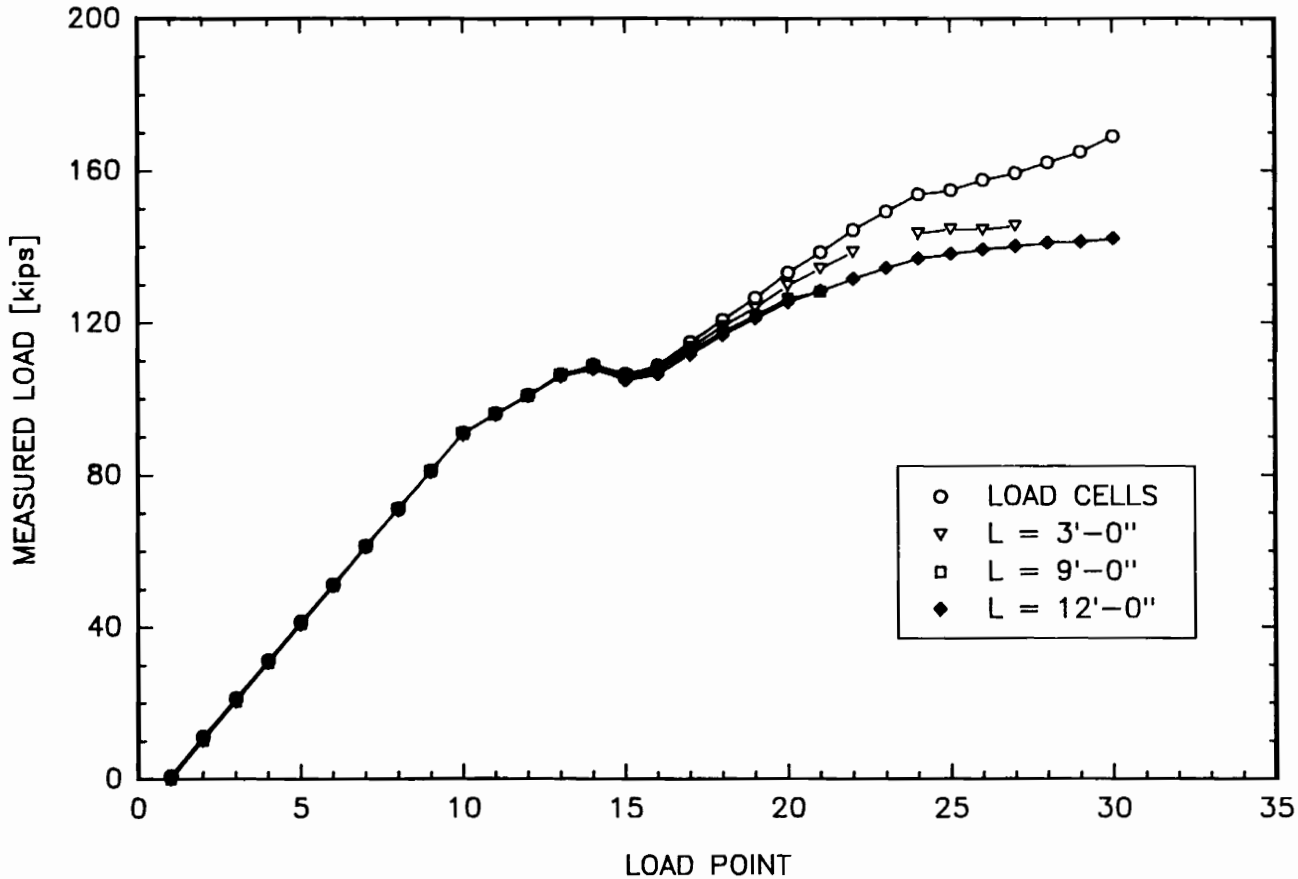

FIG. B.12 FS-2 MEASURED AXIAL LOAD IN INNER CASING

APPENDIX C

TEST FS-3 DATA

UNOCAL

TEST DATA SHEET

Test: UNOCAL FS-3

Test Date: August 1, 1990

Dimensions:

	Outer	Inner
Diameter (in.)	6.625	3.500
Wall Thickness (in.)	0.188	0.250
Yield Stress (ksi)	46.3	106.5

Parameters: Specimen Length = 13'-11"

Test Position - Vertical

Axial Load Only Applied

Max. Axial Load: 178.7 kips

Failure Mode: Stopped Test - Large Deflections

Predicted Failure Loads (AISC Criteria):

Stahl & Baur Method 112.2 kips

Manley Method 127.4 kips

Discussion:

- Inner rod made as eccentric as possible at the tip of the specimen.
- Appears as though relative maximum would have been reached at approximately 110 kips.
- Specimen continued to hold increasing amount of load up to 178.7 kips.
- Total lateral deflection at tip of specimen > 40 in.

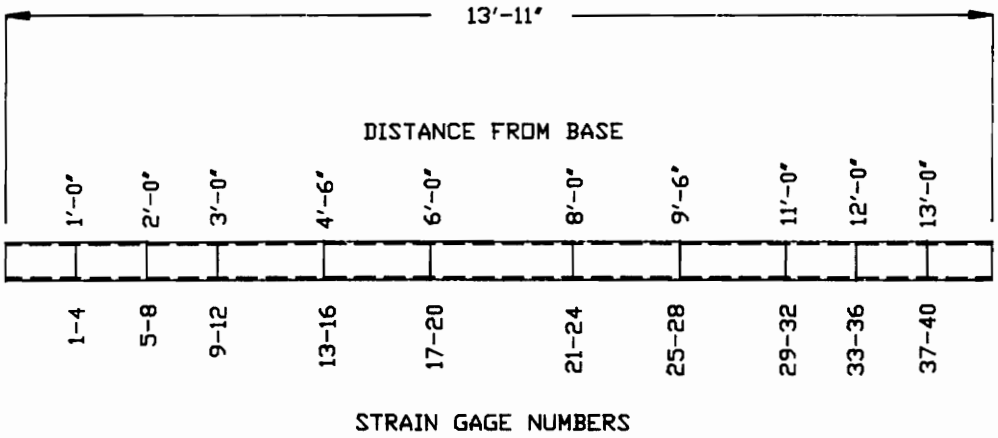

A) 6-5/8" OUTER CONDUCTOR PIPE

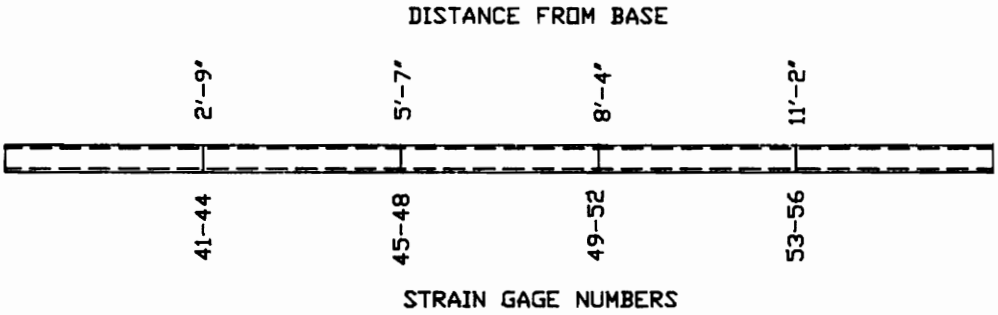

B) 3-1/2" INNER CASING PIPE

FIG. C.1 FS-3 STRAIN GAGE LOCATIONS

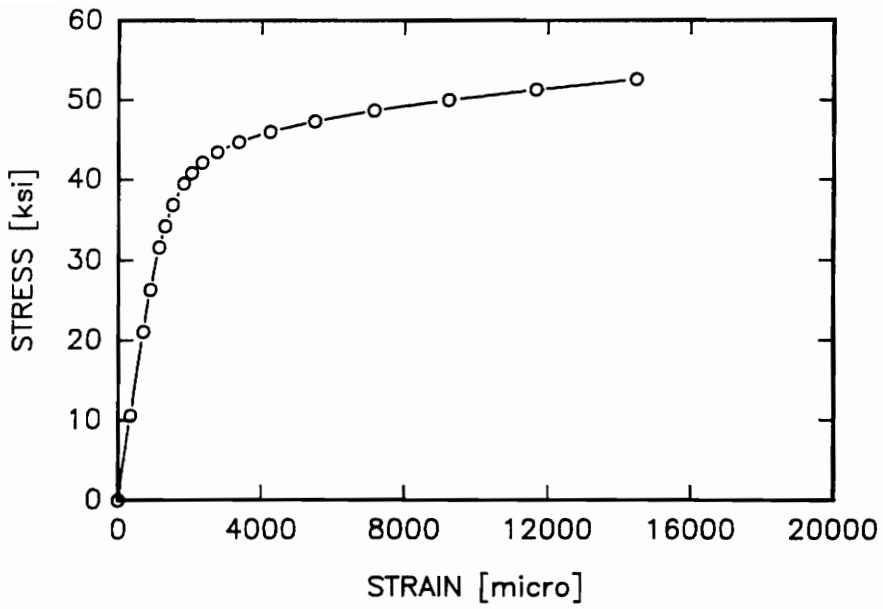

A) STUB COLUMN RESULTS

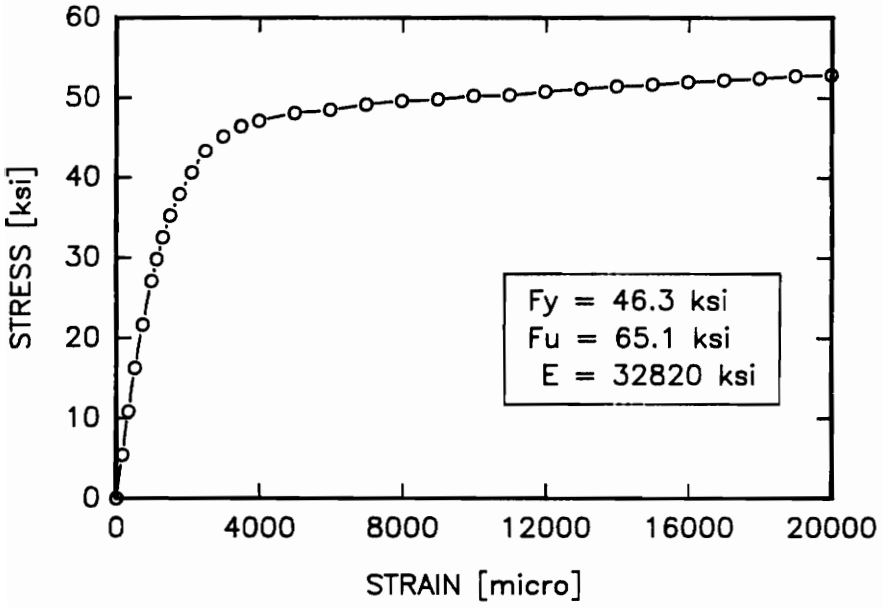

B) TENSILE COUPON RESULTS

FIG. C.2 FS–3 OUTER CONDUCTOR MATERIAL PROPERTIES

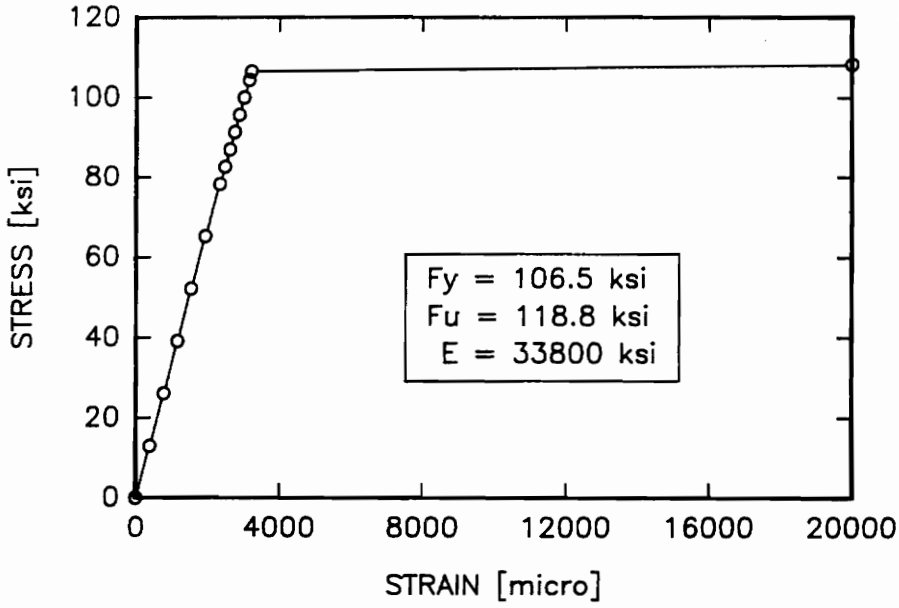

FIG. C.3 FS–3 INNER CASING MATERIAL PROPERTIES

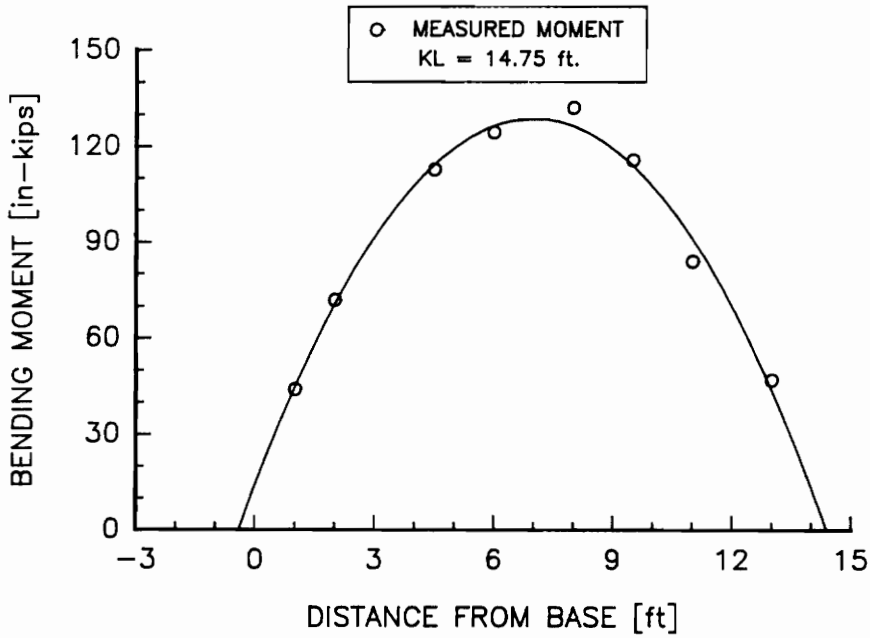

FIG. C.4 FS-3 BENDING MOMENT OVER THE LENGTH OF THE OUTER CONDUCTOR AT LOAD POINT 15.

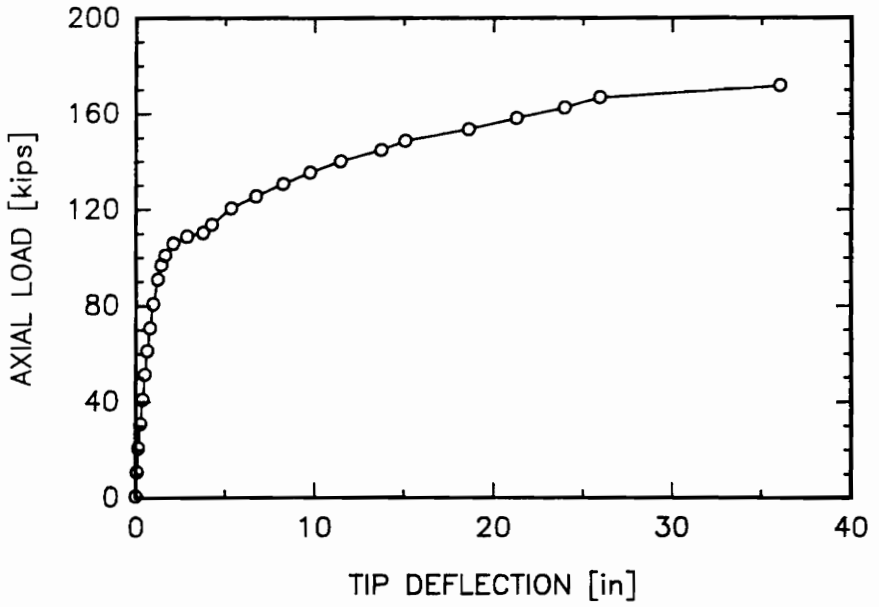

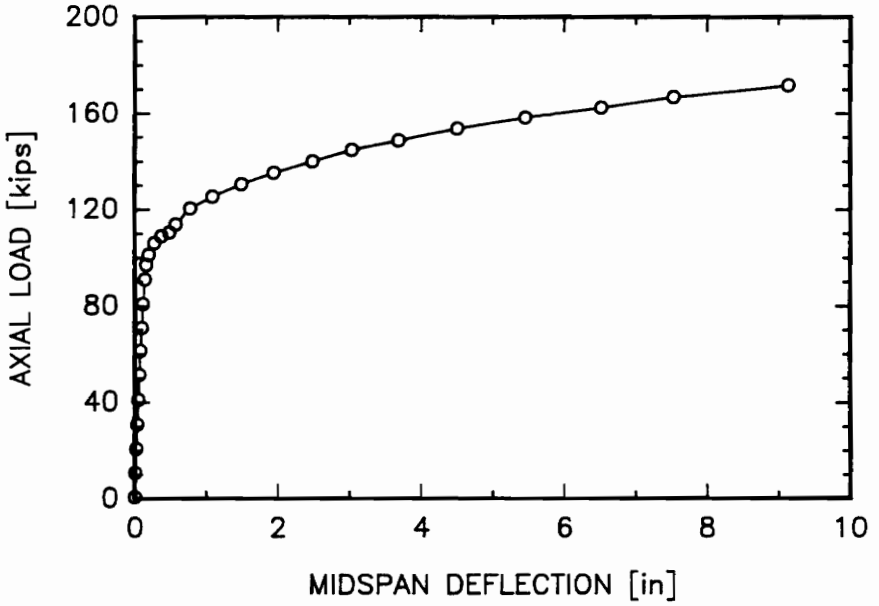

FIG. C.5 FS–3 AXIAL LOAD VS. OUTER CONDUCTOR LATERAL DEFLECTION

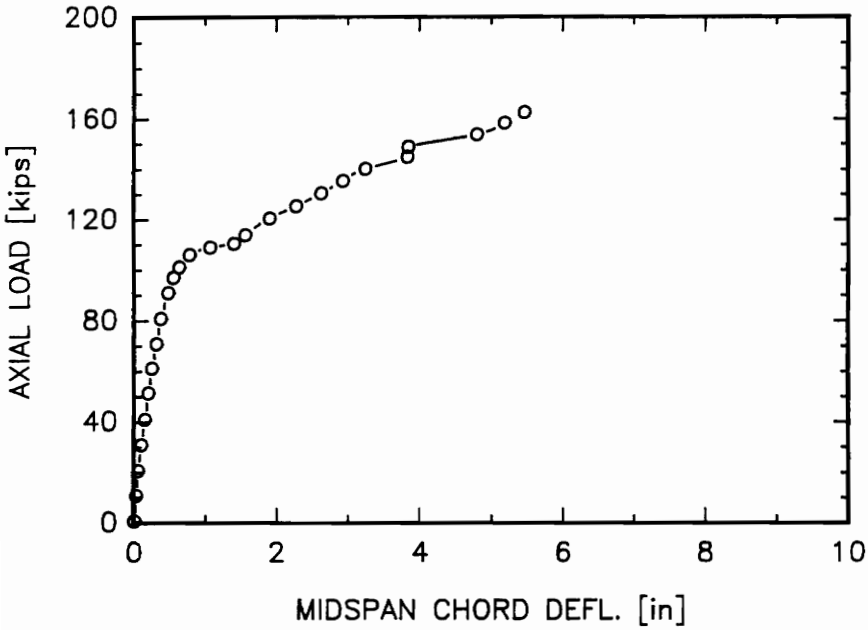

FIG. C.6 FS–3 OUTER CONDUCTOR MIDSPAN CHORD DEFLECTION

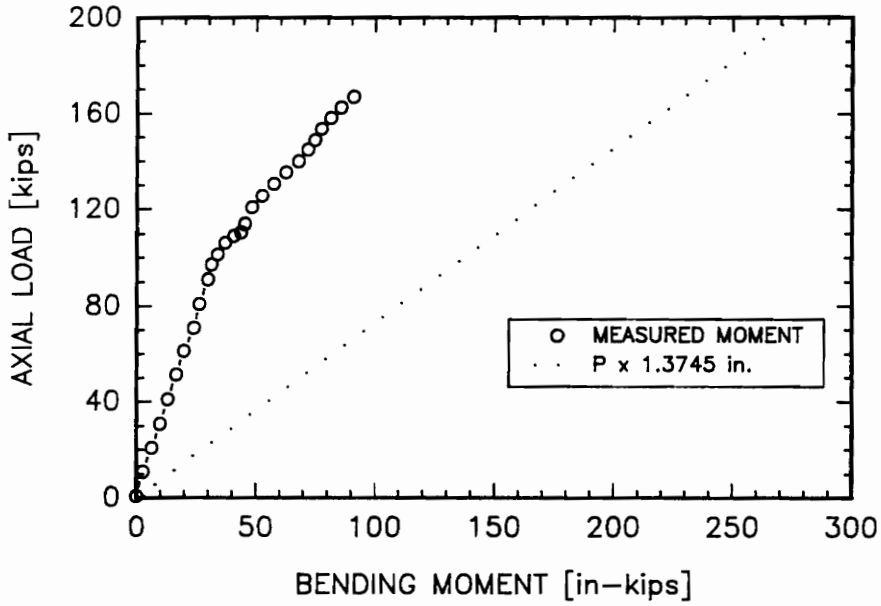

A) L = 1'-0"

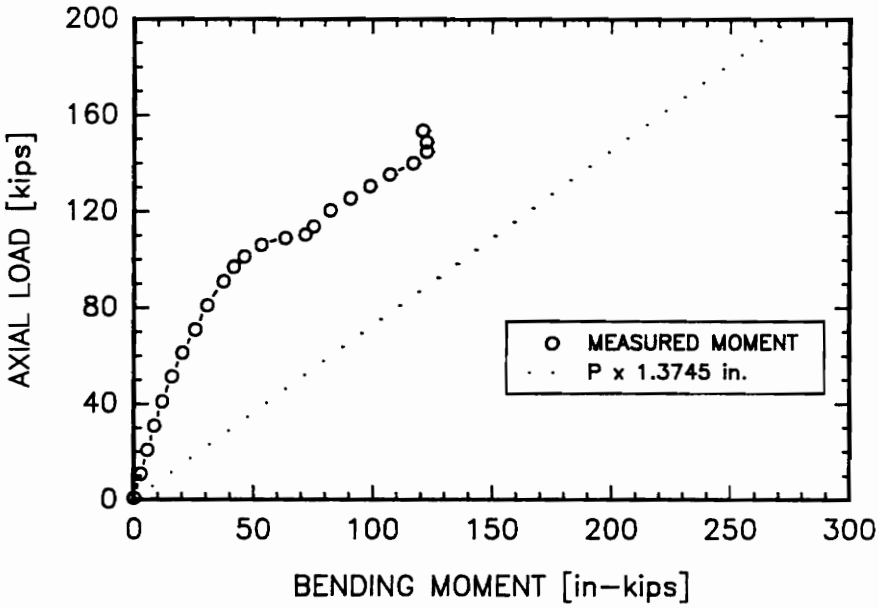

B) L = 2'-0"

FIG. C.7 FS-3 AXIAL LOAD VS. OUTER CONDUCTOR BENDING MOMENT

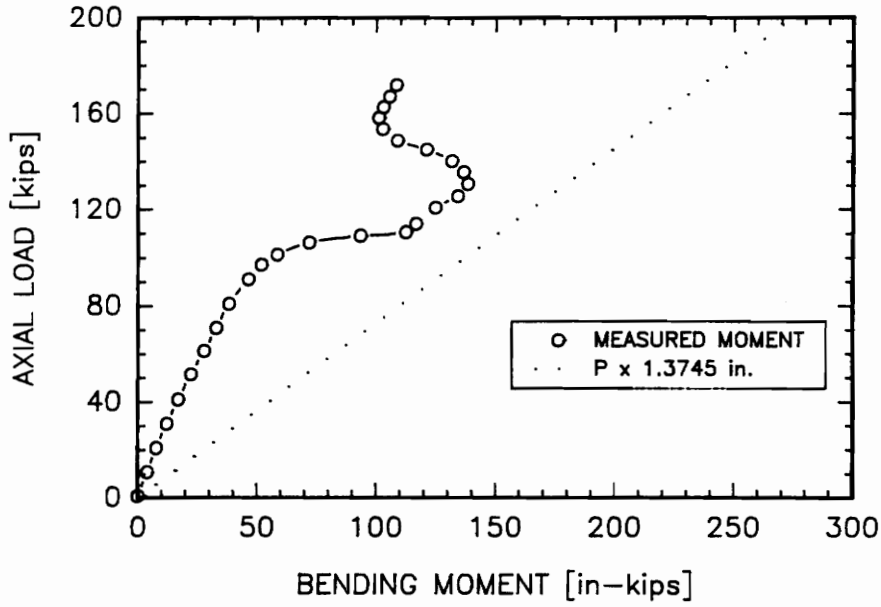

A) L = 4'-6"

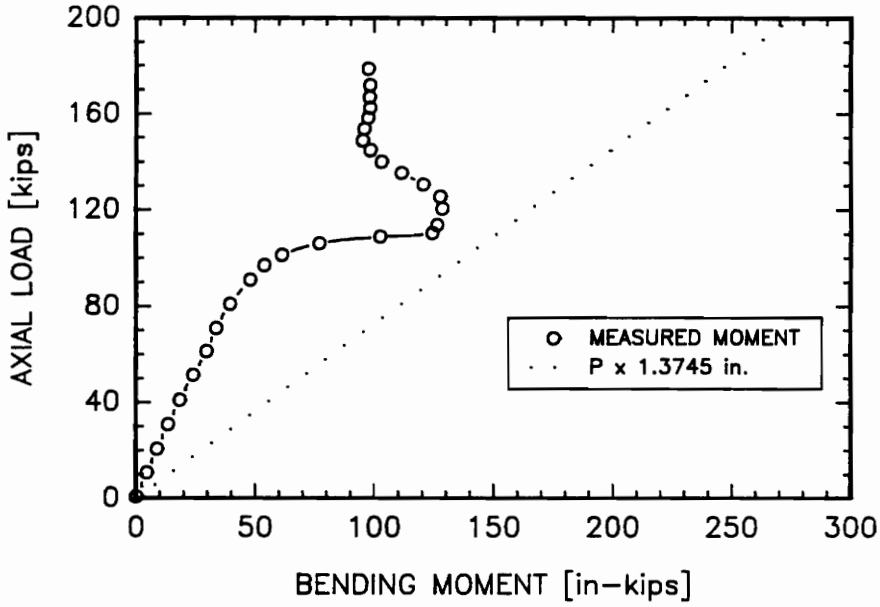

B) L = 6'-0"

FIG. C.8 FS-3 AXIAL LOAD VS. OUTER CONDUCTOR BENDING MOMENT

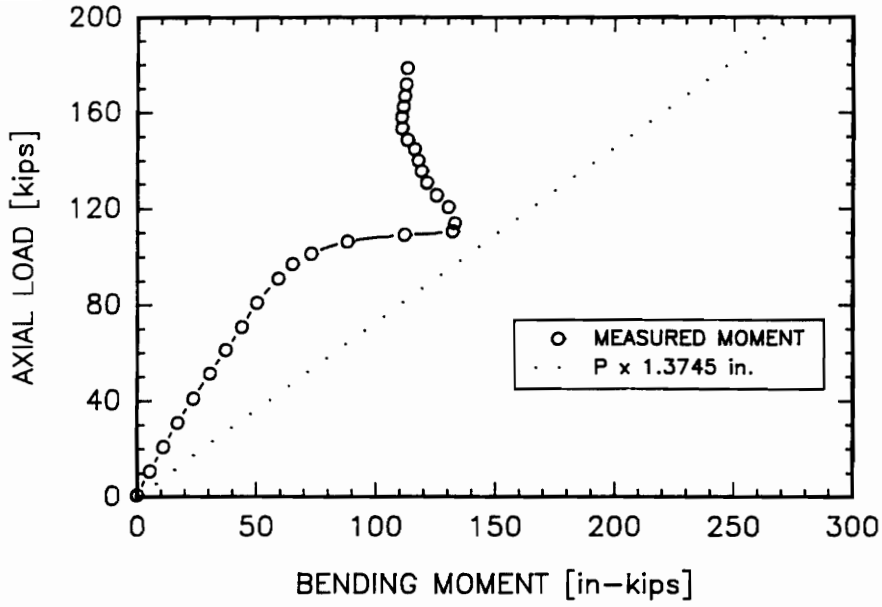

A) L = 8'-0"

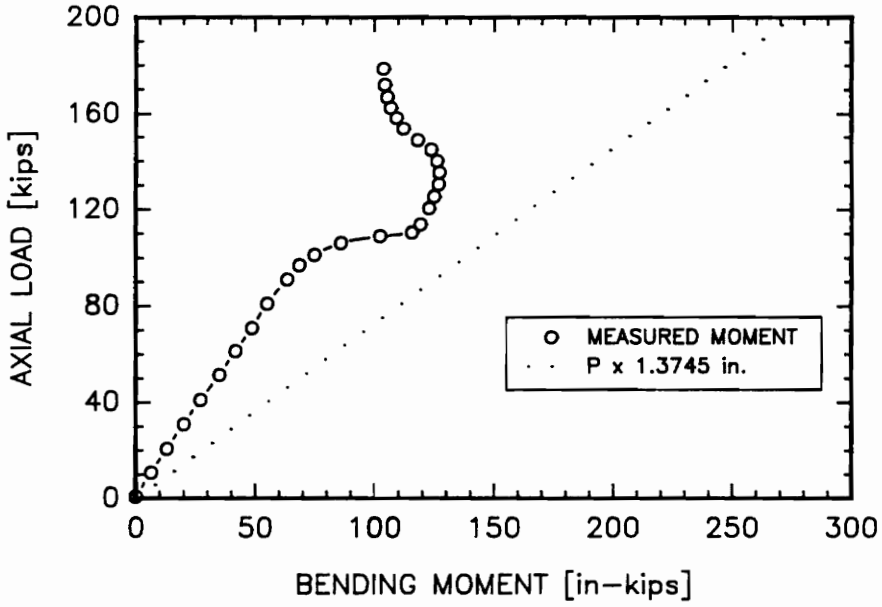

B) L = 9'-6"

FIG. C.9 FS-3 AXIAL LOAD VS. OUTER CONDUCTOR BENDING MOMENT

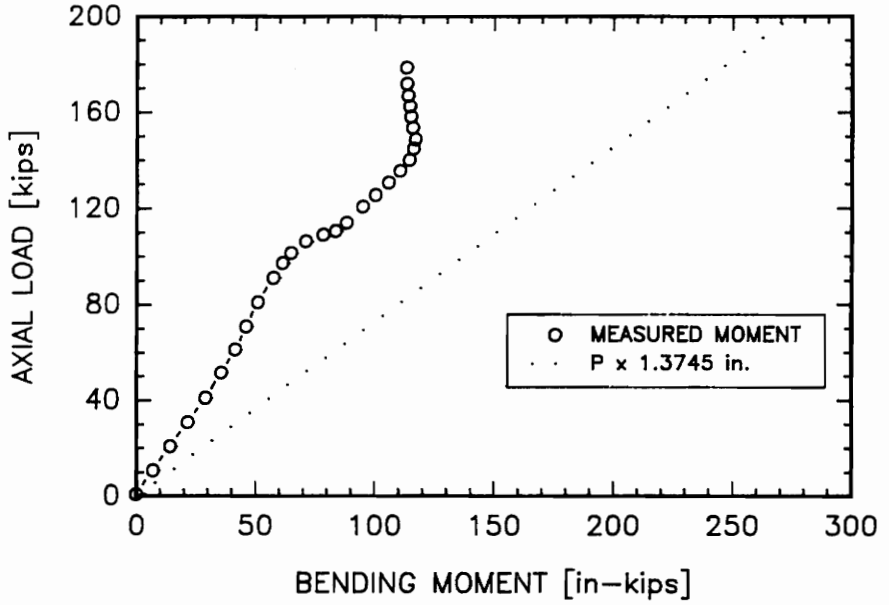

A) L = 11'-0"

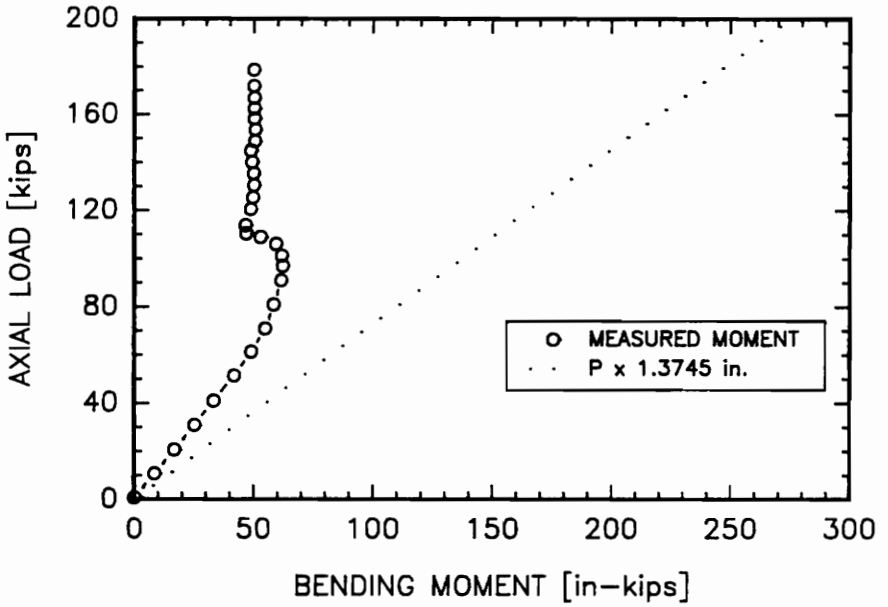

B) L = 13'-0"

FIG. C.10 FS-3 AXIAL LOAD VS. OUTER CONDUCTOR BENDING MOMENT

APPENDIX D

TEST FS-4 DATA

UNOCAL

TEST DATA SHEET

Test: UNOCAL FS-4

Test Date: September 27, 1990

Dimensions:

	Outer	Inner
Diameter (in.)	6.625	3.500
Wall Thickness (in.)	0.188	0.250
Yield Stress (ksi)	48.1	90.3

Parameters: Specimen Length = 13'-0"

Test Position - Horizontal

0.920 kips applied laterally at tip

Total applied moment is equal to 44% of outer pipe capacity and 27% of the capacity of both pipes.

Max. Axial Load: 145.5 kips

Failure Mode: Stopped Test - Large Deflections

Predicted Failure Loads (AISC Criteria):

Stahl & Baur Method 72.8 kips

Manley Method 96.8 kips

Discussion:

- Incrementally applied 0.920 kips of weight laterally at tip of cantilever, then applied axial load until failure.
- Specimen appeared to have reached relative maximum at approximately 82 kips of axial load.
- Continued to hold load up to maximum load of 145.5 kips.
- Maximum lateral deflection at tip of specimen = 30.0 in.

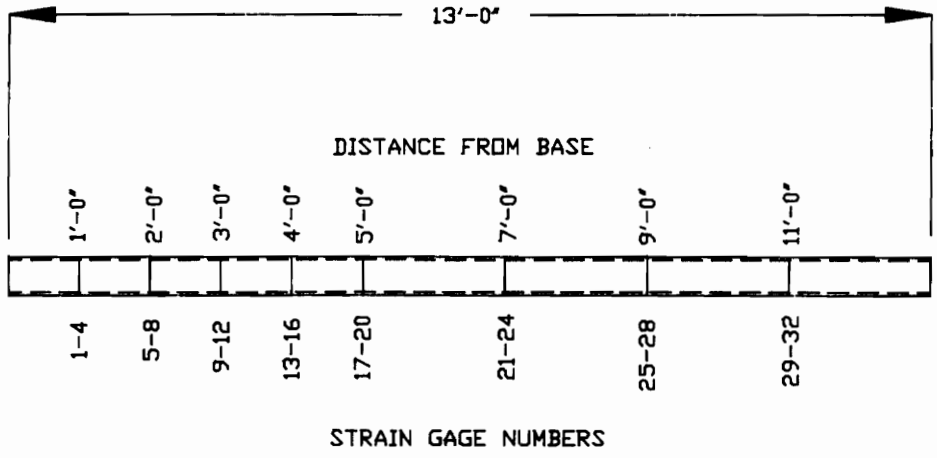

A) 6-5/8" OUTER CONDUCTOR PIPE

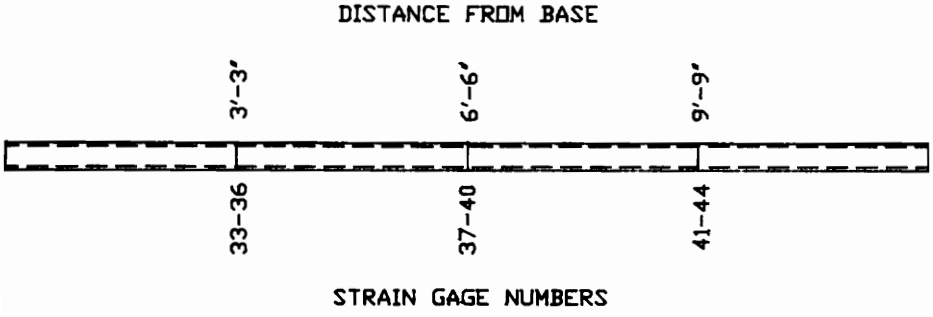

B) 3-1/2" INNER CASING PIPE

FIG. D.1 FS-4 STRAIN GAGE LOCATIONS

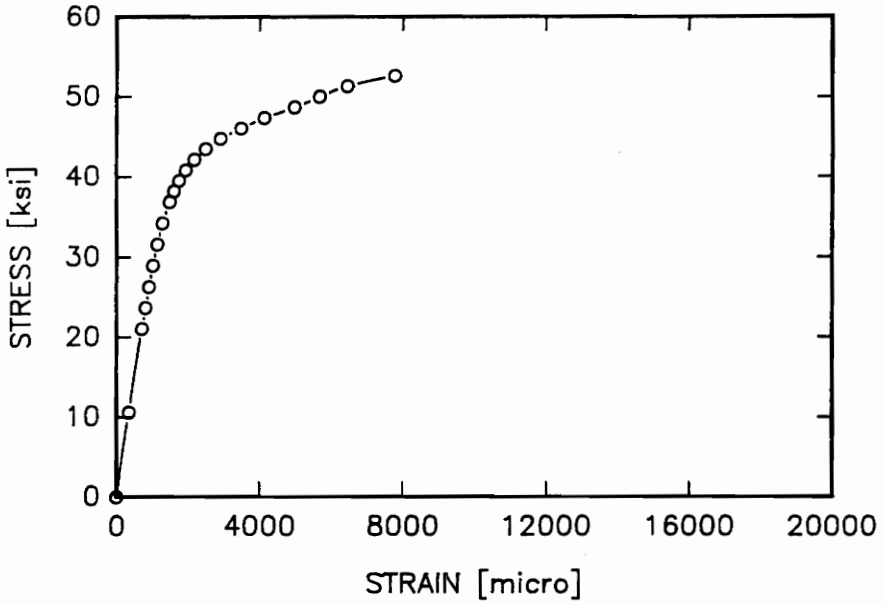

A) STUB COLUMN RESULTS

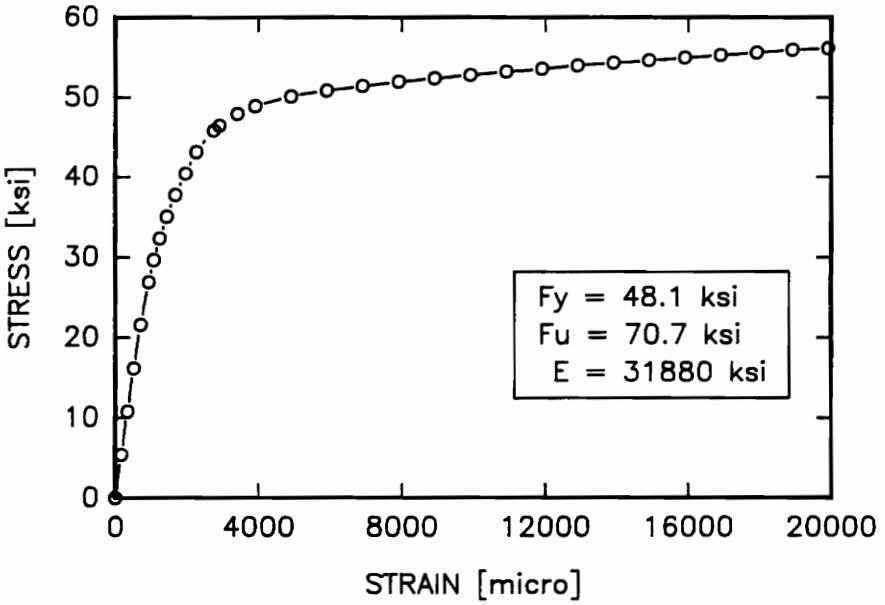

B) TENSILE COUPON RESULTS

FIG. D.2 FS–4 OUTER CONDUCTOR MATERIAL PROPERTIES

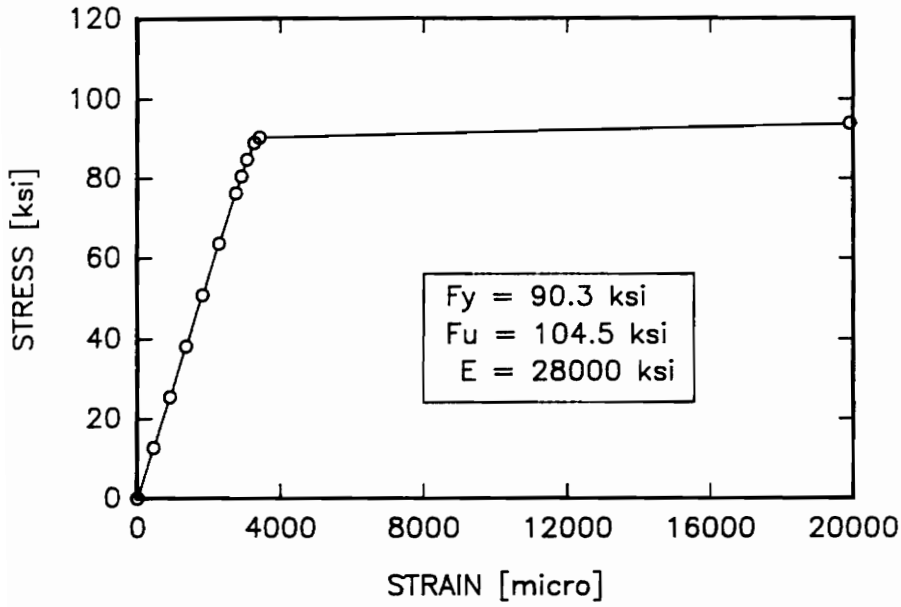

FIG. D.3 FS–4 INNER CASING MATERIAL PROPERTIES

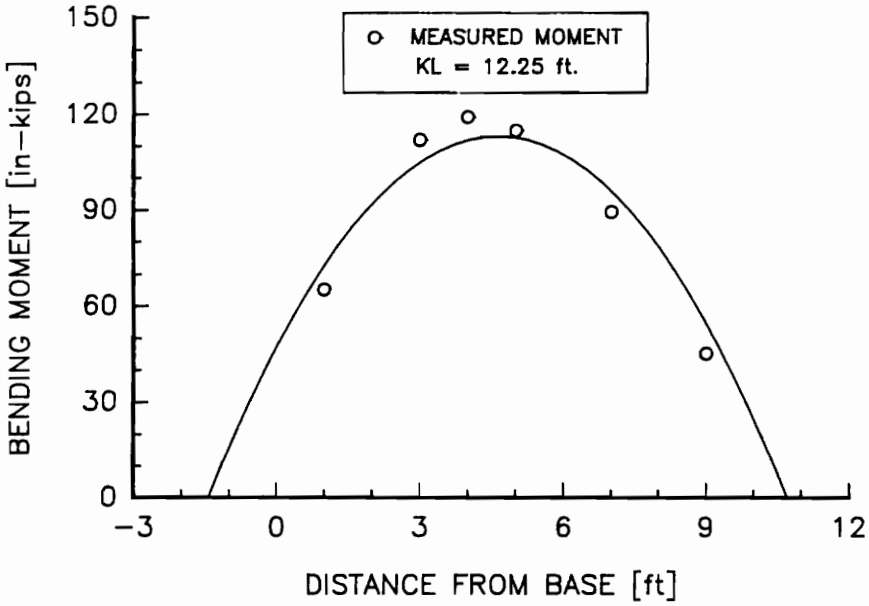

NOTE: THE BENDING MOMENT SHOWN HAS BEEN ADJUSTED TO REMOVE THE EFFECTS OF THE APPLIED LATERAL LOADING.

FIG. D.4 FS-4 BENDING MOMENT OVER THE LENGTH OF THE OUTER CONDUCTOR AT LOAD POINT 15.

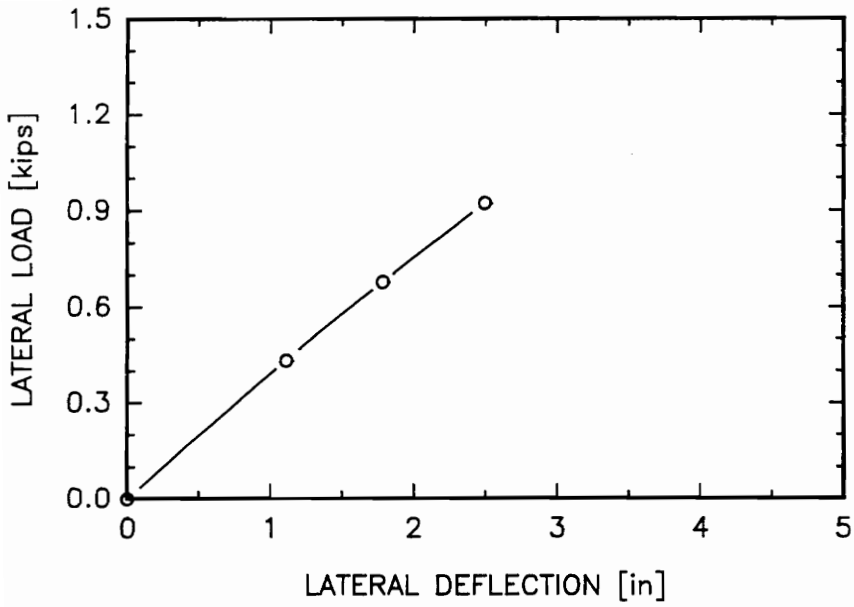

A) TIP DEFLECTION

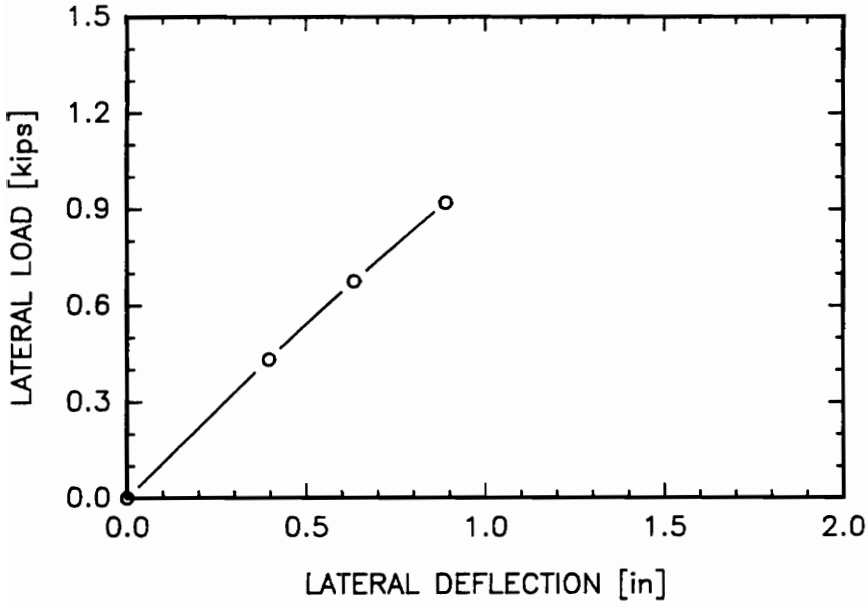

B) MIDSPAN DEFLECTION

FIG. D.5 FS–4 LATERAL LOAD VS. OUTER CONDUCTOR LATERAL DEFLECTION

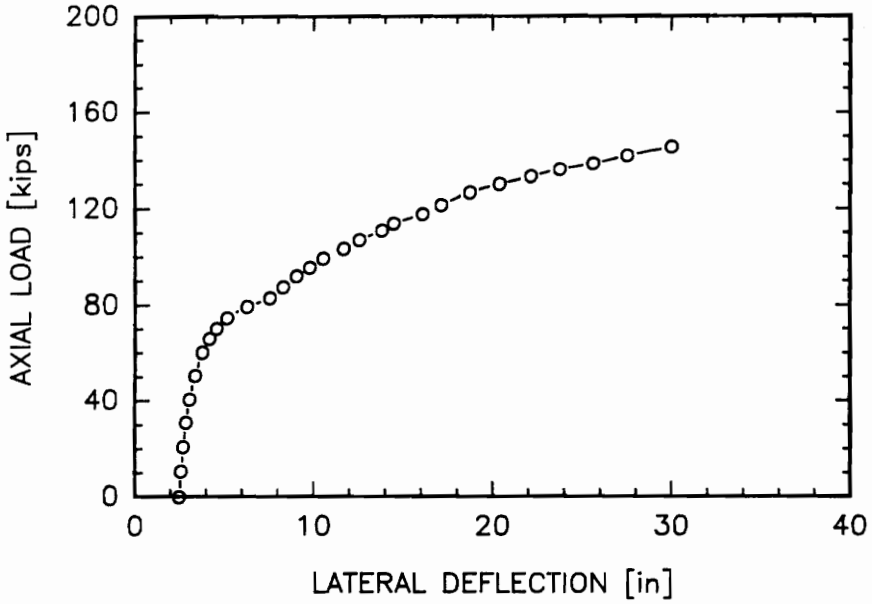

A) TIP DEFLECTION

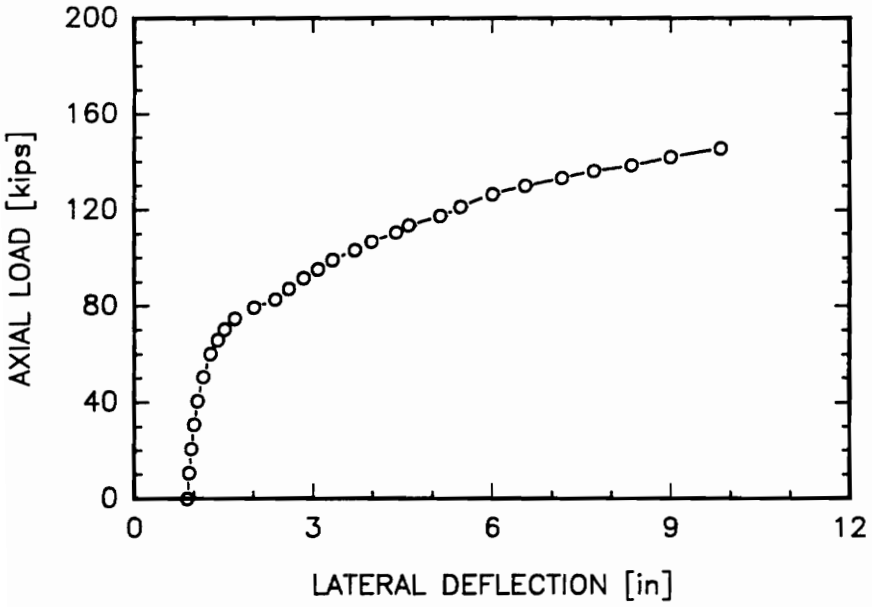

B) MIDSPAN DEFLECTION

FIG. D.6 FS–4 AXIAL LOAD VS. OUTER CONDUCTOR LATERAL DEFLECTION

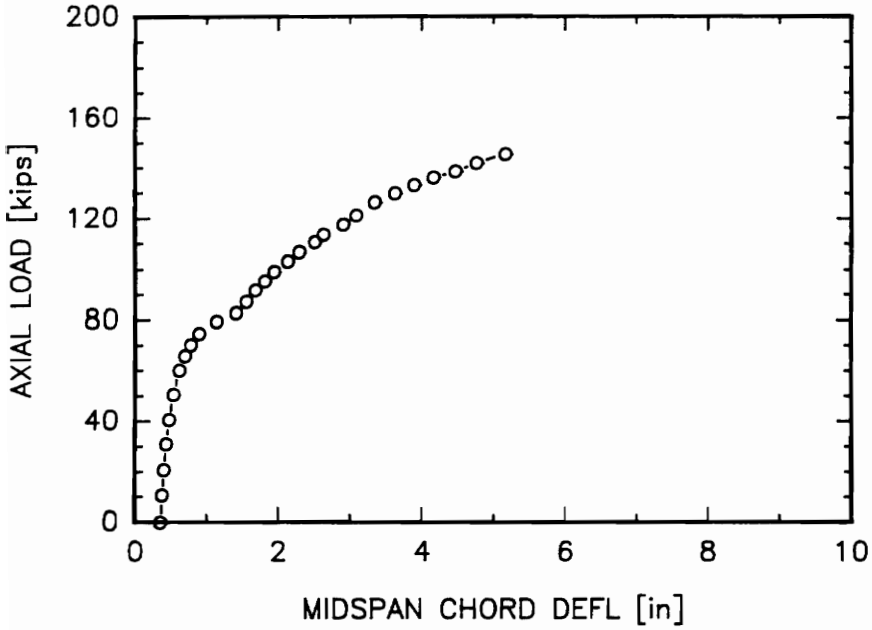

FIG. D.7 FS–4 OUTER CONDUCTOR MIDSPAN CHORD DEFLECTION

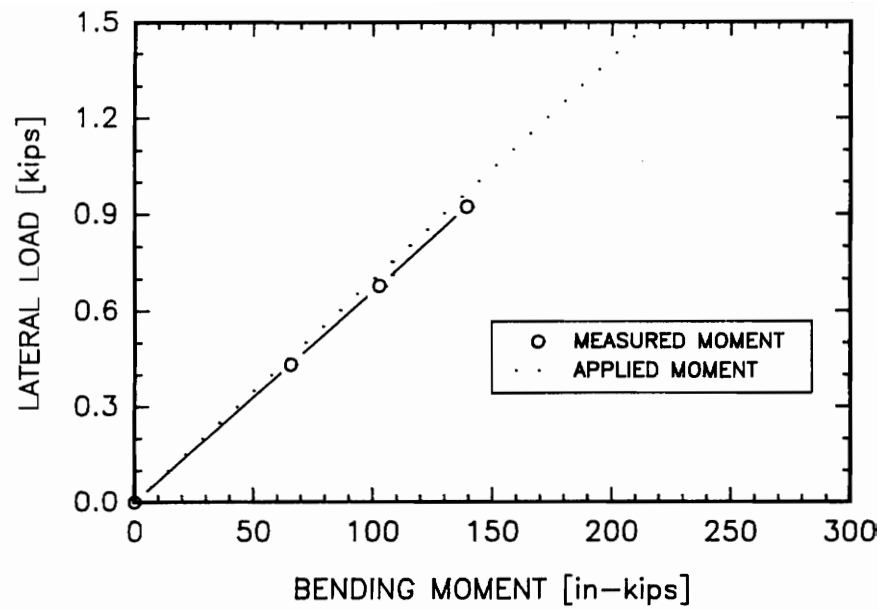

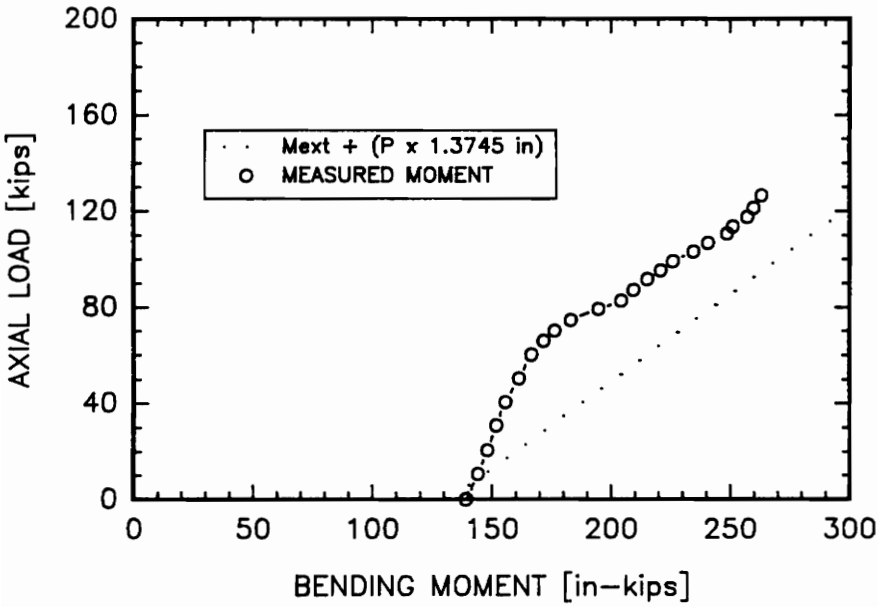

FIG. D.8 FS-4 OUTER CONDUCTOR BENDING MOMENT AT L = 1'-0"

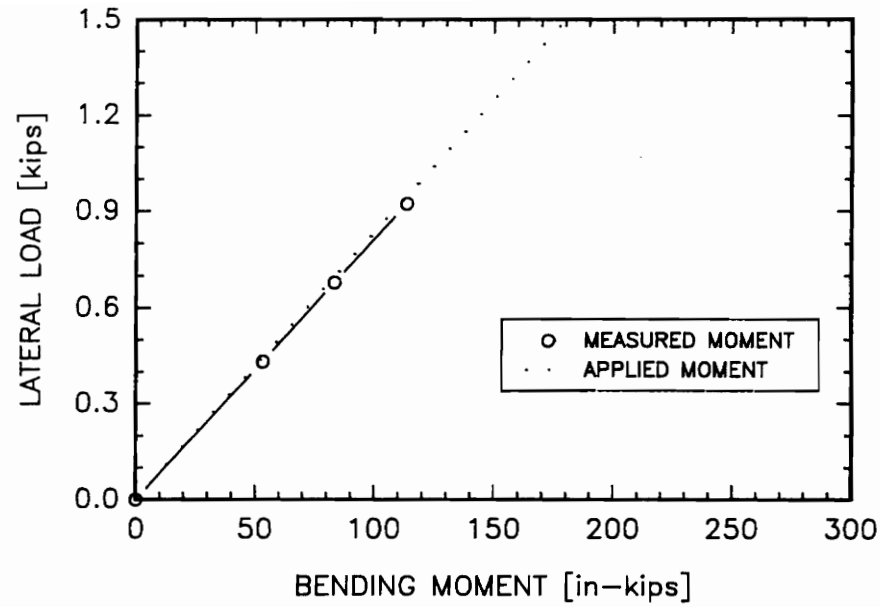

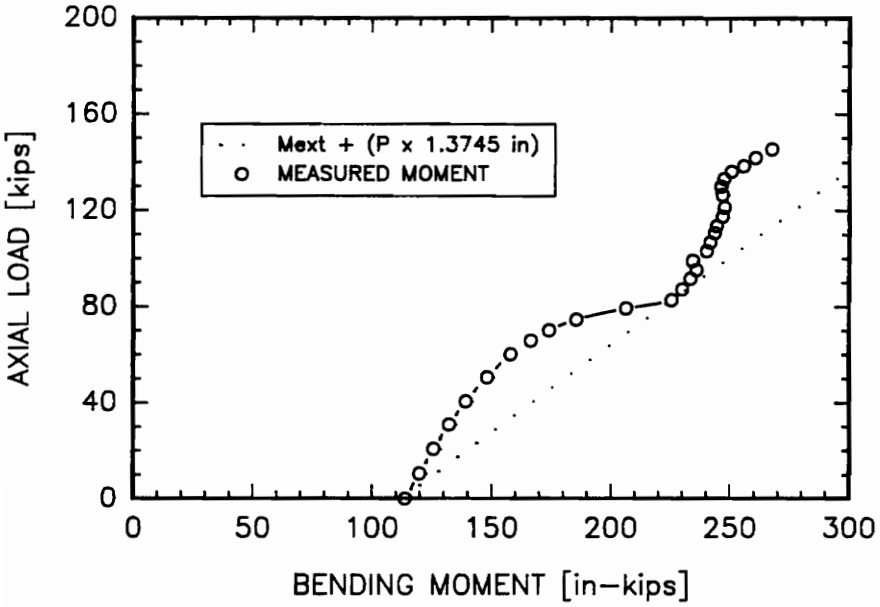

FIG. D.9 FS-4 OUTER CONDUCTOR BENDING MOMENT AT L = 3'-0"

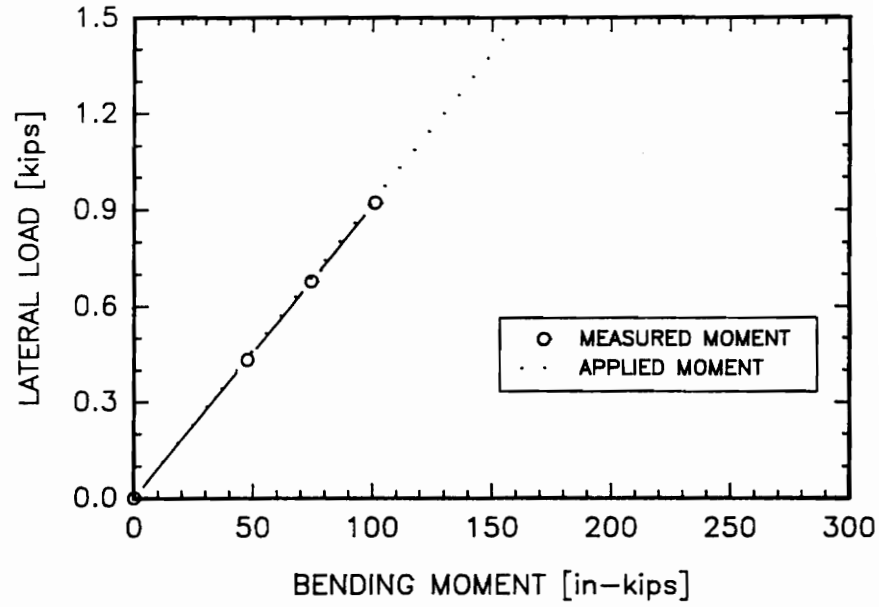

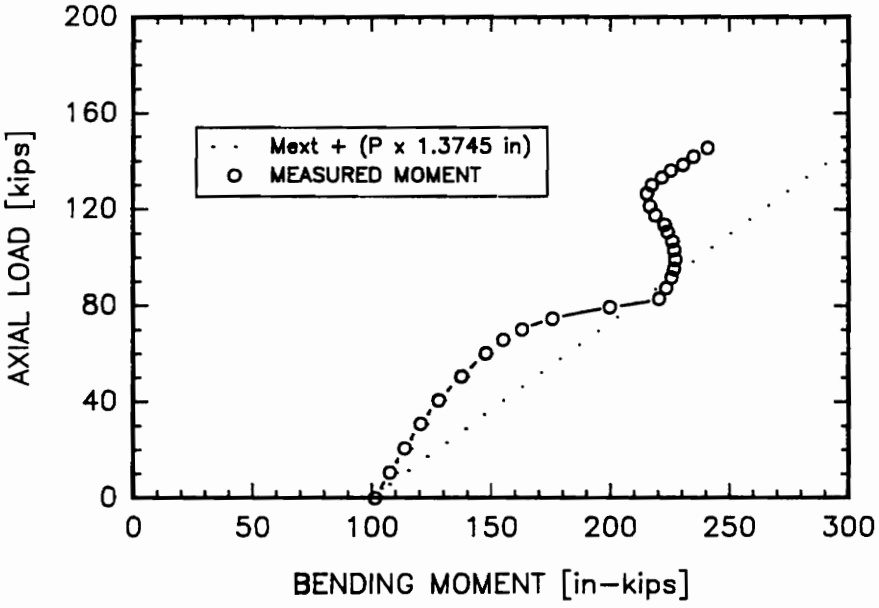

FIG. D.10 FS-4 OUTER CONDUCTOR BENDING MOMENT AT L = 4'-0"

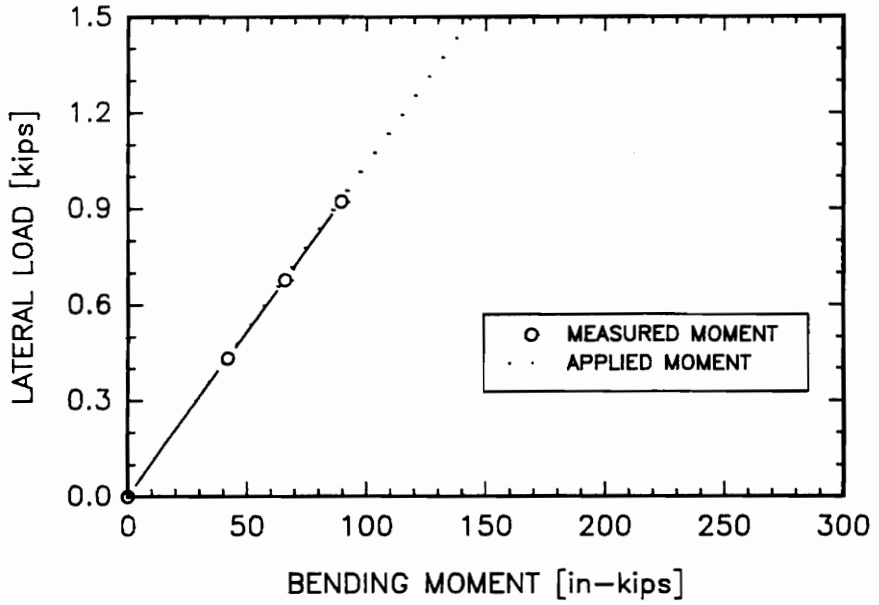

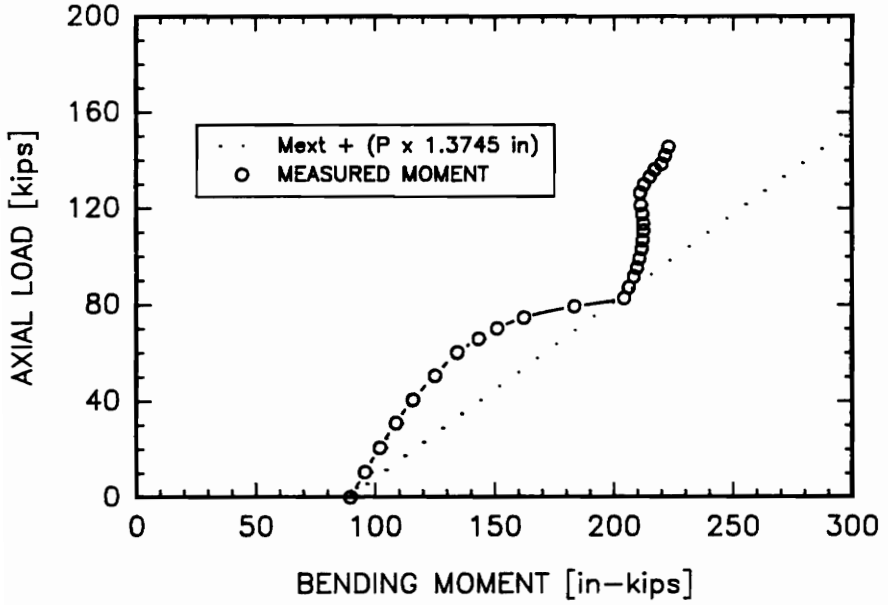

FIG. D.11 FS-4 OUTER CONDUCTOR BENDING MOMENT AT L = 5'-0"

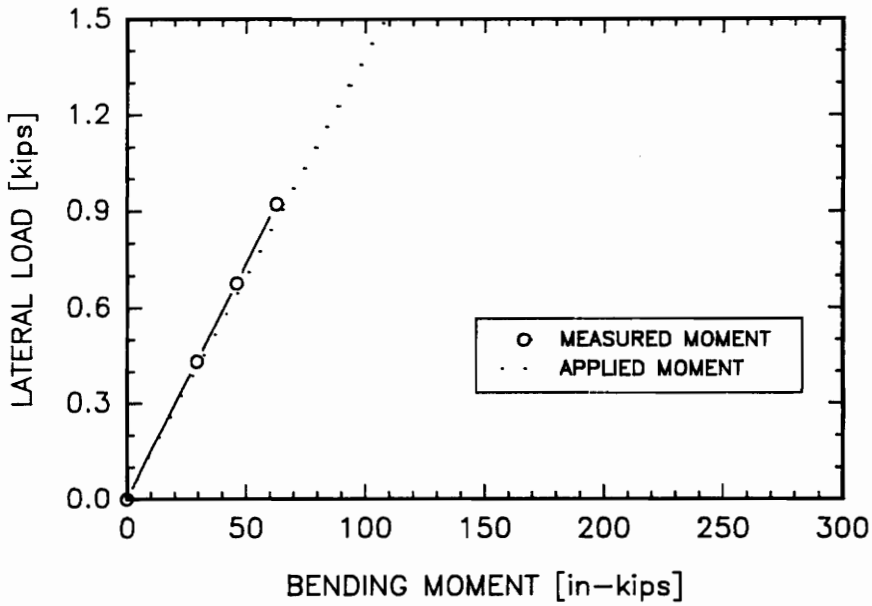

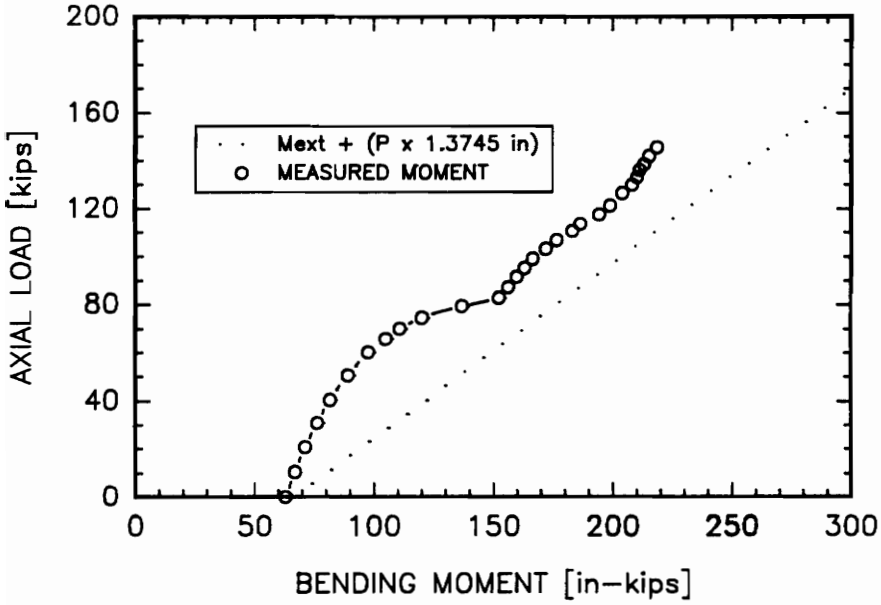

FIG. D.12 FS-4 OUTER CONDUCTOR BENDING MOMENT AT L = 7'-0"

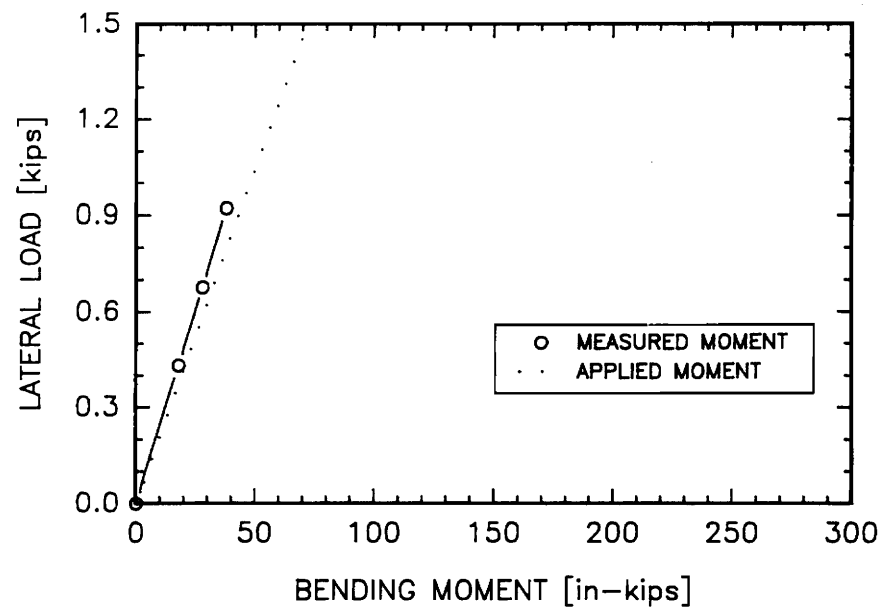

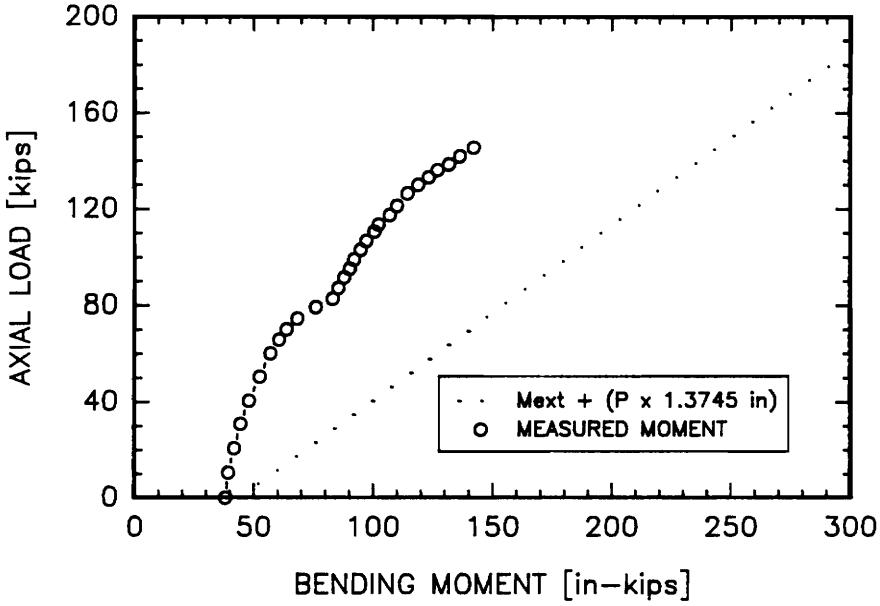

FIG. D.13 FS-4 OUTER CONDUCTOR BENDING MOMENT AT L = 9'-0"

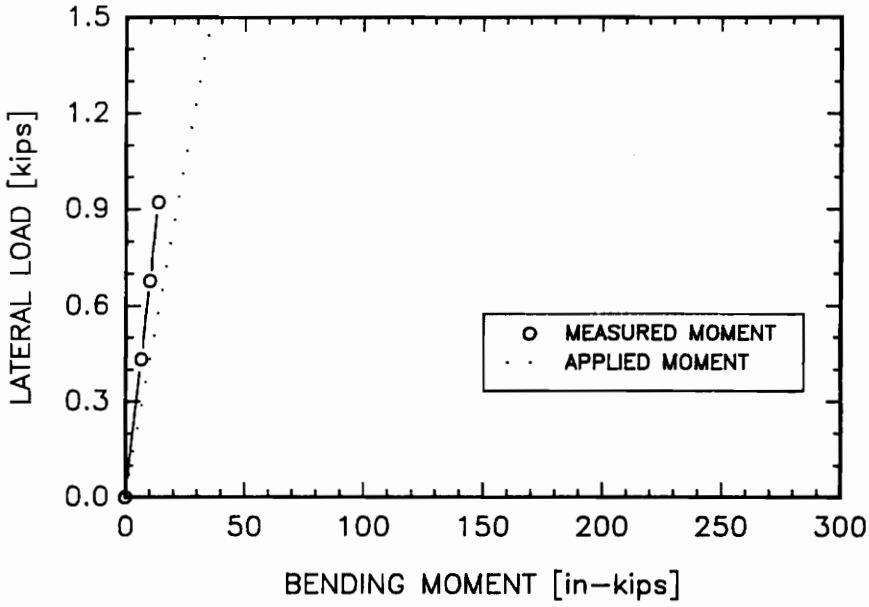

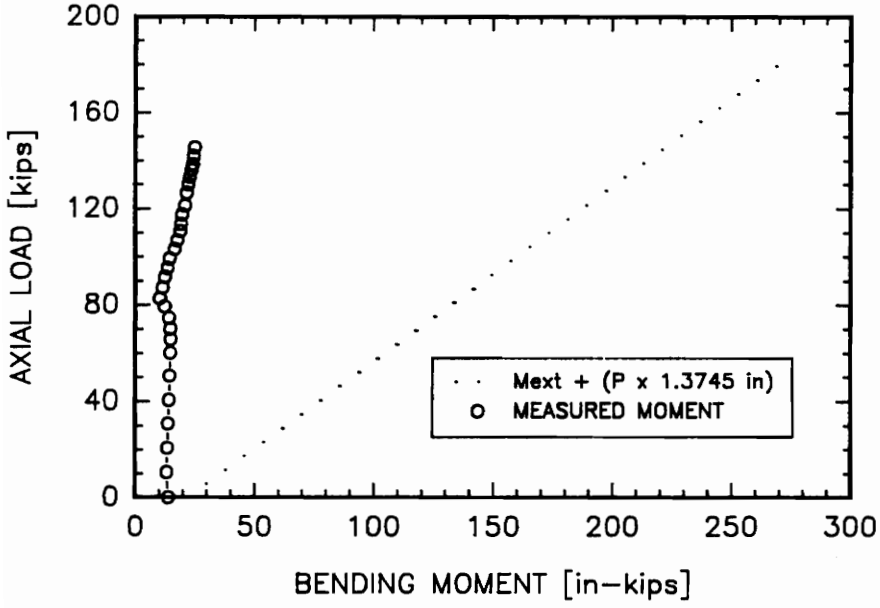

FIG. D.14 FS-4 OUTER CONDUCTOR BENDING MOMENT AT L = 11'-0"

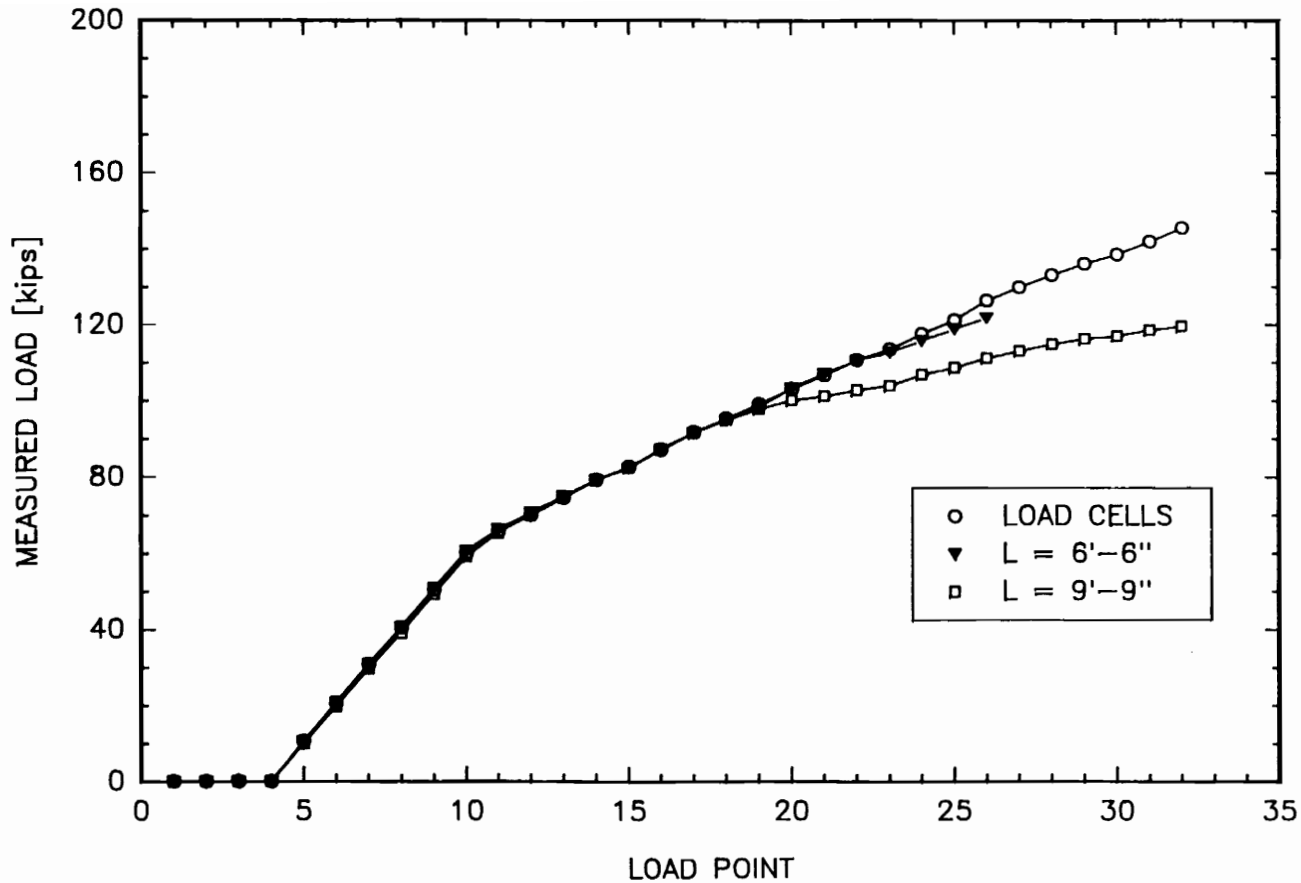

FIG. D.15 FS-4 MEASURED AXIAL LOAD IN INNER CASING

APPENDIX E

TEST FS-5 DATA

UNOCAL

TEST DATA SHEET

Test: UNOCAL FS-5

Test Date: October 16, 1990

Dimensions:

	Outer	Inner
Diameter (in.)	6.625	3.500
Wall Thickness (in.)	0.188	0.250
Yield Stress (ksi)	47.9	91.0

Parameters: Specimen Length = 13'-0"

Test Position - Horizontal

1.720 kips applied laterally at tip

Total applied moment is equal to 78% of outer pipe capacity and 47% of the capacity of both pipes.

Max. Axial Load: 100.8 kips

Failure Mode: Local Buckle in outer pipe at the support

Predicted Failure Loads (AISC Criteria):

Stahl & Baur Method 39.4 kips

Manley Method 74.8 kips

Discussion:

- Incrementally applied 1.720 kips of weight laterally at tip of cantilever, then applied axial load until failure.
- Specimen appeared to have reached relative maximum at approximately 40 kips of axial load.
- Continued to hold increasing amount of load up to 100.8 kips.
- Failed by local buckle at base of cantilever on the compression flange.

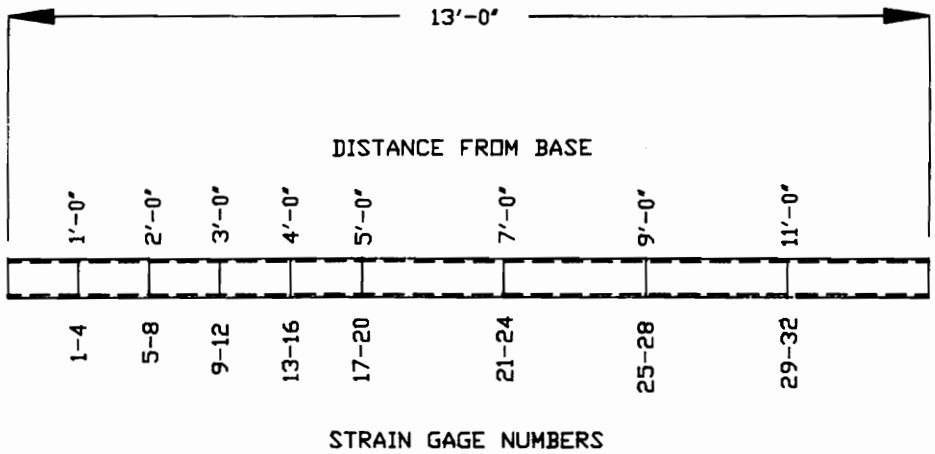

A) 6-5/8" OUTER CONDUCTOR PIPE

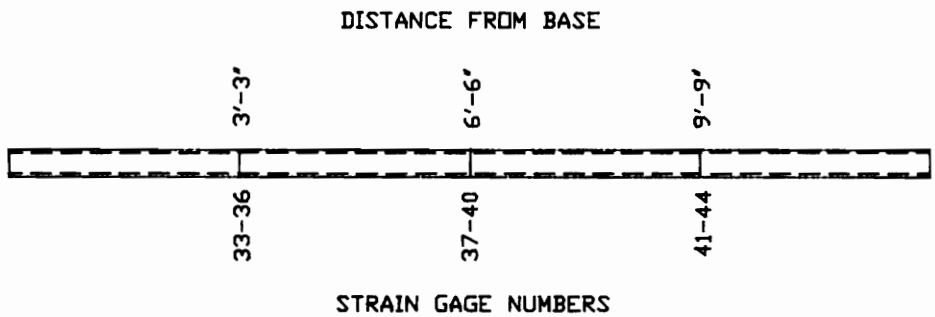

B) 3-1/2" INNER CASING PIPE

FIG. E.1 FS-5 STRAIN GAGE LOCATIONS

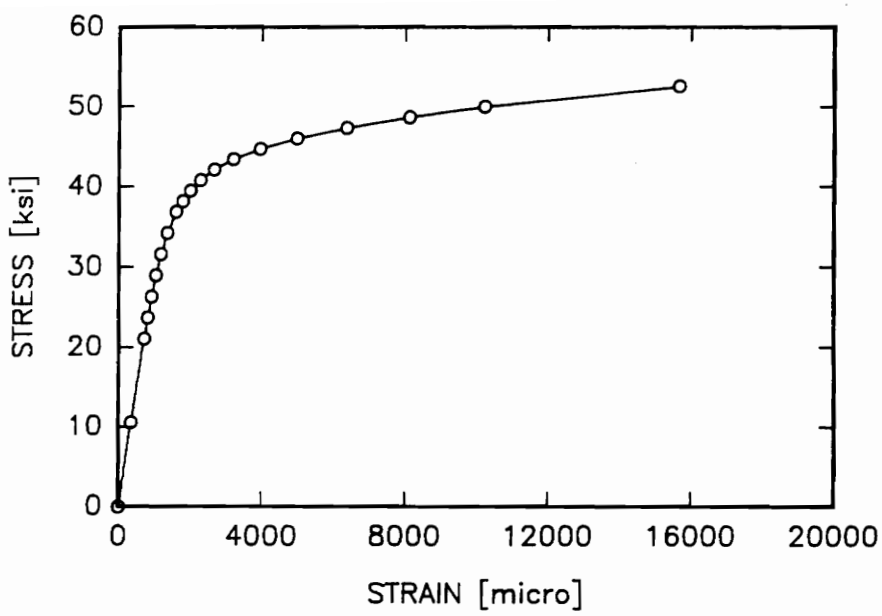

A) STUB COLUMN RESULTS

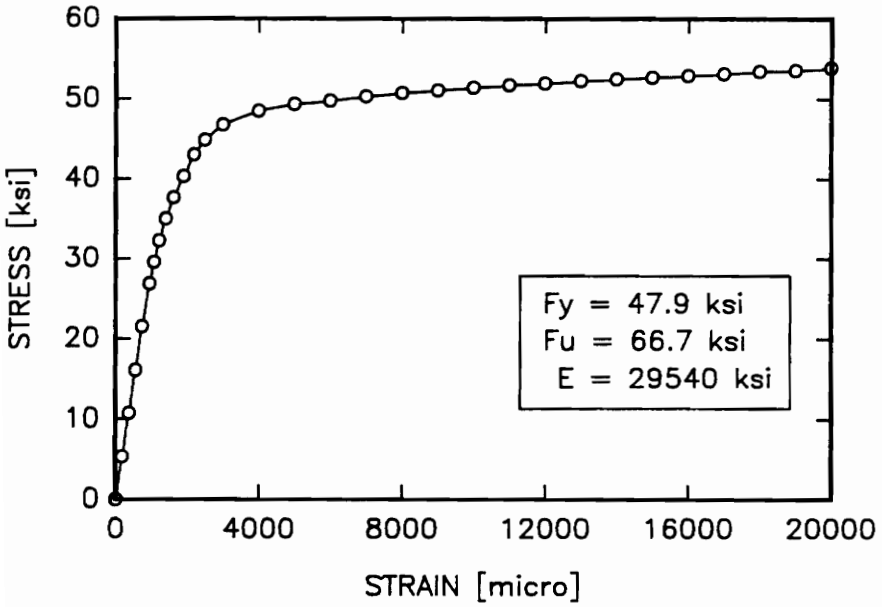

B) TENSILE COUPON RESULTS

FIG. E.2 FS–5 OUTER CONDUCTOR MATERIAL PROPERTIES

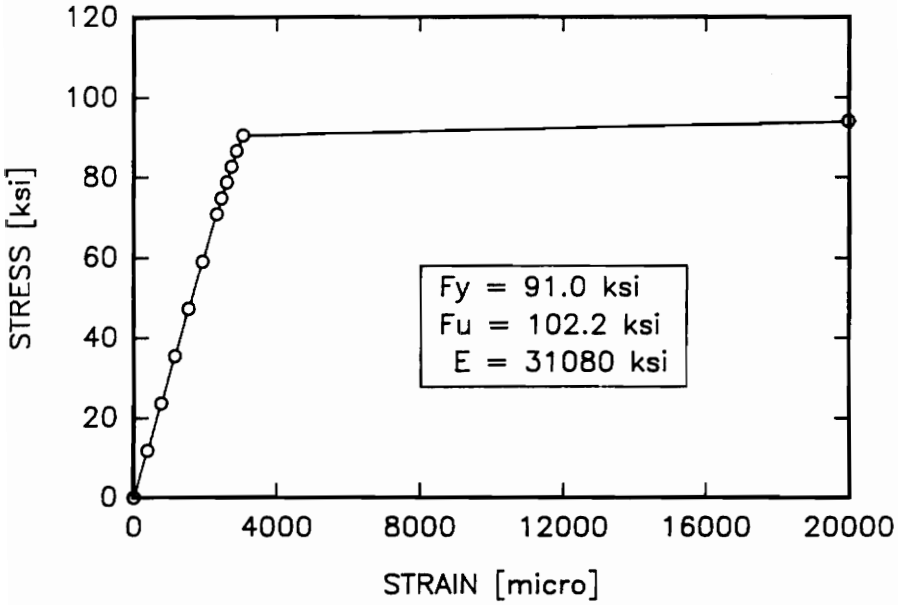

FIG. E.3 FS–5 INNER CASING MATERIAL PROPERTIES

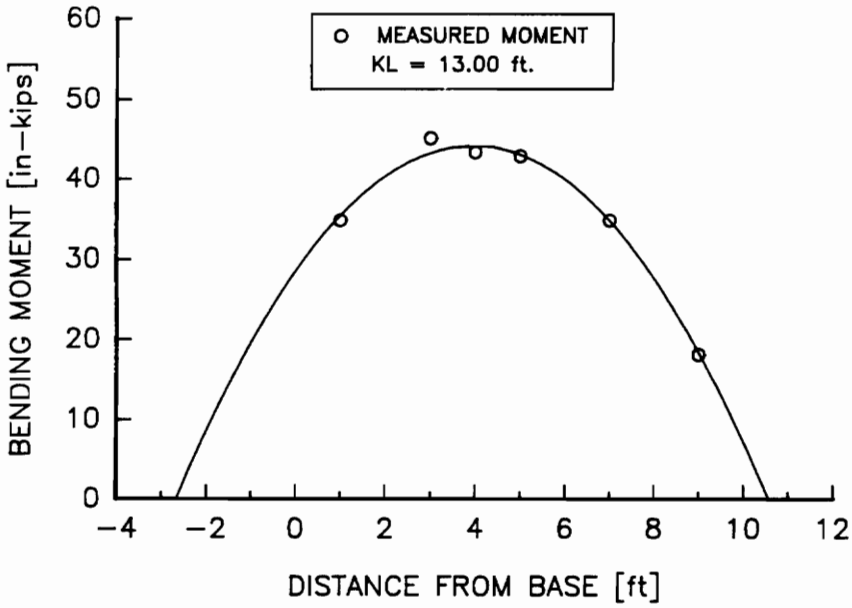

NOTE: THE BENDING MOMENT SHOWN HAS BEEN ADJUSTED TO REMOVE THE EFFECT OF THE APPLIED LATERAL LOADING.

FIG. E.4 FS-5 BENDING MOMENT OVER THE LENGTH OF THE OUTER CONDUCTOR AT LOAD POINT 12.

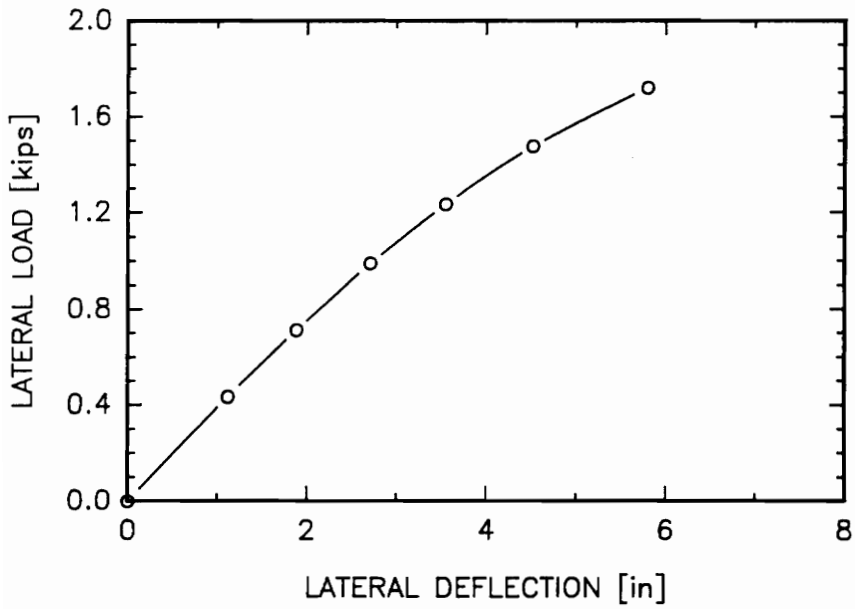

A) TIP DEFLECTION

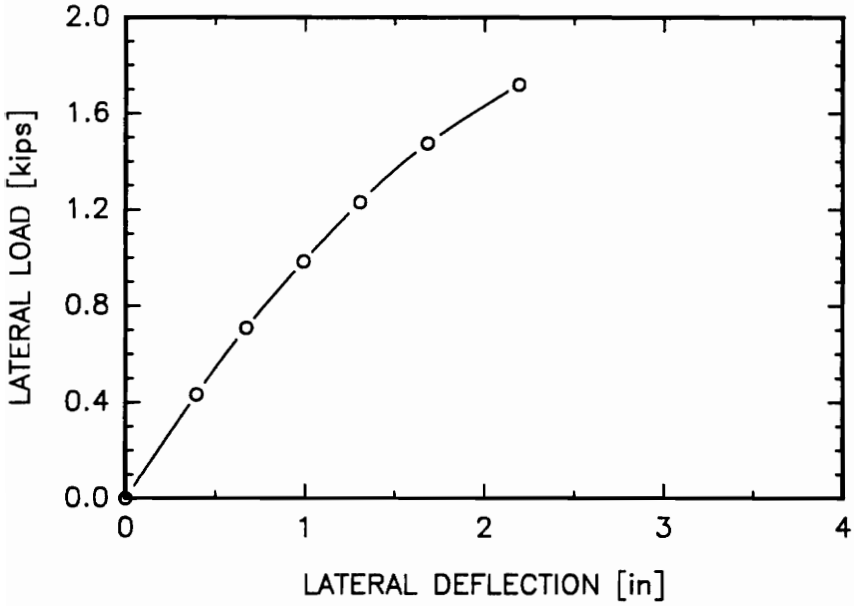

B) MIDSPAN DEFLECTION

FIG. E.5 FS–5 LATERAL LOAD VS. OUTER CONDUCTOR LATERAL DEFLECTION

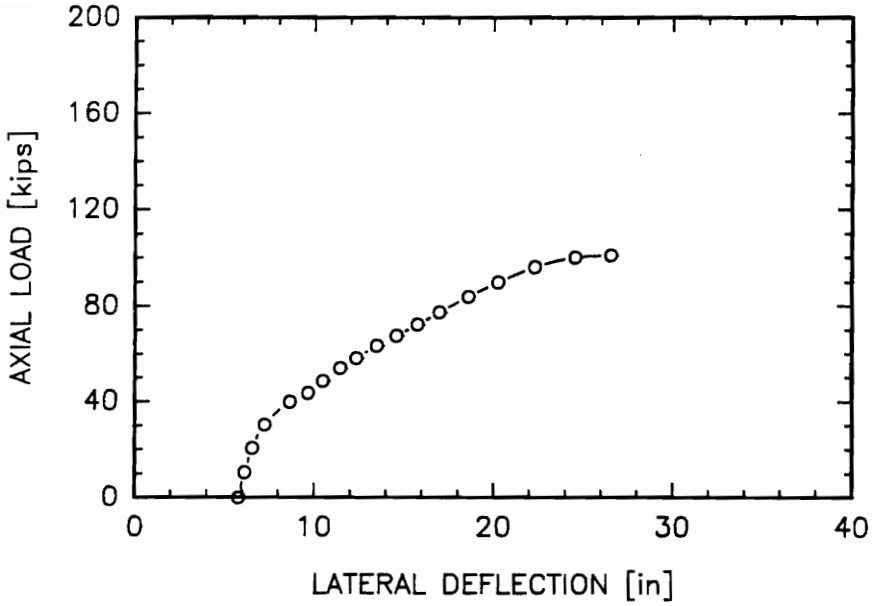

A) TIP DEFLECTION

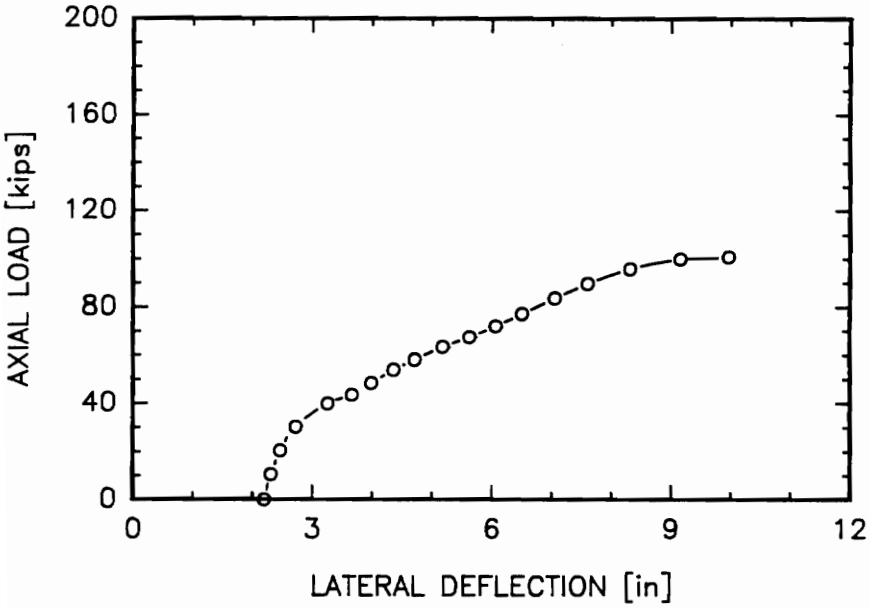

B) MIDSPAN DEFLECTION

FIG. E.6 FS–5 AXIAL LOAD VS. OUTER CONDUCTOR LATERAL DEFLECTION

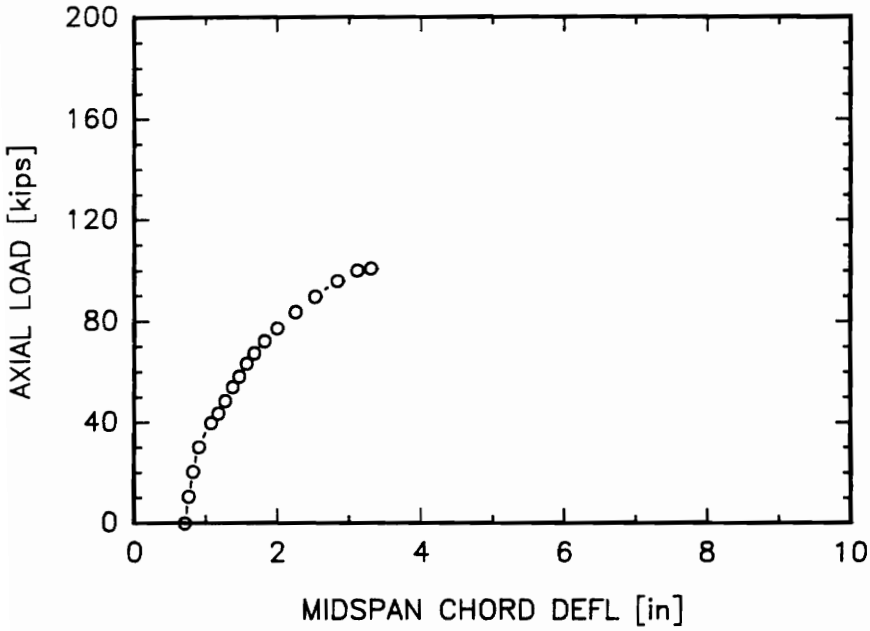

FIG. E.7 FS–5 OUTER CONDUCTOR MIDSPAN CHORD DEFLECTION

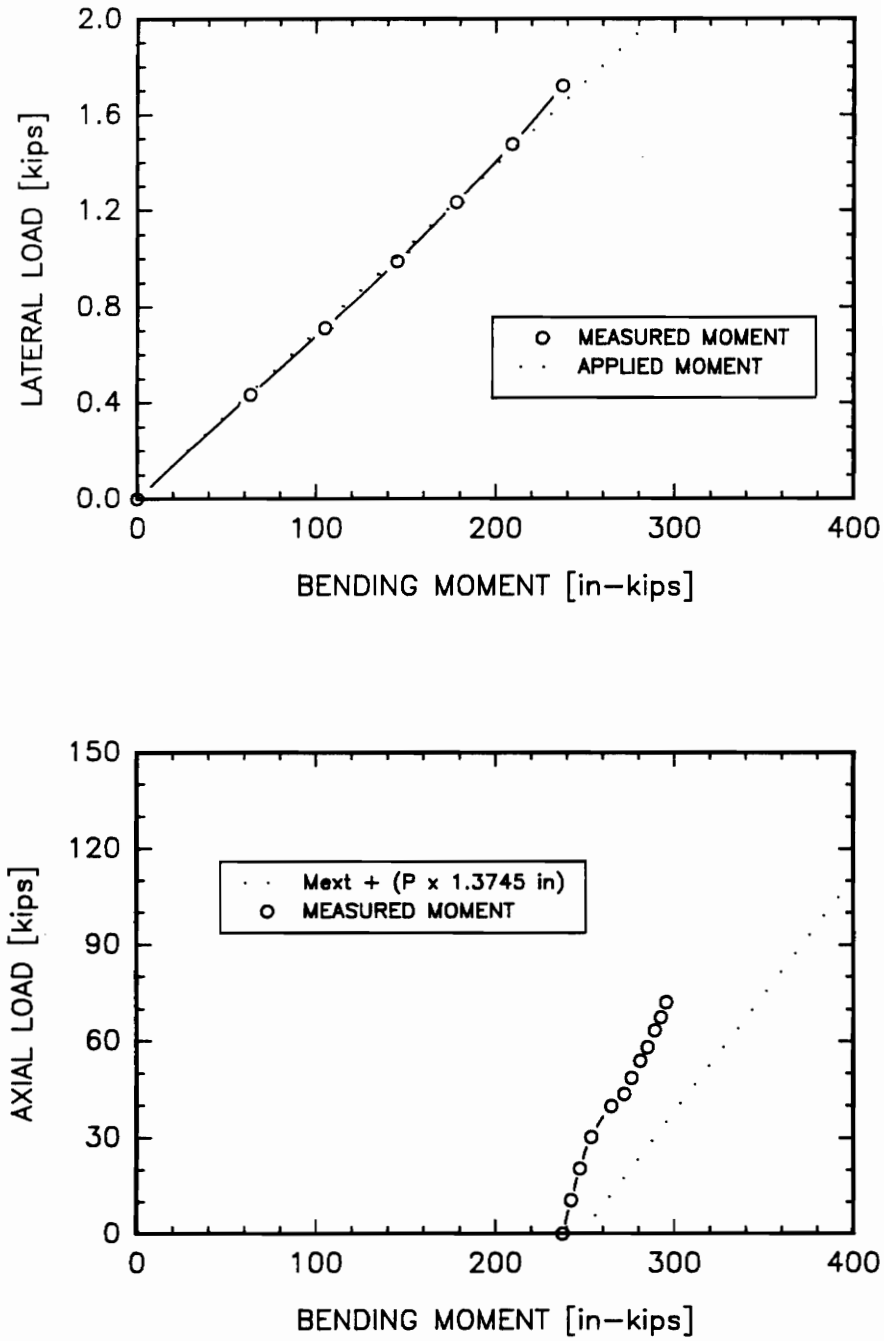

FIG. E.8 FS-5 OUTER CONDUCTOR BENDING MOMENT AT L = 1'-0"

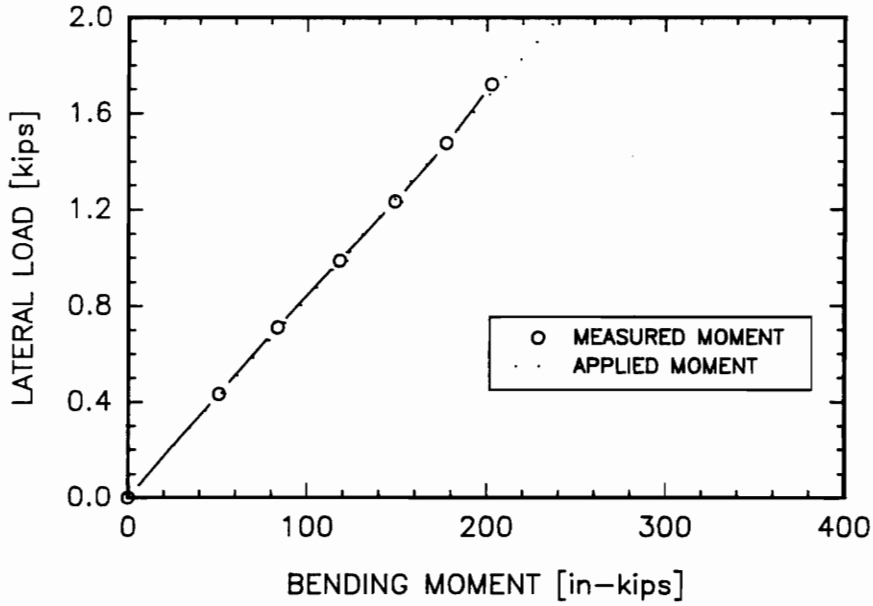

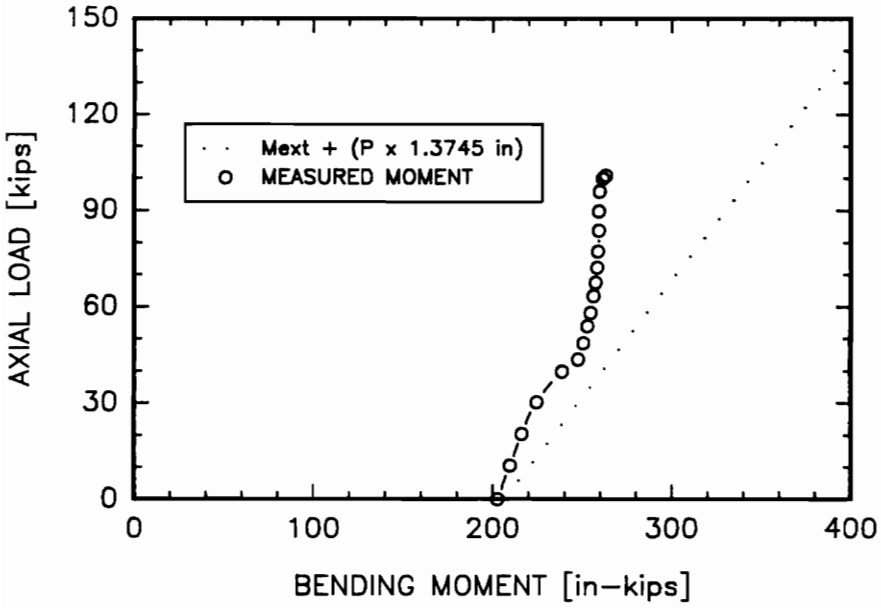

FIG. E.9 FS-5 OUTER CONDUCTOR BENDING MOMENT AT L = 3'-0"

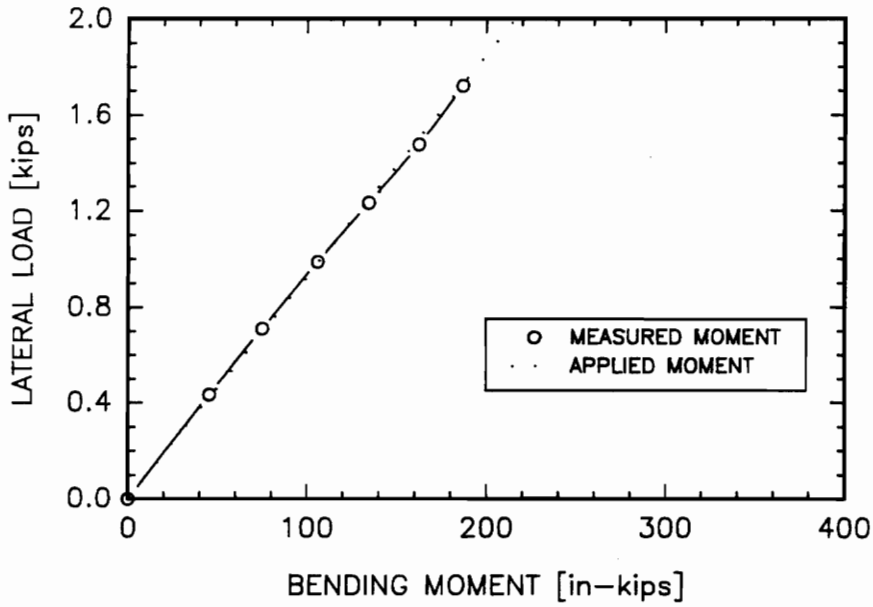

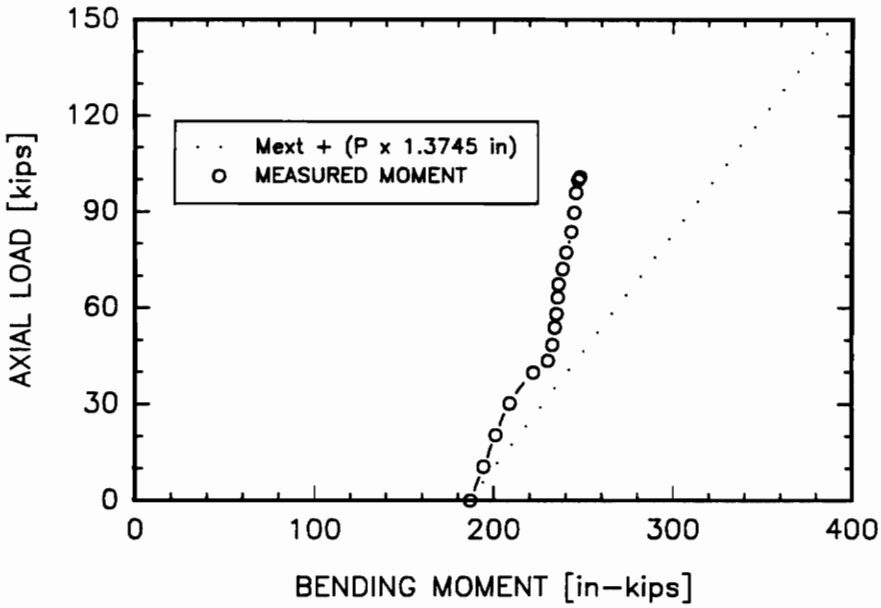

FIG. E.10 FS-5 OUTER CONDUCTOR BENDING MOMENT AT L = 4'-0"

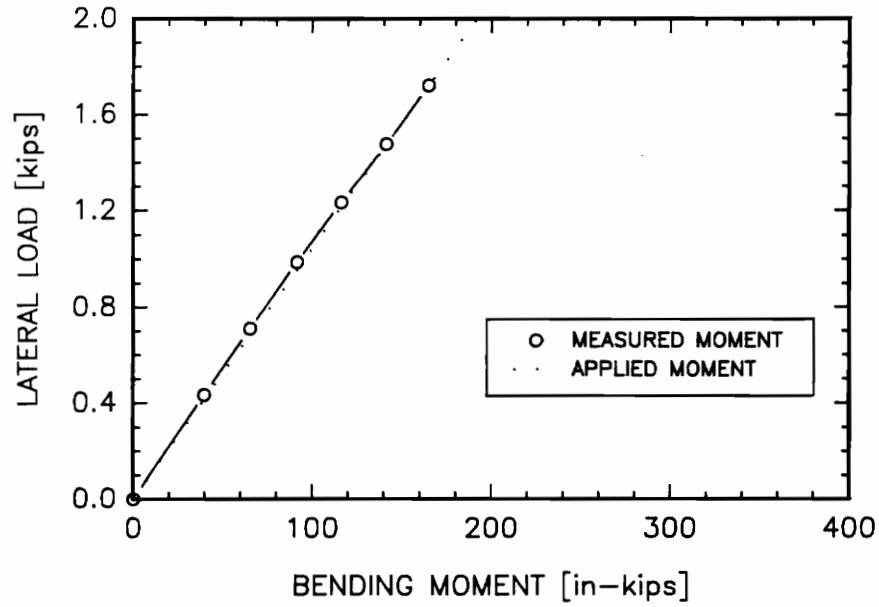

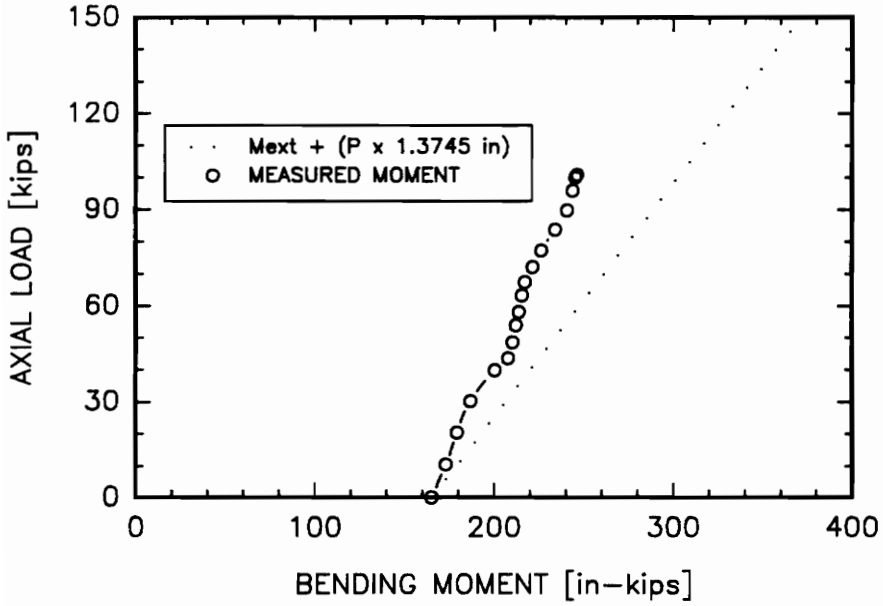

FIG. E.11 FS-5 OUTER CONDUCTOR BENDING MOMENT AT L = 5'-0"

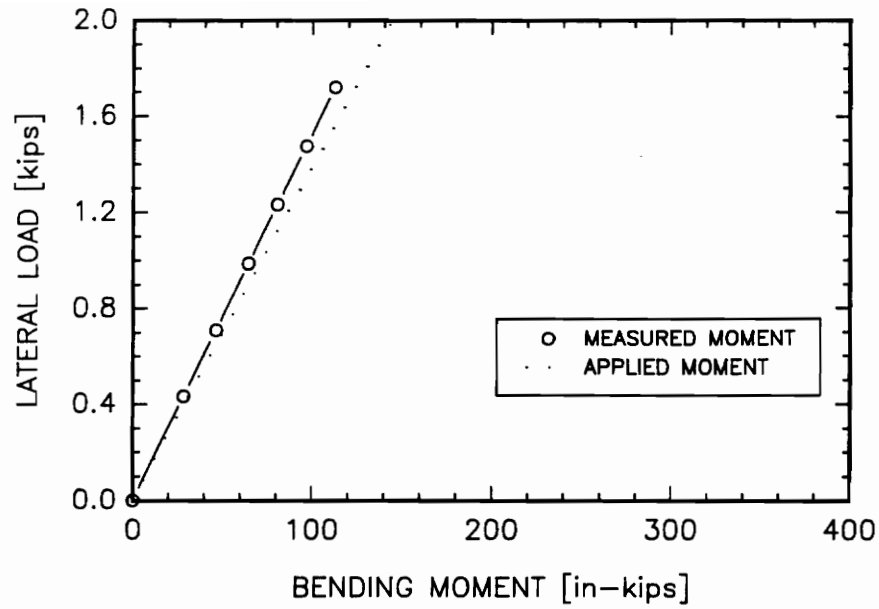

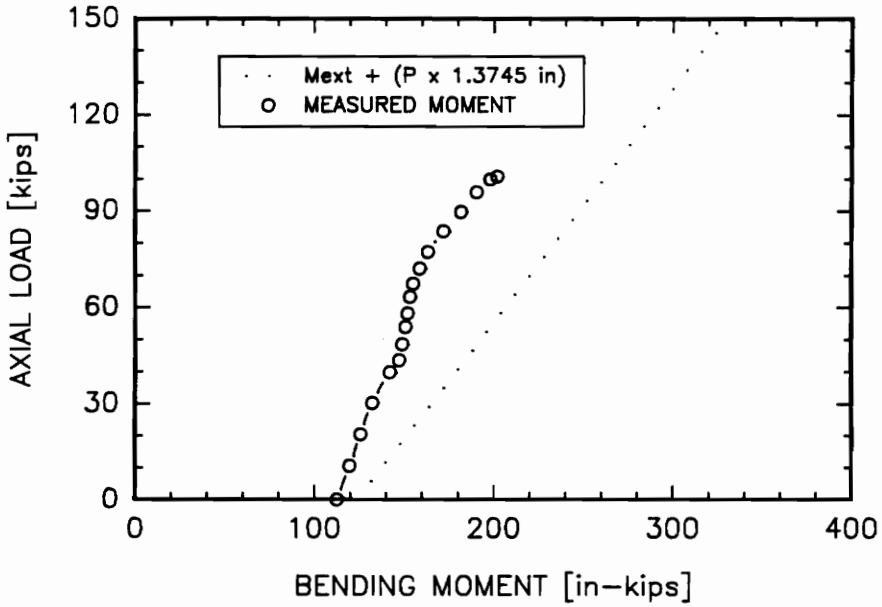

FIG. E.12 FS-5 OUTER CONDUCTOR BENDING MOMENT AT L = 7'-0"

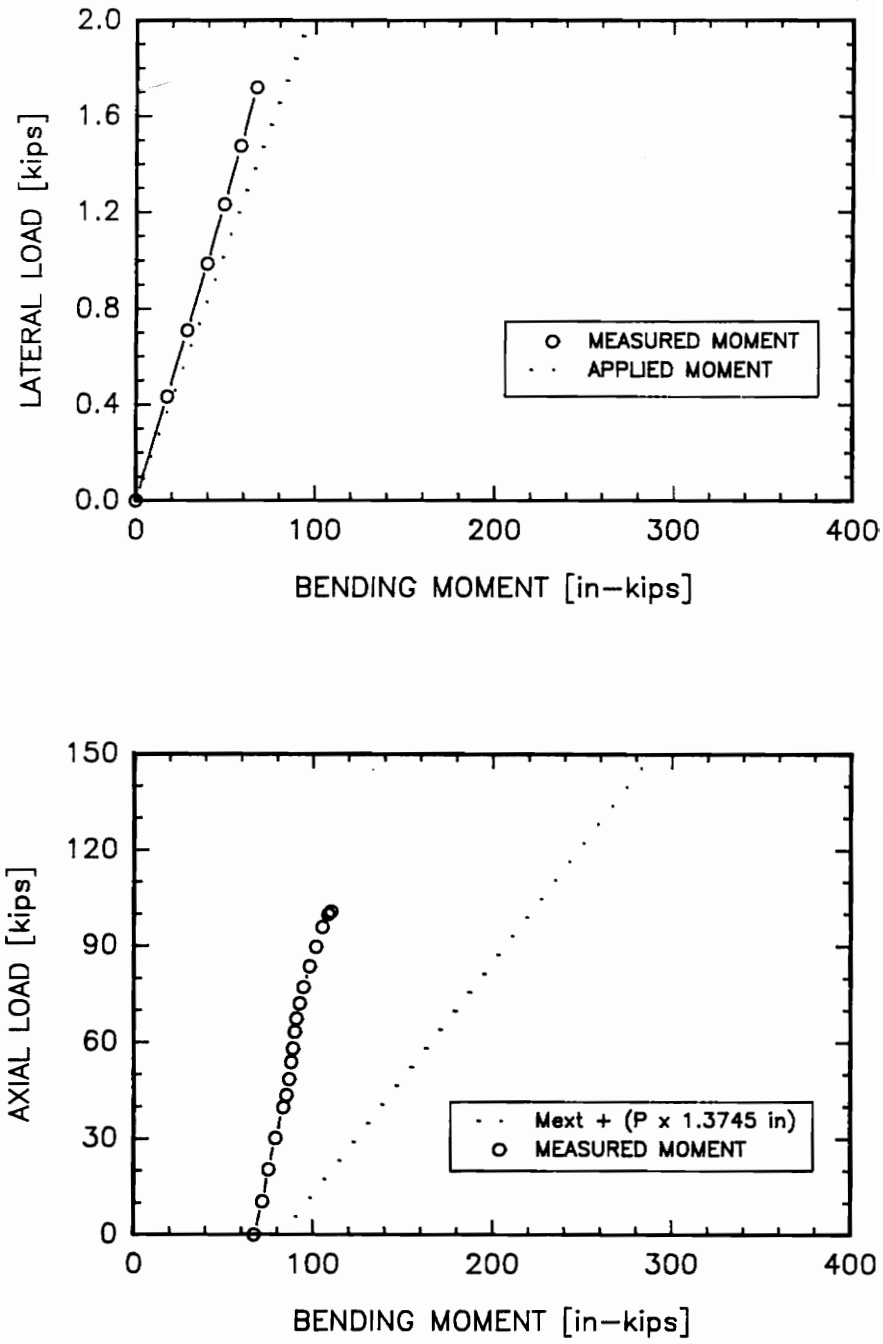

FIG. E.13 FS-5 OUTER CONDUCTOR BENDING MOMENT AT L = 9'-0"

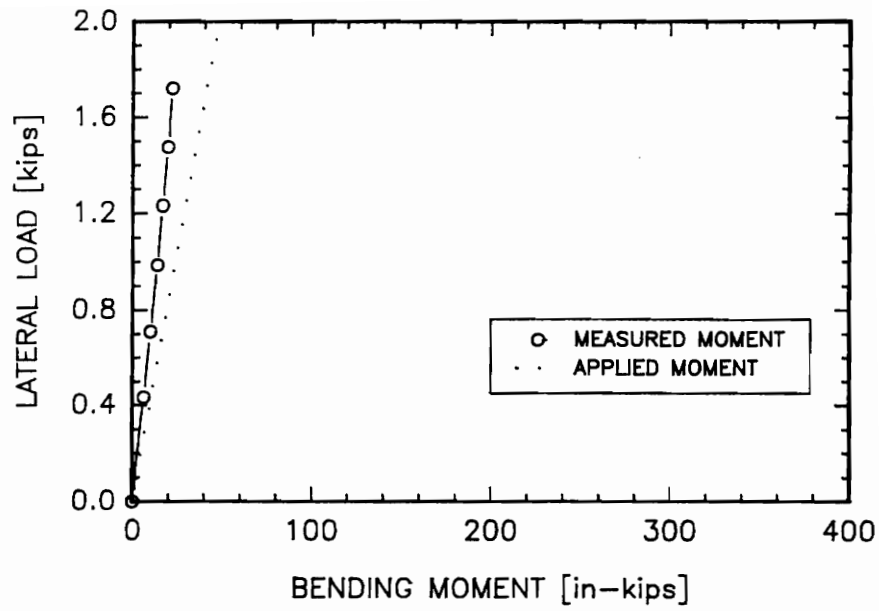

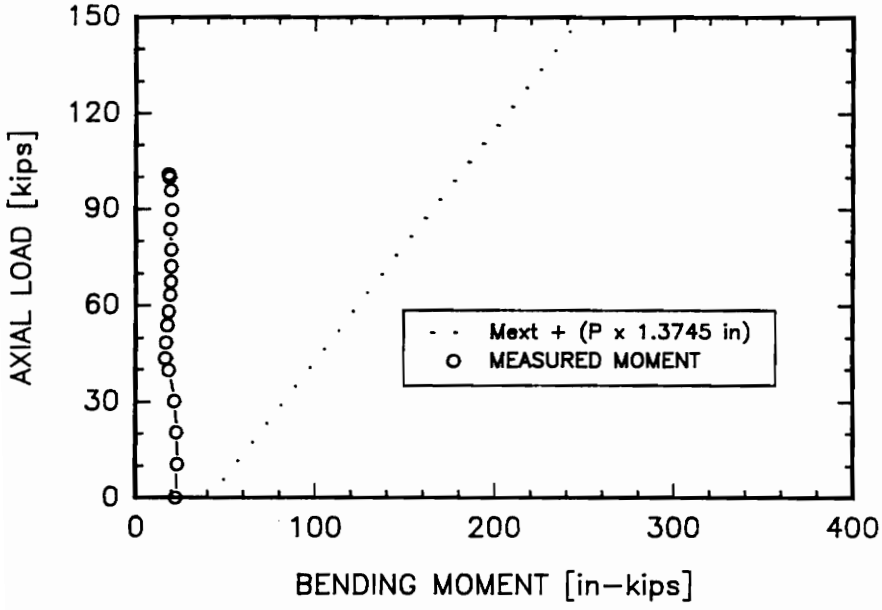

FIG. E.14 FS-5 OUTER CONDUCTOR BENDING MOMENT AT L = 11'-0"

APPENDIX F

TEST FS-6 DATA

UNOCAL

TEST DATA SHEET

Test: UNOCAL FS-6

Test Date: December 11, 1990

Dimensions:

	Outer	Inner
Diameter (in.)	6.625	3.500
Wall Thickness (in.)	0.188	0.250
Yield Stress (ksi)	47.9	106.0

Parameters: Specimen Length = 13'-0"

Test Position - Horizontal - Cantilever

0.481 kips applied laterally at tip

Total applied moment is equal to 78% of outer pipe capacity and 47% of the capacity of both pipes.

Max. Axial Load: 160.2 kips

Failure Mode: Stopped Test - Large Deflections

Predicted Failure Loads (AISC Criteria):

Stahl & Baur Method 90.6 kips

Manley Method 113.2 kips

Discussion:

- Incrementally applied 0.481 kips of weight laterally at tip of cantilever, then applied axial load until failure.
- Specimen appeared to have reached relative maximum at approximately 90.4 kips of axial load.
- Continued to hold increasing amount of load up to 160.2 kips.
- Maximum lateral deflection at tip greater than 39 inches.

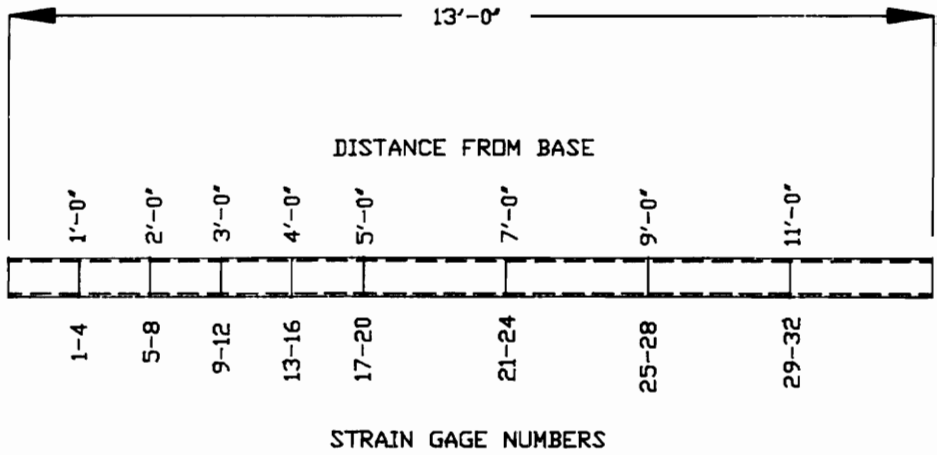

A) 6-5/8" OUTER CONDUCTOR PIPE

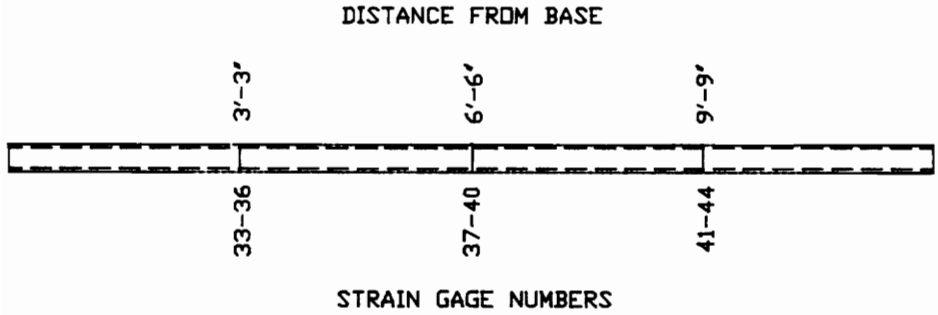

B) 3-1/2" INNER CASING PIPE

FIG. F.1 FS-6 STRAIN GAGE LOCATIONS

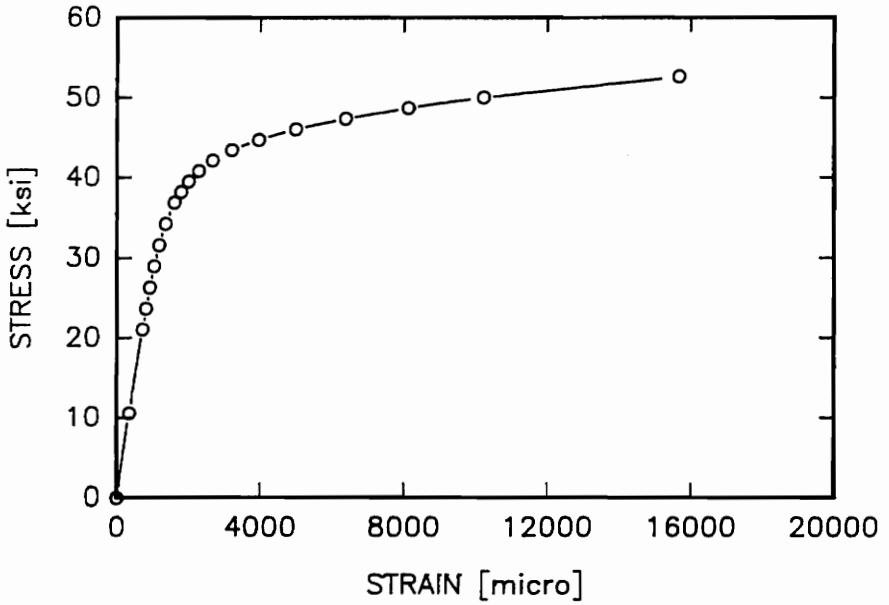

A) STUB COLUMN RESULTS

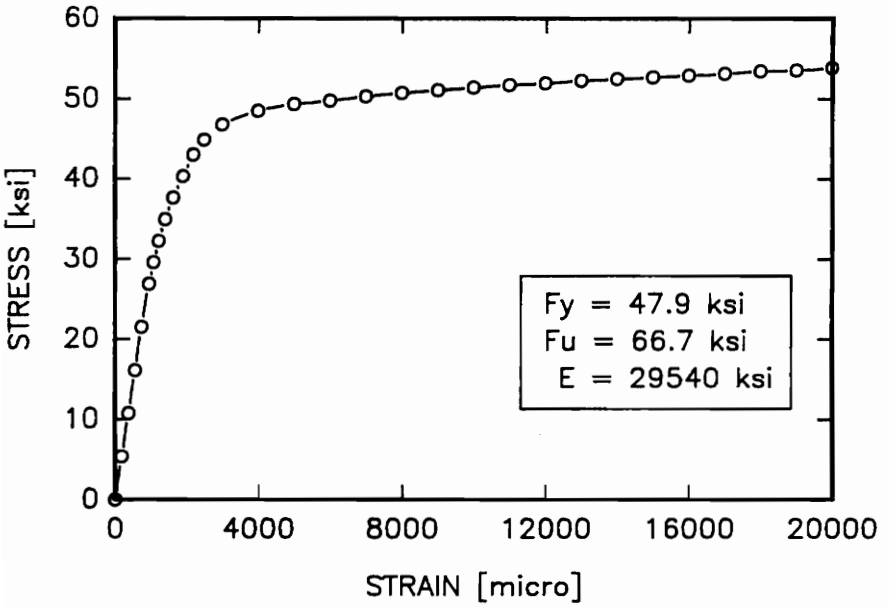

B) TENSILE COUPON RESULTS

FIG. F.2 FS–6 OUTER CONDUCTOR MATERIAL PROPERTIES

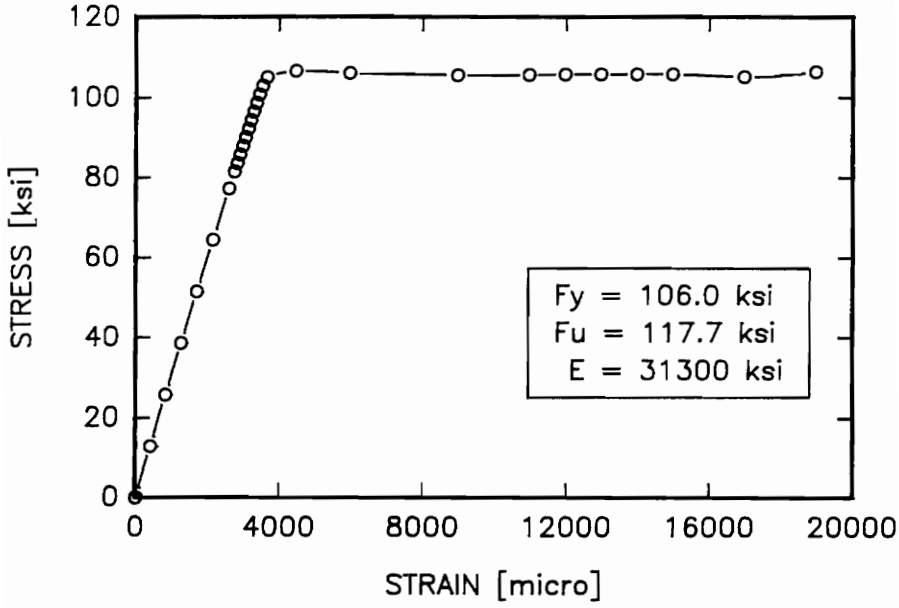

FIG. F.3 FS–6 INNER CASING MATERIAL PROPERTIES

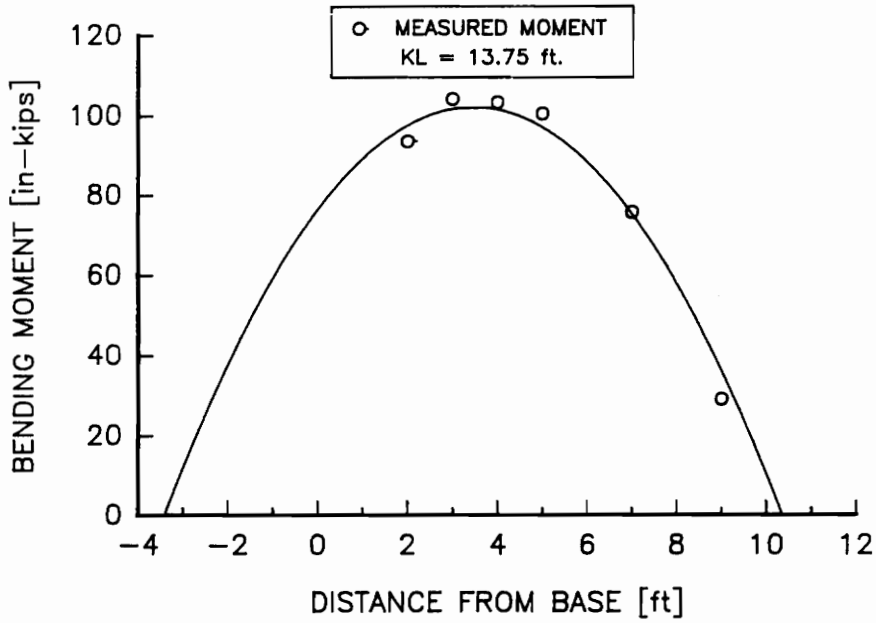

NOTE: THE BENDING MOMENT SHOWN HAS BEEN ADJUSTED TO REMOVE THE EFFECT OF THE APPLIED LATERAL LOADING.

FIG. F.4 FS-6 BENDING MOMENT OVER THE LENGTH OF THE OUTER CONDUCTOR AT LOAD POINT 13.

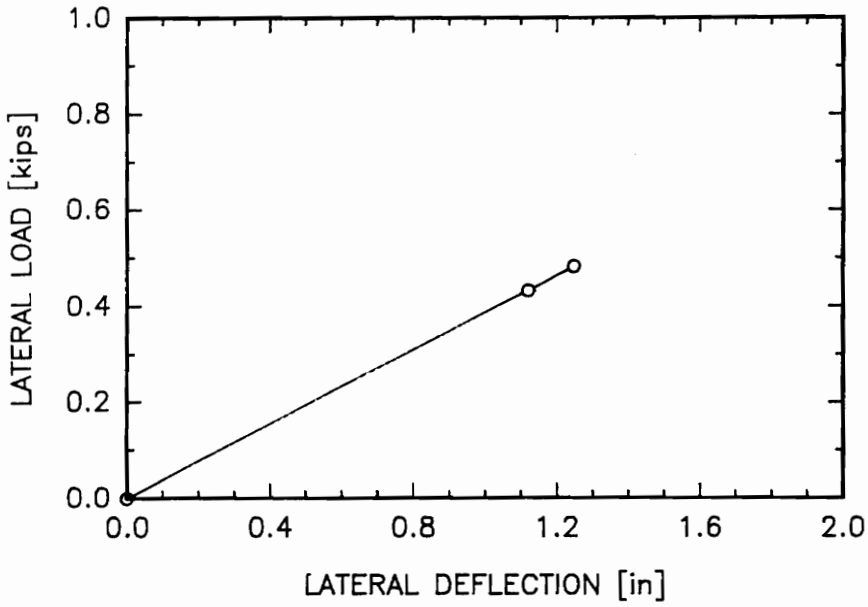

A) TIP DEFLECTION

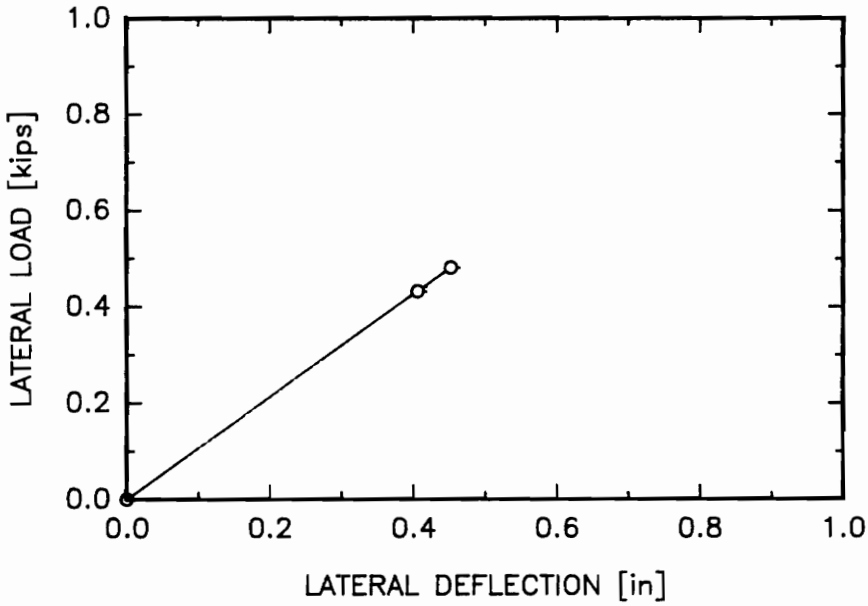

B) MIDSPAN DEFLECTION

FIG. F.5 FS–6 LATERAL LOAD VS. OUTER CONDUCTOR LATERAL DEFLECTION

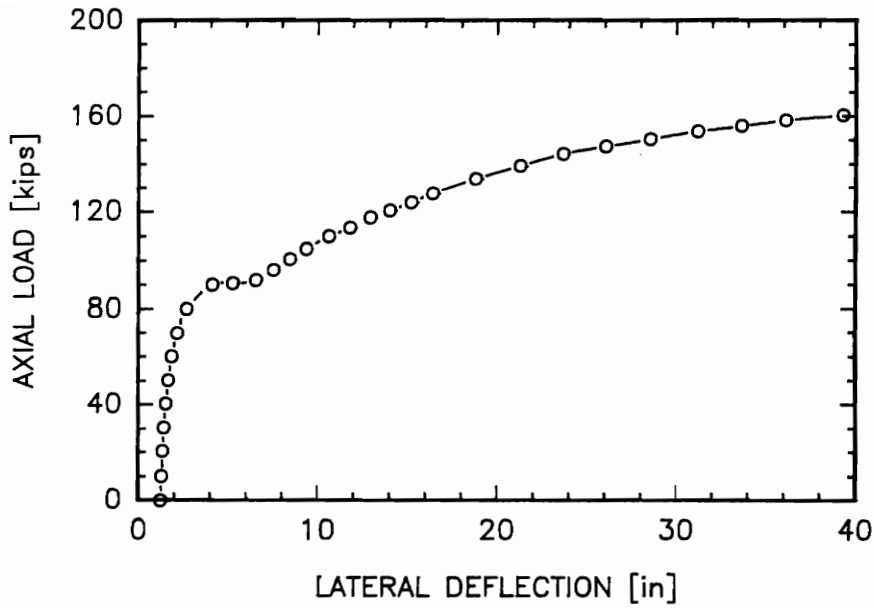

A) TIP DEFLECTION

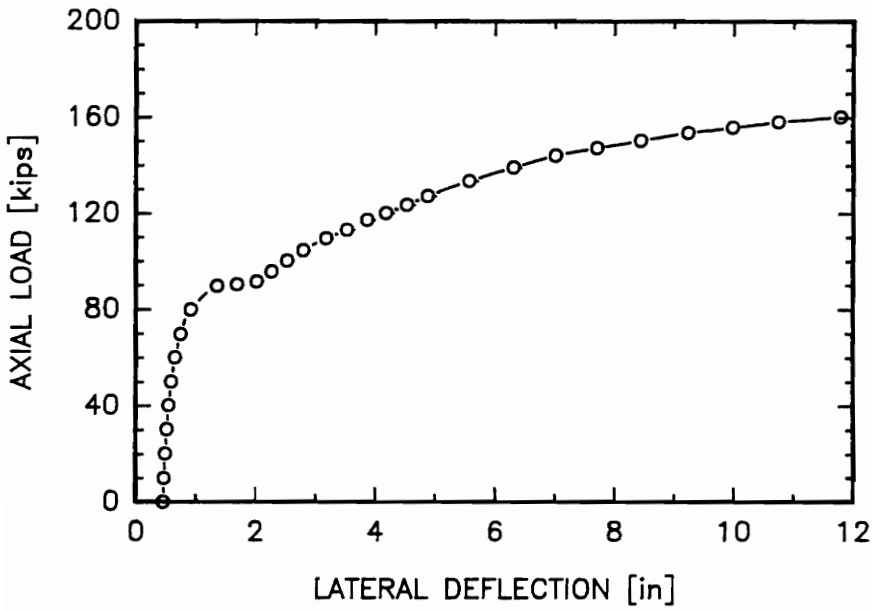

B) MIDSPAN DEFLECTION

FIG. F.6 FS–6 AXIAL LOAD VS. OUTER CONDUCTOR LATERAL DEFLECTION

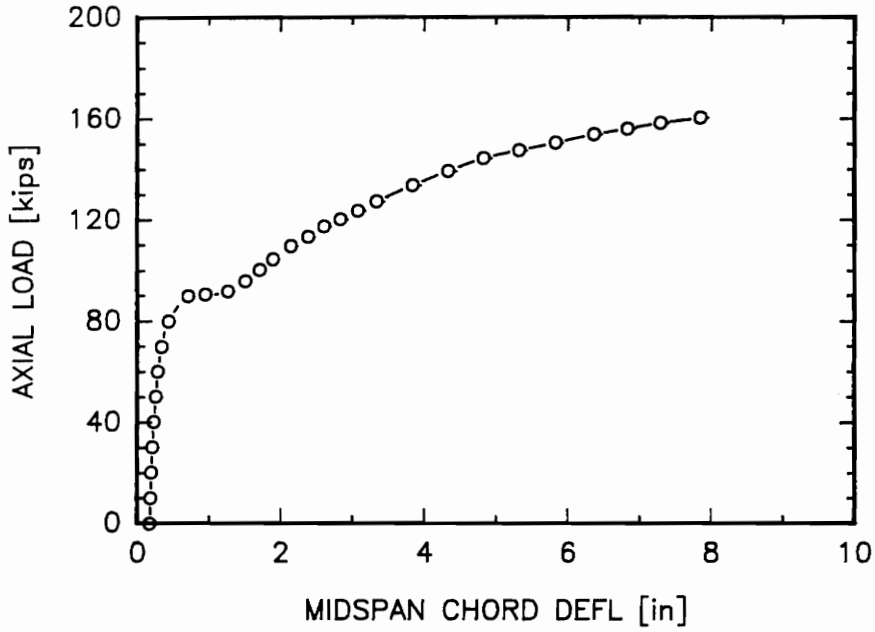

FIG. F.7 FS–6 OUTER CONDUCTOR MIDSPAN CHORD DEFLECTION

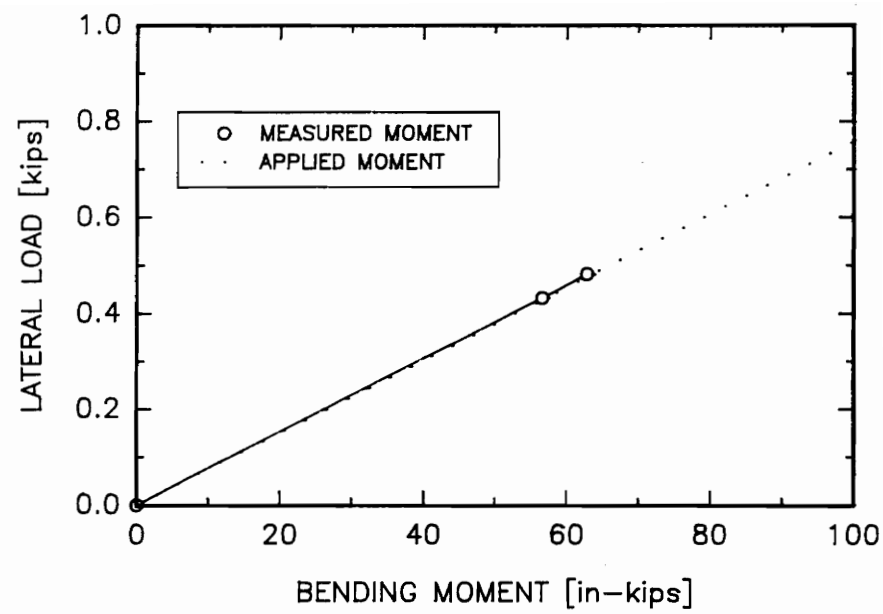

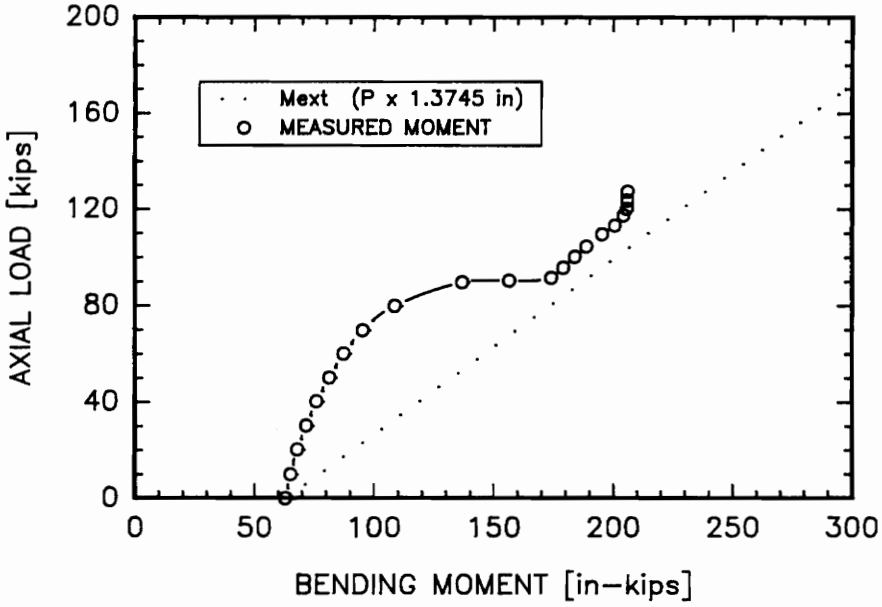

FIG. F.8 FS-6 OUTER CONDUCTOR BENDING MOMENT AT L = 2'-0"

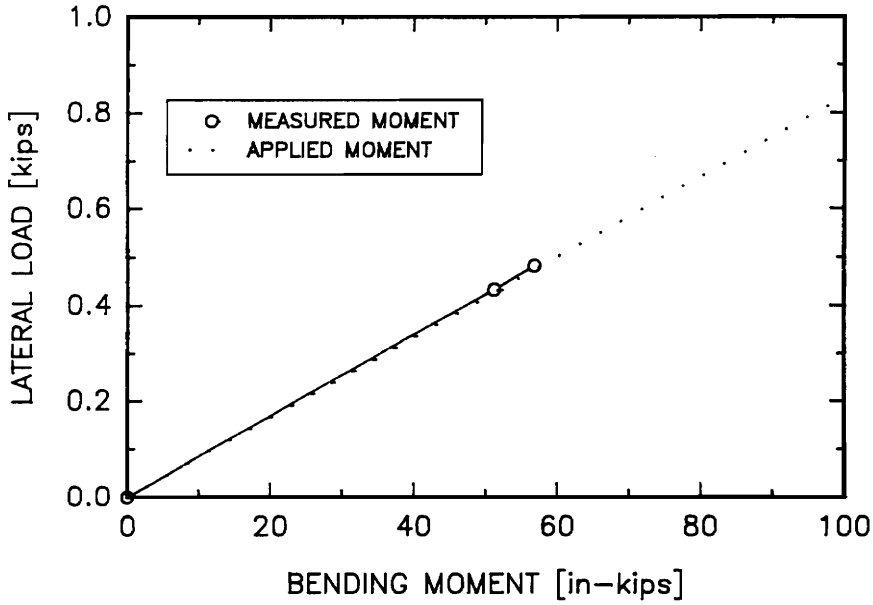

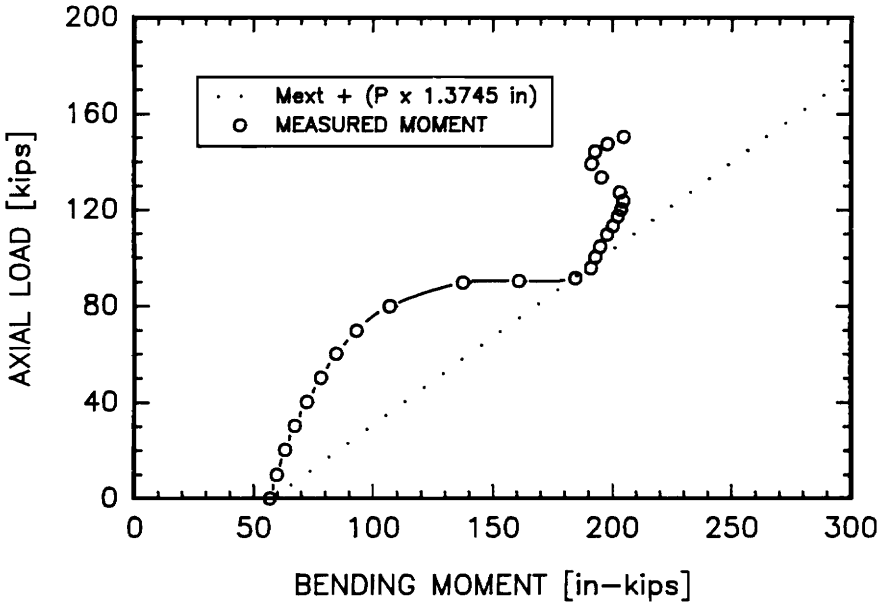

FIG. F.9 FS-6 OUTER CONDUCTOR BENDING MOMENT AT L = 3'-0"

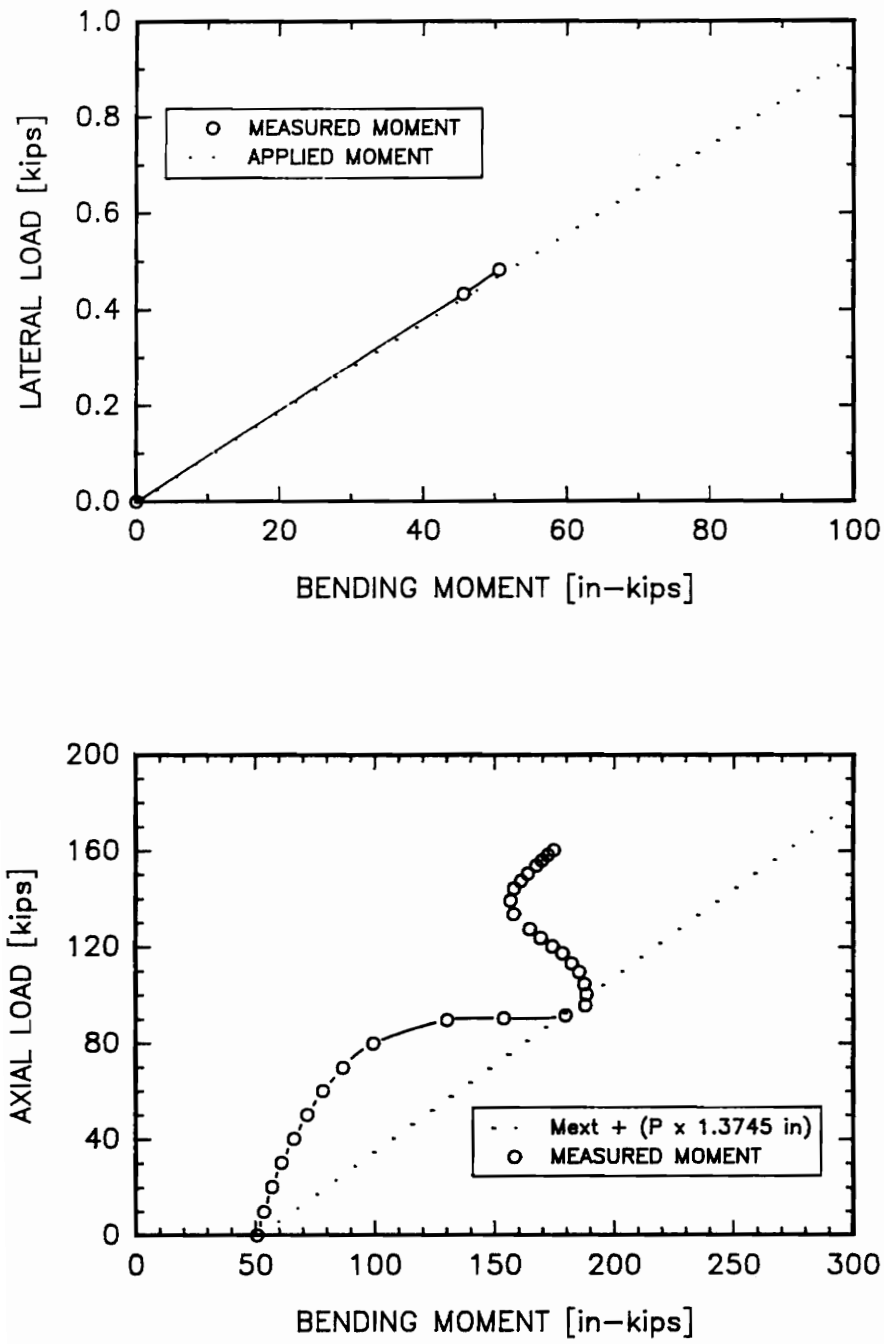

FIG. F.10 FS-6 OUTER CONDUCTOR BENDING MOMENT AT L = 4'-0"

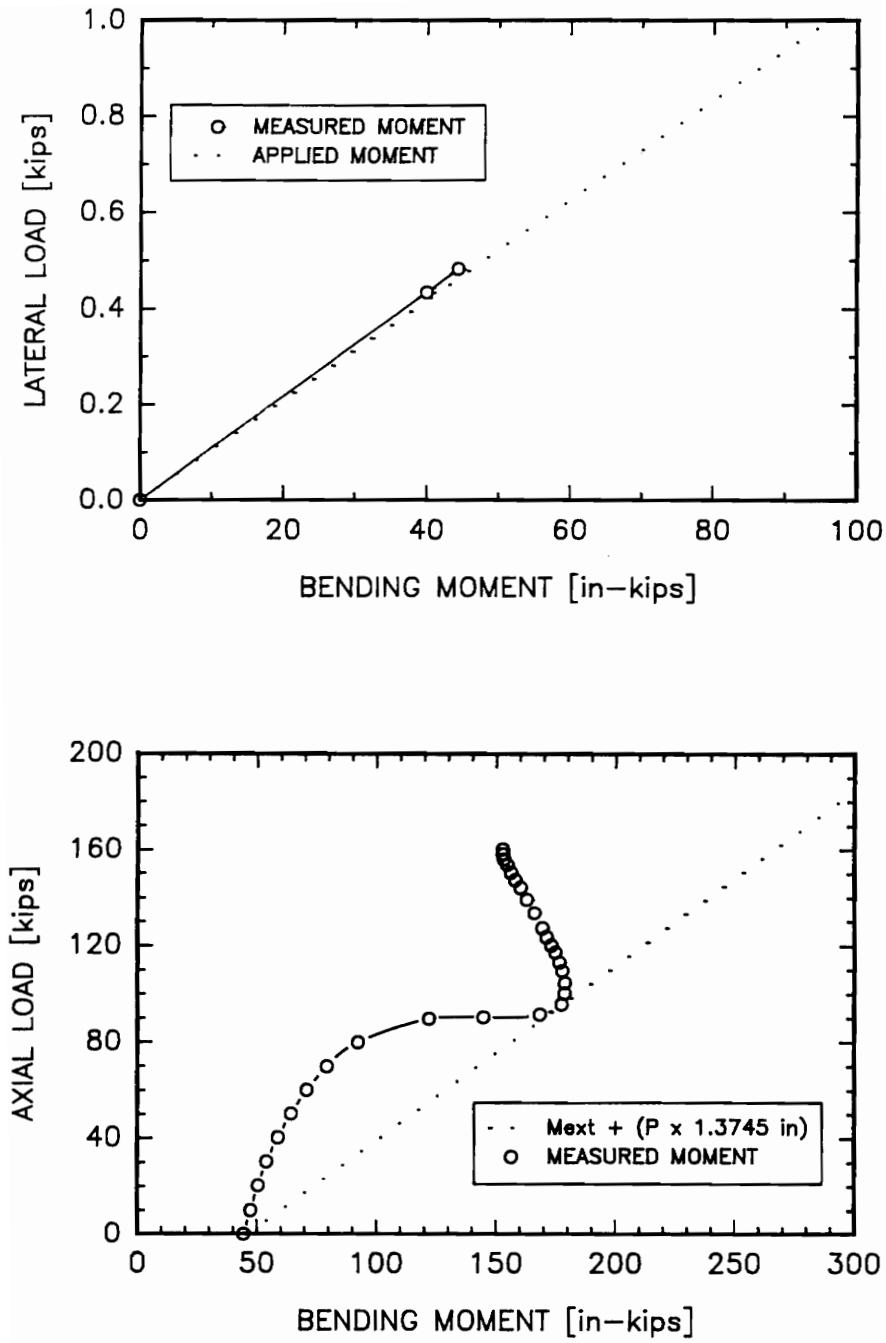

FIG. F.11 FS-6 OUTER CONDUCTOR BENDING MOMENT AT L = 5'-0"

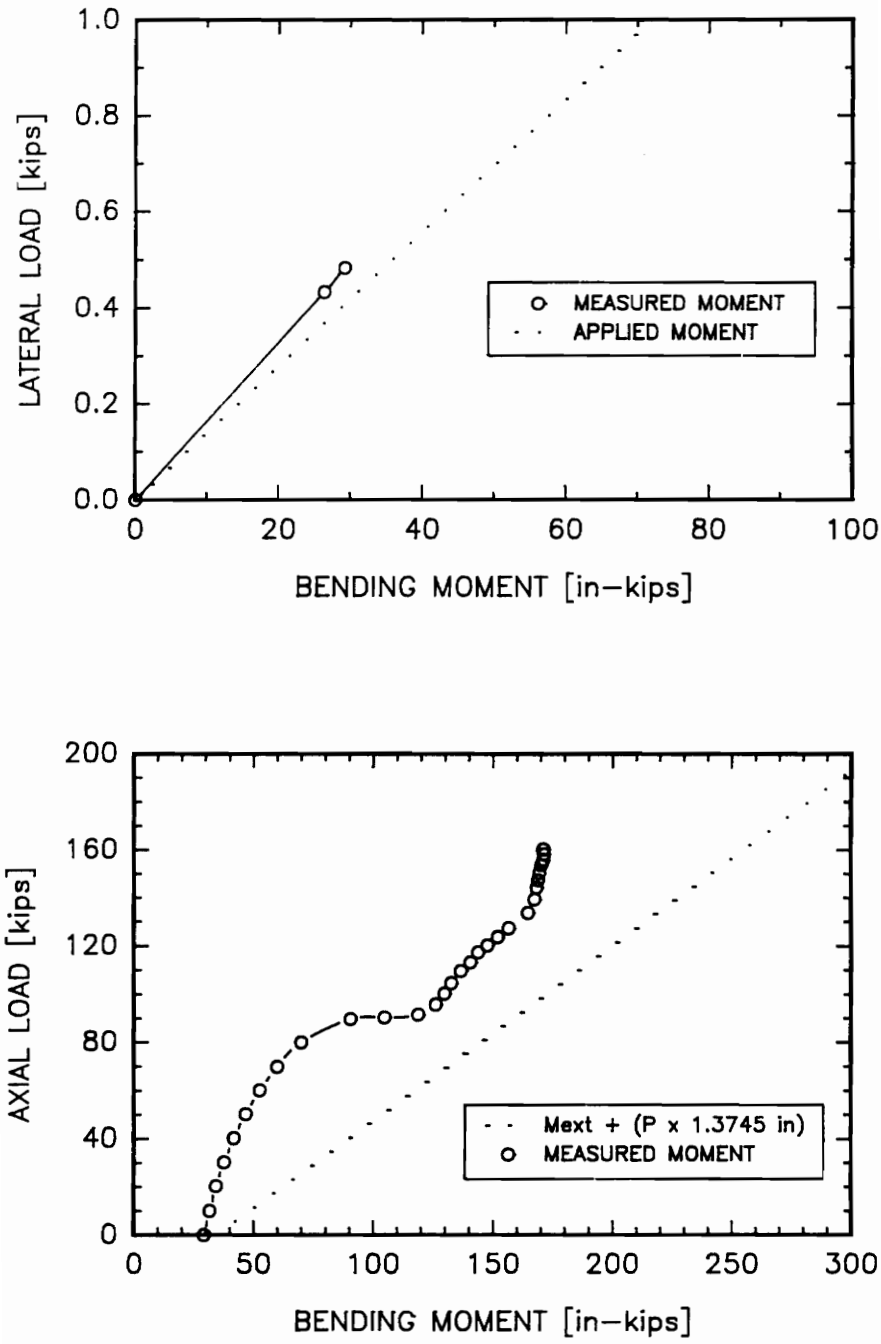

FIG. F.12 FS-6 OUTER CONDUCTOR BENDING MOMENT AT L = 7'-0"

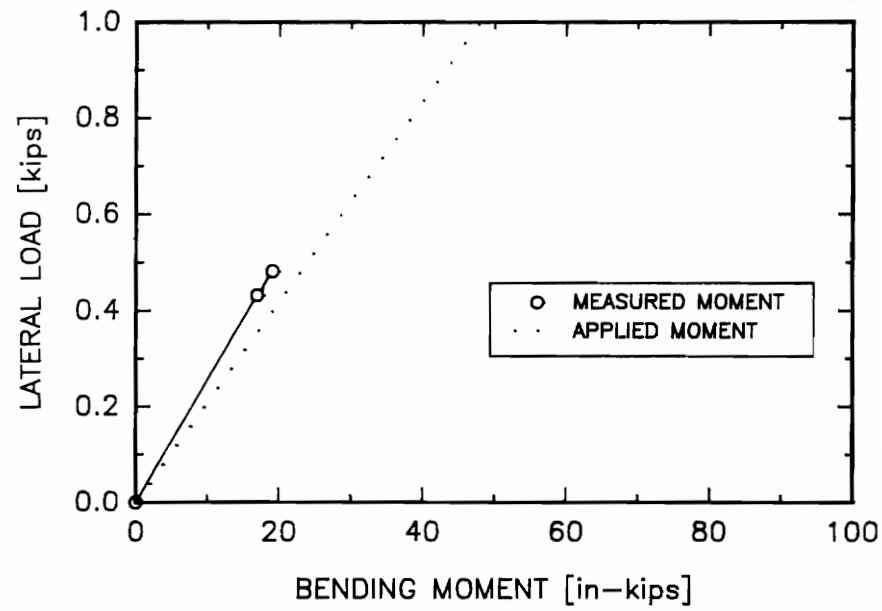

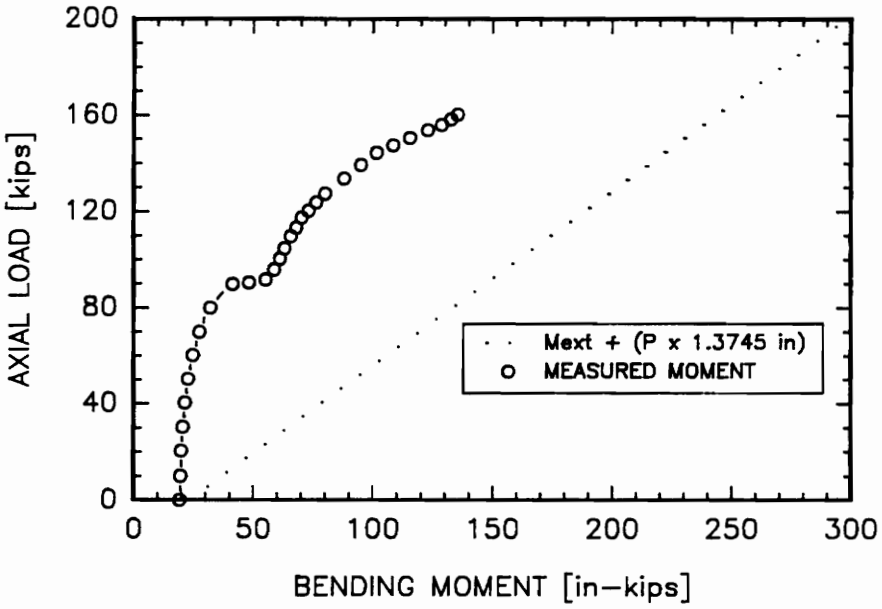

FIG. F.13 FS-6 OUTER CONDUCTOR BENDING MOMENT AT L = 9'-0"

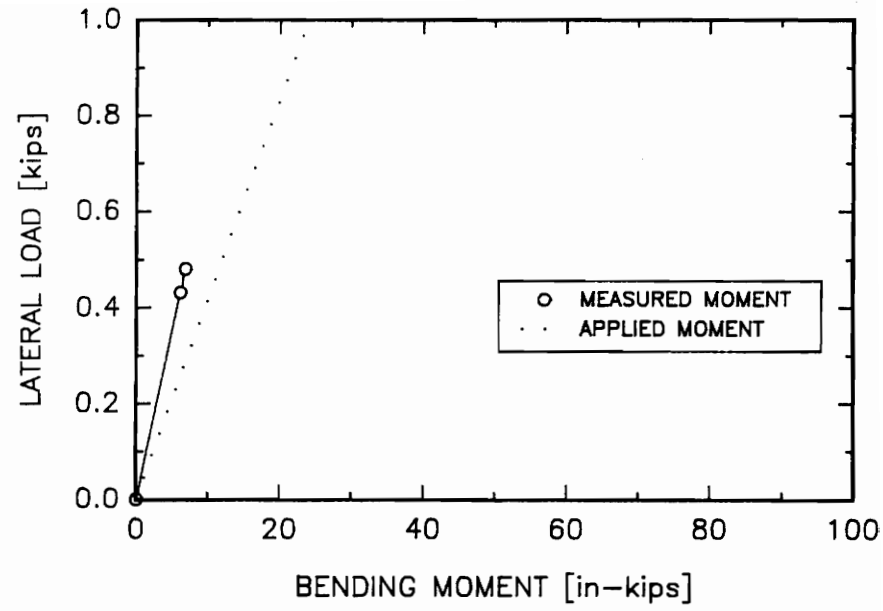

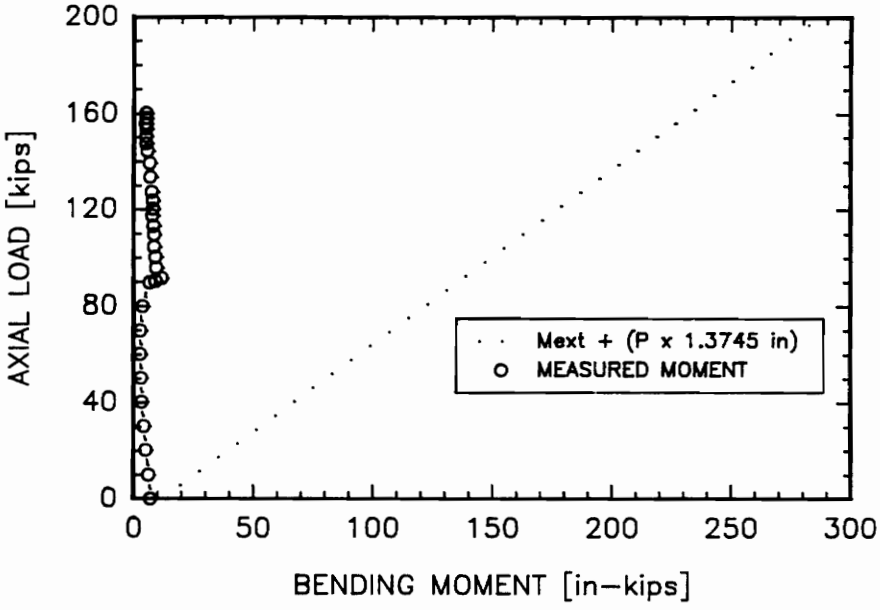

FIG. F.14 FS-6 OUTER CONDUCTOR BENDING MOMENT AT L = 11'-0"

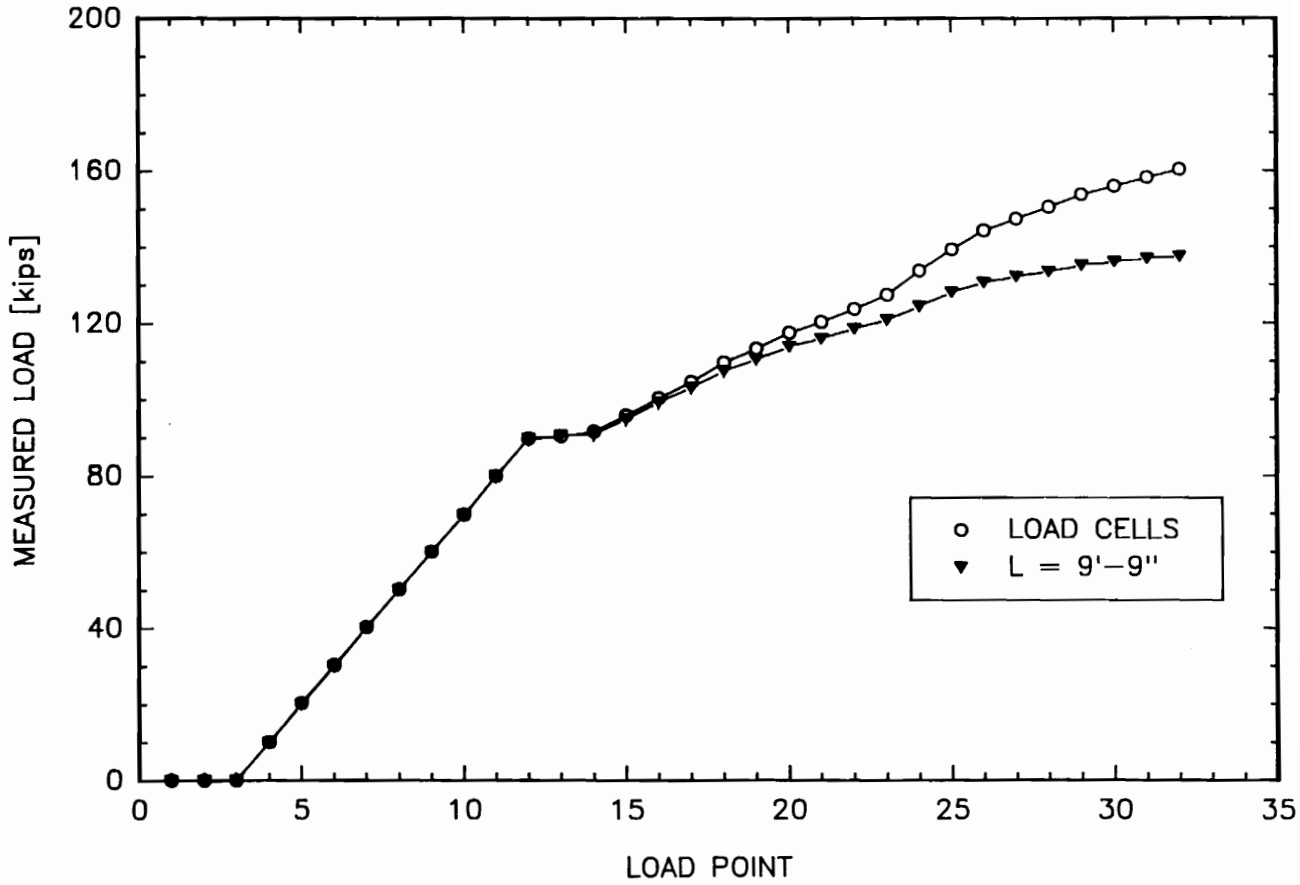

FIG. F.15 FS-6 MEASURED AXIAL LOAD IN INNER CASING

APPENDIX G

TEST FS-7 DATA

UNOCAL

TEST DATA SHEET

Test: UNOCAL FS-7

Test Date: January 24, 1991

Dimensions:

	Outer	Inner
Diameter (in.)	6.625	3.500
Wall Thickness (in.)	0.188	0.250
Yield Stress (ksi)	46.0	92.8

Parameters: Specimen Length = 16'-0"

Test Position - Horizontal: Propped Cantilever

No lateral loading - Axial load only

Max. Axial Load: 160.4 kips

Failure Mode: Stopped Test - Deflections

Predicted Failure Loads (AISC Criteria):

Stahl & Baur Method 111.5 kips

Manley Method 124.0 kips

Discussion:

- Specimen reached a relative maximum axial load of 130.6 kips after which the axial load dropped off to 124.6 kips.
- Specimen continued to hold increasing axial load up to 160.4 kips - stopped test.
- Maximum lateral deflection of approximately 7.5 inches.
- Curvature of specimen in a pronounced S-shape.

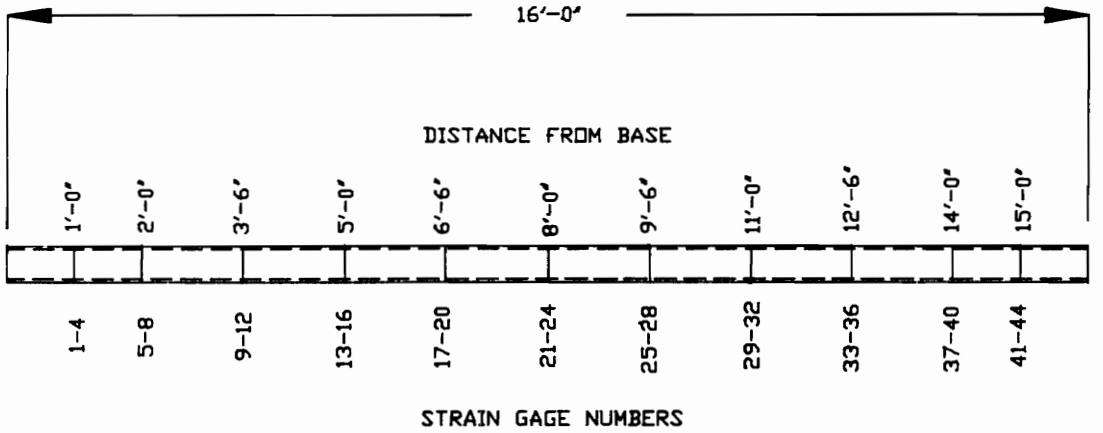

A) 6-5/8" OUTER CONDUCTOR PIPE

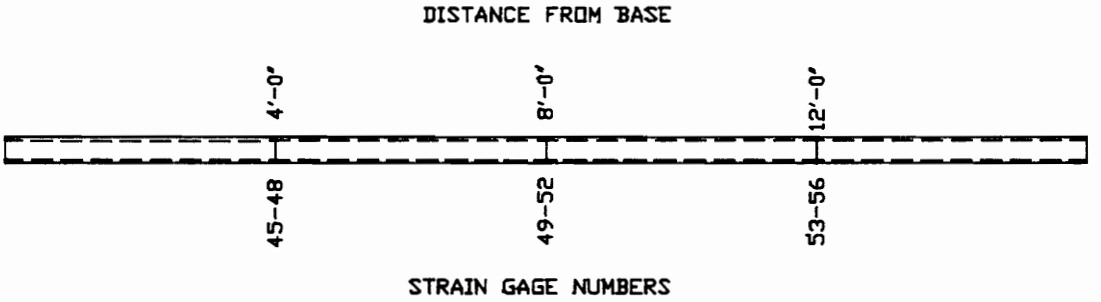

B) 3-1/2" INNER CASING PIPE

FIG. G.1 FS-7 STRAIN GAGE LOCATIONS

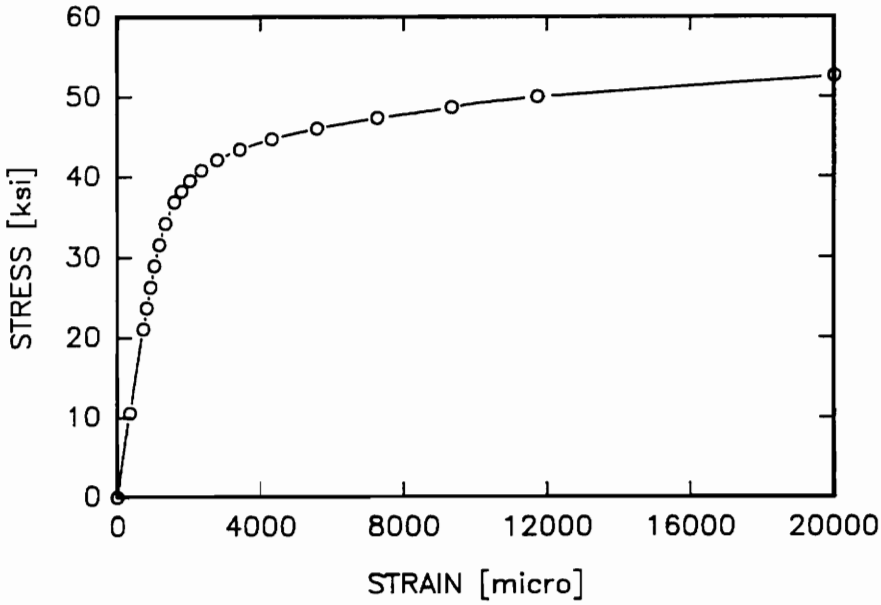

A) STUB COLUMN RESULTS

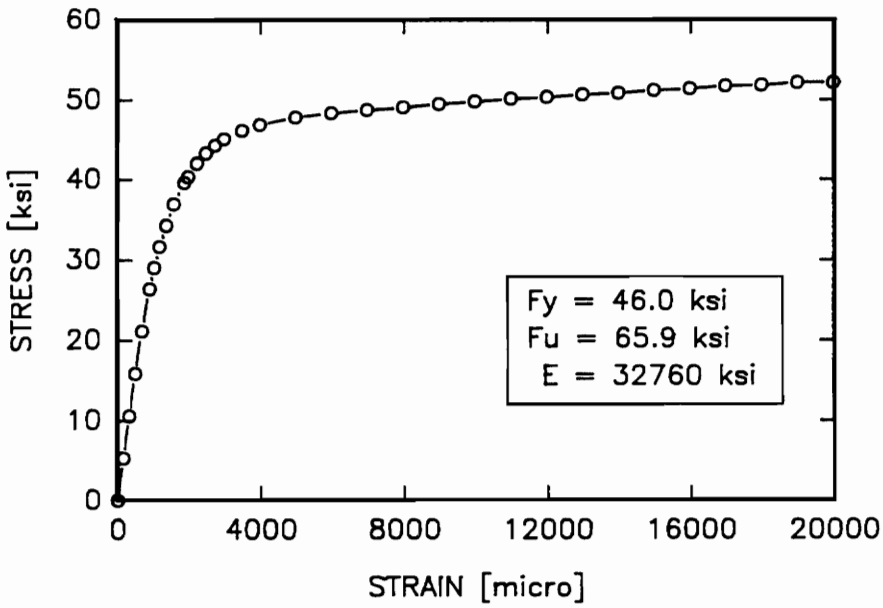

B) TENSILE COUPON RESULTS

FIG. G.2 FS–7 OUTER CONDUCTOR MATERIAL PROPERTIES

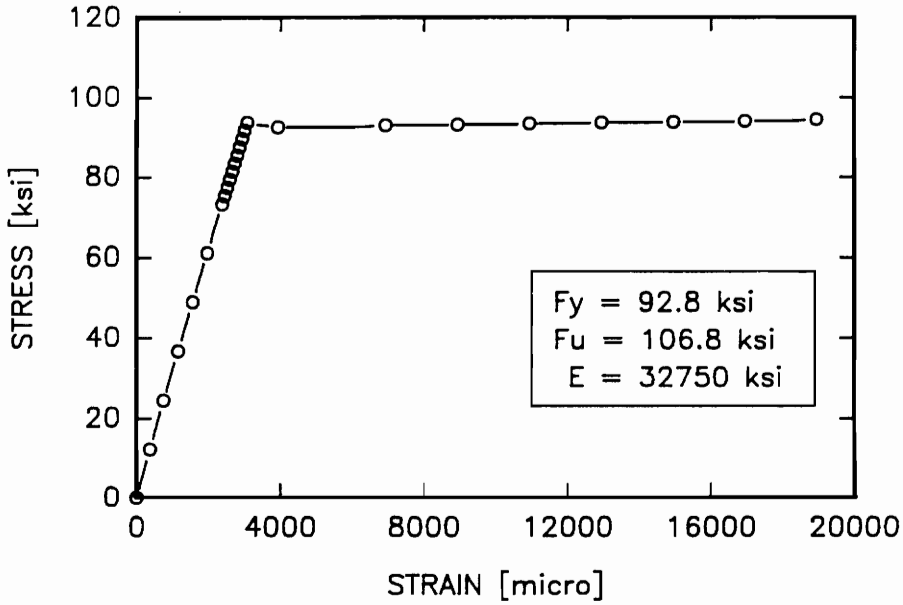

FIG. G.3 FS–7 INNER CASING MATERIAL PROPERTIES

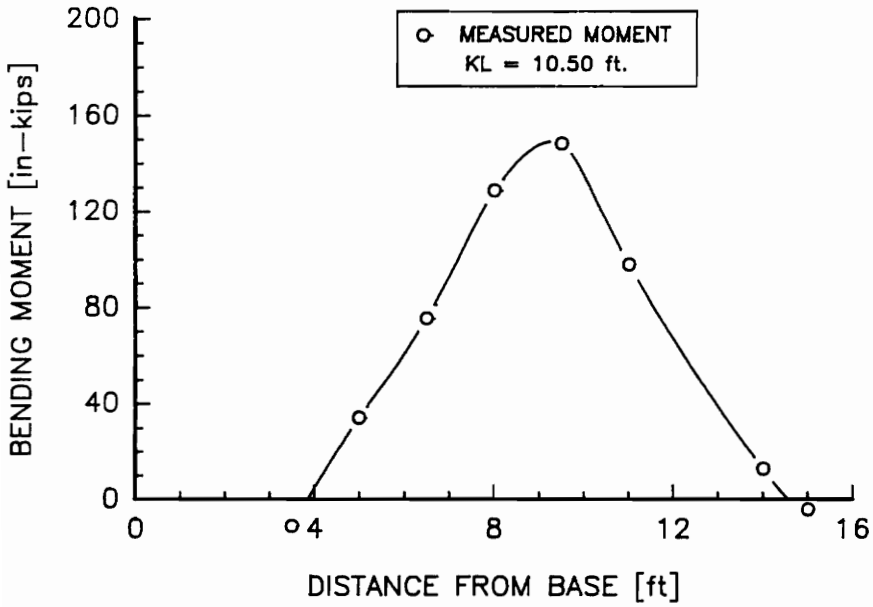

FIG. G.4 FS-7 BENDING MOMENT OVER THE LENGTH OF THE OUTER CONDUCTOR AT LOAD POINT 30.

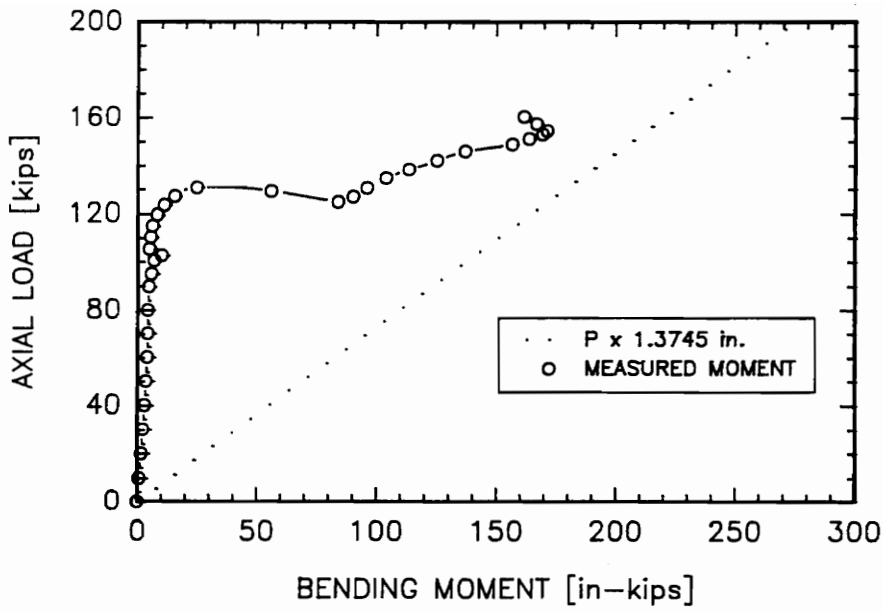

A) L = 1'-0"

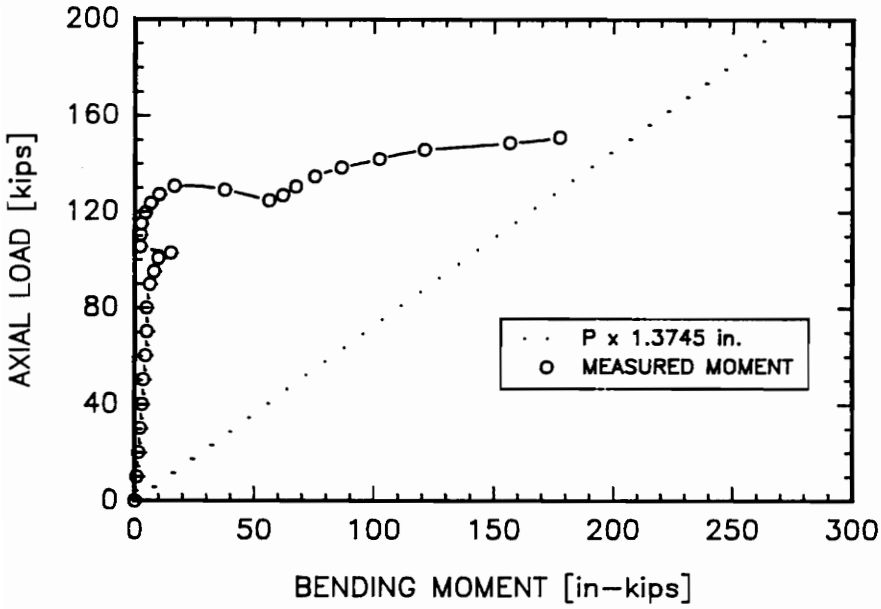

B) L = 2'-0"

FIG. G.5 FS-7 AXIAL LOAD VS. OUTER CONDUCTOR BENDING MOMENT

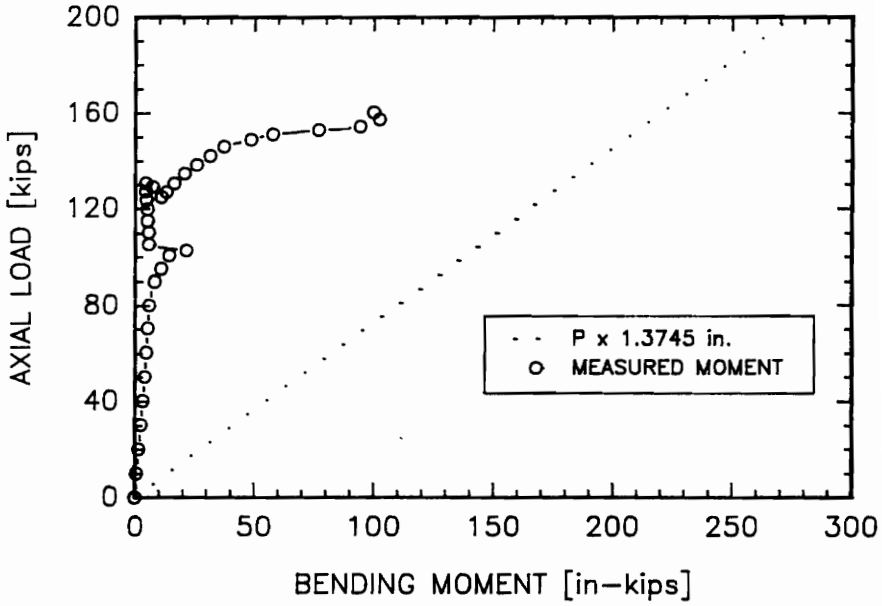

A) L = 3'-6"

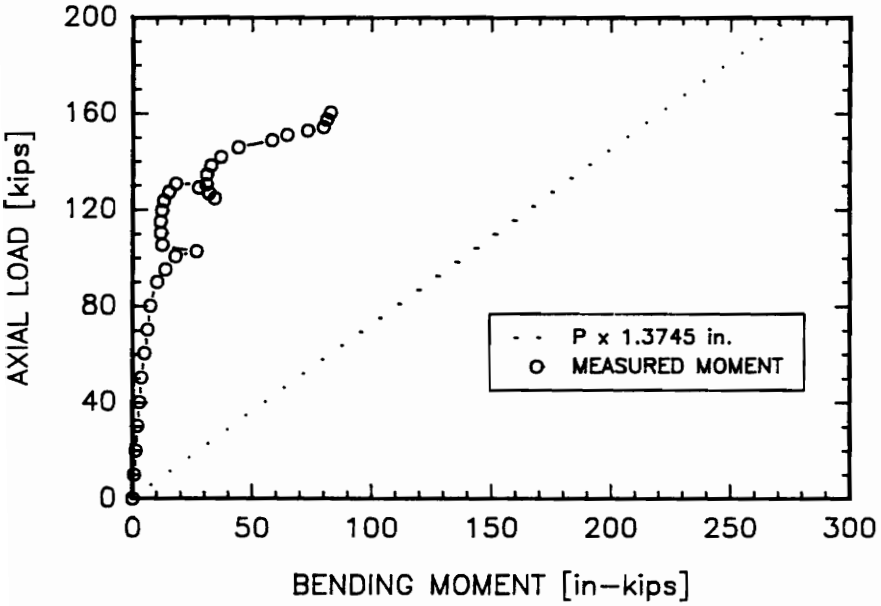

B) L = 5'-0"

FIG. G.6 FS-7 AXIAL LOAD VS. OUTER CONDUCTOR BENDING MOMENT

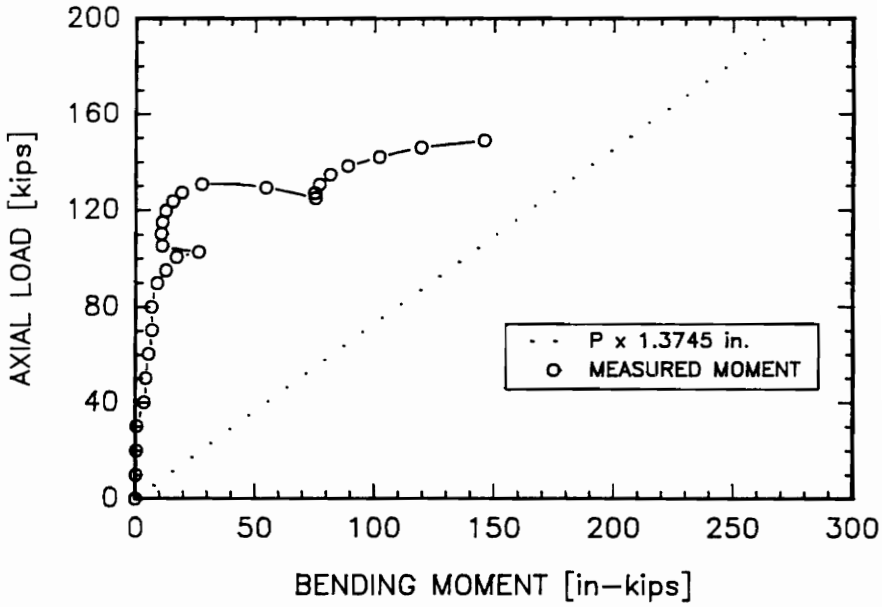

A) L = 6'-6"

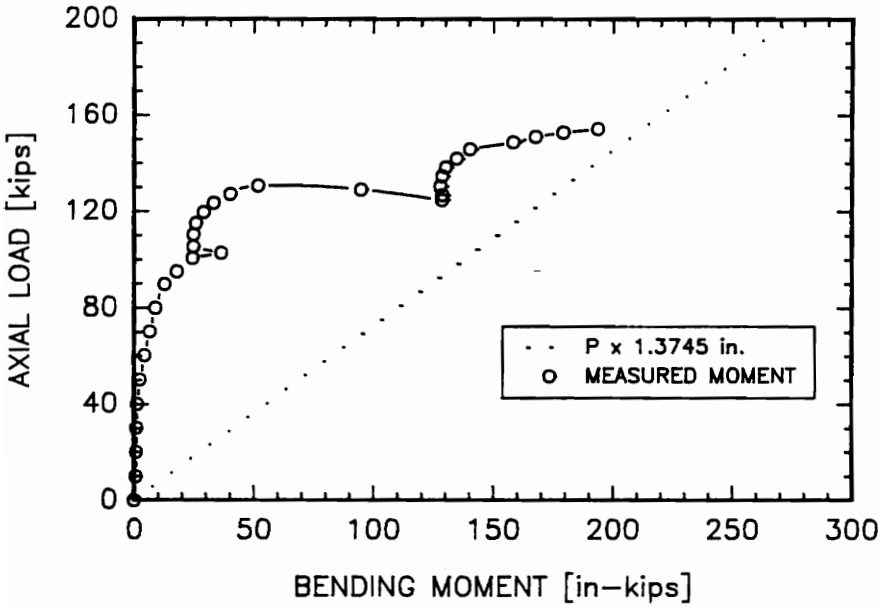

B) L = 8'-0"

FIG. G.7 FS-7 AXIAL LOAD VS. OUTER CONDUCTOR BENDING MOMENT

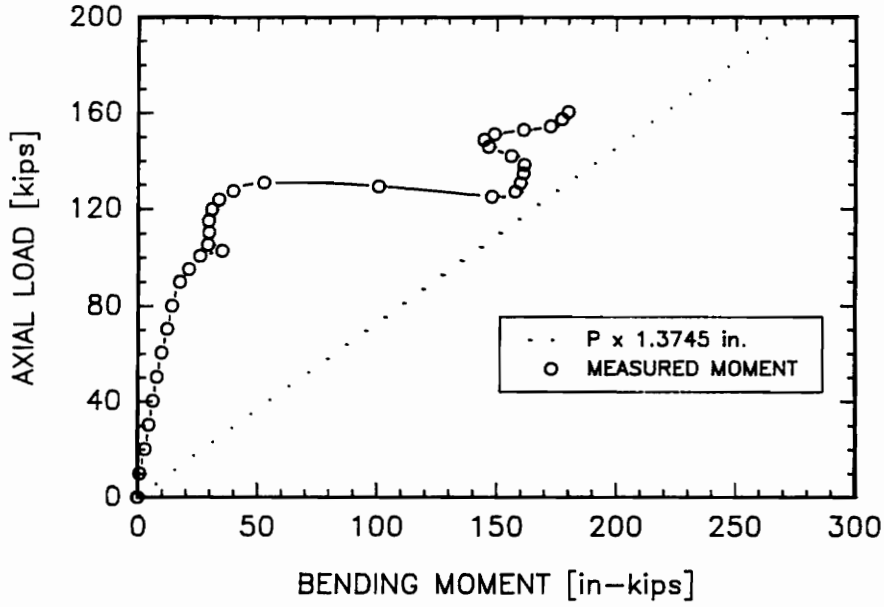

A) L = 9'-6"

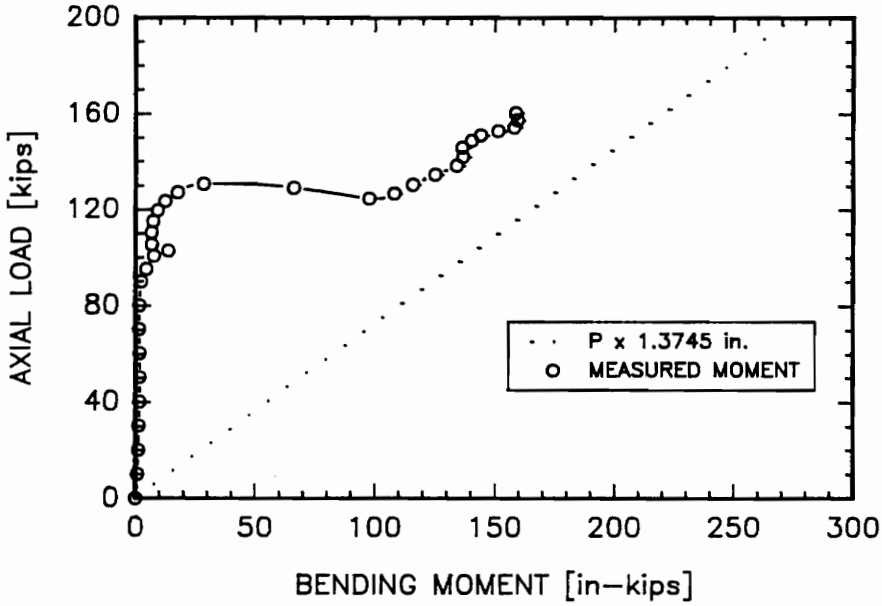

B) L = 11'-0"

FIG. G.8 FS-7 AXIAL LOAD VS. OUTER CONDUCTOR BENDING MOMENT

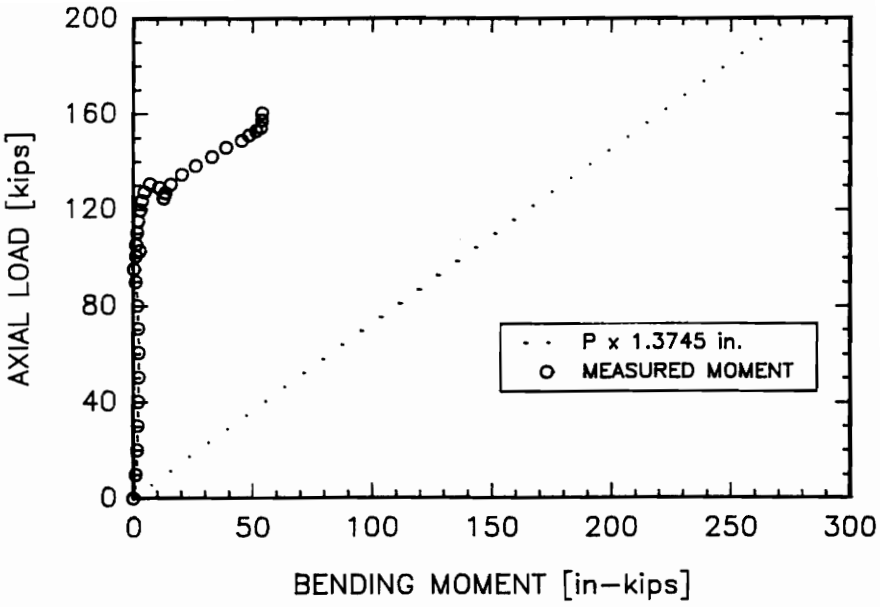

A) L = 14'-0"

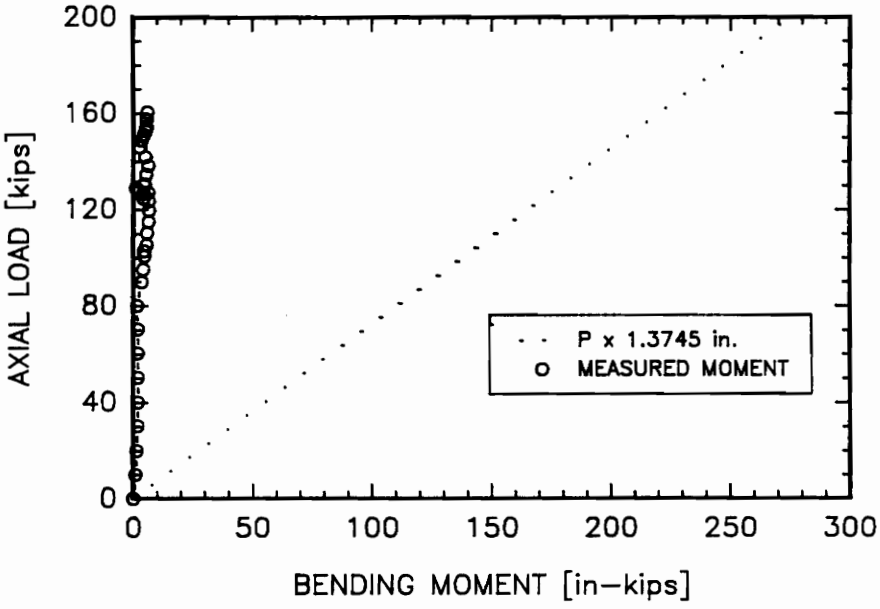

B) L = 15'-0"

FIG. G.9 FS-7 AXIAL LOAD VS. OUTER CONDUCTOR BENDING MOMENT

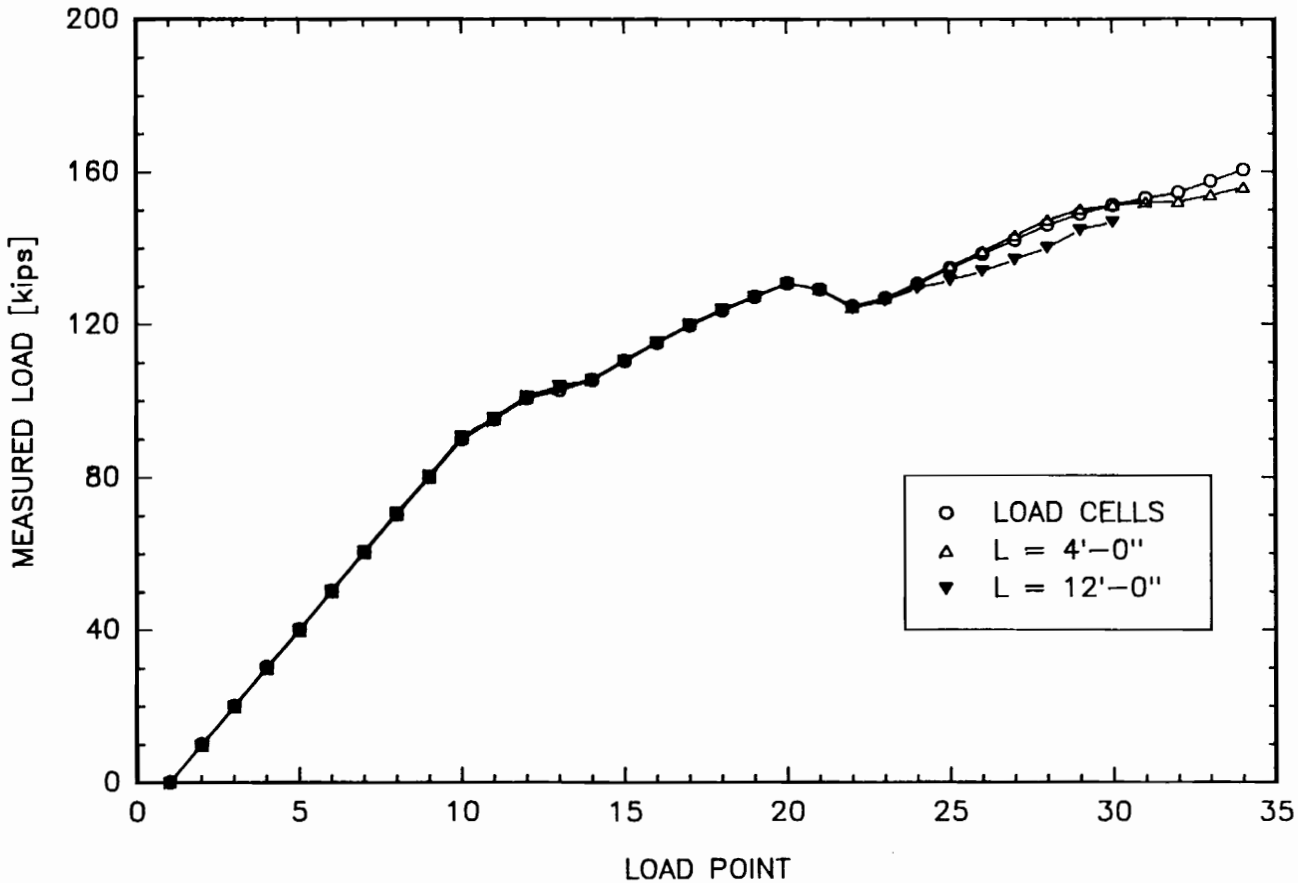

FIG. G.10 FS-7 MEASURED AXIAL LOAD IN INNER CASING

APPENDIX H

Stability Analysis: Column Strength Formula

1) AISC (ASD)

$$F_a = [1 - \frac{\lambda^2}{4}] F_y \qquad \lambda \leq \sqrt{2}$$

$$F_a = [\frac{1}{\lambda^2}] F_y \qquad \lambda \geq \sqrt{2}$$

2) Toma & Chen

$$\frac{P}{P_y} = 1 - 0.091\,\lambda - 0.22\,\lambda^2 \qquad 0 \leq \lambda \leq 1.41$$

$$\frac{P}{P_y} = 0.015 + \frac{0.84}{\lambda^2} \qquad 1.41 \leq \lambda \leq 2.00$$

3) AISC (LRFD)

$$F_a = [0.658^{\lambda^2}] F_y \qquad \lambda < 1.5$$

$$F_a = [\frac{0.877}{\lambda^2}] F_y \qquad \lambda > 1.5$$

4) AISI 76

$$F_a = [1 - 0.385\,\lambda] F_y \qquad \lambda \leq 1.73$$

$$\lambda = \frac{KL}{r\pi} (\frac{F_y}{E})^{1/2}$$

Example Calculations: FS-1

Outer Conductor	Inner Casing
F_y = 46.3 ksi	F_y = 91.8 ksi
P_y = 176.02 k	P_y = 234.32 k
M_p = 360.77 in-kips	M_p = 242.88 in-kips

Interaction Equations:

AISC Plastic Design:

$$\frac{P}{P_y} + \frac{M}{1.18\, M_p} \leq 1.0 \qquad M \leq M_p$$

Toma & Chen

$$\frac{M}{M_P} = 1 - 1.18 \left(\frac{P}{P_y}\right)^2 \qquad 0 \leq \frac{P}{P_y} \leq 0.65$$

$$\frac{M}{M_P} = 1.43 \left[1 - \frac{P}{P_y} \right] \qquad 0.65 \leq \frac{P}{P_y} \leq 1.0$$

Stahl & Baur:

$$1 - \cos\left(\frac{\pi}{2} \frac{P}{P_y}\right) + \frac{M}{M_P} \leq 1.0$$

I. Stahl & Baur Method

A) AISC Plastic Design

$$\frac{P}{176.02} + \frac{P(1.3745)}{1.18(360.77)} = 1.0$$

P(FAIL) = 112.2 kips

B) Toma & Chen

$$\frac{P(1.3745)}{360.77} = 1.43\left[1 - \frac{P}{176.02}\right]$$

$$P(FAIL) = 119.8 \text{ kips}$$

C) Stahl & Baur:

$$1 - \cos\left(\frac{\pi}{2}\frac{P}{176.02}\right) + \frac{P(1.3745)}{360.77} \leq 1.0$$

$$P(FAIL) = 121.9 \text{ kips}$$

II. Manley Method

A) AISC Plastic Design

Inner Casing:

$$\frac{P}{234.32} + \frac{M_{pr}}{1.18(242.88)} = 1.0$$

$$M_{pr} = 286.6 - 1.223\,P$$

Outer Conductor:

$$\frac{P}{176.02} + \frac{P(1.3745)}{1.18(360.77 + M_{pr})} = 1.0$$

$$P(FAIL) = 124.5 \text{ kips}$$

B) Toma & Chen

Inner Casing:

$$\frac{M_{pr}}{242.88} = 1 - 1.18 \left(\frac{P}{234.32}\right)^2$$

$$M_{pr} = 242.88 - \frac{P^2}{191.58}$$

Outer Conductor:

$$\frac{P(1.3745)}{360.77 + M_{pr}} = 1.43 \left[1 - \frac{P}{176.02}\right]$$

$$P(FAIL) = 132.3 \text{ kips}$$

C) Stahl & Baur:

Inner Casing:

$$1 - \cos\left(\frac{\pi}{2}\,\frac{P}{234.32}\right) + \frac{M_{pr}}{242.88} = 1.0$$

$$M_{pr} = 242.88 \cos\left[\frac{P}{149.17}\right]$$

Outer Conductor:

$$1 - \cos\left(\frac{\pi}{2}\,\frac{P}{176.02}\right) + \frac{P(1.3745)}{360.77 + M_{pr}} = 1.0$$

$$P(FAIL) = 134.6 \text{ kips}$$

VITA

David R. McGowan was born on March 7, 1966 in Washington D.C. He was raised in McLean, VA and graduated from Langley High School in 1984. He obtained his B.S. degree in Civil Engineering from Virginia Polytechnic Institute and State University in May 1988. After working in the steel fabrication industry for one year, he returned to graduate school. He obtained his M.S. degree in Civil Engineering from VPI & SU in April 1991.